UNIVERSITY OF BIRMINGHAM

SARCOPENIA IN CHRONIC LIVER DISEASE: NOVEL MECHANISTIC INSIGHTS

By

Sophie Louise Allen, BSc.

A thesis submitted to

The School of Sport, Exercise and Rehabilitation Sciences

The University of Birmingham

For the Degree of

DOCTOR OF PHILOSOPHY

School of Sport Exercise and Rehabilitation Sciences,

University of Birmingham

November 2021

Abstract

Sarcopenia, defined as the loss of muscle mass, quality and strength commonly occurs over the course of ageing and disease states such as chronic liver disease. In chronic liver disease sarcopenia is associated with a number of negative outcomes including an increase in mortality, increased risk of infections and an increase in length of hospital stay, presenting a major socioeconomic issue. Despite the known complications associated with the progression of sarcopenia, the mechanisms relating to its development across the different stages of chronic liver disease is largely unknown. Inflammatory cytokines and ammonia may be key systemic drivers of sarcopenia within cirrhosis. However, the investigation of these factors is limited to supraphysiological *in vitro* treatments. Therefore, in Chapter 3 we investigated the use of *ex vivo* human serum to condition C2C12 skeletal muscle cells in order to develop a more physiologically relevant model, which may be applied to a number of conditions to investigate the development of sarcopenia in both age and disease. We found that myotubes treated with serum from older individuals resulted in myotube atrophy and a blunted anabolic response to leucine provision. Based upon the *in vitro* model developed here, Chapter 4 assessed the potential mechanisms of myotube atrophy in C2C12s conditioned with serum from end-stage liver disease (ESLD), non-cirrhotic non-alcoholic fatty liver disease (NAFLD) patients and age-matched controls. We found a reduction in myotube diameter in cells treated with serum from ESLD patients, which may be characterised by a reduction in mitochondrial respiration, mitophagy and an increase in proteolysis. Following on from this *in vitro* work, in Chapter 5 we investigated fasted-state skeletal muscle regulatory protein content and gene expression in ESLD, NAFLD and age-matched controls. We found a decline in the protein content of OXPHOS complexes I and IV, alongside a decline in citrate synthase activity in ESLD patients. Additionally, we identified an upregulation in genes related to the oxidative stress response in ESLD and senescence in NAFLD patients. In

conclusion, this thesis enhanced our understanding of the potential mechanisms which may underpin the development of sarcopenia in chronic liver disease, through the development of a novel *in vitro* model of liver disease and completion of an *in vivo* human muscle biopsy trial. These findings highlight that mitochondrial dysfunction may be a key driver of sarcopenia in ESLD. Additionally, we describe a valuable model for the investigation of nutritional and pharmaceutical compounds, prior to *in vivo* trials.

Acknowledgements

Firstly, I would like to thank my supervisors Dr. Leigh Breen and Prof. Gareth Lavery. Leigh, thank you for taking a chance on me as a little third year and for giving me the opportunity to pursue a PhD. No words will ever be able to describe how grateful I am for your support and the opportunities you have given me. Thank you for your patience and constant support throughout. I have learnt so much from your leadership and can't wait to continue this over the course of my post-doc position. Here's to the next year, hopefully beyond. Gareth, thank you for allowing me to join your lab and learn the trade of cell culture. This experience, along with the consistent questioning of my methodology has made me a better researcher, for that will always be extremely grateful.

Over the course of my PhD, I have had the opportunity to work with an amazing team of clinical and academic leaders as part of the NIHR BRC Inflammatory Sarcopenia theme. I would like to thank Prof. Janet Lord and Prof. Carolyn Greig for taking time to help and support me along the way. It has been a privilege to be able to learn from you both and receive feedback. I would also like to thank Dr. Matthew Armstrong, Dr. Ahmed Elsharkawy and Dr. Amritpal Dhaliwal and Mrs Felicity Williams. Your help and support has allowed me to navigate myself through some of the clinical world to improve my understanding of this fascinating, and important field of work. I would also like to thank Dr. Yu-Chiang Lai, Dr. Alex Seabright and Dr. Jonathan Barlow for their help and expertise with the cell culture arm to this thesis. Yu-Chiang, thank you for your continued kindness and for allowing me the opportunity to attend journal clubs and lab meetings to increase my exposure to cell and animal work. This has certainly helped improve my knowledge within these areas. I would also like to thank the individuals who ensure the SportExR department keeps running (Steve, James, Dave and all the administration staff).

To past and present members of the Breen and Lavery labs, thank you for all your help and guidance. Specifically, I would like to thank Dr. Jonathan Quinlan and Dr. Paul Morgan. Jonny, thank you for being an amazing mentor over the last 3 years. You certainly helped the jump from UG to PhD seem a little easier by always being there to ask questions and discuss any issues. Paul, thank you for all you have done to keep the lab running smoothly and for your support and advice over the last 3 years but particularly over the last 6-months.

Last, but certainly not least I would like to thank my family. Mum and Dad, thank you for your endless love and support, without you both I would not have been able to complete this PhD. Dad, thank you for driving me to and from Birmingham for 4-years, hopefully it was worth it in the long run. Mommar and Grandad, Nanna and Grandad, thank you for being my biggest cheerleaders and sharing my excitement at publications and conference acceptances, even though you don't fully understand. Josh thank you for all you do for me, particularly your patience and support over the last 3-years of this PhD. I couldn't have done it without you. Hopefully the endless trips to visit me in Brum were worth it during UG and the 1st year of this PhD. I hope I continue to make you all proud.

Contents Listing

List of Conference Communications, Awards and Publications

Author Declaration and Candidate Contributions

List of Abbreviations

Table of Contents

List of Tables

List of Figures

List of Conference Communications, Awards and Publications

Data obtained and presented at conference communications during postgraduate study:

1. 12th Annual Muscle Health Awareness Day, May 2021. Oral Communication. The effect of young and old *ex vivo* human serum on cellular protein synthesis and growth in an *in vitro* model of ageing.
2. International Liver Congress, June 2021. Poster Communication. *In vitro* skeletal muscle cell atrophy and mitochondrial dysfunction after exposure to human serum from patients with ESLD and NAFLD.
3. The Inaugural Birmingham Inflammation, Repair and Ageing (BIRA), July 2021. Oral Communication. *In-vitro* skeletal muscle cell atrophy and proteolysis after exposure to human serum from patients with ESLD and NAFLD
4. The International Conference on Frailty and Sarcopenia and Research, September 2021. Oral Communication. The effect of young and old *ex vivo* human serum on cellular protein synthesis and growth in an *in vitro* model of ageing.

Articles published during the period of postgraduate study:

1. **Allen, S. L., Quinlan, J. I., Dhaliwal, A., Armstrong, M. J., Elsharkawy, A. M., Greig, C. A., Lord, J. M., Lavery, G. G. & Breen, L.** (2021) Sarcopenia in Chronic Liver Disease: Mechanisms and Countermeasures. *American Journal of Physiology: Gastrointestinal and Liver Physiology.* 320 (3):G241-G257.
2. **Allen, S. L., Marshall, R. N., Edwards, S. J., Lord, J. M., Lavery, G. G. & Breen, L.** (2021) The effect of young and old ex vivo human serum on cellular protein synthesis and growth in an in vitro model of ageing. *American Journal of Physiology: Cell Physiology*. 321 (1):C26-C37.

3. **Morgan, P. T., Harris, D. O., Marshall, R. N., Quinlan, J. I., Edwards, S. J., Allen, S. L. & Breen, L.** (2021) Protein source and quality for skeletal muscle anabolism in young and older adults: a systematic review and meta-analysis. *Journal of Nutrition.* 151 (7): 1901-1920.

Under Review:

1. **Edwards, S. J., Carter, S. Nicholson, T., Allen, S. L., Morgan, P. T., Jones, S. W., Rendeiro, C. & Breen, L.** (-)-Epicatechin and its colonic metabolite hippuric acid protect against dexamethasone-induced atrophy in skeletal muscle cells. *Free Radical Biology & Medicine.*
2. **Allen, S. L., Seabright, A. P., Quinlan, J. I., Dhaliwal, A., Williams, F. R., Fine, N. H. F., Hodson, D. J., Armstrong, M. J., Elsharkawy, A. M., Greig, C. A., Y-C. Lai., Lord, J. M., Lavery, G. G. & Breen, L.** Impaired mitochondrial function, proteostasis and growth in C2C12 skeletal muscle cells treated with *ex vivo* serum from Liver Disease patients. *Cells.*

Awards during the period of postgraduate study:

1. MHAD12 Abstract award, elevated to an oral communication at the 12th Annual Muscle Health Awareness Day, May 2021. The effect of young and old *ex vivo* human serum on cellular protein synthesis and growth in an *in vitro* model of ageing.
2. International Liver Congress. June 2021. Young Investigator Bursary. *In vitro* skeletal muscle cell atrophy and mitochondrial dysfunction after exposure to human serum from patients with ESLD and NAFLD.
3. American Physiological Society Select Article. July 2021. The effect of young and old ex vivo human serum on cellular protein synthesis and growth in an in vitro model of ageing.

Author Declarations and Candidate Contributions

I declare that the work outlined within this thesis is my own, as described in detail, with the following exceptions:

Chapter 2 –

- I completed all methods development experiments and analysis.

Chapter 3 –

- I completed all participant visits, *in vitro* experiments, data analysis and writing of the manuscript.

Chapter 4 –

- I helped with a number of patient visits (ESLD and NAFLD). During these visits the candidate assisted in the taking of muscle biopsies, muscle strength testing, physical performance assessments and body composition assessments.
- I completed all control participant visits.
- I completed all *in vitro* experiments, data analysis and writing of the manuscript.
- Mito-QC cells were kindly provided by Dr. Yu Chiang Lai and Dr. Alex Seabright.

Chapter 5 –

- I helped with a number of patient visits (ESLD, NAFLD and CON). These visits consisted of assisting with muscle biopsies, muscle strength testing, physical performance assessments and body composition assessments.
- I completed all western blot analysis.
- RNA extractions and blood work were conducted by Dr. Thomas Nicholson.
- RNA sequencing and library preparation was performed by the Genomic Facility at the University of Birmingham.
- I completed data mapping and RNA-sequencing analysis.

List of Abbreviations

25(OH)D	25-hydroxyvitamin D
3-MH	3-methylhistidine
4EBP-1	eukaryotic translation initiation factor 4E- binding protein 1
6MWT	6-minute walk test
AA	amino acid
AAA	aromatic amino acid
ActRIIB	anti-activin receptor IIB
AdipoR1	adiponectin receptor 1
Akt	protein kinase B
Akt1S1	proline-rich Akt1 substrate 1
ALT	alanine amino transferase
AMPK	AMP kinase
APOE	apolipoprotein E
ArLD	alcohol related liver disease
ATF4	activating transcription factor 4
ATCC	American type culture collection
ATP	adenosine triphosphate
AV	arteriovenous
BAM	binary alignment map
BAM-15	N^5,N^6-bis(2-Fluorophenyl)-[1,2,5]oxadiazolo[3,4-B]pyrazine-5,6-diamine
BCAA	branched-chain amino acid
BIA	bioelectrical impedance analysis

BF	body fat
BMI	body mass index
BSA	bovine serum albumin
CCF	CO_2 contribution factor
CCCP	carbonyl cyanide m-chlorophenyl hydrazone
CITED2	Cpb/P300 interacting transactivator 2
CLD	chronic liver disease
Con PT	concentric peak torque
CPET	cardiopulmonary exercise test
CRP	c-reactive protein
CON/CTR	control
CS	citrate synthase
CST	cell signalling technology
CT	computed tomography
DC Protein Assay	detergent compatible protein assay
DEX	dexamethasone
DEXA	dual-energy x-ray absorptiometry
Deg/s	degrees per second
DMEM	Dulbecco's modified Eagle medium
DMSO	dimethyl sulfoxide
DRP-1	dynamic-related protein 1
DTNB	5,5-dithio-bis-(2-nitrobenzoic acid)
EASL	European Association for the Study of Liver
ECAR	extracellular acidification rate

ECM	extracellular matrix
Ecc PT	eccentric peak torque
eEF2	eukaryotic elongation factor 2
EDTA	ethylenediaminetetraacetic
eIF-4E	eukaryotic translation initiation factor 4E
eIF2α	eukaryotic initiation factor 2α
EIF4G1	eukaryotic translation initiation factor 4 gamma 1
ELISA	enzyme-linked immunosorbent assay
ESLD	end stage liver disease
ESPEN	European Society for Clinical Nutrition and Metabolism
ETC	electron transport chain
EWGSOP	European Working Group on Sarcopenia in Older People
FBS	fetal bovine serum
FFA	free fatty acids
FFM	fat-free mass
FIS1	mitochondrial fission protein 1
FM	fat mass
FOXO	forkhead box O
GCN2	general control non-depressed 2
GDH	glutamate dehydrogenase
GFP	green fluorescent protein
GH	growth hormone
GSR	glutathione reductase
H_2O_2	hydrogen peroxide
Hb	haemoglobin

HCC	hepatocellular carcinoma
HE	hepatic encephalopathy
HEPES	4-(2-hydroxyethyl)-1-piperazineethanesulfonic acid
HGF	hepatocyte growth factor
HGS	hand-grip strength
HMB	hydroxymethylbutyrate
HOMA-IR	homeostatic model assessment of insulin resistance
HRP	horseradish peroxidase
HS	horse serum
IGF-1	insulin-like growth factor-1
IGFBP2	insulin-like growth factor binding protein 2
IGFBP-3	insulin-like growth factor-binding protein 3
IKZF3	IKARSO family zinc finger 3
ILK	integrin linked kinase
IL-1β	interleukin-1β
IL-4	interleukin-4
IL-6	interleukin-6
IL-9	interleukin-9
IL-16	interleukin-16
INR	international normalised ratio
ISR	integrated stress response
JNK	c-Jun N-terminal Kinase
kDa	kilodalton
Kg	kilogram
L3	third lumbar vertebrae

LC3 A/B	microtubule-associated protein 1A/1B- light chain 3
Leu	leucine
LES	late evening snack
LFI	liver frailty index
LGI	low grade inflammation
LPS	lipopolysaccharide
LT	liver transplant
MAFbx	muscle atrophy-box
MAMC	midarm muscle circumference
MAPK	mitogen activated protein kinase
MELD	model for end-stage liver disease
MFF	mitochondrial fission factor
MFN2	mitofusin 2
Mito-QC	mitophagy reporter cell line
mL	millilitre
mM	millimolar
MPB	muscle protein breakdown
MPS	muscle protein synthesis
MRI	magnetic resonance spectroscopy
mRNA	messenger ribonucleic acid
$mtFIS1_{101-152}$	mitochondrial targeting sequence of FIS1 (amino acids 101-152)
mTOR	mammalian target of rapamycin
mTORC1	mammalian target of rapamycin complex 1
MuRF1	muscle RING finger-1

MyoD	myoblast determination protein 1
Myf5	myogenic factor 5
NAFL	non-alcoholic fatty liver
NAFLD	non-alcoholic fatty liver disease
NASH	non-alcohol steatohepatitis
NDRG1	N-myc downstream regulated 1
NFI	nuclear fusion index
NF-κB	nuclear factor-κB
NOSTRIN	nitric oxide synthase trafficking
NPB	net protein balance
NRF2	nuclear factor erythroid factor 2 related factor 2
NSAIDs	non-steroidal anti-inflammatory drugs
OCR	oxygen consumption rate
OM	oligomycin
OPA-1	optic atrophy protein 1
ORF	open reading frame
OXPHOS	oxidative phosphorylation
p62	sequestome 1
PAGE	polyacrylamide gel electrophoresis
Pax7	paired box 7
p70S6k	ribosomal protein S6 kinase
PBS	phosphate-buffered saline
PCA	portacaval anastomosis
pg	picogram
pH	potential of hydrogen

PI3K	phosphoinositide 3-kinase
PMI	psoas muscle index
PP2A	protein phosphatase 2A
PPARGC1A	PPAR coactivator alpha
PPR	proton production rate
P/O	per mol of oxygen atoms consumed
PRKAA2	protein kinase AMP-activated catalytic subunit alpha 2
P/S	penicillin/streptomycin
PVDF	polyvinylidene fluoride
QoL	quality of life
RAF1	v-Raf-1 murine leukaemia viral oncogene homolog 1
RET	resistance exercise training
Rhbg	Rh B glycoprotein
Rhcg	Rh C glycoprotein
RIPA	radioimmunoprecipitation assay
RNA	ribonucleic acid
ROS	reactive oxygen species
RPS6	s6 protein
SARC-F	simple five-item questionnaire
SC	satellite cell
SDS	sodium dodecyl sulphate
SEM	standard error of the mean
Ser	serine
SF-36	short form 36
SLC75A/LAT1	large neutral amino acid transporter 1

SLC28A2/SNAT2	sodium-coupled neutral amino acid transporter 2
SMM	skeletal muscle mass
SMI	skeletal muscle mass index
SPPB	short physical performance battery
SUnSET	surface sensing of translation
TBST	tris-buffered saline and 0.1% tween-20
TCA	tricarboxylic acid cycle
TGFB1	transforming growth factor beta 1
TSC 1/2	tuberous sclerosis complex 1/2
TEM	transmission electron microscopy
Thr	threonine
TNF-α	tumor necrosis factor-α
TNF-β	tumor necrosis factor-β
TNB	5-thio-2-nitrobenzoic acid
TNFR1	tumor necrosis receptor 1
tRNA	transfer ribonucleic acid
UA	urolithin A
μg	microgram
UK	United Kingdom
UKLED	United Kingdom Model of End Stage Liver Disease
μL	microlitre
μM	micromolar
UPP	ubiquitin proteasome pathway
UTR	untranslated region

WBFM	whole body fat mass
WbPB	whole-body protein breakdown
WHO	World Health Organisation
WPR	work per repetition
YNG	young
α-KG	alpha ketoglutarate

Table of Contents

Chapter 1 – General Introduction 1

1.1 Chronic Liver Disease 2

1.1.1 Epidemiology of Chronic Liver Disease and the Health Care Burden 4

1.2 Malnutrition, Sarcopenia and Chronic Liver Disease 5

1.2.1 The Definition of Sarcopenia 7

1.2.2 Diagnosis of Sarcopenia in Chronic Liver Disease 8

1.2.3 The Clinical Impact of Sarcopenia in Cirrhosis 10

1.3 Alterations in Muscle Protein Turnover in Chronic Liver Disease 12

1.3.1 Hyperammonemia, Myostatin and Muscle Protein Turnover 15

1.3.2 Energy Expenditure and Amino acid Availability in Chronic Liver Disease 19

1.3.3 Alcohol and Chronic Liver Disease 20

1.3.4 Abnormalities in Endocrine Function 21

1.3.5 Non-Alcoholic Fatty Liver Disease and Obesity 22

1.3.6 Potential Drivers of Chronic Liver Disease Which May Influence Sarcopenia Progression 25

1.4 Cell Culture: Current Perspectives, Limitations and Future Directions 27

1.4.1 In Vitro Models of Atrophy 27

1.4.2 Making Cell Culture More Physiologically Relevant 29

1.5 Overview and Thesis Aims 31

1.6 References 33

Chapter 2 –Methods Development 46

2.1 Cell Culture 47

2.1.1 C2C12 Cell Line 47
2.1.2 Thawing Cells 47
2.1.3 Freezing Cells 47
2.1.4 Cell Maintenance 48
2.1.5 Cell Counting 49
2.1.6 Cell Differentiation 49
2.2 Cell Treatments *49*
2.2.1 The Investigation of Conditioning C2C12 Skeletal Muscle Cells with Ex Vivo Human Serum 49
2.2.2 In Vitro Leucine Treatment 51
2.2.3 Conditioning with Ex vivo Human Serum Prior to In Vitro Leucine Treatment 52
2.3 Muscle Protein Synthesis *52*
2.4 Protein Analysis *53*
2.4.1 Cell Lysis 53
2.4.2 Sample Preparation – Cell Lysates 53
2.4.3 Gel Preparation and Electrophoresis 53
2.4.4 Transfer and Blocking 53
2.4.5 Antibodies 54
2.4.6 Image Capture and Analysis 56
2.5 Myotube Morphology *56*
2.5.1 Staining for Myotube Diameter 56
2.5.2 Myotube Diameter and Nuclear Fusion Index Quantification 57
2.6 Mitochondrial Respirometry *58*
2.6.1 Cell Seeding, Maintenance and Preparation 58

2.6.2 Mitochondrial Stress Test....58
2.6.3 Estimation of ATP Production....59
2.6.4 Normalisation....61
2.7 Mitophagy....*62*
2.7.1 Mito-QC Cell Line....62
2.7.2 Sample Preparation....62
2.7.3 Image Analysis and Quantification....62
2.8 Statistical Analysis....*63*
2.9 References....*65*
Chapter 3 – Development of an In Vitro Model of Ageing....67
3.1 Abstract....*69*
3.2 Introduction....*70*
3.3 Materials and Methods....*72*
3.3.1 Subject Characteristics and Ethical Approval....72
3.3.2 Study Design....72
3.3.3 Body Composition....73
3.3.4 Handgrip Strength....73
3.3.5 Leg Strength....74
3.3.6 Blood Analyses....74
3.3.7 Cell Culture....74
3.3.8 Myotube Diameter....75
3.3.9 Muscle Protein Synthesis....75
3.3.10 Immunoblotting....76
3.3.11 Statistical Analysis....77

3.4 Results *78*

3.4.1 Body Composition and Strength 78

3.4.2 Inflammatory Markers and Blood Analysis 79

3.4.3 Myotube Diameter and Nuclear Fusion Index 79

3.4.4 Muscle Protein Synthesis 81

3.4.5 Anabolic Signalling 83

3.4.6 Catabolic Signalling 84

3.5 Discussion *85*

3.6 References *91*

Chapter 4 – The Development of a Novel In Vitro Model of Liver Disease 96

4.1 Abstract *98*

4.2 Introduction *100*

4.3 Methods *102*

4.3.1 Participant Characteristics and Ethical Approval 102

4.3.2 Study Design 103

4.3.3 Blood Analyses 103

4.3.4 Cell Culture 103

4.3.5 Myotube Diameter 104

4.3.6 Muscle Protein Synthesis 105

4.3.7 Immunoblotting 105

4.3.8 Mitochondrial Respirometry 106

4.3.9 Mitophagy Assay 107

4.3.10 Statistical Analysis 107

4.4 Results *108*

4.4.1 Body Composition and Strength 108
4.4.2 Blood Analysis 109
4.4.3 Muscle Protein Synthesis and Anabolic Signalling 112
4.4.4 Proteolytic Signalling 114
4.4.5 Mitochondrial Respiration 116
4.4.6 Mitophagy 119
4.4.7 Mitochondrial Content 121
4.5 Discussion *121*
4.6 References *129*
Chapter 5 – The Regulatory Protein and Gene Expression Profile of Skeletal Muscle in Chronic Liver Disease Patients 133
5.2 Introduction *137*
5.3 Methods *139*
5.3.1 Participant Characteristics and Ethical Approval 139
5.3.2 Study Design 140
5.3.3 Blood Analyses 140
5.3.4 Muscle Sample Preparation 141
5.3.5 Immunoblotting 141
5.3.6 RNA Sequencing Analysis 143
5.3.7 Citrate Synthase Activity Assay 144
5.3.8 Statistical Analysis 144
5.4 Results *145*
5.4.1 Body Composition, Muscle Mass and Strength 145
5.4.2 Blood Analysis 146

5.4.3 Anabolic Signalling 147

5.4.4 Catabolic Signalling 149

5.4.5 Mitochondrial Markers and Activity 151

5.4.6 Regulatory Markers 153

5.4.7 RNA Sequencing Analysis 154

5.5 Discussion *157*

5.6 References *166*

Chapter 6 – General Discussion 170

6.1 Introduction *171*

6.2 In Vitro Models of Age-Related Sarcopenia *172*

6.2.1 Inflammation, Insulin Resistance and Sarcopenia 174

6.2.2 Future Directions and Implications 176

6.3 In Vitro Models of Chronic Liver Disease *177*

6.3.1 Muscle Atrophy and Protein Turnover in Chronic Liver Disease 181

6.3.2 Mitochondrial Dysfunction and Chronic Liver Disease 183

6.3.3 Model Limitations and Future Directions 185

6.4 Sarcopenia in Chronic Liver Disease: Translation of an In Vitro Model of ESLD, to In Vivo Work *186*

6.4.3 Limitations and Future Directions 192

6.4.4 Implications and Potential Therapeutic Targets 192

6.5 Conclusions *194*

6.6 References *196*

List of Tables

Table 1.1 Aetiology of end stage liver disease 5

Table 1.2 Key diagnostic criteria for sarcopenia and cachexia 7

Table 1.3 Overview of modes used to assess sarcopenia in chronic liver disease..... 8

Table 2.1 Antibodies 56

Table 2.2 Respiratory analysis..... 60

Table 2.3 Estimation of ATP production..... 62

Table 3.1 Participant characteristics for anthropometric, body composition and strength data in young and old males 79

Table 4.1 Participant characteristics for anthropometric, body composition and strength data in healthy control, NAFLD and ESLD participants..... 110

Table 5.1 Co-morbidities in NAFLD and ESLD patients..... 141

Table 5.2 Participant characteristics for anthropometric, body composition and strength data in healthy control, NAFLD and ESLD participants..... 147

List of Figures

Figure 1.1 Trajectory of chronic liver disease 3

Figure 1.2 Schematic representation of muscle protein turnover in response to anabolic stimuli (protein feeding with/ without exercise) in healthy and chronic liver disease 12

Figure 1.3 Molecular regulation of muscle protein turnover 14

Figure 1.4 The proposed molecular alterations which contribute to ammonia induced changes in muscle protein turnover 18

Figure 1.5 The molecular regulation of muscle protein synthesis and muscle protein breakdown in chronic liver disease 24

Figure 2.1 Western blot of puromycin incorporation for leucine dose response 53

Figure 3.1 Myotube diameter and NFI 81

Figure 3.2 Measures of MPS and anabolic signalling in response to the addition of ex vivo human serum with and without leucine treatment 83

Figure 3.3 Changes in markers of catabolic signalling in response to the addition of ex vivo human serum with and without leucine treatment 85

Figure 4.1 Serum from NAFLD and ESLD patients induces myotube atrophy 112

Figure 4.2 Measures of MPS and anabolic signalling in response to treatment with CON, NAFLD and ESLD serum 114

Figure 4.3 Markers of catabolic signalling are elevated in myotubes treated with serum from ESLD patients for 4 hours and a 30-minute treatment with leucine 116

Figure 4.4 Serum from NAFLD and ESLD patients induces impairments in mitochondrial respiration, despite no changes in markers of mitochondrial content.....119

Figure 4.5 Serum from NAFLD and ESLD patients induces a reduction in mitophagy.....121

Figure 4.6 ESLD serum induces a reduction in myotube diameter, mitochondrial function and an increase in markers of MPB, with no change in MPS 123

Figure 5.1 Western blot analysis of anabolic signalling targets in CON, NAFLD and ESLD patients 150

Figure 5.2 Markers of proteolytic signalling in CON, NAFLD and ESLD patients 152

Figure 5.3 Markers of mitochondrial fission, fusion and content in CON, NAFLD and ESLD patients 154

Figure 5.4 Regulatory protein content in CON, NAFLD and ESLD patients 155

Figure 5.5 RNA-sequencing analysis of CON, NAFLD and ESLD muscle biopsy samples 158

Figure 6.1 Plasma IL-6 and CRP concentrations and HOMA-IR in young and old males ...177

Figure 6.2 Myotube diameter is significantly decreased within NAFLD and ESLD treated myotubes compared to untreated control C2C12s 181

Figure 6.3 Proton efflux rate and ATP production 186

Figure 6.4 Updated schematic representation of muscle protein turnover in response to anabolic stimuli (protein feeding) in healthy, non-cirrhotic non-alcoholic fatty liver disease 192

CHAPTER 1 – GENERAL INTRODUCTION

1.1 Chronic Liver Disease

Chronic liver disease (CLD) is a term given to a group of heterogenous disease states, which result in damage to the liver structure and hepatic function in response to inflammation and insults to the liver (1, 2). Under normal conditions, the liver contains a small amount of fibrotic tissue, however in response to chronic damage to liver cells, an accumulation of fibrillar extracellular matrix (ECM) develops (3, 4). This accumulation of fibrillar ECM arises due to a defective liver and represents the outcome of continuous wound healing in response to damage to the liver (4, 5). This stage of liver damage can be reversed to restore a state of normal liver function with an appropriate intervention (5). However, in the absence of interventions an advanced stage of liver disease may arise, known as cirrhosis, regardless of the underlying aetiology (5). Cirrhosis represents end stage liver disease (ESLD) and is defined as the structural development of regenerative nodules that are encompassed by fibrous bands (6). The progression to ESLD is heterogenous and can be dependent on genetic and environmental factors, however most cases develop over 20-40 years. The presentation of fibrosis is largely asymptomatic, however the development of cirrhosis leads to significant increases in mortality (3). Once patients develop cirrhosis they may progress through compensated cirrhosis, an asymptomatic phase, followed by the development of decompensated cirrhosis, defined as the development of liver failure and portal hypertension (3), predicted to occur at a rate of 5-7% per year (7).

The stage of CLD progression can be classified by a number of factors including fibrosis, steatosis, inflammation, hepatocellular injury and miscellaneous features (8, 9). In 2005 Kleiner et al (8) outlined the validation of a histological scoring system, specific to non-alcoholic fatty liver disease (NAFLD) and non-alcoholic steatohepatitis (NASH). Within this definition Kleiner et al (8) defined the stage of liver fibrosis by a 4-point scale (F1-4), with 1 representing mild fibrosis and 4 representing cirrhosis. Once a stage of fibrosis reaches the

end of the spectrum (cirrhosis) and is considered ESLD, alternative scales may be used to classify an individual's stage of ESLD (Figure 1.1).

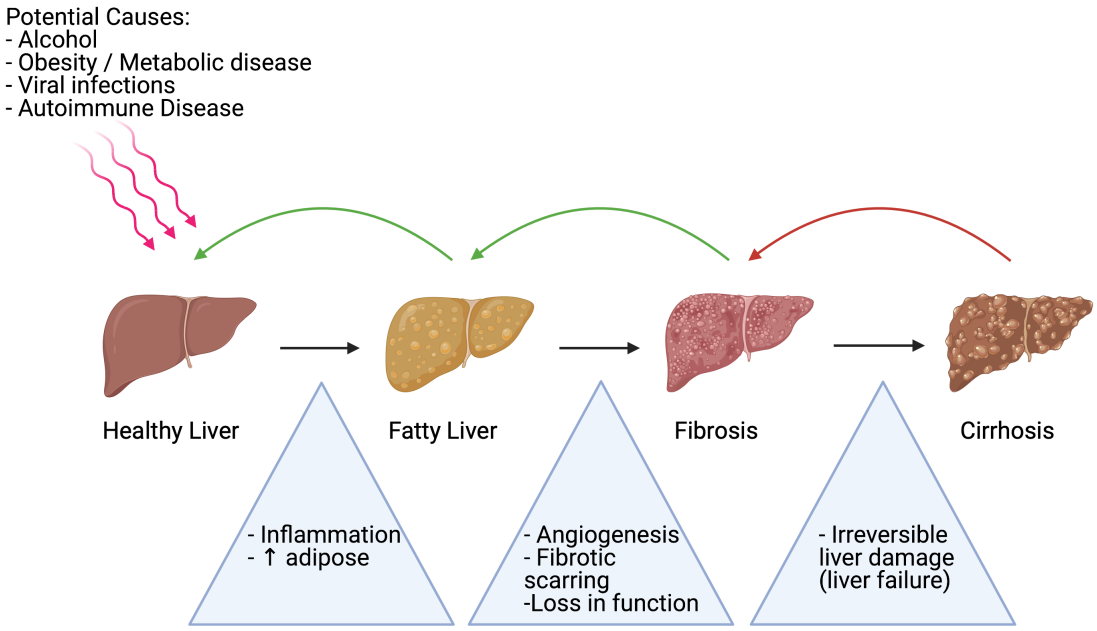

Figure 1.1. Trajectory of chronic liver disease. A healthy liver experiences insults which causes an increase in inflammation and adipose tissue which progress to the development of a fatty liver. A fatty liver may deteriorate further and develop angiogenesis, fibrotic scarring and a loss of liver function. At a stage of fibrosis, the degree of liver damage is reversible with the adherence to appropriate interventions. A stage of fibrosis may then progress to the development of cirrhosis, irreversible liver damage.

Over the last 50 years a number of models have been proposed to characterise the stages of ESLD including; Child-Turcotte score (10), Child-Pugh score (11), model for end stage liver disease (MELD) (12) and the United Kingdom (UK) model of end stage liver disease (UKLED) (13). One of the first proposed models was the Child-Turcotte score, which aimed to predict the outcome after portal hypertension surgery (10). This was later modified to form the Child-Pugh scoring system which categorises patients into 3 grades; grade A, B and C,

with grade C accounting for the most severe cases (11). Individuals are scored based upon the grade of encephalopathy, ascites, bilirubin, albumin and prothrombin time, providing a 'multiorgan' assessment of patients (11, 14). In comparison, MELD incorporates 3 factors into the diagnosis of ESLD; international normalised ratio (INR), serum creatine, total serum bilirubin and the etiology of cirrhosis (12). MELD was originally developed to assess morality risk post transjugular intrahepatic portosystemic shunt (15). Although MELD has been shown to accurately predict ESLD in patients with cirrhosis, it cannot accurately predict mortality in those with ascites (12, 16, 17). As a result, serum sodium was suggested to be a key predictor of morality in patients with ascites (16, 18, 19). This led to the development of MELD-Na, an updated version of the MELD scoring system which includes the level of serum sodium level within the mortality assessment (17).

In the UK, patients are allocated a position on the transplant list based upon their UKLED scores. This model scores patients based upon sodium, serum bilirubin, creatinine and INR in addition to patient specific factors (13). A score of >49 predicts that individuals have a 1-year mortality risk of 9%, the minimum criteria required to enter patients onto the UK waiting list in this category (13, 20). This model was developed through the analysis of 1103 patients and later validated in a cohort of 452 patients (20). This study identified that a UKLED score below 49 in those without hepatocellular carcinoma (HCC) represents a predicted 1-year mortality of 9%, suggesting that this is a suitable score (20).

1.1.1 Epidemiology of Chronic Liver Disease and the Health Care Burden

ESLD can arise due to a range of factors including both genetic and environmental factors such as excessive alcohol consumption, obesity, hepatitis B and hepatitis C infections (Table 1.1) (2, 21, 22). In the western world and industrialised countries, alcoholic liver disease (ArLD) and NAFLD are the two most common aetiologies of ESLD, whilst in low income countries viral hepatitis infections equate to the highest prevalence of ESLD aetiology (22).

Table 1.1. Aetiology of end stage liver disease (1, 23).

Cause	Type of Liver Disease
Lifestyle e.g., alcohol and diet	Alcoholic liver disease (ArLD) Non-alcoholic fatty liver disease (NAFLD)
Viral	Hepatitis B, C, D
Autoimmune	Autoimmune hepatitis Primary biliary cirrhosis Primary sclerosing cholangitis

ESLD is associated with a number of consequences, including portal hypertension, HCC and reductions in liver function (6). ESLD is associated with a reduced quality of life (QoL), which does not differ between the type of disease, but worsens with age and disease severity (24). Patients with CLD also suffer from a range of physical and psychosocial symptoms including fatigue, anxiety, reduced self-esteem, muscle spasms and reduced physical function, highlighting the burden of the disease (24, 25). While mild to moderate fibrosis is partially reversible with successful treatment of the underlying liver disease, regardless of the initial etiology, cirrhosis represents a state of irreversible liver damage requiring a liver transplant (26).

The socioeconomic burden of ESLD is rapidly increasing worldwide, with cirrhosis and liver cancer attributing to 3.5% of deaths (22). In 2014, ESLD was responsible for a total of 151,513 deaths across Europe, with two-thirds occurring in individuals under the age of 65-years old (21). In the UK, ESLD constitutes as the third leading cause of premature death, increasing at a more rapid rate than other European countries (27). Ultimately, ESLD presents a considerable burden on healthcare resources both within the UK (28, 29) and United States (30) equating to annual health care costs of ~£3.4billon and $2.5 billon respectively. This is largely attributed to excessive alcohol consumption and obesity (21, 29).

1.2 Malnutrition, Sarcopenia and Chronic Liver Disease

Malnutrition, defined by the World Health Organisation (WHO) as an imbalance, deficiency or excess in an individual's energy and nutrient intake is commonly identified in cirrhotic patients (31, 32). One of the most widely accepted components of malnutrition affecting ESLD patients is sarcopenia (33, 34). The term sarcopenia was first proposed in 1989 by Irwin Rosenberg to describe the loss of muscle mass identified throughout the course of ageing and was derived from the words "sarco" meaning flesh and "penia" meaning poverty (35). Although sarcopenia is widely recognised in elderly individuals, many other causes have been identified (36). This led to the development of two distinct categories: primary sarcopenia and secondary sarcopenia. Primary sarcopenia is considered to be age-related, whilst secondary sarcopenia is identified when factors apart from, or in addition to ageing are present (36). Secondary sarcopenia is often classified in one of three categories, activity-related, nutrition-related and disease-related (37). However, the etiology of sarcopenia is often multifactorial, consequently it may not be possible to distinguish between primary and secondary sarcopenia (37, 38). Therefore, the same diagnostic criteria are utilised for both primary and secondary sarcopenia (36-38). In contrast, the term cachexia is also used to describe a metabolic syndrome which is associated with a loss of muscle mass, with or without the loss of fat mass (39). While the term cachexia has been linked to malnutrition in liver cirrhosis, the vast majority of literature choose to focus on the incorporation of sarcopenia. This is likely due to the fact that weight loss has been identified as a key clinical feature associated with cachexia (40). Table 1.2 highlights the key differences in definitions of sarcopenia and cachexia. Importantly, sarcopenia is not associated with weight loss and may be reflective in a 'pre-cachectic' state without fat loss (39). Indeed, liver disease patients often experience a loss of muscle mass, often masked by an increase in adipose tissue i.e., sarcopenic obesity (41). Therefore, for the purpose of this thesis, the definition of secondary sarcopenia will be focused upon throughout.

Table 1.2 Key diagnostic criteria for sarcopenia and cachexia

Sarcopenia (EWGSOP Guidelines) (36)	(1) Low muscle strength (2) Low muscle mass or quality (3) Low physical performance
Cachexia (Evans et al) (39)	(1) Weight loss of ≥5% in 12 months (2) Prescence of 3/5 of the following criteria (A) Decreased muscle strength (B) Fatigue (C) Anorexia (D) Low fat-free mass index (E) Abnormal biochemistry (increased inflammation (e.g. CRP, IL-6), anaemia (Hb <12g/dl), low serum albumin (< 3.2 g/dl)

CRP, c-reactive protein, EWGSOP, European Working Group on Sarcopenia in Older People, Hb, haemoglobin, IL-6, interleukin-6.

1.2.1 The Definition of Sarcopenia

Over the last two decades the definition of sarcopenia has been updated to reflect advances in research. Initially, sarcopenia was identified through the use of appendicular skeletal muscle mass (kg/height^2) (42). Baumgartner et. al. (42) classified individuals as sarcopenic if the appendicular skeletal muscle mass was two or more standard deviations below that of a young control group. In 2002, this definition was expanded by Janssen et al (43) who utilised bioelectrical impedance analysis (BIA) to estimate skeletal muscle mass index (SMI). The researchers defined sarcopenia in two classes; class I was diagnosed when individuals were within one to two standard deviations below the mean of young individuals, whilst class II sarcopenia was identified as those that were two or more standard deviations below that of the young reference values (43).

In 2010, the European Working Group on Sarcopenia in Older People (EWGSOP) suggested that a loss of muscle mass was central to the development of sarcopenia, along with the presence of low muscle strength and/ or reduced physical performance (37). However, in 2019

the EWGSOP updated their previous description of sarcopenia to " *a progressive and generalised skeletal muscle disorder that is associated with increased likelihood of adverse outcomes including falls, fractures, physical disability and mortality*" (36). The diagnosis of sarcopenia was based on three outcome measures; muscle strength, quantity, quality and reduced physical performance (36). Probable sarcopenia (stage 1) can be defined by a reduction in muscle strength only. Sarcopenia (stage 2) can be described by low muscle strength accompanied with either low muscle quality or quantity. Severe sarcopenia can be diagnosed when individuals present with low muscle strength, quality and quantity alongside reductions in physical performance (36).

1.2.2 Diagnosis of Sarcopenia in Chronic Liver Disease

In CLD there are currently no standardized definitions or cut-off values specific to liver-related sarcopenia (44). This is likely a consequence of the significant heterogeneity in the methods utilised to assess and define sarcopenia (Table 1.3) (44). This variability generates a major challenge and a degree of uncertainty that limits the assessment of sarcopenia in routine clinical care (45). Further, many retrospective studies which have investigated the prevalence of sarcopenia only utilise one measure of sarcopenia, most commonly the measurement of muscle mass (46), potentially underestimating the prevalence and severity in this patient group.

Table 1.3. Overview of modes used to assess sarcopenia in chronic liver disease (45, 47).

	Mode of Assessment
Muscle Mass	MAMC, DEXA, BIA, ultrasound, CT, MRI
Muscle Strength	HGS, isokinetic dynamometry
Physical Performance	SPPB, gait speed, timed up and go, 6MWD, CPET, LFI

MAMC, midarm muscle circumference, DEXA, dual-energy x-ray absorptiometry, CT, computed tomography, MRI, magnetic resonance imaging, HGS, handgrip strength, SPPB, short physical performance battery, 6MWD, 6-minute walk distance, CPET, cardiopulmonary exercise test, LFI, liver frailty index.

The most common measure of muscle mass in patients with CLD is the SMI of the third lumbar vertebrae (L3), imaged through computed tomography (CT) (48). While SMI incorporates the measure of the psoas, paraspinal and abdominal muscles at L3, the measurement of psoas muscle index (PMI) also obtained through CT imaging may be utilised (49, 50). Whilst CT scans are expensive and irradiating, abdominal imaging is often completed in the routine assessment of transplant candidates and cancer screening (49, 51), thereby allowing identification of sarcopenia without the need for additional imaging. However, the application of SMI in a clinical setting remains limited due to a lack of standardised definitions and sex-specific cut off values. Nonetheless, recent work by Carey et al (52) sought to generate specific SMI cut off values for sarcopenia in CLD patients. The authors reported these cut offs as $<50cm^2/m^2$ and $<39cm^2/m^2$ in men and women with CLD respectively. Importantly, these cut-off values were shown to correlate with liver transplant (LT) wait list mortality (52) and are considered to be the most robust definition of sarcopenia within CLD patients to date (44). In contrast, when compared with SMI, the use of PMI was unable to identify LT-list patients with a higher mortality risk (49).

As mentioned earlier, the latest EWGSOP update shows appreciation of the importance of muscle strength and physical performance (36). As a result, the use of self-reported questionnaires which evaluate aspects of sarcopenia such as the simple five-item questionnaire (SARC-F) can be used to screen for the risk of sarcopenia development (53). The SARC-F incorporates questions which evaluate an individual's muscle strength, ability to walk, rise from chairs, climb stairs and the incidence of falls and has shown to be a valid assessment of sarcopenia risk (53). Additionally, high SARC-F scores have been more frequently identified with the progression CLD (54). After the risk of sarcopenia has been identified further assessment of muscle strength should be conducted. The use of handgrip strength (HGS) assessment has been identified as a key, reproducible measure of sarcopenia and is now

typically incorporated in clinical assessments (55). HGS forms part of the recommended diagnostic criteria for patients with liver failure in both the European Association for the Study of Liver (EASL) and the European Society for Clinical Nutrition and Metabolism (ESPEN) guidelines (55, 56). HGS is seen as a valuable tool as it is a quick, validated and cost effective measure of muscle strength, which can be conducted at the bedside in patients with CLD, and correlates with mortality (57). In addition to muscle strength, measures of physical performance and muscle function, including the 6-minute walk distance (6MWD) (58), the short physical performance battery test (SPPB) (59) and gait speed (60) are all practical as a measure of sarcopenia in CLD. In patients with cirrhosis awaiting liver transplantation a distance of less than 250m achieved within the 6MWD (58) and each 1-unit decrease in SPPB score (59) are associated with an increase in mortality risk, while a reduced gait speed is associated with an increased risk of complications, such as hepatic encephalopathy (HE), gastrointestinal bleeding and infections (60).

1.2.3 The Clinical Impact of Sarcopenia in Cirrhosis

Globally, the prevalence of sarcopenia in CLD patients awaiting liver transplantation is estimated to range from ~25-70%, with a higher prevalence identified amongst males (61). Sarcopenia has consistently been identified as a predictor of mortality risk both pre- (51, 62) and post-LT (50). It has been shown that the addition of sarcopenia to the MELD scoring system improves the predictive accuracy of mortality, particularly in patients with MELD scores below 15 (62). Sarcopenia is also associated with a number of poor clinical outcomes including a risk of decompensation (63), HE (64), increased risk of infection (i.e. sepsis) (46, 51, 61), duration of mechanical ventilation, duration of hospital admission and length of admission to intensive care post-LT (65, 66). It is therefore unsurprising that sarcopenic patients have increased hospital costs in comparison to those associated with non-sarcopenic patients (67).

Whilst sarcopenia has clear implications for overall health outcomes, it is also associated with reduction in QoL in liver cirrhosis patients (68). Recent research found that CLD patients with 'pre-sarcopenia', defined as a loss of muscle mass without subsequent decreases in muscle strength and performance (37) experience greater reductions in QoL in comparison to non-sarcopenic patients (68). One of the most frequently reported symptoms of CLD is sleep disturbance (69), which can have a large impact upon many aspects of QoL including fatigue (70). Sleep disturbances are often associated with the presence of HE, and are believed to arise in CLD due to a number of mechanisms which include alterations in the metabolism of melatonin and glucose (71) and disturbances to the intestinal microbiome (70). However, it is largely unclear whether the poor QoL identified within CLD patients arises as a consequence of muscle loss or functional disabilities (68). Furthermore, it is possible that factors such as clinical characteristics, disease severity and cirrhosis-specific complications also contribute to reductions in QoL (72).

Whilst LTs are thought to reverse complications such as ascites and portal hypertension, sarcopenia may remain, or even worsen post-LT (73, 74). Indeed, previous research identified the presence of post-LT sarcopenia in both individuals with and without pre-LT sarcopenia, whilst only 6.1% of patients experienced a reversal of sarcopenia post-LT (74). Alongside changes in muscle mass, patients often experience an increase in body weight post-LT (73). This is largely attributed to an increase in fat mass (75), and a slower, incomplete restoration of muscle mass (73). These changes are thought to closely resemble the onset of sarcopenic-obesity, identified frequently in NAFLD (76). Collectively, current data highlights the need for better nutritional and functional assessment and the implementation of interventions pre- and post-LT to reduce sarcopenia.

1.3 Alterations in Muscle Protein Turnover in Chronic Liver Disease

Skeletal muscle protein exists in a constant state of turnover, with simultaneous synthesis and breakdown (77). Alterations in muscle protein turnover occur on a daily basis due to a number of environmental stimuli, such as the ingestion of dietary protein (78) and physical activity (79). These alterations in muscle protein turnover contribute to changes in net protein balance (NPB), whereby muscle loss may occur when muscle protein breakdown (MPB) is greater than muscle protein synthesis (MPS) and muscle growth may occur when MPS is greater than MPB (77). Although protein ingestion alone can be sufficient to maintain muscle mass in young healthy individuals (77), the combination of exercise and protein ingestion can synergistically augment MPS (80) (Figure 1.2a).

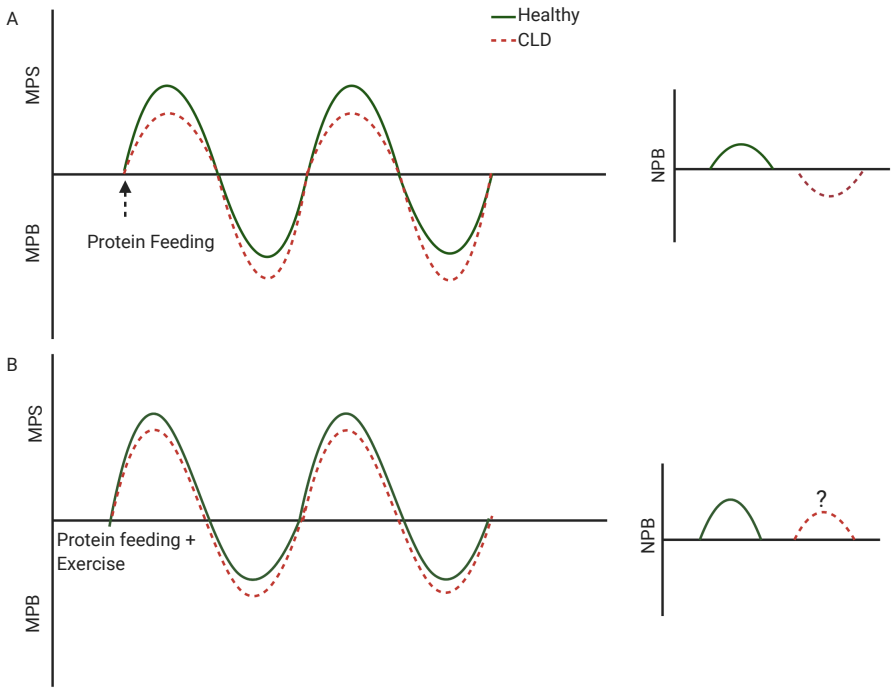

Figure 1.2. Schematic representation of muscle protein turnover in response to anabolic stimuli (protein feeding with/without exercise) in healthy and chronic liver disease. We

hypothesize that the primary reason for muscle loss in chronic liver disease (CLD) patients is a blunted muscle protein synthesis (MPS) in response to protein ingestion which coincides with an increase in muscle protein breakdown (MPB) (A). This likely equates to a reduction in net protein balance (NPB) within CLD patients, in response to the proposed alterations in muscle protein turnover. However, exercise in combination with protein ingestion may partially restore the MPS response in CLD patients (B).

Muscle protein turnover is regulated by a number of key molecular pathways, including the mammalian target of rapamycin complex one (mTORC1) signalling cascade, satellite cell (SC) signalling and the ubiquitin proteasome pathway (UPP) (Figure 1.3). mTORC1 is a critical serine/threonine protein kinase (81), which is activated by a number of factors including amino acids, growth factors e.g. insulin-like growth factor-1 (IGF-1), energy status and mechanical stress (82). This subsequently leads to the phosphorylation of two key effectors translation initiation factor eukaryotic translation factor 4E-binding protein 1 (4EBP1) and ribosomal protein S6 kinase (p70S6K) (81). Additionally, SC play a key role in the growth, repair and regeneration of muscle fibres and are regulated by a number of factors such as interleukin-6 (IL-6), IGF-1 and myostatin (83-85). Several factors contribute to MPB including inflammation, inactivity, mitochondrial dysfunction and myostatin. Myostatin is thought to inhibit MPS through the inhibition of the IGF-1/ phosphoinositide 3-kinase (PI3K)/ protein kinase B (Akt)/mTORC1 pathway and SCs (84, 86, 87). Additionally, myostatin has been suggested to activate the UPP, contributing to an increase in MPB, resulting in negative protein balance (87). However, the activation of Akt, and inhibition of the transcription factor, Forkhead box O (FOXO) can prevent the activation of the ubiquitin ligases, muscle RING finger-1 (MuRF-1) and muscle atrophy box (MAFbx) (88).

It is hypothesized that those suffering from CLD have a dysregulated muscle protein turnover that underpins the progression of sarcopenia (Figure 1.2b). Indeed, initial studies investigating muscle protein turnover in cirrhotic patients suggested that protein synthesis may be lower in comparison to healthy controls, when utilising arteriovenous (AV) balance and whole-body tracer methodologies (89-91). However, for whole-body protein breakdown (WbPB), previous work has yielded conflicting results with different studies reporting that MPB rates in cirrhotic patients were increased, decreased or even remained unaltered (91-94). These inconsistent findings are likely due to a range of factors, including differences in methodology and patient characteristics such as age, severity of CLD and disease aetiology (48).

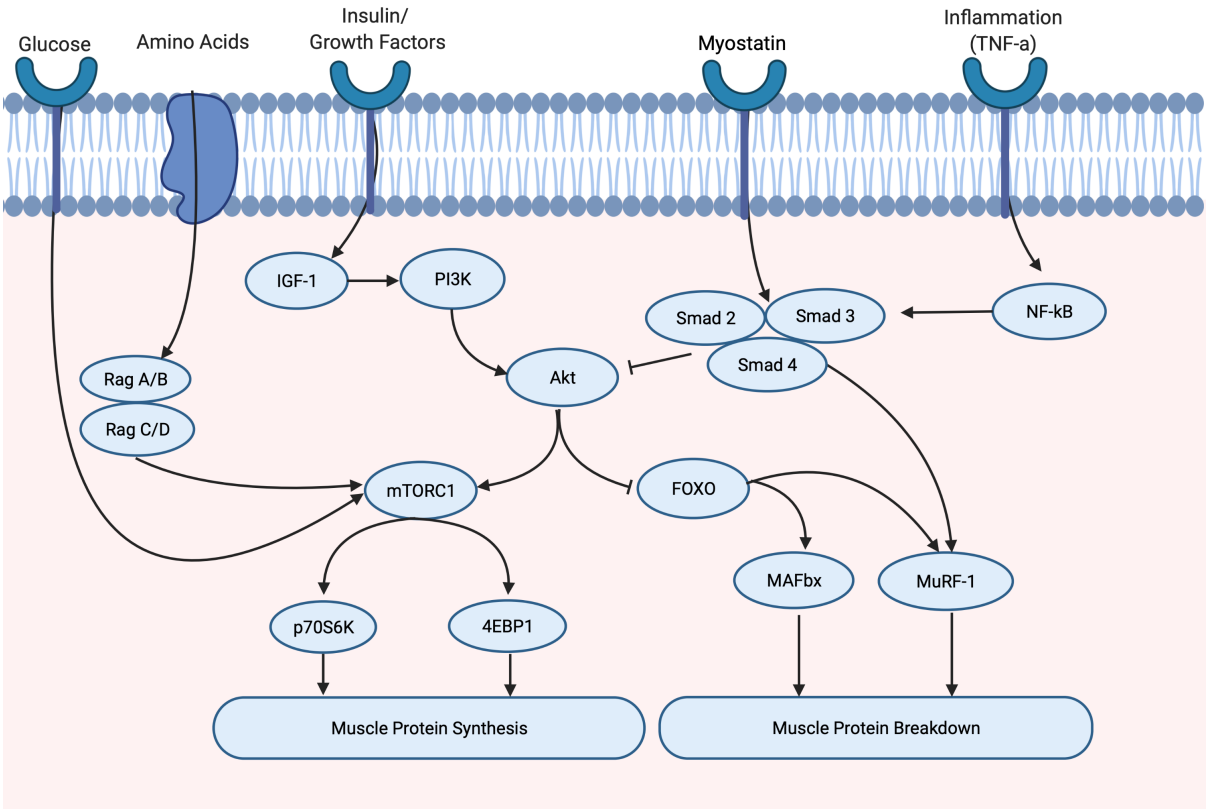

Figure 1.3. Molecular regulation of muscle protein turnover. Muscle protein turnover is regulated by muscle protein synthesis and breakdown. Muscle protein synthesis is regulated by a number of signals including, energy status, amino acids and growth factors e.g. insulin growth factor-1 (IGF-1). This leads to the activation of phosphoinositide 3-kinase (PI3K).

protein kinase B (Akt) regulates muscle protein turnover through the activation of mammalian target of rapamycin complex 1 (mTORC1) and inhibition of forkhead box O (FOXO). In turn the activation of mTORC1 leads to the phosphorylation of eukaryotic translation initiation factor 4E-binding protein 1 (4EBP-1) and ribosomal protein S6 kinase (p70S6K), which contribute to muscle protein synthesis. Muscle protein breakdown is influenced by a number of factors including inflammation and myostatin which lead to an increase in muscle atrophy box (MAFbx) and muscle ring finger 1 (MuRF-1).

However, it is known that in age-related sarcopenia a phenomenon known as muscle 'anabolic resistance' is present, referring to a blunted MPS response to the ingestion of amino acids (95), or exercise (96) in comparison to young individuals. It has been proposed that cirrhotic patients experience a similar state of muscle anabolic resistance (97), but to the best of our knowledge no study has investigated the MPS response to the ingestion of protein or exercise stimuli in CLD patients. The absence of such studies may be due to concerns relating to obtaining muscle biopsy samples from CLD patients, due to the perceived elevated risks related to platelet dysfunction, coagulopathy and thrombocytopenia (98). However, more recently muscle biopsies have been shown to be safe in patients with Childs Pugh A cirrhosis (98), which will therefore enable a greater understanding of the dysregulation in muscle protein turnover that underpins muscle wasting in CLD patients.

1.3.1 Hyperammonemia, Myostatin and Muscle Protein Turnover

Hyperammonemia is a consistent abnormality in cirrhotic patients caused by hepatocellular dysfunction, portosystemic shunting and impaired ureagenesis, which in turn results in the increased concentration of ammonia within skeletal muscle (99, 100). The increased uptake of ammonia by skeletal muscle has been proposed as a protective mechanism in CLD, with the aim of preventing ammonia neurotoxicity (100, 101). The specific mechanism driving the

increased uptake of ammonia is currently unknown, although it has been suggested that the expression of the ammonia transporters, Rh B glycoprotein (Rhbg) and Rh C glycoprotein (Rhcg) may both play a role (102). However, the resultant accumulation of ammonia is not without consequence and may contribute to the development of sarcopenia (101, 103, 104) (Figure 1.4) thus reducing the muscle mass available to remove excess ammonia.

Mechanistically, *in vitro* experiments have shown that hyperammonemia induced activation of nuclear factor-κB (NF-κB) is associated with an increase in myostatin expression, an inhibitor of myogenesis, and a reduction in myotube diameter (101). In cirrhotic patients, skeletal muscle hyperammonemia was also associated with an increase in myostatin expression and activation of NF-κB, resulting in impaired MPS, increased autophagy and a reduction in skeletal muscle mass (101, 103, 105, 106). As a consequence, hyperammonemia is considered a key regulator in the liver-muscle axis (101).

The elevated myostatin expression in cirrhotic patients is thought to be one of the key drivers of muscle anabolic resistance (105) as it is associated with a reduction in p70S6K, s6 protein (RPS6) and 4EBP-1 protein content, indicating an impaired activation of the mTORC1 pathway which is critical in the regulation of MPS (98). This is consistent with *in vivo* data suggesting that myostatin inhibits MPS via impaired Akt signalling, and subsequently reduces MPS via the Akt/mTORC1/p70S6K pathway (86). Myostatin may also influence MPS through the impairment of SC function. In a portacaval anastomosis rat (PCA) model, myostatin expression was threefold higher than control rats and was associated with a decline in SC function mediated via a reduction in myogenic transcription factors myoblast determination protein 1 (MyoD), myogenic factor 5 (myf5) and myogenin (104, 107). In addition, hyperammonemia induced upregulation of myostatin may contribute to a reduction in skeletal muscle mass through an increase in MPB. Cirrhotic patients have been shown to exhibit increased WbPB, alongside an increase in the expression of myostatin, beclin1, sequestome 1

(p62) degradation and LC3 lipidation, representing an increase in autophagy compared to healthy adults (98). However, this increase in WbPB and autophagy occurred with no change in ubiquitinated proteins or MuRF1 messenger ribonucleic acid (mRNA) at baseline, or after branched chain amino acid (BCAA)/ leucine ingestion in healthy control and cirrhotic participants (98, 103, 107). Collectively, this suggests that hyperammonemia induced increases in MPB may largely occur through changes in autophagy, rather than the UPP.

Hyperammonemia may also contribute to a decrease in MPS through mitochondrial dysfunction. Anaplerosis is the first reaction in the tricarboxylic acid (TCA) cycle, whereby glutamine and glutamate are converted to α-ketoglutarate (α-KG) and ammonia (108). This reaction is catalysed by the enzyme glutamate dehydrogenase (GDH) (108), and under physiological conditions this reaction is favoured as GDH has a low affinity for ammonia, resulting in the conversion of glutamate to α-KG (109). However, due to the high concentrations of ammonia present in the skeletal muscle of cirrhotic patients; it is likely that cataplerosis, i.e. the removal of TCA intermediates, (108) may be favoured and in turn cause a reduction in α-KG availability and impaired mitochondrial function (48, 101). The consequence of reduced TCA cycle intermediates is a reduction in adenosine triphosphate (ATP) synthesis (110), which may contribute to a reduction in MPS as translation initiation is an energy intensive process (48). However, hyperammonaemia has also been found to increase reactive oxygen species (ROS) and oxidative damage in both rats and humans (110). This suggests that ROS may overwhelm the adaptive antioxidant defence systems and in turn lead to muscle loss and tissue injury (110). Thus, hyperammonaemia may influence mitochondrial functioning through impairments in TCA cycle metabolism, oxidative damage and, consequently, a decrease in cellular energy status and subsequently MPS. However, this remains to be clearly demonstrated.

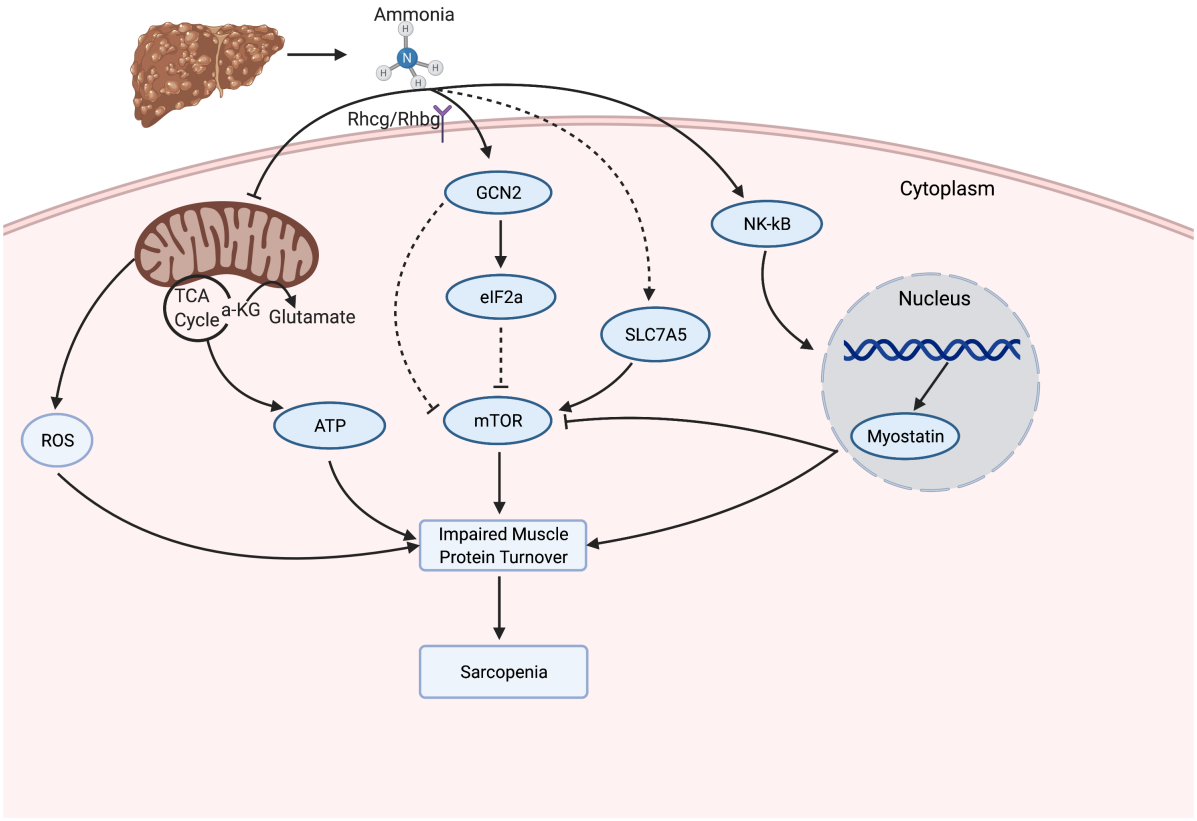

Figure 1.4. The proposed molecular alterations which contribute to ammonia induced changes in muscle protein turnover. Ammonia enters the skeletal muscle through the Rhcg/Rhbg receptors. Subsequently, ammonia contributes to mitochondrial dysfunction, an impaired integrated stress response and an increase in myostatin transcription. These contribute to an impairment in protein turnover and sarcopenia.

4EBP-1, eukaryotic translation initiation factor 4E- binding protein 1; eIF2α, eukaryotic initiation factor 2α; IGF-1, insulin growth factor 1; MAFbx, muscle atrophy-box; mTORC1, mammalian target of rapamycin complex 1; MuRF1, Muscle RING finger-1; NF-κB, nuclear factor-κB; PI3K, phosphoinositide 3-kinase; p70S6K, ribosomal protein S6 kinase; Rhbg, Rh B glycoprotein; Rhcg, Rh C glycoprotein; ROS, reactive oxygen species; TNF-α, tumor necrosis factor-α; TCA cycle, tricarboxylic acid cycle; α-KG, alpha ketoglutarate

1.3.2 Energy Expenditure and Amino acid Availability in Chronic Liver Disease

Cirrhosis is associated with an accelerated state of starvation (111). An overnight fast has been shown to accelerate fat oxidation, gluconeogenesis, ketogenesis and a catabolic state in cirrhotic patients compared to healthy individuals (111, 112). As a consequence of the increased gluconeogenesis, amino acids are often utilised as an energy source (111, 113), resulting in a low concentration of skeletal muscle BCAA in cirrhotic patients (114). In response to a state of cellular stress, such as amino acid deprivation, an integrated stress response (ISR) is activated in order to promote the restoration of cellular homeostasis (115). In a state of amino acid deficiency the ISR is mediated through the activation of general control non-depressed 2 (GCN2), an amino acid deficiency sensor (116). This leads to the phosphorylation of eukaryotic initiation factor 2 (eIF2α), which subsequently causes a reduction in global protein synthesis and an increase in activating transcription factor 4 (ATF4) mRNA, thus reducing the requirement for amino acids (116, 117). The activation of ATF4 leads to the inhibition of mTORC1 signalling and promotes autophagy in an attempt to restore and preserve levels of amino acids (115). Once this balance has been restored, ATF4 signalling contributes to the de-phosphorylation of eIF2α, restoring normal levels of protein synthesis (118).

Cirrhotic patients display increased GCN2 activation and eIF2α phosphorylation alongside a reduction in mTORC1 signalling, similar to the ISR seen in response to intracellular amino acid deficiency (98, 106). However, hyperammonemia induces a state of cellular stress which impairs the ISR by preventing an increase in ATF4 mRNA (106). This failure to induce an increase in ATF4 mRNA may contribute to a further decline in MPS and an increase in autophagy, due to the inability to terminate the ISR and return to normal levels of protein synthesis (106, 115). Therefore, cirrhotic patients have been suggested to experience an adaptive ISR, in which a second pathway is activated in response to increased ammonia

concentrations (106) (Figure 1.4). This second signalling pathway appears to be mediated by large neutral amino acid transporter 1 (SLC7A5/LAT1), an amino acid transporter, which is increased in cirrhotic patients (98, 106). SLC7A5/LAT1 appears to act as an amino acid exchanger, resulting in an increase in L-leucine uptake (98, 106). This increase in L-leucine concentration is thought to occur in order to utilise this amino acid to generate acetyl-CoA within the mitochondria, in order to generate an increase in energy output (119). Under normal conditions the transport of leucine relies on glutamine transport via the glutamine exchanger sodium-coupled neutral amino acid transporter 2 (SLC38A2/SNAT2) (120), but under a state of hyperammonemia glutamine is primarily utilised for the detoxification of ammonia (106, 119). Taken collectively, the activation of the ISR in cirrhotic patients results in an impairment in mTORC1 signalling and an increase in autophagy (98, 106); which may contribute to the development of sarcopenia.

1.3.3 Alcohol and Chronic Liver Disease

Alcohol intake and CLD are both believed to contribute to sarcopenia in ArLD (121). As a consequence, it is often challenging to distinguish between the specific effects of CLD and that of alcohol. While ethanol is primarily metabolised in the liver and the brain, it can also be metabolised in skeletal muscle (122, 123). ArLD is frequently associated with a reduction in skeletal muscle mass, alongside alterations in muscle protein turnover (123) and ethanol can inhibit mTORC1 stimulation (124). Further, excessive alcohol intake has been linked to increased myostatin, which is assumed to mediate impairments in MPS (123, 125). Nonetheless, markers of the UPP remain unaltered in animal models of ArLD, and are decreased in human ArLD patients, suggesting that autophagy is likely responsible for an increase in MPB (123). Similar to hyperammonemia, ethanol may also contribute to reductions in MPS through impairment of mitochondrial function, resulting in the generation of ROS and

activation of autophagy (126). In turn, the above may impair MPS through a reduction in ATP generation and mRNA translation (121).

1.3.4 Abnormalities in Endocrine Function

CLD is associated with a number of endocrine abnormalities that could contribute to sarcopenia, including low serum testosterone (127). In male cirrhotic patients, low levels of testosterone may arise as a consequence of changes in the hypothalamic-pituitary-gonadal axis (128). This can lead to a decrease in testosterone production and an increase in aromatase activity, an enzyme responsible for the conversion of testosterone to estradiol, similar to that seen in ageing males (129) and PCA rats (130). PCA rats exhibit lower levels of testosterone alongside a reduced growth rate, attributed to a reduction in food intake and efficiency, calculated as the increase in body weight per gram of food eaten (130). Inhibition of aromatase in this model led to an increase in testosterone and improved body weight, alongside improvements in food intake and efficiency (130). However, further research is required in human cirrhotic patients in order to confirm this relationship.

CLD is also associated with an increase in the secretion of growth hormone (GH) and a reduction in serum IGF-1 concentration (131), a change also seen in human ageing. IGF-1 can promote muscle growth through the activation of the Akt/PI3K/mTORC1 signalling cascade, which leads to an increase in MPS (132, 133). Furthermore, IGF-1 also contributes to a reduction in muscle atrophy through the activation of Akt and inhibition of the transcription factor FOXO; in turn, preventing the activation of the ubiquitin ligases MuRF-1 and MAFbx (88). GH has been associated with an increase in myostatin expression and impairments in IGF-1 signalling and therefore may further contribute to impairments in MPS (131, 134). Again, the relative contribution of changes in the GH/IGF-1 axis to sarcopenia in CLD remain poorly understood (48).

1.3.5 Non-Alcoholic Fatty Liver Disease and Obesity

NAFLD is currently predicted to be the most common cause of CLD, with an estimated global prevalence of ~25% (135). NAFLD is an umbrella term used to describe the spectrum of disease from non-alcoholic fatty liver (NAFL), identified through the presence of ≥5% steatosis, to non-alcoholic steatohepatitis (NASH) and cirrhosis (136, 137). In contrast, progression to NASH is characterised by the presence of hepatic steatosis alongside inflammation and hepatocellular injury with, or without the presence of fibrosis, this in turn may lead to the development of cirrhosis and HCC (136, 137). NAFLD is a growing cause of CLD, largely attributed to the increase in the incidence of obesity (21). However, obesity in this cohort may occur alongside the development of sarcopenia (sarcopenic obesity) (41). There are a number of risk factors associated with the development of both NAFLD and sarcopenia, with physical inactivity, insulin resistance and chronic inflammation believed to play key roles (138). It is therefore unsurprising that NAFLD and sarcopenia are typically associated with increased sedentary behaviour, alongside a reduction in physical activity (139, 140). Unfortunately, this physical inactivity likely contributes to an increased risk of metabolic syndrome due to an increase in visceral fat accumulation and insulin resistance (141).

A state of insulin resistance may directly lead to the development of sarcopenia through an increase in MPB and a decrease in MPS. Insulin resistance in adipose tissue stimulates lipolysis and the release of free-fatty acids (FFAs) to the liver (142, 143). In turn, FFA inhibit IGF-1 signalling which subsequently impair PI3K/Akt signalling (144) and reduce MPS (145) (Figure 1.5). Impairments in Akt signalling increase FOXO phosphorylation which activates the UPP, leading to an increase in MAFbx and MuRF1 expression (144, 145). Combined, these alterations in protein turnover are thought to contribute to the muscle loss identified in type II diabetes (145). Therefore, increased insulin resistance may cause similar effects in CLD patients with a NAFLD etiology. Insulin resistance also leads to the development of

hyperinsulinemia within hepatocytes which can contribute to a decrease in gluconeogenesis, an increase in lipogenesis and inhibition of ß-oxidation (142, 143). This leads to the accumulation of lipids within liver and muscle, termed myosteatosis (142, 145). Obesity and a reduction in muscle quality, calculated as the ratio of muscle strength to muscle mass are often associated with the development of insulin resistance and a reduction in muscle mass and strength (146, 147). Furthermore, sarcopenia likely contributes to the development of insulin resistance, independent of obesity as skeletal muscle is the primary tissue facilitating the uptake of glucose mediated by insulin (148). This suggests that the pathology of NAFLD and sarcopenia are closely intertwined (143).

Chronic inflammation and oxidative damage are also important factors associated with the development of CLD (149) and sarcopenia (150). NAFLD is associated with an accumulation of FFAs and increased adiposity, which contribute to an increase in pro-inflammatory cytokines (151-153). Adipose tissue contains immune cells such as macrophages and also senescent cells which are highly pro-inflammatory (154). In addition, adipose tissue produces its own cytokines, termed adipokines, which can also contribute to an increased inflammatory status (155). One key cytokine, tumor necrosis factor-α (TNF-α) appears to have a significant role in the impairment of muscle protein turnover in CLD (156, 157). In rats, TNF-α impairs MPS through a reduction in the phosphorylation of key signalling proteins involved in the mTORC1 pathway, such as eukaryotic translation initiation factor 4E (eIF-4E) (156). In addition, *in vitro* work has shown that TNF-α may also increase MPB through an increase in UPP activity, as shown by an increase in MAFbx expression (157, 158). Further *in vitro* work has shown that TNF-α induced MPB is thought to arise through an increase in type 1 TNF-α receptor (TNFR1) binding and consequently an increase in ROS which leads to the subsequent activation of NF-κB (157, 159). An increase in NF-κB signalling enhances protein degradation through the activation of the UPP, reduction of myogenesis and a further increase in

inflammation (157, 160). This increase in proinflammatory cytokines may further contribute to the development of NAFLD and muscle loss (150, 161). Together, this suggests that an increase in circulating proinflammatory cytokines, in particular TNF-α may contribute to a reduction in MPS and increase in MPB.

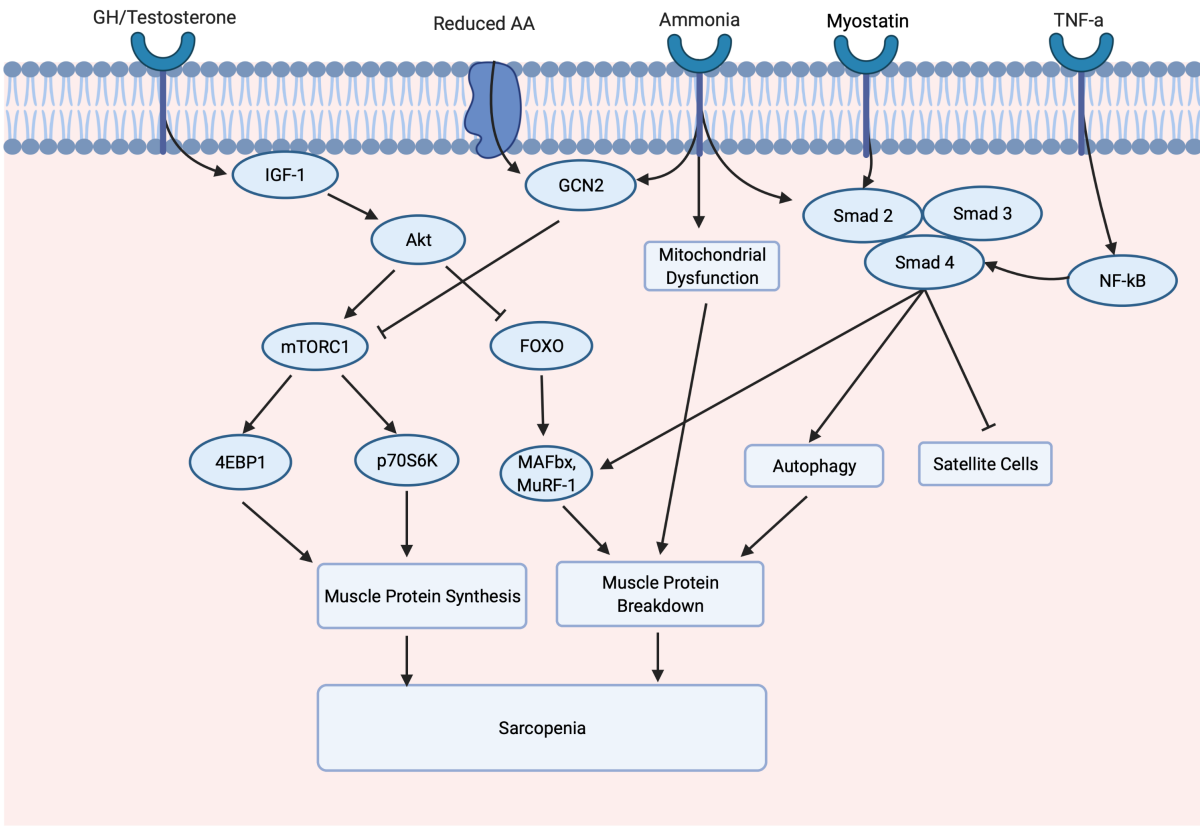

Figure 1.5. The molecular regulation of muscle protein synthesis and muscle protein breakdown in chronic liver disease. The mammalian target of rapamycin complex 1 (mTORC1) can be activated in response to the activation of insulin growth factor-1 (IGF-1) which leads to the activation of protein kinase B (Akt) and inhibited through general control non-depressed 2 (GCN2), activated by a reduction in amino acids (AA) and ammonia. mTORC1 activation leads to the activation of eukaryotic translation initiation factor 4E-binding protein 1 (4EBP1) and ribosomal protein S6 kinase (p70S6K). Akt regulates forkhead box O (FOXO), and the subsequent activation of muscle atrophy-box (MAFbx) and muscle ring finger-1 (MuRF-1). Inflammatory cytokines e.g. tumor necrosis factor-α (TNF-

α) and ammonia activate nuclear factor-κB (NF-κB), which leads to the activation of myostatin. Myostatin results in an increase in autophagy and inhibition of satellite cells.

1.3.6 Potential Drivers of Chronic Liver Disease Which May Influence Sarcopenia Progression

In addition to the factors outlined above, adiponectin, vitamin D deficiency and alterations in intestinal function may contribute to the progression of sarcopenia in CLD. Adiponectin is an adipokine which plays an integral role in the regulation of glucose metabolism and oxidation of fatty acids in an insulin dependent manner (162). In skeletal muscle, adiponectin binds to adiponectin receptor I (AdipoR1), which is responsible for the regulation of insulin sensitivity and fatty acid oxidation (163, 164). Therefore, a reduction in circulating levels of adiponectin as seen in obesity (165) may contribute to impairments in muscle protein turnover as a consequence of insulin resistance (166). In obese individuals, myostatin expression is positively associated with a state of insulin resistance (167). Therefore, this increase in myostatin is believed to contribute to muscle wasting through impairments in mTORC1 signalling and increased autophagy, as discussed previously (86, 101, 103). As a consequence, it is plausible to suggest that crosstalk between myostatin and adiponectin exists, and warrants further investigation in CLD and NAFLD (143, 166).

Vitamin D deficiency has been shown to contribute to insulin resistance, metabolic syndrome and NAFLD (168, 169). Evidence from animal models of NAFLD suggest that rats fed a vitamin D deficient western diet experienced an increase in NAFLD activity, inflammation and oxidative stress in comparison to those fed a vitamin D replete western diet (170). Thus, it would seem that vitamin D deficiency may exacerbate NAFLD severity partly through an inflammatory-mediated mechanism (169). Vitamin D has also been suggested to contribute to an increased risk of age-related sarcopenia (171). In older individuals low levels of vitamin D

are independently associated with a greater risk of sarcopenia (171), and is thought to contribute to muscle loss through a number of mechanisms including a reduction in MPS, an increase in muscle atrophy and mitochondrial dysfunction (172). However, it is currently unclear whether low 25-hydroxyvitamin D (25(OH)D) levels are a cause or a consequence of age-related sarcopenia (173). As CLD patients experience vitamin D deficiency, similar to that identified within older sarcopenic individuals, it is possible that low levels of vitamin D contribute to the pathology of sarcopenia within these patients. However, CLD patients often experience a number of fat soluble vitamin deficiencies, including vitamin A, D, E and K, which are affected by malabsorption, impaired synthesis and storage (174).

Cirrhosis is also associated with alterations in the gut microbiome such as an increase in bacterial translocation which may lead to an increase in the level of circulating endotoxins, pro-inflammatory cytokines and ROS (175, 176). The changes identified in the gut microbiome diversity, include an increase in pathogenic and a decrease in autochthonous taxa, which contribute to the development of endotoxemia and worsen with the severity of CLD (177). In addition to the activation of immune cells which raise cytokine levels, elevated endotoxin can activate circulating inflammatory cells and Kupffer cells in the liver, leading to an increase in the production of TNF-α via binding to soluble TNF-α-receptors (178). Indeed, previous work has found that elevated levels of endotoxins within the portal and hepatic veins correlate with the level of soluble TNF-α receptors (178). This increase in inflammation may potentially contribute to increasing portal pressure and associate with the severity of liver dysfunction (178, 179).

1.4 Cell Culture: Current Perspectives, Limitations and Future Directions

Due to the limited number of human trials conducted in cirrhotic patients, the mechanisms which underpin the development of sarcopenia in cirrhotic patients is largely unknown. Therefore, it is unsurprising that a number of *in vitro* and *in vivo* models of cirrhosis have been developed to investigate the potential mechanisms of cirrhotic-like myotube, and muscle atrophy. These include the use of *in vitro* ammonia (103) and ethanol (180) treatment, and *in vivo* trials using PCA rats (181). Although these models allow for insights into one potential mechanistic driver of sarcopenia in CLD, the treatments utilised here are likely to be supraphysiological, and therefore translation to *in vivo* human work may be limited, yielding conflicting results. Additionally, a number of systemic factors may contribute to the atrophy identified in cirrhotic patients (48). Consequently, the extent to which isolated factors may contribute to the development of sarcopenia within cirrhosis is unknown. Similarly, key hallmarks associated with the progression of disease severity and sarcopenia in ESLD e.g. inflammation are yet to be investigated in detail, highlighting a clear knowledge gap.

1.4.1 In Vitro Models of Atrophy

Currently, *in vitro* models which probe the mechanisms of sarcopenia have been conducted using pharmacological treatments such as dexamethasone (DEX) (88, 182-184), TNF-α (185, 186) and hydrogen peroxide (H_2O_2) (187). DEX, a synthetic glucocorticoid has previously been utilised as a model of atrophy, confirmed through its ability to decrease myotube diameter by ~40% (184). This model has allowed for the investigation of the potential mechanisms of atrophy, highlighting a blockage of MPS through the Akt/mTORC1 pathway, and an upregulation of MPB through an increase in MuRF-1, MAFbx and myostatin (88, 183, 184). However, it is unclear if DEX treatment induces age-related changes such as an increase in

inflammation, and senescence, therefore it is unlikely to replicate a true model of age-related atrophy (188).

Inflammation is considered a key hallmark of ageing (189) and correlates with a decline in muscle mass (190). In particular, *in vitro* treatment with TNF-α has been shown to suppress myotube formation and induce apoptosis (185). Similarly, Sharples et al (186) found that TNF-α treatment in C2C12 skeletal muscle cells reduced proliferation, which occurred alongside a reduction in the expression of key regulatory proteins such as MyoD, myogenin and IGF-1. Furthermore, Wang et al (191) found that TNF-α induced a decrease in myotube diameter within C2C12s, alongside an increase in markers of MPB; MAFbx and MuRF-1 and a reduction in anabolic markers including Akt, mTORC1 and p70S6K. Taken together, this suggests that TNF-α treatment provides a useful model to investigate inflammatory related sarcopenia. However, the dosage of TNF-α utilised is supraphysiological, therefore the ability to translate this model to *in vivo* trials is unclear.

Additionally, H_2O_2 treatment has been utilised to induce a model of atrophy as ROS are associated with the presence of sarcopenia (188, 192). Previous research which has utilised H_2O_2 to investigate oxidative stress-induced damage has been shown to induce autophagy (193) and mitochondrial dysfunction (194). While this model provides a suitable avenue for the investigation of oxidative stress, it lacks many fundamental characteristics commonly associated with the progression of sarcopenia.

Alternative models of age-related atrophy have investigated the use of replicative ageing, in which C2C12 skeletal muscle cells are subject to multiple passages, providing a potential model of musculoskeletal ageing. In cells subjected to multiple passages, Sharples et al (195), demonstrated a decline in IGF-1, myogenic regulatory factors and a reduced capacity for myoblast differentiation, associated with a decrease in Akt signalling. While this model provides a useful model to study age-related sarcopenia, cellular senescence, a key hallmark of

ageing (189) is not induced (195). Therefore, replicative ageing cannot be considered a true model of musculoskeletal ageing.

1.4.2 Making Cell Culture More Physiologically Relevant

Traditional methods of culturing C2C12 cell lines involve supplementation with animal-derived serums. More specifically, fetal bovine serum (FBS) is used to allow for proliferation, while horse serum (HS) is used to induce differentiation (196). In order to improve the physiological relevance of the *in vitro* models outlined above, more recent work has modified culturing techniques by using *ex vivo* human serum (197-200) or plasma (201, 202) to condition cell culture media and thus change the systemic environment of the cells in culture. These studies have investigated a range of factors, including myotube growth (202), regulatory signalling pathways (197, 201) and MPS (199, 200), in response to a diverse range of stimuli including, ageing, injury / illness e.g. sepsis, burns and nutrient status. Recent work by Kalampouka et al (202) showed an increase in myotube diameter in C2C12s treated with 5% human plasma from young, in comparison to old participants. These findings are in line with *in vivo* research, highlighting an increase in the prevalence of sarcopenia with advancing age (203). In addition, plasma from septic shock patients has been found to induce a reduction in myosin content and an increase in markers of proteolysis, highlighting the induction of myotube atrophy (201). Similarly, Corrick et al (197) identified a decrease in markers of anabolic signalling within human primary myoblasts in response to treatment with serum from burns patients. These studies, highlight the potential applications in which *ex vivo* human plasma can be used to study myotube atrophy across a range of disease states and illness. Therefore, this model may provide a more physiologically relevant model which can be used to study the potential drivers of sarcopenia in CLD.

In addition, more recent models have aimed to utilise *ex vivo* human serum to investigate changes in MPS in response to different nutrient compositions (199, 204). In 2018, Carson et

al (199) identified an increase in MPS in response to an acute, 4-hour treatment with *ex vivo* human serum obtained 60-minutes after the ingestion of whey protein ingestion, in comparison to myotubes treated with fasted serum. Furthermore, the authors aimed to investigate the ability of serum obtained postprandial after the ingestion of whey protein hydrolysate, or non-essential amino acids to stimulate MPS in C2C12 skeletal muscle cells (204). Results highlighted a significant increase in MPS in myotubes conditioned with whey protein hydrolysate fed serum, in contrast to non-essential amino acid fed serum, highlighting the importance of amino acid composition. This work supports findings from *in vivo* human trials which show that non-essential amino acids are not required to stimulate MPS (205). Therefore, it is plausible to suggest that conditioning C2C12s with *ex vivo* human serum can be utilised to investigate the effectiveness of nutraceutical compounds, prior to the completion of *in vivo* human trials.

Alternative models have utilised human primary skeletal muscle cells with varied findings. Indeed, previous work investigating myotube growth within samples obtained from young and old participants failed to identify a difference between the two conditions (206). It is therefore plausible to suggest that without the systemic environment induced by human serum or plasma, primary cell cultures may have a limited capability of withholding the specific phenotype. However, when human myoblasts obtained from young individuals were treated with human serum from young or old donors, no difference in myogenic fusion index was identified (207). In contrast to these findings, previous work investigating the myogenic fusion index in muscle samples obtained from old sarcopenic and middle-aged individuals identified a significantly slower fusion index in older myotubes (208). Similarly, Bechshøft et al (209) showed that myotubes obtained from older individuals maintained their phenotype, exhibited with a lower myogenic fusion index. Therefore, this highlights the potential use of human primary skeletal muscle cells to improve the physiological relevance of *in vitro* work.

Additionally, more recent work has investigated the potential to utilise human serum to condition human primary SCs, obtained from the vastus lateralis over the course of 5 days of differentiation in comparison to normal growth conditions (i.e. FBS) (198). The authors found that culturing with human serum from healthy individuals throughout the course of differentiation preserved the cell-dependent variability, in contrast to FBS controls, while serum from chronic obstructive pulmonary disease (COPD) induced myotube atrophy (198). However, similar to *in vivo* human work, reproducibility may be reduced due to the biological variability in human samples (198). In order to overcome this variability, pooling blood samples from a number of individuals may provide a suitable solution (198). Future research should therefore aim to investigate the utility of human primary cell cultures with *ex vivo* human serum to create a more physiologically relevant model of cell culture. Thus, undoubtedly creating the 'gold-standard' approach to improving the physiological relevance of cell culture.

1.5 Overview and Thesis Aims

As described in this introductory chapter, sarcopenia is a common complication affecting CLD patients and is associated with a number of adverse outcomes. CLD is characterised by a state of hyperammonemia, increased catabolism, systemic inflammation, physical inactivity and poor nutritional status, all of which may contribute to the development of sarcopenia through alterations in muscle protein turnover. However, the molecular mechanisms which contribute to the development of sarcopenia remain largely unclear. Therefore, based upon the identified gaps within the literature surrounding the mechanisms of sarcopenia in CLD patients, the studies presented in this thesis aimed to improve our understanding on the molecular mechanisms which may underpin the development of sarcopenia in decompensated ESLD patients and non-cirrhotic NAFLD patients, through the use of *in vitro* experiments and an observational study. **Chapter 2** describes the methods developed, particularly in reference to

the leucine dosage and serum parameters utilised throughout the *in vitro* work within this thesis. This chapter also describes methodological considerations for the incorporation of *ex vivo* human blood samples *in vitro*. **Chapter 3** describes a methods development study in which *ex vivo* human serum from young and old participants was used to condition C2C12 skeletal muscle cells to investigate changes in myotube diameter, MPS and anabolic signalling. We hypothesized that myotubes treated with *ex vivo* serum from young participants would exhibit elevated levels of MPS and anabolic signalling, alongside increases in myotube diameter in comparison to those treated with serum from older participants. This model offers the potential to study the regulators of sarcopenia in inflammatory disease conditions such as chronic liver disease. **Chapter 4** describes an *in vitro* study in which we utilised *ex vivo* human serum from ESLD patients and age-matched control participants to investigate changes in MPS, anabolic signalling and myotube diameter, as previously described in the methods development study outlined in Chapter 3. We hypothesized that myotubes treated with *ex vivo* serum from ESLD patients will lead to reductions in myotube diameter in comparison to those treated with serum from age-matched control individuals. **Chapter 5** describes the analysis of muscle biopsy samples obtained from ESLD, NAFLD and control patients during an observational study, which aimed to characterise the markers of intracellular signalling pathways that may underpin the development of sarcopenia in CLD. We investigated the protein and ribonucleic acid (RNA) content of key anabolic, catabolic and mitochondrial signalling proteins. We hypothesized that ESLD patients would exhibit an increase in catabolic markers, and mitochondrial function in comparison to healthy age-matched control individuals. **Chapter 6** discusses the main findings of the studies described in the contents of this thesis and provides an overview of the conclusions identified in these studies. This chapter aims to incorporate these results with evidence from the literature which has emerged since the start of this doctoral study.

1.6 References

1. **Heidelbaugh JJ, and Bruderly M**. Cirrhosis and Chronic Liver Failure: Part I. Diagnosis and Evaluation. *Am Fam Physician* 74: 756-762, 2006.
2. **Hernandez-Gea V, and Friedman SL**. Pathogenesis of liver fibrosis. *Annu Rev Pathol* 6: 425-456, 2011.
3. **Garcia-Tsao G, Friedman S, Iredale J, and Pinzani M**. Now there are many (stages) where before there was one: In search of a pathophysiological classification of cirrhosis. *Hepatology* 51: 1445-1449, 2010.
4. **Pinzani M, Rombouts K, and Colagrande S**. Fibrosis in chronic liver diseases: diagnosis and management. *J Hepatol* 42 Suppl: S22-36, 2005.
5. **Friedman SL**. Liver fibrosis – from bench to bedside. *J Hepatol* 38: 38-53, 2003.
6. **Schuppan D, and Afdhal NH**. Liver Cirrhosis. *Lancet* 371: 838-851, 2008.
7. **Samonakis DN, Koulentaki M, Coucoutsi C, Augoustaki A, Baritaki C, Digenakis E, Papiamonis N, Fragaki M, Matrella E, Tzardi M, and Kouroumalis EA**. Clinical outcomes of compensated and decompensated cirrhosis: A long term study. *World J Hepatol* 6: 504-512, 2014.
8. **Kleiner DE, Brunt EM, Van Natta M, Behling C, Contos MJ, Cummings OW, Ferrell LD, Liu YC, Torbenson MS, Unalp-Arida A, Yeh M, McCullough AJ, Sanyal AJ, and Nonalcoholic Steatohepatitis Clinical Research N**. Design and validation of a histological scoring system for nonalcoholic fatty liver disease. *Hepatology* 41: 1313-1321, 2005.
9. **Goodman ZD**. Grading and staging systems for inflammation and fibrosis in chronic liver diseases. *J Hepatol* 47: 598-607, 2007.
10. **Child CG, and Turcotte JG**. Surgery and portal hypertension. *Major Probl Clin Surg* 1: 1-85, 1964.
11. **Pugh RN, Murray-Lyon IM, Dawson JL, Pietroni MC, and Williams R**. Transection of the oesophagus for bleeding oesophageal varies. *Br J Surg* 60: 646-649, 1973.
12. **Kamath PS, Wiesner RH, Malinchoc M, Kremers W, Therneau TM, Kosberg CL, D'Amico G, Dickson ER, and Kim WR**. A model to predict survival in patients with end-stage liver disease. *Hepatology* 33: 464-470, 2001.
13. **Neuberger J, Gimson A, Davies M, Akyol M, O'Grady J, Burroughs A, and Hudson M**. Selection of patients for liver transplantation and allocation of donated livers in the UK. *Gut* 57: 252-257, 2008.
14. **Durand F, and Valla D**. Assessment of the prognosis of cirrhosis: Child-Pugh versus MELD. *J Hepatol* 42: S100-107, 2005.
15. **Malinchoc M, Kamath PS, Gordon FD, Peine CJ, Rank J, and ter Borg PC**. A model to predict poor survival in patients undergoing trans jugular intrahepatic portosystemic shunts. *Hepatology* 31: 864-871, 2000.
16. **Heuman DM, Abou-Assi SG, Habib A, Williams LM, Stravitz RT, Sanyal AJ, Fisher RA, and Mihas AA**. Persistent ascites and low serum sodium identify patients with cirrhosis and low MELD scores who are at high risk for early death. *Hepatology* 40: 802-810, 2004.
17. **Kim WR, Biggins SW, Kremers WK, Wiesner RH, Kamath PS, Benson JT, Edwards E, and Therneau TM**. Hyponatremia and mortality among patients on the liver-transplant waiting list. *N Engl J Med* 359: 1018-1026, 2008.
18. **Biggins SW, Kim WR, Terrault NA, Saab S, Balan V, Schiano T, Benson J, Therneau T, Kremers W, Wiesner R, Kamath P, and Klintmalm G**. Evidence-based incorporation of serum sodium concentration into MELD. *Gastroenterology* 130: 1652-1660, 2006.

19. **Ruf AE, Kremers WK, Chavez LL, Descalzi VI, Podesta LG, and Villamil FG**. Addition of serum sodium into the MEDL score predicts waiting list mortality better than MELD alone. *Liver Transpl* 11: 336-343, 2005.
20. **Barber K, Madden S, Allen J, Collett D, Neuberger J, and Gimson A**. Elective liver transplant list mortality: development of a United Kingdom end-stage liver disease score. *Transplantation* 92: 469-476, 2011.
21. **Pimpin L, Cortez-Pinto H, Negro F, Corbould E, Lazarus JV, Webber L, and Sheron N**. Burden of liver disease in Europe: Epidemiology and analysis of risk factors to identify prevention policies. *J Hepatol* 69: 718-735, 2018.
22. **Asrani SK, Devarbhavi H, Eaton J, and Kamath PS**. Burden of liver diseases in the world. *J Hepatol* 70: 151-171, 2019.
23. **Wiegand J, and Berg T**. The Etiology, Diagnosis and Prevention of Liver Cirrhosis. Part 1 of a series on liver cirrhosis. *Etsch Arztebl Int* 110: 85-91, 2013.
24. **Younossi ZM, Boparai N, Price LL, Kiwi ML, McCormick M, and Guyatt G**. Health-related quality of life in chronic liver disease: the impact of type and severity of disease. *Am J Gastroenterol* 96: 2199-2205, 2001.
25. **Younossi ZM, Guyatt G, Boparai N, and King D**. Development of a disease specific questionnaire to measure health related quality of life in patients with chronic liver disease. *Gut* 45: 295-300, 1999.
26. **Bataller R, and Brenner DA**. Liver fibrosis. *J Clin Invest* 115: 209-218, 2005.
27. **Williams R, Aspinall R, Bellis M, Camps-Walsh G, Cramp M, Dhawan A, Ferguson J, Forton D, Foster G, Gilmore SI, Hickman M, Hudson M, Kelly D, Langford A, Lombard M, Longworth L, Martin N, Moriarty K, Newsome P, O'Grady J, Pryke R, Rutter H, Ryder S, Sheron N, and Smith T**. Addressing liver disease in the UK: a blueprint for attaining excellence in health care and reducing premature mortality from lifestyle issues of excess consumption of alcohol, obesity, and viral hepatitis. *The Lancet* 384: 1953-1997, 2014.
28. **Scarborough P, Bhatnagar P, Kremlin KW, Allender S, Foster C, and Rayer M**. The economic burden of ill health due to diet, physical inactivity, smoking, alcohol and obesity in the UK: an update to 2006-07 NHS costs. *J Public Health (Oxf)* 33: 527-535, 2011.
29. **Williams R, Alexander G, Armstrong I, Baker A, Bhala N, Camps W, G., Cramp ME, de Lusignan S, Day N, Dhawan A, Dillon J, Drummond C, Dyson J, Foster G, Gilmore I, Hudson M, Kelly D, Langford A, McDougall N, Meier P, Moriarty K, Newsome P, O'Grady J, Pryke R, Rolfe L, Rice P, Rutter H, Sheron N, Taylor A, Thompson J, Thorburn D, Verne J, Wass J, and Yeoman A**. Disease burden and costs from excess alcohol consumption, obesity and viral hepatitis: forth report of the Lancet Standing Commission on Liver Disease in the UK. *Lancet* 391: 1097-1107, 2018.
30. **Neff GW, Duncan CW, and Schiff ER**. The current economic burden of cirrhosis. *Gastroenterol Hepatol (N Y)* 7: 661-671, 2011.
31. **WHO**. Malnutrition https://www.who.int/news-room/fact-sheets/detail/malnutrition. [17/02/2020].
32. **Anand AC**. Nutrition and Muscle in Cirrhosis. *J Clin Exp Hepatol* 7: 340-357, 2017.
33. **Roongpisuthipong C, Sobhonslidsuk A, Nantiruj K, and Songchitsomboon S**. Nutritional assessment in various stages of liver cirrhosis. *Nutrition* 17: 761-765, 2001.
34. **Dasarathy S**. Consilience in sarcopenia of cirrhosis. *J Cachexia Sarcopenia Muscle* 3: 225-237, 2012.
35. **Rosenberg IH**. Summary comments: epidemiological and methodological problems in determining nutritional status of older persons. *Am J Clin Nutr* 50: 1231-1233, 1989.

36. **Cruz-Jentoft AJ, Bahat G, Bauer J, Boirie Y, Bruyere O, Cederholm T, Cooper C, Landi F, Rolland Y, Sayer AA, and Schneider SM**. Sarcopenia: revised European consensus on definition and diagnosis. *Age Ageing* 48: 16-31, 2019.
37. **Cruz-Jentoft AJ, Baeyens JP, Bauer JM, and al. e**. Sarcopenia: European consensus on definition and diagnosis: Report of the European Working Group on Sarcopenia in Older People. *Age Ageing* 39: 412-423, 2010.
38. **Muscaritoli M, Anker SD, Argiles J, Aversa Z, Bauer JM, Biolo G, Boirie Y, Bosaeus I, Cederholm T, Costelli P, Fearon KC, Laviano A, Maggio M, Rossi Fanelli F, Schneider SM, Schols A, and Sieber CC**. Consensus definition of sarcopenia, cachexia and pre-cachexia: joint document elaborated by Special Interest Groups (SIG) "cachexia-anorexia in chronic wasting diseases" and "nutrition in geriatrics". *Clin Nutr* 29: 154-159, 2010.
39. **Evans WJ, Morley JE, Argiles J, Bales C, Baracos V, Guttridge D, Jatoi A, Kalantar-Zadeh K, Lochs H, Mantovani G, Marks D, Mitch WE, Muscaritoli M, Najand A, Ponikowski P, Rossi Fanelli F, Schambelan M, Schols A, Schuster M, Thomas D, Wolfe R, and Anker SD**. Cachexia: a new definition. *Clin Nutr* 27: 793-799, 2008.
40. **Rolland Y, Abellan van Kan G, Gillette-Guyonnet S, and Vellas B**. Cachexia versus sarcopenia. *Curr Opin Clin Nutr Metab Care* 14: 15-21, 2011.
41. **Montano-Loza AJ, Angulo P, Meza-Junco J, Prado CM, Sawyer MB, Beaumont C, Esfandiari N, Ma M, and Baracos VE**. Sarcopenic obesity and myosteatosis are associated with higher mortality in patients with cirrhosis. *J Cachexia Sarcopenia Muscle* 7: 126-135, 2016.
42. **Baumgartner RN, Koehler KM, Gallagher D, Heymsfield SB, Ross RR, Garry PJ, and Lindeman RD**. Epidemiology of sarcopenia among the elderly in New Mexico. *Am J Epidemiol* 147: 755-763, 1998.
43. **Janssen I, Heymsfield SB, and Ross R**. Low relative skeletal muscle mass (sarcopenia) in older persons is associated with functional impairment and physical disability. *J Am Geriatr Soc* 50: 889-896, 2002.
44. **Carey EJ, Lai JC, Sonnenday C, Tapper EB, Tandon P, Duarte-Rojo A, Dunn MA, Tsien C, Kallwitz ER, Ng V, Dasarathy S, Kappus M, Bashir MR, and Montano-Loza AJ**. A North American Expert Opinion Statement on Sarcopenia in Liver Transplantation. *Hepatology* 70: 1816-1829, 2019.
45. **Sinclair M**. Controversies in diagnosing sarcopenia in cirrhosis-moving from research into clinical practice. *Nutrients* 11: 2454, 2019.
46. **van Vugt JL, Levolger S, de Bruin RW, van Rosmalen J, Metselaar HJ, and Ijzermans JN**. Systematic review and meta-analysis of the impact of computed tomography-assessed skeletal muscle mass on outcome in patients awaiting or undergoing liver transplantation. *Am J Transplant* 16: 2277-2292, 2016.
47. **Dhaliwal A, Williams FR, El-sherif O, and Armstrong MJ**. Sarcopenia in Liver Transplantation: an Update. *Curr Hepatol Rep,* 2020.
48. **Dasarathy S, and Merli M**. Sarcopenia from mechanism to diagnosis and treatment in liver disease. *J Hepatol* 65: 1232-1244, 2016.
49. **Ebadi M, Wang CW, Lai JC, Dasarathy S, Kappus MR, Dunn MA, Carey EJ, and Montano-Loza AJ**. Poor performance of psoas muscle index for identification of patients with higher waitlist mortality risk in cirrhosis. *J Cachexia Sarcopenia Muscle* 9: 1053-1062, 2018.
50. **Englesbe MJ, Patel SP, He K, Lynch RJ, Schaubel DE, Harbaugh C, Holcombe SA, Wang SC, Segev DL, and Sonnenday CJ**. Sarcopenia and mortality after liver transplantation. *J Am Coll Surg* 211: 271-278, 2010.

51. **Montano-Loza AJ, Meza-Junco J, Prado CM, Lieffers JR, Baracos VE, Bain VG, and Sawyer MB**. Muscle wasting is associated with mortality in patients with cirrhosis. *Clin Gastroenterol Hepatol* 10: 166-173, 2012.
52. **Carey EJ, Lai JC, Wang CW, Dasarathy S, Lobach I, Montano-Loza AJ, and Dunn MA**. A multicenter study to define sarcopenia in patients with end-stage liver disease. *Liver Transpl* 23: 625-633, 2017.
53. **Malmstrom TK, Miller DK, Simonsick EM, Ferrucci L, and Morley JE**. SARC-F: a symptom score to predict persons with sarcopenia at risk for poor functional outcomes. *J Cachexia Sarcopenia Muscle* 7: 28-36, 2016.
54. **Hiraoka A, Nagamatsu K, Izumoto H, Yoshino T, Adachi T, Tsuruta M, Aibiki T, Okudaira T, Yamago H, Suga Y, Iwasaki R, Mori K, Miyata H, Tsubouchi E, Ninomiya T, Hirooka M, Abe M, Matsuura B, Hiasa Y, and Michitaka K**. SARC-F combined with a simple tool for assessment of muscle abnormalities in outpatients with chronic liver disease. *Hepatol Res* 50: 502-511, 2020.
55. **European Association for the Study of the Liver. Electronic address eee, and European Association for the Study of the L**. EASL Clinical Practice Guidelines on nutrition in chronic liver disease. *J Hepatol* 70: 172-193, 2019.
56. **Plauth M, Bernal W, Dasarathy S, Merli M, Plank LD, Schutz T, and Bischoff SC**. ESPEN guideline on clinical nutrition in liver disease. *Clin Nutr* 38: 485-521, 2019.
57. **Sinclair M, Chapman B, Hoermann R, Angus PW, Testro A, Scodellaro T, and Gow PJ**. Handgrip strength adds more prognostic value to the model for end-stage liver disease score than imaging-based measures of muscle mass in men with cirrhosis. *Liver Transpl* 25: 1480-1487, 2019.
58. **Carey EJ, Steidley DE, Agel BA, Mekeel KL, Rakela J, Vargas HE, and Douglas DD**. Six-minute walk distance predicts mortality in liver transplant candidates. *Liver Transpl* 16: 1373-1378, 2010.
59. **Lai JC, Feng S, Terrault NA, Lizaola B, Hayssen H, and Covinsky K**. Frailty predicts waitlist mortality in liver transplant candidates. *Am J Transplant* 14: 1870-1879, 2014.
60. **Dunn MA, Josbeno DA, Tevar AD, Rachakonda V, Ganesh SR, Schmotzer AR, Kallenborn EA, Behari J, Landsittel DP, DiMartini AF, and Delitto A**. Frailty as Tested by Gait Speed is an Independent Risk Factor for Cirrhosis Complications that Require Hospitalization. *Am J Gastroenterol* 111: 1768-1775, 2016.
61. **Kim G, Kang SH, Kim MY, and Back SK**. Prognostic value of sarcopenia in patients with liver cirrhosis: A systematic review and meta-analysis. *PLoS One* 12: e0186990, 2017.
62. **Montano-Loza AJ, Duarte-Rojo A, Meza-Junco J, Baracos VE, Sawyer MB, Pang JX, Beaumont C, Esfandiari N, and Myers RP**. Inclusion of Sarcopenia Within MELD (MELD-Sarcopenia) and the Prediction of Mortality in Patients With Cirrhosis. *Clin Transl Gastroenterol* 6: e102, 2015.
63. **Bhanji RA, Carey EJ, Yang L, and Watt KD**. The Long Winding Road to Transplant: How Sarcopenia and Debility Impact Morbidity and Mortality on the Waitlist. *Clin Gastroenterol Hepatol* 15: 1492-1497, 2017.
64. **Bhanji RA, Moctezuma-Velazquez C, Duarte-Rojo A, Ebadi M, Ghosh S, Rose C, and Montano-Loza AJ**. Myosteatosis and sarcopenia are associated with hepatic encephalopathy in patients with cirrhosis. *Hepatol Int* 12: 377-386, 2018.
65. **DiMartini A, Cruz Jr RJ, Dew MA, Myaskovsky L, Goodpaster B, Fox K, Kim KH, and Fontes P**. Muscle mass predicts outcomes following liver transplant. *Liver Transpl* 19: 1172-1180, 2015.

66. **Merli M, Giusto M, Gentili F, Novelli G, Ferretti G, Riggio O, Corradini SG, Siciliano M, Farcomeni A, Attili AF, Berloco P, and Rossi M**. Nutritional status: its influence on the outcome of patients undergoing liver transplantation. *Liver Int* 30: 208-214, 2010.
67. **van Vugt JLA, Buettner S, Alferink LJM, Bossche N, de Bruin RWF, Darwish Murad S, Polak WG, Metselaar HJ, and JNM IJ**. Low skeletal muscle mass is associated with increased hospital costs in patients with cirrhosis listed for liver transplantation-a retrospective study. *Transpl Int* 31: 165-174, 2018.
68. **Ohashi K, Ishikawa T, Imai M, Suzuki M, Hoshii A, Abe H, Koyama F, Nakano T, Ueki A, Noguchi H, Hasegawa E, Hirosawa S, Kobayashi M, Hirosawa H, Sato K, Munakata M, and Yoshida T**. Relationship between pre-sarcopenia and quality of life in patients with chronic liver disease: a cross-sectional study. *Eur J Gastroenterol Hepatol* 31: 1408-1413, 2019.
69. **Peng JK, Hepgul N, Higginson IJ, and Gao W**. Symptom prevalence and quality of life patients with end-stage liver disease: A systematic review and meta-analysis. *Palliat Med* 33: 24-36, 2019.
70. **Ghabril M, Jackson M, Gotur R, Weber R, Orman E, Vuppalanchi R, and Chalasani N**. Most Individuals With Advanced Cirrhosis Have Sleep Disturbances, Which Are Associated With Poor Quality of Life. *Clin Gastroenterol Hepatol* 15: 1271-1278 e1276, 2017.
71. **Montagnese S, De Pitta C, De Rui M, Corrias M, Turco M, Merkel C, Amodio P, Costa R, Skene DJ, and Gatta A**. Sleep-wake abnormalities in patients with cirrhosis. *Hepatology* 59: 705-712, 2014.
72. **Younossi Z, and Henry L**. Overall health-related quality of life in patients with end-stage liver disease. *Clin Liver Dis (Hoboken)* 6: 9-14, 2015.
73. **Dasarathy S**. Posttransplant sarcopenia: an underrecognized early consequence of liver transplantation. *Dig Dis Sci* 58: 3103-3111, 2013.
74. **Tsien C, Garber A, Narayanan A, Shah SN, Barnes D, Eghtesad B, Fung J, McCullough AJ, and Dasarathy S**. Post-liver transplantation sarcopenia in cirrhosis: a prospective evaluation. *J Gastroenterol Hepatol* 29: 1250-1257, 2014.
75. **Everhart JE, Lombardero M, Lake JR, Wisner RH, Zetterman RK, and Hoofnagle JH**. Weight Change and Obesity After Liver Transplantation: Incidence and Risk Factors. *Liver Transpl Surg* 4: 285-296, 1998.
76. **El Sherif O, Dhaliwal A, Newsome PN, and Armstrong MJ**. Sarcopenia in nonalcoholic fatty liver disease: new challenges for clinical practice. *Expert Rev Gastroeterol Hepatol* 23: 1-9, 2020.
77. **Breen L, and Phillips SM**. Skeletal muscle protein metabolism in the elderly: Interventions to counteract the 'anabolic resistance' of ageing. *Nutr Metab* 8: 2011.
78. **Bohe J, Low A, Wolfe RR, and Rennie MJ**. Human muscle protein synthesis is modulated by extracellular, not intramuscular amino acid availability: a dose-response study. *J Physiol* 552: 315-324, 2003.
79. **Phillips SM, Tipton KD, Aarsland A, Wolf SE, and Wolfe RR**. Mixed muscle protein synthesis and breakdown after resistance exercise in humans. *Am J Physiol* 273: E99-107, 1997.
80. **Biolo G, Tipton KD, Klein S, and Wolfe RR**. An abundant supply of amino acids enhances the metabolic effect of exercise on muscle protein. *Am J Physiol* 273: E122-E129, 1997.
81. **Kim DH, Sarbassov DD, Ali SM, King JE, Latek RR, Erdjument-Bromage H, Tempst P, and Sabatini DM**. mTOR interacts with raptor to form a nutrient-sensitive complex that signals to the cell growth machinery. *Cell* 110: 163-175, 2002.

82. **Jewell JL, Russell RC, and Guan KL**. Amino acid signalling upstream of mTOR. *Nat Rev Mol Cell Biol* 14: 133-139, 2014.
83. **McKay BR, De Lisio M, Johnston AP, O'Reilly CE, Phillips SM, Tarnopolsky MA, and Parise G**. Association of interleukin-6 signalling with the muscle stem cell response following muscle-lengthening contractions in humans. *PLoS One* 4: e6027, 2009.
84. **McKay BR, Ogborn DI, Bellamy LM, Tarnopolsky MA, and Parise G**. Myostatin is associated with age-related human muscle stem cell dysfunction. *FASEB J* 26: 2509-2521, 2012.
85. **McKay BR, O'Reilly CE, Phillips SM, Tarnopolsky MA, and Parise G**. Co-expression of IGF-1 family members with myogenic regulatory factors following acute damaging muscle-lengthening contractions in humans. *J Physiol* 586: 5549-5560, 2008.
86. **Trendelenburg AU, Meyer A, Rohner D, Boyle J, Hatakeyama S, and Glass DJ**. Myostatin reduces Akt/TORC1/p70S6K signaling, inhibiting myoblast differentiation and myotube size. *Am J Physiol Cell Physiol* 296: C1258-C1270, 2009.
87. **Lokireddy S, Mouly V, Butler-Browne G, Gluckman PD, Sharma M, Kambadur R, and McFarlane C**. Myostatin promotes the wasting of human myoblast cultures through promoting ubiquitin-proteasome pathway-mediated loss of sarcomeric proteins. *Am J Physiol Cell Physiol* 301: C1316-C1324, 2011.
88. **Stitt TN, Drujan D, Clarke BA, Panaro F, Timofeyva Y, Kline WO, Gonzalez M, Yancopoulos GD, and Glass DJ**. The IGF-1/PI3K/Akt pathway prevents expression of muscle atrophy-induces ubiquitin ligases by inhibiting FOXO transcription factors. *Mol Cell* 14: 395-403, 2004.
89. **Morrison WL, Bouchier IA, Gibson JN, and Rennie MJ**. Skeletal muscle and whole-body protein turnover in cirrhosis. *Clin Sci (Lond)* 78: 613-619, 1990.
90. **Tessari P, Barazzoni R, Kiwanuka E, Davanzo G, De Pergola G, Orlando R, Vettore M, and Zanetti M**. Impairment of albumin and whole body postprandial protein synthesis in compensated liver cirrhosis. *Am J Physiol Endocrinol Metab* 282: E394-E311, 2002.
91. **Tessari P, Kiwanuka E, Vettore M, Barazzoni R, Zanetti M, Cecchet D, and Orlando R**. Phenylalanine and tyrosine kinetics in compensated liver cirrhosis: effects of meal ingestion. *Am J Physiol Gastrointest Liver Physiol* 295: G598-G604, 2008.
92. **Tessari P, Vettore M, Millioni R, Puricelli L, and Orlando R**. Effect of liver cirrhosis on phenylalanine and tyrosine metabolism. *Curr Opin Clin Nutr Metab Care* 13: 81-86, 2010.
93. **McCullough AJ, Mullen KD, Tavill AS, and Kalhan SC**. In vivo differences between the turnover rates of leucine and leucine's ketoacid in stable cirrhosis. *Gastroenterology* 103: 571-578, 1992.
94. **Tessari P, Inchiostro S, Barazzoni R, Zanetti M, Orlando R, Biolo G, Sergi G, Pino A, and Tiengo A**. Fasting and postprandial phenylalanine and leucine kinetics in liver cirrhosis. *Am J Physiol* 267: E140-E149, 1994.
95. **Cuthbertson D, Smith K, Babraj J, Leese G, Waddell T, Atherton P, Wackerhage H, Taylor PM, and Rennie MJ**. Anabolic signaling deficits underlie amino acid resistance of wasting, aging muscle. *FASEB J* 19: 422-424, 2005.
96. **Brook MS, Wilkinson DJ, Mitchell WK, Lund JN, Phillips BE, Szewczyk NJ, Greenhaff PL, Smith K, and Atherton PJ**. Synchronous deficits in cumulative muscle protein synthesis and ribosomal biogenesis underlie age-related anabolic resistance to exercise in humans. *J Physiol* 594: 7399-7417, 2016.
97. **Tsien C, McCullough AJ, and Dasarathy S**. Late evening snack: exploiting a period of anabolic opportunity in cirrhosis. *J Gastroenterol Hepatol* 27: 430-441, 2012.

98. **Tsien C, Davuluri G, Singh D, Allawy A, Ten Have GA, Thapaliya S, Schulze JM, Barnes D, McCullough AJ, Engelen MP, Deutz NE, and Dasarathy S**. Metabolic and molecular responses to leucine-enriched branched chain amino acid supplementation in the skeletal muscle of alcoholic cirrhosis. *Hepatology* 61: 2018-2029, 2015.
99. **Shangraw RE, and Jahoor F**. Effect of Liver Disease and Transplantation on Urea Synthesis in Humans: Relationship to Acid-Base Status. *Am J Physiol* 276: G1145-G1152, 1999.
100. **Olde Damink SW, Jalan R, and Dejong CH**. Interorgan ammonia trafficking in liver disease. *Metab Brain Dis* 24: 169-181, 2009.
101. **Qiu J, Thapaliya S, Runkana A, Yang Y, Tsien C, Mohan ML, Narayanan A, Eghtesad B, Mozdziak PE, McDonald C, Stark GR, Welle S, Naga Prasad SV, and Dasarathy S**. Hyperammonemia in cirrhosis induces transcriptional regulation of myostatin by an NF-kappaB-mediated mechanism. *Proc Natl Acad Sci U S A* 110: 18162-18167, 2013.
102. **Takeda K, and Takemasa T**. Expression of ammonia transporters Rhbg and Rhcg in mouse skeletal muscle and the effect of 6-week training on these proteins. *Physiol Rep* 3: e12596, 2015.
103. **Qiu J, Tsien C, Thapalaya S, Narayanan A, Weihl CC, Ching JK, Eghtesad B, Singh K, Fu X, Dubyak G, McDonald C, Almasan A, Hazen SL, Naga Prasad SV, and Dasarathy S**. Hyperammonemia-mediated autophagy in skeletal muscle contributes to sarcopenia of cirrhosis. *Am J Physiol Endocrinol Metab* 303: E983-E993, 2012.
104. **Dasarathy S, Muc S, Hisamuddin K, Edmison JM, Dodig M, McCullough AJ, and Kalhan SC**. Altered expression of genes regulating skeletal muscle mass in the portacaval anastomosis rat. *Am J Physiol Gastrointest Liver Physiol* 292: G1105-1113, 2007.
105. **Nishikawa H, Enomoto H, Ishii A, Iwata Y, Miyamoto Y, Ishii N, Yuri Y, Hasegawa K, Nakano C, Nishimura T, Yoh K, Aizawa N, Sakai Y, Ikeda N, Takashima T, Takata R, Iijima H, and Nishiguchi S**. Elevated serum myostatin level is associated with worse survival in patients with liver cirrhosis. *J Cachexia Sarcopenia Muscle* 8: 915-925, 2017.
106. **Davuluri G, Krokowski D, Guan BJ, Kumar A, Thapaliya S, Singh D, Hatzoglou M, and Dasarathy S**. Metabolic adaptation of skeletal muscle to hyperammonemia drives the beneficial effects of l-leucine in cirrhosis. *J Hepatol* 65: 929-937, 2016.
107. **Dasarathy S, Dodig M, Muc SM, Kalhan SC, and McCullough AJ**. Skeletal muscle atrophy is associated with an increased expression of myostatin and impaired satellite cell function in the portacaval anastamosis rat. *Am J Physiol Gastrointest Liver Physiol* 287: G1124-1130, 2004.
108. **Owen OE, Kalhan SC, and Hanson RW**. The key role of anaplerosis and cataplerosis for citric acid cycle function. *J Biol Chem* 277: 30409-30412, 2002.
109. **Zaganas I, Pajecka K, Wendel Nielsen C, Schousboe A, Waagepetersen HS, and Plaitakis A**. The effect of pH and ADP on ammonia affinity for human glutamate dehydrogenases. *Metab Brain Dis* 28: 127-131, 2013.
110. **Davuluri G, Allawy A, Thapaliya S, Rennison JH, Singh D, Kumar A, Sandlers Y, Van Wagoner DR, Flask CA, Hoppel C, Kasumov T, and Dasarathy S**. Hyperammonaemia-induced skeletal muscle mitochondrial dysfunction results in cataplerosis and oxidative stress. *J Physiol* 594: 7341-7360, 2016.
111. **Owen OE, Trapp VE, Reichard GAJ, Mozzoli MA, Moctezuma J, Paul P, Skutches CL, and Boden G**. Nature and quantity of fuels consumed in patients with alcoholic cirrhosis. *J Clin Invest* 72: 1821-1832, 1983.
112. **Nakaya Y, Harada N, Kakui S, Okada K, Takahashi A, Inoi J, and Ito S**. Severe catabolic state after prolonged fasting in cirrhotic patients: effect of oral branched-chain amino-acid-enriched nutrient mixture. *J Gastroenterol* 37: 531-536, 2002.

113. **Brosnan JT**. Comments on metabolic needs for glucose and the role of gluconeogenesis. *Eur J Clin Nutr* 53: S107-S111, 1999.
114. **Tajiri K, and Shimizu Y**. Branched-chain amino acids in liver diseases. *World J Gastroenterol* 19: 7620-7629, 2013.
115. **Pakos-Zebrucka K, Koryga I, Mnich K, Ljujic M, Samali A, and Gorman AM**. The integrated stress response. *EMBO Rep* 17: 1374-1395, 2016.
116. **Harding HP, Novoa I, Zhang Y, Zeng H, Wek R, Schapira M, and Ron D**. Regulated translation initiation controls stress-induced gene expression in mammalian cells. *Mol Cell* 6: 1099-1108, 2000.
117. **Lu PD, Harding HP, and Ron D**. Translation reinitiation at alternative open reading frames regulates gene expression in an integrated stress response. *J Cell Biol* 167: 27-33, 2004.
118. **Novoa I, Zeng H, Harding HP, and Ron D**. Feedback Inhibition of the Unfolded Protein Response by GADD34-Mediated Dephosphorylation of eIF2 a. *J Cell Biol* 153: 1011-1022, 2001.
119. **Holecek M, Kandar R, Sispera L, and Kovarik M**. Acute hyperammonemia activates branched-chain amino acid catabolism and decreases their extracellular concentrations: different sensitivity of red and white muscle. *Amino Acids* 40: 575-584, 2011.
120. **Nicklin P, Bergman P, Zhang B, Triantafellow E, Wang H, Nyfeler B, Yang H, Hild M, Kung C, Wilson C, Myer VE, MacKeigan JP, Porter JA, Wang YK, Cantley LC, Finan PM, and Murphy LO**. Bidirectional transport of amino acids regulates mTOR and autophagy. *Cell* 136: 521-534, 2009.
121. **Dasarathy J, McCullough AJ, and Dasarathy S**. Sarcopenia in Alcoholic Liver Disease: Clinical and Molecular Advances. *Alcohol Clin Exp Res* 41: 1419-1431, 2017.
122. **Estonius M, Svensson S, and Höög JO**. Alcohol Dehydrogenase in Human Tissues: Localisation of Transcripts Coding for Five Classes of the Enzyme. *FEBS Lett* 397: 338-342, 1996.
123. **Thapaliya S, Runkana A, McMullen MR, Nagy LE, McDonald C, Naga Prasad SV, and Dasarathy S**. Alcohol-induced autophagy contributes to loss in skeletal muscle mass. *Autophagy* 10: 677-690, 2014.
124. **Steiner JL, and Lang CH**. Alcohol impairs skeletal muscle protein synthesis and mTOR signalling in a time-dependent manner following electrically stimulate muscle contraction. *J Appl Physiol (1985)* 117: 1170-1179, 2014.
125. **Lang CH, Frost RA, Svanberg E, and Vary TC**. IGF-I/IGFBP-3 ameliorates alterations in protein synthesis, eIF4E availability, and myostatin in alcohol-fed rats. *Am J Physiol Endocrinol Metab* 286: E916-E926, 2004.
126. **Bonet-Ponce L, Saez-Atienzar S, da Casa C, Flores-Bellver M, Barcia JM, Sancho-Pelluz J, Romero FJ, Jordan J, and Galindo MF**. On the mechanism underlying ethanol-induced mitochondrial dynamic disruption and autophagy response. *Biochim Biophys Acta* 1852: 1400-1409, 2015.
127. **Sinclair M, Grossmann M, Gow PJ, and Angus PW**. Testosterone in men with advanced liver disease: abnormalities and implications. *J Gastroenterol Hepatol* 30: 244-251, 2015.
128. **Van Thiel DH, Kumar S, Gavaler JS, and Tarter RE**. Effect of liver transplantation on the hypothalamic-pituitary-gonadal axis of chronic alcoholic men with advanced liver disease. *Alcohol Clin Exp Res* 14: 478-481, 1990.
129. **Kaufman JM, and Vermeulen A**. The decline of androgen levels in elderly men and its clinical and therapeutic implications. *Endocr Rev* 26: 833-876, 2005.

130. **Dasarathy S, Mullen KD, Dodig M, Donofrio B, and McCullough AJ**. Inhibition of aromatase improves nutritional status following portacaval anastomosis in male rats. *J Hepatol* 45: 214-220, 2006.
131. **Cuneo RC, Hickman PE, Wallace JD, Teh BT, Ward G, Veldhuis JD, and Waters MJ**. Altered endogenous growth hormone secretory kinetic and diurnal GH-binding protein profiles in adults with chronic liver disease. *Clin Endocrinol (Oxf)* 43: 265-275, 1995.
132. **Rommel C, Bodine SC, Clarke BA, Rossman R, Nunez L, Stitt TN, Yancopoulos GD, and Glass DJ**. Mediation of IGF-1-induced skeletal myotube hypertrophy by PI(3)K/Akt/mTOR and PI(3)K/Akt/GSK3 pathways. *Nat Cell Biol* 3: 1009-1013, 2001.
133. **Bodine SC, Stitt TN, Gonzalez M, Kline WO, Stover GL, Bauerlein R, Zlotchenko E, Scrimgeour A, Lawrence JC, Glass DJ, and Yancopoulos GD**. Akt/mTOR pathway is a crucial regulator of skeletal muscle hypertrophy and can prevent myscle atrophy in vivo. *Nat Cell Biol* 3: 1014-1019, 2001.
134. **Liu W, Thomas SG, Asa SL, Gonzalez-Cadavid N, Bhasin S, and Ezzat S**. Myostatin is a skeletal muscle target of growth hormone anabolic action. *J Clin Endo Metab* 88: 5490-5496, 2003.
135. **Younossi ZM, Koenig AB, Abdelatif D, Fazel Y, Henry L, and Wymer M**. Global epidemiology of nonalcoholic fatty liver disease-Meta-analytic assessment of prevalence, incidence, and outcomes. *Hepatology* 64: 73-84, 2016.
136. **Chalasani N, Younossi Z, Lavine JE, Charlton M, Cusi K, Rinella M, Harrison SA, Brunt EM, and Sanyal AJ**. The diagnosis and management of nonalcoholic fatty liver disease: Practice guidance from the American Association for the Study of Liver Diseases. *Hepatology* 67: 328-357, 2018.
137. **European Association for the Study of the L, European Association for the Study of D, and European Association for the Study of O**. EASL-EASD-EASO Clinical Practice Guidelines for the Management of Non-Alcoholic Fatty Liver Disease. *Obes Facts* 9: 65-90, 2016.
138. **Lee YH, Jung KS, Kim SU, Yoon HJ, Yun YJ, Lee BW, Kang ES, Han KH, Lee HC, and Cha BS**. Sarcopenia is associated with NAFLD independently of obesity and insulin resistance: nationwide surveys (KNHANES 2008-2011). *J Hepatol* 63: 486-493, 2015.
139. **Hallsworth K, Thoma C, Moore S, Ploetz T, Anstee QM, Taylor R, Day CP, and Trenell MI**. Non-alcoholic fatty liver disease is associated with higher levels of *objectively* measured sedentary behaviour and lower levels of physical activity than matched healthy controls. *Frontline Gastroenterol* 6: 44-51, 2015.
140. **Sanchez-Sanchez JL, Manas A, Garcia-Garcia FJ, Ara I, Carnicero JA, Walter S, and Rodriguez-Manas L**. Sedentary behaviour, physical activity, and sarcopenia among older adults in the TSHA: isotemporal substitution model. *J Cachexia Sarcopenia Muscle* 10: 188-198, 2019.
141. **Kim TN, Yang SJ, Yoo HJ, Lim KI, Kang HJ, Song W, Seo JA, Kim SG, Kim NH, Baik SH, Choi DS, and Choi KM**. Prevalence of sarcopenia and sarcopenic obesity in Korean adults: the Korean sarcopenic obesity study. *Int J Obes (Lond)* 33: 885-892, 2009.
142. **Utzschneider KM, and Kahn SE**. Review: The role of insulin resistance in nonalcoholic fatty liver disease. *J Clin Endocrinol Metab* 91: 4753-4761, 2006.
143. **Bhanji RA, Narayanan P, Allen AM, Malhi H, and Watt KD**. Sarcopenia in hiding: The risk and consequence of underestimating muscle dysfunction in nonalcoholic steatohepatitis. *Hepatology* 66: 2055-2065, 2017.
144. **Wang X, Hu Z, Hu J, Du J, and Mitch WE**. Insulin resistance accelerates muscle protein degradation: Activation of the ubiquitin-proteasome pathway by defects in muscle cell signaling. *Endocrinology* 147: 4160-4168, 2006.

145. **Kalyani RR, Corriere M, and Ferrucci L**. Age-related and disease-related muscle loss: the effect of diabetes, obesity, and other diseases. *Lancet Diabetes Endocrinol* 2: 819-829, 2014.
146. **Kim TN, Park MS, Lim KI, Choi HY, Yang SJ, Yoo HJ, Kang HJ, Song W, Choi H, Baik SH, Choi DS, and Choi KM**. Relationships between sarcopenic obesity and insulin resistance, inflammation, and vitamin D status: the Korean Sarcopenic Obesity Study. *Clin Endocrinol (Oxf)* 78: 525-532, 2013.
147. **Koster A, Ding J, Stenholm S, Caserotti P, Houston DK, Nicklas BJ, You T, Lee JS, Visser M, Newman AB, Schwartz AV, Cauley JA, Tylavsky FA, Goodpaster BH, Kritchevsky SB, Harris TB, and Health ABCs**. Does the amount of fat mass predict age-related loss of lean mass, muscle strength, and muscle quality in older adults? *J Gerontol A Biol Sci Med Sci* 66: 888-895, 2011.
148. **Srikanthan P, Hevener AL, and Karlamangla AS**. Sarcopenia exacerbates obesity-associated insulin resistance and dysglycemia: findings from the National Health and Nutrition Examination Survey III. *PLoS One* 5: e10805, 2010.
149. **Koyama Y, and Brenner DA**. Liver inflammation and fibrosis. *J Clin Invest* 127: 55-64, 2017.
150. **Dalle S, Rossmeislova L, and Koppo K**. The Role of Inflammation in Age-Related Sarcopenia. *Front Physiol* 8: 1045, 2017.
151. **Cusi K**. Role of obesity and lipotoxicity in the development of nonalcoholic setatohepatitis: pathphysiology and clinical implications. *Gastroenterology* 142: 711-725, 2012.
152. **Feldstein AE, Weneburg NW, Canbay A, Guicciardi ME, Bronk SF, Rydzewski R, Burgart LJ, and Gores GJ**. Free fatty acids promote hepatic lipotoxicity by stimulating TNF-alpha expression via a lysosomal pathway. *Hepatology* 40: 185-194, 2004.
153. **Marí M, Caballero F, Colell A, Morales A, Caballeria J, Fernandez A, Enrich C, Fernandez-Checa JC, and García-Ruiz C**. Mitochondrial free cholesterol loading sensitises to TNF- and Fas- mediated steatohepatitis. *Cell Metab* 4: 185-198, 2006.
154. **Tchkonia T, Morbeck DE, Von Zglinicki T, Van Deursen J, Lustgarten J, Scrable H, Khosla S, Jensen MD, and Kirkland JL**. Fat tissue, aging, and cellular senescence. *Aging Cell* 9: 667-684, 2010.
155. **Trayhurn P, and Wood IS**. Adipokines: inflammation and the pleiotropic role of white adipose tissue. *Br J Nutr* 92: 347-355, 2004.
156. **Lang CH, Frost RA, Nairn AC, MacLean DA, and Vary TC**. TNF-alpha impairs heart and skeletal muscle protein synthesis by altering translation initiation. *Am J Physiol Endocrinol Metab* 282: E336-E247, 2002.
157. **Reid MB, and Li Y-P**. Tumor necrosis factor-α and muscle wasting: a cellular perspective. *Respir Res* 2: 269-272, 2001.
158. **Li YP, Chen Y, John J, Moylan J, Jin B, Mann DL, and Reid MB**. TNF-alpha acts via p38 MAPK to stimulate expression of the ubiquitin ligase atrogin1/MAFbx in skeletal muscle. *FASEB J* 19: 362-370, 2005.
159. **Li YP, Schwartz RJ, Waddell ID, Holloway BR, and Reid MB**. Skeletal muscle myocytes undergo protein loss and reactive oxygen-mediated NF-kappaB activation in response to tumor necrosis factor alpha. *FASEB J* 12: 871-880, 1998.
160. **Thoma A, and Lightfoot AP**. NF-kB and Inflammatory Cytokine Signalling: Role in Skeletal Muscle Atrophy. *Adv Exp Med Biol* 1088: 267-279, 2018.
161. **Wree A, Kahraman A, Gerken G, and Canbay A**. Obesity affects the liver - the link between adipocytes and hepatocytes. *Digestion* 83: 124-133, 2011.
162. **Chandran M, Phillips SA, Ciaraldi T, and Henry RR**. Adiponectin: More than just another fat cell hormone? *Diabetes Care* 26: 2442-2450, 2003.

163. **Combs TP, and Marliss EB**. Adiponectin Signaling in the Liver. *Rev Endocr Metad Disord* 15: 137-147, 2014.
164. **Ruan H, and Dong LQ**. Adiponectin signaling and function in insulin target tissues. *J Mol Cell Biol* 8: 101-109, 2016.
165. **Liu T, Xu L, Chen FH, and Zhou YB**. Association of Serum Vitamin D Level and Nonalcoholic Fatty Liver Disease: A Meta-Analysis. *Eur J Gastronenterol Hepatol* 32: 140-147, 2020.
166. **Dasarathy S**. Is the adiponectin-AMPK-mitochondrial axis involves in progression of nonalcoholic fatty liver disease? *Hepatology* 60: 22-25, 2014.
167. **Amor M, Itariu BK, Moreno-Viedma V, Keindl M, Jürets A, Prager G, Langer F, Grablowitz V, Zelda M, and Stulnig TM**. Serum Myostatin Is Upregulated in Obesity and Correlates With Insulin Resistance in Humans. *Exp Clin Endocrinol Diabetes* 127: 550-556, 2019.
168. **Barchetta I, De Bernardinis M, Capoccia D, Baroni MG, Fontana M, Fraioli A, Morini S, Leonetti F, and Cavallo MG**. Hypovitaaminosis D Is Independently Association With Metabolic Syndrome in Obese Patients. *PLoS One* 8: e68689, 2013.
169. **Eliades M, Spyrou E, Agrawal N, Lazo M, Brancati FL, Potter JJ, Koteish AA, Clark JM, Guallar E, and Hernaez R**. Meta-analysis: Vitamin D and Non-Alcoholic Fatty Liver Disease. *Aliment Pharmacol Ther* 38: 246-254, 2013.
170. **Roth CL, Elfers CT, Fidlewicz DP, Melhorn SJ, Morton GJ, Hoofnagle A, Yeh MM, Nelson JE, and Kowdley KV**. Vitamin D Deficiency in Obese Rats Exacerbates Nonalcoholic Fatty Liver Disease and Increases Hepatic Resistin and Toll-like Receptor Activation. *Hepatology* 55: 1103-1111, 2012.
171. **Visser M, Deeg DJ, Lips P, and Longitudinal Aging Study A**. Low vitamin D and high parathyroid hormone levels as determinants of loss of muscle strength and muscle mass (sarcopenia): the Longitudinal Aging Study Amsterdam. *J Clin Endocrinol Metab* 88: 5766-5772, 2003.
172. **Dzik KP, and Kaczor JJ**. Mechanisms of Vitamin D on Skeletal Muscle Function: Oxidative Stress, Energy Metabolism and Anabolic State. *Eur J Appl Physiol* 119: 825-839, 2019.
173. **Kim MK, Baek KH, Song KH, Il Kang M, Park CY, Lee WY, and Oh KW**. Vitamin D deficiency is associated with sarcopenia in older Koreans, regardless of obesity: the Fourth Korea National Health and Nutrition Examination Surveys (KNHANES IV) 2009. *J Clin Endocrinol Metab* 96: 3250-3256, 2011.
174. **Kozeniecki M, Ludke R, Kerner J, and Patterson B**. Micronutrients in Liver Disease: Roles, Risk Factors for Deficiency, and Recommendations for Supplementation. *Nutr Clin Pract* 35: 50-62, 2020.
175. **Wiest R, Lawson M, and Geuking M**. Pathological bacterial translocation in liver cirrhosis. *J Hepatol* 60: 197-209, 2014.
176. **Bellot P, Francés R, and Such J**. Pathological bacterial translocation in cirrhosis: pathophysiology, diagnosis and clinical implications. *Liver Int* 33: 31-39, 2013.
177. **Bajaj JS, Heuman DM, Hylemon PB, Sanyal AJ, White MB, Monteith P, Noble NA, Unser AB, Daita K, Fisher AR, Sikaroodi M, and Gillevet PM**. Altered profile of human gut microbiome is associated with cirrhosis and its complications. *J Hepatol* 60: 940-947, 2014.
178. **Trebicka J, Krag A, Gansweid S, Appenodt B, Schiedermaier P, Sauerbruch T, and Spengler U**. Endotoxin and tumor necrosis factor-receptor levels in portal and hepatic vein of patients wit alcoholic liver cirrhosis receiving elective trans jugular intrahepatic portosystemic shunt. *Eur J Gastroenterol Hepatol* 23: 1218-1225, 2011.

179. **Fukui H**. Gut-liver axis in liver cirrhosis: How to manage leaky gut and endotoxemia. *World J Hepatol* 7: 425-442, 2015.
180. **Crossland H, Smith K, Atherton PJ, and Wilkinson DJ**. The metabolic and molecular mechanisms of hyperammonaemia- and hyperethanolaemia-induced protein catabolism in skeletal muscle cells. *J Cell Physiol* 233: 9663-9673, 2018.
181. **Kumar A, Davuluri G, Silva RNE, Engelen M, Ten Have GAM, Prayson R, Deutz NEP, and Dasarathy S**. Ammonia lowering reverses sarcopenia of cirrhosis by restoring skeletal muscle proteostasis. *Hepatology* 65: 2045-2058, 2017.
182. **Crossland H, Smith K, Atherton PJ, and Wilkinson DJ**. A novel stable isotope tracer method to simultaneously quantify skeletal muscle protein synthesis and breakdown. *Metabolism Open* 5: 100021, 2020.
183. **Desler MM, Jones SJ, Smith CW, and Woods TL**. Effects of Dexamethasone and Anabolic Agents on Proliferation and Protein Synthesis and Degradation in C2C12 Myogenic Cells. *J Anim Sci* 74: 1265-1273, 1996.
184. **Sandri M, Sandri C, Gilbert A, Skurk C, Calabria E, Picard A, Walsh K, Schiaffino S, Lecker SH, and Goldberg AL**. Foxo Transcription Factors Induce the Atrophy-Related Ubiquitin Ligase Atrogin-1 and Cause Skeletal Muscle Atrophy. *Cell* 117: 399-412, 2004.
185. **Stewart CE, Newcomb PV, and Holly JM**. Multifaceted roles of TNF-alpha in myoblast destruction: a multitude of signal transduction pathways. *J Cell Physiol* 198: 237-247, 2004.
186. **Sharples AP, Al-Shanti N, and Stewart CE**. C2 and C2C12 murine skeletal myoblast models of atrophic and hypertrophic potential: relevance to disease and ageing? *J Cell Physiol* 225: 240-250, 2010.
187. **Pomies P, Blaquiere M, Maury J, Mercier J, Gouzi F, and Hayot M**. Involvement of the FoxO1/MuRF1/Atrogin-1 Signaling Pathway in the Oxidative Stress-Induced Atrophy of Cultured Chronic Obstructive Pulmonary Disease Myotubes. *PLoS One* 11: e0160092, 2016.
188. **Mankhong S, Kim S, Moon S, Kwak HB, Park DH, and Kang JH**. Experimental Models of Sarcopenia: Bridging Molecular Mechanism and Therapeutic Strategy. *Cells* 9: 1385, 2020.
189. **Lopez-Otin C, Blasco MA, Partridge L, Serrano M, and Kroemer G**. The hallmarks of aging. *Cell* 153: 1194-1217, 2013.
190. **Wahlin-Larsson B, Wilkinson DJ, Strandberg E, Hosford-Donovan A, Atherton PJ, and Kadi F**. Mechanistic Links Underlying the Impact of C-Reactive Protein on Muscle Mass in Elderly. *Cell Physiol Biochem* 44: 267-278, 2017.
191. **Wang DT, Yin Y, Yang YJ, Lv PJ, Shi Y, Lu L, and Wei LB**. Resveratrol prevents TNF-alpha-induced muscle atrophy via regulation of Akt/mTOR/FoxO1 signaling in C2C12 myotubes. *Int Immunopharmacol* 19: 206-213, 2014.
192. **Sullivan-Gunn MJ, and Lewandowski PA**. Elevated hydrogen peroxide and decreased catalase and glutathione peroxidase protection are associatef with aging sarcopenia. *BMC Geriatrics* 13: 104, 2013.
193. **Siu PM, Wang Y, and Alway SE**. Apoptotic signaling induced by H2O2-mediated oxidative stress in differentiated C2C12 myotubes. *Life Sci* 84: 468-481, 2009.
194. **Fan X, Hussien R, and Brooks GA**. H2O2-induced mitochondrial fragmentation in C2C12 myocytes. *Free Radic Biol Med* 49: 1646-1654, 2010.
195. **Sharples AP, Al-Shanti N, Lewis MP, and Stewart CE**. Reduction of myoblast differentiation following multiple population doublings in mouse C2 C12 cells: a model to investigate ageing? *J Cell Biochem* 112: 3773-3785, 2011.

196. **van der Valk J, Brunner D, De Smet K, Fex Svenningsen A, Honegger P, Knudsen LE, Lindl T, Noraberg J, Price A, Scarino ML, and Gstraunthaler G**. Optimization of chemically defined cell culture media--replacing fatal bovine serum in mammalian in vitro methods. *Toxicol In Vitro* 24: 1053-1063, 2010.
197. **Corrick KL, Stec MJ, Merritt EK, Windham ST, Thomas SJ, Cross JM, and Bamman MM**. Serum from human burn victims impairs myogenesis and protein synthesis in primary myoblasts. *Front Physiol* 6: 184, 2015.
198. **Catteau M, Gouzi F, Blervaque L, Passerieux E, Blaquière M, Ayoub B, Bughin F, Mercier J, Hayot M, and Pomiès P**. Effects of a human microenvironment on the differentiation of human myoblasts. *Biochem Biophsy Res Commun* 525: 968-973, 2020.
199. **Carson BP, Patel B, Amigo-Benavent M, Pauk M, Kumar Gujulla S, Murphy SM, Kiely PA, and Jakeman PM**. Regulation of muscle protein synthesis in an in vitro cell model using ex vivo human serum. *Exp Physiol* 103: 783-789, 2018.
200. **Patel B, Pauk M, Amigo-Benavent M, Nongonierma AB, Fitzgerald RJ, Jakeman PM, and Carson BP**. A cell-based evaluation of a non-essential amino acid formulation as a non-bioactive control for activation and stimulation of muscle protein synthesis using ex vivo human serum. *PLoS One* 14: e0220757, 2019.
201. **van Hees HW, Schellekens WJ, Linkels M, Leenders F, Zoll J, Donders R, Dekhuijzen PN, van der Hoeven JG, and Heunks LM**. Plasma from septic shock patients induces loss of muscle protein. *Crit Care* 15: R233, 2011.
202. **Kalampouka I, van Bekhoven A, and Elliott BT**. Differing effects of younger and older human plasma on C2C12 myocytes in vitro. *Front Physiol* 9: 2018.
203. **Ethgen O, Beaudart C, Buckinx F, Bruyere O, and Reginster JY**. The Future Prevalence of Sarcopenia in Europe: A Claim for Public Health Action. *Calcif Tissue Int* 100: 229-234, 2017.
204. **Patel B, Pauk M, Amigo-Benavent M, Nongonierma AB, Fitzgerald RJ, Jakeman PM, and Carson BP**. A cell-based evaluation of a non-essential amino acid formulation as a non-bioactive control for activation and stimulation of muscle protein synthesis using ex vivo human serum. *PLoS One* 14: e0220757, 2019.
205. **Tipton KD, Gurkin BE, Matin S, and Wolfe RR**. Nonessential amino acids are not necessary to stimulate net muscle protein synthesis in healthy volunteers. *J Nutr Biochem* 10: 89-95, 1999.
206. **Alsharidah M, Lazarus NR, George TE, Agley CC, Velloso CP, and Harridge SD**. Primary human muscle precursor cells obtained from young and old donors produce similar proliferative, differentiation and senescent profiles in culture. *Aging Cell* 12: 333-344, 2013.
207. **George T, Velloso CP, Alsharidah M, Lazarus NR, and Harridge SD**. Sera from young and older humans equally sustain proliferation and differentiation of human myoblasts. *Exp Gerontol* 45: 875-881, 2010.
208. **Brzeszczynska J, Meyer A, McGregor R, Schilb A, Degen S, Tadini V, Johns N, Langen R, Schols A, Glass DJ, Roubenoff R, Ross JA, Fearon KCH, Greig CA, and Jacobi C**. Alterations in the in vitro and in vivo regulation of muscle regeneration in healthy ageing and the influence of sarcopenia. *J Cachexia Sarcopenia Muscle* 9: 93-105, 2018.
209. **Bechshoft CJL, Jensen SM, Schjerling P, Andersen JL, Svensson RB, Eriksen CS, Mkumbuzi NS, Kjaer M, and Mackey AL**. Age and prior exercise in vivo determine the subsequent in vitro molecular profile of myoblasts and nonmyogenic cells derived from human skeletal muscle. *Am J Physiol Cell Physiol* 316: C898-C912, 2019.

CHAPTER 2 –METHODS DEVELOPMENT

2.1 Cell Culture

Cell culture was utilised in chapters 3 and 4 of this thesis. In Chapter 3, we describe the development of an *in vitro* model of ageing through the use of *ex vivo* human serum to improve the physiological relevance of cell culture. This model aimed to allow for the investigation of the potential mechanisms of age-related atrophy. In Chapter 4, *ex vivo* human serum was used to create an *in vitro* model of ESLD and non-cirrhotic NAFLD, to investigate the processes which may underpin the progression of sarcopenia across the spectrum of chronic liver disease. Specific information regarding ethical approval and participant recruitment are detailed within the appropriate chapters. Details regarding the preparation of human skeletal muscle for analysis are described in Chapter 5.

2.1.1 C2C12 Cell Line

Mouse skeletal muscle C2C12 myoblasts were obtained from the American Type Culture Collection (ATCC, Manassas, VA, USA). This vial of cells was expanded and frozen down for future use after serial passages.

2.1.2 Thawing Cells

To begin experiments using a fresh culture of C2C12s, a cryovial of cells was removed from liquid nitrogen storage and thawed quickly. Once thawed, the cell suspension was added immediately to 9ml of pre-heated growth media (see section 2.1.4) in a T25cm^2 flask and incubated overnight. The next day confluency of the flask was assessed, and media was changed if needed. The cells were then grown as outlined in the following section (2.1.4).

2.1.3 Freezing Cells

To preserve stocks of C2C12 myoblasts, excess C2C12 myoblasts were frozen down and stored for future use. Cells were cultured in T75cm^2 flasks and washed in 5ml of phosphate-buffered

saline (PBS) (Gibco, 10010015). Following this wash, cells were trypsinsed with TrypLE Express Enzyme (2ml) (Thermo Fisher Scientific, Massachusetts, USA) at a confluency of ~70%. Cells were incubated for 2-5 minutes to allow for dissociation. Once dissociated 8ml of growth media was added to the flask and transferred to a falcon tube. Cells were then centrifuged at 10,000 x g for 5-minutes. The supernatant was discarded, and the cell pellet was resuspended in 1ml of media supplemented with 10% dimethyl sulfoxide (DMSO) and added to a cryovial. Cryovials were stored at -80°C for 24-hours in a NALGENE^{TM} Cryo 1°C Freezing container, containing 500ml of isopentane to freeze cells at a slow rate of -1°C/minute. Subsequently, vials were transferred to liquid nitrogen storage.

2.1.4 Cell Maintenance

Murine C2C12 skeletal muscle cells were cultured in Dulbecco's modified Eagle medium (DMEM) (11966025, Gibco) supplemented with 10% (v/v) fetal bovine serum (FBS) (F9665, Sigma-Aldrich, St. Louis, MO, USA), 1% (v/v) penicillin/streptomycin (P/S) (15070-063, Gibco), 5mM glucose (G7021, Sigma-Aldrich), 1mM sodium pyruvate and 1mM GlutaMAX^{TM} (35050-038, Gibco) (growth media) in standard conditions (5% CO_2, 100% humidity, 37°C). Media was changed every 48-hours until a confluency of ~70% was reached. Passage numbers between 10-12 were selected to ensure C2C12s prior to treatment, showed normal levels of muscle protein synthesis (MPS) and growth were present, in contrast to using cells considered as an ageing model, investigated in previous work (1). Once a confluency of ~70% was achieved, cells were washed in PBS and trypsinised as previously described in section 2.1.3. The supernatant was discarded, and cells were subsequently resuspended in 1ml growth media. 9ml of growth media was subsequently added to this mixture. At this stage, cells were transferred to a number of T75 flasks to passage, or seeded into 6-well plates, or 24-well plates for experimentation at a density of $2.0x10^5$ and $5.0x10^4$ cells. mL^{-1} respectively.

2.1.5 Cell Counting

Cells were counted using a Countess™ II FL Automated Cell Counter (Thermo Fisher Scientific). 10 μl of cell suspension was added to the counting chamber. The slide was inputted into the cell counter and brightfield illumination and focus was automatically adjusted. The number of live and dead cells was then calculated. This was conducted twice, with an average of the two values used for the calculation of total cell number as part of the following equation:

Total cell count = (Value 1 + Value 2) / 2

Average of cell count / 2 = number of cells /1ml

(Number of cells /1ml) / 1000 = number of cells /1μl

The appropriate volume of cell suspension was added to the necessary volume of growth media and mixed to ensure uniform distribution across the plates.

2.1.6 Cell Differentiation

At a confluency of ~90% myoblasts were differentiated in DMEM supplemented with 2% (v/v) horse serum (HS) (16050, Gibco), 1% (v/v) P/S, 5mM glucose, 1mM sodium pyruvate and 1mM GlutaMAX™, (differentiation media) over the course of 5-7 days. During the differentiation period media was changed every 24 hours.

2.2 Cell Treatments

2.2.1 The Investigation of Conditioning C2C12 Skeletal Muscle Cells with Ex Vivo Human Serum

C2C12 myoblasts were seeded in 6-well plates at a density of $2.0x10^5$ cells. mL^{-1} and maintained in DMEM supplemented with FBS as described above in the '2.1.4 cell maintenance' section. Once a confluency of ~90% was reached, growth media was replaced

with differentiation media and changed every 24 hours (see section 2.1.5). On day 7 of differentiation myotubes were changed to an amino acid, and serum free media (D9800-13, US Biological, Salem, MA, USA) (pH 7.3) and underwent a 1-hour serum and amino acid starvation period prior to treatment. Myotubes were subsequently treated with media containing 10% human serum from fasted young or old participants for 4-hours. This time period of 'preconditioning' was chosen as previous research has shown that MPS induced by growth medium is reduced within 30-60 minutes of serum and amino acid starvation and is significantly downregulated alongside key mammalian target of rapamycin complex 1 (mTORC1) pathway signaling proteins (2, 3). A range of plasma and serum doses have previously been utilised in previous investigations with similar outcomes, ranging from 5-20% (2, 4, 5). Therefore, given limited serum sample availability and the detection of protein expression during preliminary experiments, a dilution of 10% was deemed optimal for the current experimental outcomes. Additionally, conditioned media containing 10% human serum has been shown to exhibit high cell adherence and viability throughout a 4-hour time-course treatment (2).

In addition to serum treatment, we also compared the use of plasma treatment *in vitro*. However, we found that plasma treatment greater than 5% resulted in cell viability issues, identified through visible cell peeling and was significantly less tolerated. This is similar to work shown by Kalampouka et. al. (4) who utilised a dilution of 5% plasma throughout *ex vivo* plasma treatments. However, we also found clotting of the cell culture media in plasma treated wells when compared to both serum treated and control wells. This finding is likely a consequence of plasma collection in ethylenediaminetetraacetic (EDTA) tubes, in comparison to lithium heparin coated vacutainers. Lithium heparin treated vacutainers are desirable for the use of *ex vivo* treatments due to their ability to inhibit coagulation through the activation of antithrombin and subsequent inhibition of thrombin.

All *in vitro* experiments involving treatment with *ex vivo* human serum were performed with n=4 in each group and were repeated in triplicate.

2.2.2 In Vitro Leucine Treatment

Unfortunately fed blood samples were not obtained from ESLD and NAFLD patients. To overcome this issue, we aimed to utilise *in vitro* leucine treatment, within an *in vitro* model of ageing to establish whether *in vitro* leucine treatment was appropriate for further investigation. Prior to conditioning with human serum, the appropriate dosage of leucine needed to be determined. Therefore, preliminary data aimed to investigate a dose response to leucine treatment with dosages of 2mM, 5mM, 10mM and 15mM investigated (Figure 2.1). The dosages used for preliminary investigation were selected based upon previous work by Areta et al (6) who compared the phosphorylation of a number of anabolic targets including; ribosomal protein S6 kinase (p70S6K), eukaryotic translation initiation factor 4E- binding protein 1 (4EBP-1), s6 protein (RPS6), eukaryotic elongation factor 2 (eEF2), alongside the incorporation of phenylalanine to investigate MPS in response to 1.5mM, 3.2mM, 5mM and 16.5mM leucine treatment. In this study a 1-hour serum starvation was performed, prior to treatment with leucine for 30 minutes. The authors identified an increase the phosphorylation of mTORC1, 4EBP-1 and RPS6 in C2C12 myotubes, in response to 5mM of leucine treatment (6). Similarly, we conducted a 1-hour serum and amino acid starve as previously described (section 2.2.1). Subsequently cells were treated with leucine for 30-minutes, with the addition of puromycin to measure MPS. We found that 5mM induced a significant increase in MPS, measured through the incorporation of puromycin in comparison to the control. Additionally, no other dosage appeared to have a significant increase in MPS, therefore 5mM was utilised for *in vitro* treatment after conditioning with *ex vivo* human serum. The *in vitro* leucine stimulation used provides an alternative model to investigate the effect of a nutritional supplement, providing us with an alternative ‘fed’ state.

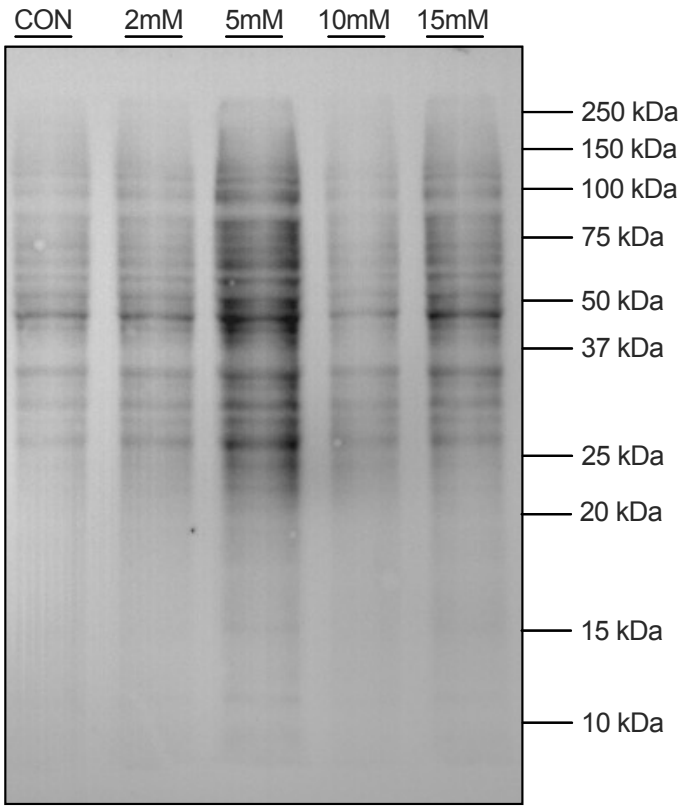

Figure 2.1. Western blot of puromycin incorporation for leucine dose response.

2.2.3 Conditioning with Ex vivo Human Serum Prior to In Vitro Leucine Treatment

C2C12 skeletal muscle cells were seeded into 6-well plates and grown as previously described (section 2.2.1). On day 7 of differentiation, myotubes underwent a 1-hour amino acid and serum starvation. Subsequently, myotubes were treated with 10% *ex vivo* human serum for 4-hours as previously described. In a subset of C2C12 myotubes, 5mM leucine was added to wells for 30-minutes after the 4-hour serum conditioning treatment with *ex vivo* human serum in order to investigate the anabolic response to the addition of an essential amino acid.

2.3 Muscle Protein Synthesis

Acute measures of MPS were assessed using the surface sensing of translation (SUnSET) technique, as previously described (7). Briefly, this method utilises the antibiotic puromycin, a tyrosyl-tRNA analogue and immunoblotting to assess the incorporation level of puromycin

into newly synthesized peptide chains (7, 8). Myotubes were incubated with puromycin (P8833, Sigma-Aldrich) (1μmol/L) for the final 30-minutes of treatment.

2.4 Protein Analysis

2.4.1 Cell Lysis

After the relevant treatment, culture media was aspirated and cells were washed with cold PBS, 3 times over ice. The PBS was removed and ice cold 1X radioimmunoprecipitation assay (RIPA) lysis buffer (Merck Millipore, Watford, UK) (150μl) was added to each well to lyse the cells and left for 20-minutes. Subsequently, cell lysates were collected into Eppendorfs and centrifuged at 13,000rpm for 15-minutes at 4°C.

2.4.2 Sample Preparation – Cell Lysates

The concentration of protein lysates was determined using a detergent compatible (DC) protein assay (Bio-Rad, Hercules, California, USA) using an FLUOstar Omega plate reader (BMG Labtech, Aylesbury, UK). The lysate concentrations were read at an absorbance of 750nm. Subsequently, equal amounts of protein from each sample were added to 1x Laemmli sample buffer and left for 24-hours on the benchtop to allow for denaturing of protein, before being transferred to storage at -80°C until further analysis.

2.4.3 Gel Preparation and Electrophoresis

Samples were thawed and allowed to come to room temperature prior to use. Protein (15-30 μg) was loaded onto 4-20% graded pre-cast gels (561095, Bio-Rad). Protein was separated by electrophoresis at 100V for 10-minutes and 140V for 1-hour.

2.4.4 Transfer and Blocking

After electrophoresis, proteins were transferred from the gel to a nitrocellulose membrane (Whatman, Dassel, Germany) at 100V for 1-hour. After transfer, membranes were stained

with Ponceau S solution as a loading control (9) and subsequently blocked with 5% bovine serum albumin (BSA) (Fisher Scientific, Thermo Fisher Scientific) or 5% milk diluted in Tris-buffered saline and 0.1% Tween-20 (TBST) for 1-hour.

2.4.5 Antibodies

Following blocking, membranes were incubated overnight at 4°C with the primary antibodies detailed in Table 2.3 After an overnight incubation, membranes were washed with TBST for 15-minutes and incubated for 1-hour in the appropriate secondary antibody, listed in Table 2.1. All antibodies were prepared using 5% BSA.

Table 2.1. Antibodies

Primary antibody	Code	Company	Host	Dilution
IgG2a monoclonal anti-puromycin	clone 12D10	Merck Millipore	Mouse	1:1000
Phopho-mTOR^{Ser2448}	#2971	CST	Rabbit	1:1000
Total-mTOR	#2972	CST	Rabbit	1:1000
Phospho-eEF2^{Thr56}	#2331	CST	Rabbit	1:1000
Total-eEF2	#2332	CST	Rabbit	1:1000
Phospho-p70S6K^{Thr389}	#9205	CST	Rabbit	1:500
Total-p70S6K	#9202	CST	Rabbit	1:1000
Phospho-Akt^{Ser473}	#3787	CST	Rabbit	1:1000
Total-Akt	#9272	CST	Rabbit	1:1000
Phospho-RPS6$^{Ser240/244}$	#5364	CST	Rabbit	1:1000
Total-RPS6	#2217	CST	Rabbit	1:1000
Phospho-4EBP-1$^{Thr37/46}$	#9459	CST	Rabbit	1:1000
Total-4EBP-1	#9452	CST	Rabbit	1:1000
MuRF-1	#sc-398608	SC	Mouse	1:1000
MAFbx	AM3141	ECM BioSciences	Rat	1:1000
Caspase-3	#14220	CST	Rabbit	1:1000
LC3A/B	#12741	CST	Rabbit	1:1000
Myostatin	ab201954	ABCAM	Rabbit	1:1000
OXPHOS	ab110413	ABCAM	Mouse	1:1000
OPA-1	BD61260	BD BioSciences (New Jersey, USA)	Mouse	1:1000
DRP1 (D8H5)	#5391	CST	Rabbit	1:1000
FIS1	ab156865	ABCAM	Rabbit	1:1000
MFN2 (D2D10)	#9482	CST	Rabbit	1:1000
MFF	#84580	CST	Rabbit	1:1000
Anti-myosin (skeletal muscle, slow)	M8421	Sigma-Aldrich	Mouse	1:1000
Anti-myosin (skeletal muscle, fast)	M4276	Sigma-Aldrich	Mouse	1:1000
Pax7	PA1-117	Thermo Fisher Scientific	Rabbit	1:1000
MyoD	#13812	CST	Rabbit	1:500
Myogenin	SC-12732	SC	Mouse	1:500
Anti-ubiquitinylated proteins, clone FK2	04-263	Merck Millipore	Mouse	1:1000
Secondary antibody				
Anti-rabbit IgG HRP-conjugated secondary antibody	#7074	CST	Rabbit	1:10000
Anti-rat IgG, HRP-linked antibody	#7077	CST	Rat	1:500
Anti-mouse IgG, HRP-linked antibody	#7076	CST	Mouse	1:1000

4EBP-1, eukaryotic translation initiation factor 4E binding protein 1, Akt, protein kinase B, CST, Cell Signalling Technology, DRP1, dynamic related protein 1, eEF2, eukaryotic

elongation factor 2, FIS1, mitochondrial fission protein 1, HRP, horseradish peroxidase LC3 A/B, microtubule-associated protein 1A/B- light chain 3, MAFbx, muscle atrophy-box, MFF, mitochondrial fission factor, MFN2, mitofusin 2, mTOR, mammalian target of rapamycin, MuRF-1, muscle ring finger 1, myo D, myoblast determination protein 1, OPA-1, optic atrophy protein 1, p70S6K, ribosomal protein S6 kinase, Pax7, paired box 7, RPS6- s6 ribosomal protein, SC, Santa Cruz Biotechnology (Texas, USA), ECM BioSciences (Kentucky, USA), Ser, serine, Thr, threonine.

2.4.6 Image Capture and Analysis

After incubation with the secondary antibody, membranes were washed in TBST for 15-minutes. Protein content was quantified using Immobilon Western chemiluminescent horseradish peroxidase (HRP) substrate (Merck Millipore). Images were captured on a G:BOX Chemi XT4 imager using GeneSys capture software (Syngene, Cambridge, UK). Subsequent band quantification was conducted using ImageJ software (US National Institutes of Health, Bethesda, MD, USA). For puromycin blots the whole lane was quantified in order to account for the range of proteins which incorporate puromycin (7). Relative arbitrary units were normalised to a protein band stained with ponceau S solution (9).

2.5 Myotube Morphology

2.5.1 Staining for Myotube Diameter

C2C12 cells were seeded in 24-well plates at a density of $5.0x10^4$ cells. mL^{-1} as previously described in section 2.1.4. At a confluency of ~90% cells were differentiated for 6 days as described in section 2.1.6. Myotubes were subsequently incubated in differentiation media supplemented with 10% *ex vivo* human serum for 24-hours. A subset of myotubes were maintained in differentiation media throughout the treatment period, providing a comparison to normal growth conditions. Similar to previous work by Kalampouka *et al* (4) we chose to add serum to differentiation media, as we aimed to observe growth following normal conditions, rather than after the stress of a serum and amino acid starvation period. After a 24-

hour incubation period, media was removed and myotubes were washed with PBS. Myotubes were incubated with 2% paraformaldehyde for 30-minutes. Following a PBS wash, cells were incubated for 10-minutes with 100% methanol. Cells were washed 3 times in PBS prior to blocking in 5% (v/v) goat serum in PBS. After 3 PBS washes, cells were then incubated with the primary antibody Desmin (1:100, D8281, Sigma-Aldrich) for 1-hour. After incubation, cells were washed twice with PBS and incubated with the secondary antibody (1:200, Alexa Fluor Plus 488 goat anti-rabbit IgG H+L, A32731, Thermo Fisher Scientific) for 1-hour in darkness. Cells were washed once with PBS and incubated in the dark with DAPI (1:5,000, 4083, Cell Signaling Technology (CST), Leiden, Netherlands) for 5-minutes. Finally, cells were washed with PBS prior to the addition of mountant (P36930, Thermo Fisher Scientific) to each well. A 13mm coverslip was applied and image acquisition was performed after an overnight incubation using a fluorescent microscope (Leica DMI6000B, Leica Microsystems, Wetzlar, Hessen, Germany).

2.5.2 Myotube Diameter and Nuclear Fusion Index Quantification

For analysis, approximately 10 fields per well were randomly selected, with at least 100 myotubes included in the analysis of each well (10). Myotubes for this work were defined as a desmin positive structure with 3 or more nuclei. The mean of five measurements along each myotube was used to calculate the average myotube diameter. The mean of 10 images, with 10 myotubes per image was used for analysis. Nuclear fusion index (NFI) was defined as the number of nuclei within myotubes, expressed as a percentage of the total number of nuclei in a field of view (11). Images were analysed using ImageJ software.

2.6 Mitochondrial Respirometry

2.6.1 Cell Seeding, Maintenance and Preparation

Mitochondrial respiration was measured in intact, attached cells as described previously (12). Briefly, C2C12s were seeded at $4.0x10^4$ cells. mL^{-1} on XFe24 cell culture plates (Seahorse Bioscience, Agilent Technologies, Manchester, UK) and were grown to a confluency of ~70% prior to differentiation. On day 5 of differentiation, myotubes underwent a 24-hour treatment with DMEM conditioned with 10% *ex vivo* human serum.

2.6.2 Mitochondrial Stress Test

After the 24-hour treatment, myotubes were washed in Agilent Seahorse XF Base medium (DMEM) supplemented with 5mM of glucose, 1 mM of sodium pyruvate, 2 mM of L-glutamine and 5mM 4-(2-hydroxyethyl)-1-piperazineethanesulfonic acid (HEPES) (15630106, Thermo Fisher Scientific), pre-warmed to 37°C. The cells were then transferred to a non-CO_2 incubator for 50-minutes at 37°C. Subsequently, cells were transferred to a Seahorse XFe24 extracellular flux analyzer (controlled at 37°C) for a 10-minute calibration. Following calibration, 4 measurement cycles were completed to obtain the recording of basal cellular respiration. Following baseline measures, oligomycin (1μM), N^5,N^6-bis(2-Fluorophenyl)-[1,2,5]oxadiazolo[3,4-B]pyrazine-5,6-diamine (BAM 15) (3μM), and a mixture of rotenone (1μM) and antimycin A (2μM) were added to sequentially inhibit adenosine triphosphate (ATP) synthase, uncouple oxidative phosphorylation and determine non-mitochondrial rates of respiration. Throughout the experiment, a total of 4 measurement cycles were recorded after the addition of each compound. For all respirometry experiments each measurement cycle involved a 1-minute mix, 2-minute wait, and 3-minute measurement period. A calculation for respiratory parameters obtained through the completion of the mitochondrial stress test can be found in Table 2.2.

Table 2.2. Respiratory analysis

Respiratory Parameter	Definition	Calculation
Basal Respiration	O_2 consumption required to meet the cellular ATP demand from proton leak respiration.	Final rate measurement obtained before OM injection – non-mitochondrial respiration rate
Maximal Respiration	The maximum rate of oxygen consumption, visible after the addition of an uncoupler. Representative of the maximum rate of respiration a cell can achieve.	Maximum rate measurement taken after BAM-15 injection – non-mitochondrial respiration
Protein Leak Respiration	Basal respiration which is not accounted for by ATP coupled respiration.	Minimum rate measurement taken after OM injection – non-mitochondrial respiration
ATP Coupled Respiration	ATP produced within the mitochondria to meet metabolic demands, shown by a decrease in oxygen consumption rate after the injection of an ATP synthase inhibitor.	Last rate measurement before OM injection – minimum rate after OM injection
Spare Respiratory Capacity	The ability of a cell to respond to changes in energetic demand.	Maximal respiration – basal respiration
Coupling Efficiency	The percentage of basal respiration rate attributed to ATP coupled respiration.	ATP production rate / basal respiration rate x 100
Basal Glycolysis	The conversion of glucose into lactate (within a Seahorse XFe analyser)	The last proton efflux rate measurement before the first injection
Compensatory Glycolysis	The rate of glycolysis, after the addition of an ATP synthase inhibitor	The maximum proton efflux rate measurement after the injection of rotenone and antimycin A.

ATP, adenosine triphosphate, BAM-15, N^5,N^6-bis(2-Fluorophenyl)-[1,2,5]oxadiazolo[3,4-B]pyrazine-5,6-diamine, OM, oligomycin

2.6.3 Estimation of ATP Production

Estimation of intracellular rates of glycolysis and ATP production were conducted utilising both the oxygen consumption rate (OCR), which measures oxidative phosphorylation and extracellular acidification rate (ECAR), a measure of glycolysis (13). Previous work has measured the rate of glycolysis utilising the rate of lactate and proton production, however more recent work has investigated the measurement of extracellular proton production (PPR)

to calculate glycolysis (14, 15). The measurement of PPR can be determined through the measurement of potential of hydrogen (pH) to measure the rate of acidification simultaneously with measures of oxygen consumption rate. However, most current analyses which compare the ECAR to oxygen consumption are problematic. In order to overcome these potential issues, Mookerjee et. al. (14) created a new method in which total ATP production ($J_{ATPproduction}$) is calculated. ATP can be produced through both glycolytic (ATP_{glyc})) and oxidative reactions (ATP_{ox}). The authors of this method described ATP_{glyc} as the amount of ATP formed during the glycolytic reaction which results in the formation of pyruvate from glycose, thereby describing the overall flux of glycolysis (14). ATP_{ox} was defined as the amount of ATP formed during oxidative metabolism e.g., through the tricarboxylic acid (TCA) cycle and oxidative phosphorylation (14). Therefore, based upon the calculations outlined by Mookerjee et. al. (14), the equations outlined in Table 2.3 were utilised to calculate ATP production, from both glycolytic (ATP_{glyc}) and oxidative capacities (ATP_{ox}).

Table 2.3. Estimation of ATP production

Respiratory Parameter	Definition	Calculation
OCR_{mito}	Mitochondrial oxygen consumption rate (OCR)	(OCR_{tot} – $OCR_{rot/AA}$) / μg of protein
$OCR_{coupled}$	OCR coupled to oxidative phosphorylation	((OCR_{tot} – OCR_{oli}) x 0.908) / μg of protein
PPR_{tot}	Total proton production rate (PPR)	($ECAR_{tot}$ / buffer factor) / μg of protein
PPR_{resp}	Proton production rate associated with HCO_3^- production	OCR_{mito} x CCF (0.61) (16)
PPR_{glyc}	Proton production rate associated with lactate production	PPR_{tot} = PPR_{resp}
J_{ATPox}	Amount of ATP produced by oxidative reactions	($OCR_{coupled}$ x $2P/O_{oxphos}$ (2.486)) + (OCR_{mito} x $2P/O_{TCA}$ (0.121))
$J_{ATPglyc}$	Amount of ATP produced by conversion of glucose to pyruvate via glycolysis	(PPR_{glyc} x ATP/lactate) + (OCR_{mito} X$2P/O_{glyc}$ (0.2420))
$J_{ATPproduction}$	Total amount of ATP produced.	ATP (J_{ATPox}) + ATP ($J_{ATPglyc}$)
ATP (J_{ATPox}) (%)	Percentage of total ATP produced by oxidative reactions	(ATP (J_{ATPox}) / ATP $J_{ATPproduction}$) x 100
ATP ($J_{ATPglyc}$) (%)	Percentage of total ATP produced by glycolytic reactions	(ATP ($J_{ATPglyc}$) / ATP $J_{ATPproduction}$) x 100

CCF, CO_2 Contribution Factor = $PPR_{mito}/OCR_{mito,}$ OCR_{tot}, Total OCR; $OCR_{rot/AA}$, OCR in the presence of rotenone/ antimycin, P/O, per mol of oxygen atoms consumed.

2.6.4 Normalisation

After completion of the experiment, cells were lysed in ice cold 1X RIPA lysis buffer and stored at -80°C until further analysis. Upon thawing, protein concentration was determined using a DC protein assay as previously described (section 2.4.2). Data was normalised to the total protein content quantified by a DC protein assay (17), and corrected for background. A total of 3 experimental runs was included for analysis, across 3 different passage numbers.

2.7 Mitophagy

2.7.1 Mito-QC Cell Line

Mitophagy was measured using a mitophagy reporter cell line (mito-QC) in C2C12s, kindly provided by Dr Yu-Chiang Lai (University of Birmingham). Briefly, the mito-QC C2C12 cell line express a stable functional insert tandem mCherry- green fluorescent protein (GFP) tag, which is fused to the mitochondrial targeting sequence of mitochondrial fission protein 1 (FIS1) (residues 101-152) (18). Under basal conditions, the mitochondria fluoresce two colours; red (mCherry) and green (GFP), which when merged appear gold in colour (17). However, mitophagy induces an acidic environment within the lysosomes which quench the signal of GFP, but not mCherry. As a consequence, an increase in mCherry signal is visible in the mitochondrial network.

2.7.2 Sample Preparation

C2C12 myoblasts expressing the stable mCherry-GFP-mt-FIS1 were seeded onto imaging dishes with a polymer coverslip bottom (Ibidi, Gräfelfing, Germany) at a seeding density of $6x10^4$ cells. mL^{-1}. After 24-hours, cells were treated with *ex vivo* human serum or 10 μM of carbonyl cyanide m-chlorophenyl hydrazone (CCCP) for 24-hours. After treatment, cells were washed twice with PBS and fixed in 3.7% formaldehyde with 200mM HEPES (pH 7.0) for 10-minutes. Following fixation, cells were washed and incubated for a further 10-minutes in DMEM supplemented with HEPES (10mM, pH 7.0) and washed with PBS. Subsequently, a mounting solution was added to the wells.

2.7.3 Image Analysis and Quantification

After an overnight incubation in the dark, images were taken using a Crest X-Light spinning disk system coupled to a Nikon Ti-E base, 60x/1.4 NA (CFI Plan Apo Lambda) air objective and Photometrics Delta Evolve EM-CCD. Excitation was required during imaging and

delivered at λ= 458-482nm and λ= 563-587 for GFP and mCherry respectively. Signals were detected at λ=500-550nm and λ= 602-662 respectively.

Mitophagy was quantified using mean fluorescence intensity of mCherry and GFP, alongside the measurement of circularity and Feret's diameter, measured in 25 cells across at least 15 fields of view within each condition within ImageJ software (17). Myoblasts expressing the mCherry-GFP construct display a yellow color upon merging the red and green, fluorescent signals. An increase in mitophagy was detected through changes in pH induced by an increase in mitochondrial delivery to the lysosome, which lowers the pH and quenches the GFP signal (19). Subsequently, this allows for a stronger mCherry signal, therefore the quantification of mitophagy at the cellular level was conducted through the relative increase in mCherry/GFP ratio. The mCherry/GFP ratio was normalised to control serum treated samples.

2.8 Statistical Analysis

Statistical analysis was performed using IBM SPSS Statistics version 26 (IBM SPSS inc. Chicago, Illinois, USA). Data were tested for normality using Shapiro-Wilk test, and for homogeneity of variances using Levene's test. In Chapter 3, independent samples t-tests were used to investigate changes in arthrometric measures, body composition, strength and blood analyses. A one-way ANOVA was utilised for the analysis of myotube diameter, NFI, puromycin incorporation, markers anabolic and catabolic signaling. In Chapter 4, a one-way ANOVA was used to assess differences in arthrometric measures, body composition, strength and blood analyses between groups (i.e., control, non-alcoholic fatty liver disease (NAFLD) and end stage liver disease (ESLD). A 3 (group) x 2 (treatment) ANOVA was used to assess differences in puromycin incorporation, anabolic and catabolic signalling. A one-way ANOVA was used to assess differences in myotube diameter, NFI, mitophagy and respirometry between groups. In Chapter 5, a one-way ANOVA was used to assess differences in arthrometric

measures, body composition, strength and blood analyses between groups (i.e., control, NAFLD, ESLD). Additionally, one-way ANOVA was used to assess differences in anabolic, regulatory, catabolic and mitochondrial signalling markers. Where the results of the one-way, or two-way ANOVAs revealed a positive interaction effect, post-hoc analysis t-tests were completed using Tukey's HSD. Effect size was calculated using Cohen's d for t-test and post-hoc comparisons, while partial eta squared (η^2) was used for omnibus tests. Cohen's d was calculated using the equation:

(Mean 1 – Mean 2) / ((Standard deviation 1 + Standard deviation 2) / 2))

Effect size assessed by Cohen's d can be classified as small (d = 0.2), medium (d = 0.5) and large (d < 0.8) (20). Effect size assessed by partial eta squared was classified as small (η^2 = 0.01), medium (η^2 = 0.06) and large (η^2 = 0.14). Statistical significance was set at $p < 0.05$. The data presented throughout tables in this thesis include the mean of each participant, over the 3 passage numbers to provide one data point per participant ± standard deviation unless stated otherwise. The data presented in figures throughout this thesis are expressed as the mean (cross), median (central horizontal line), 25th and 75th percentiles (box) and the minimum and maximum values (vertical lines), Figures were generated in GraphPad Prism V8.4.3. Data presented in tables include the mean of each participant ± standard deviation, unless stated otherwise.

2.9 References

1. **Sharples AP, Al-Shanti N, Lewis MP, and Stewart CE**. Reduction of myoblast differentiation following multiple population doublings in mouse C2 C12 cells: a model to investigate ageing? *J Cell Biochem* 112: 3773-3785, 2011.
2. **Carson BP, Patel B, Amigo-Benavent M, Pauk M, Kumar Gujulla S, Murphy SM, Kiely PA, and Jakeman PM**. Regulation of muscle protein synthesis in an in vitro cell model using ex vivo human serum. *Exp Physiol* 103: 783-789, 2018.
3. **Ham DJ, Caldow MK, Lynch GS, and Koopman R**. Arginine protects muscle cells from wasting in vitro in an mTORC1-dependent and NO-independent manner. *Amino Acids* 46: 2643-2652, 2014.
4. **Kalampouka I, van Bekhoven A, and Elliott BT**. Differing effects of younger and older human plasma on C2C12 myocytes in vitro. *Front Physiol* 9: 2018.
5. **Patel B, Pauk M, Amigo-Benavent M, Nongonierma AB, Fitzgerald RJ, Jakeman PM, and Carson BP**. A cell-based evaluation of a non-essential amino acid formulation as a non-bioactive control for activation and stimulation of muscle protein synthesis using ex vivo human serum. *PLoS One* 14: e0220757, 2019.
6. **Areta JL, Hawley JA, Ye JM, Chan MH, and Coffey VG**. Increasing leucine concentration stimulates mechanistic target of rapamycin signaling and cell growth in C2C12 skeletal muscle cells. *Nutr Res* 34: 1000-1007, 2014.
7. **Goodman CA, Mabrey DM, Frey JW, Miu MH, Schmidt EK, Pierre P, and Hornberger TA**. Novel insights into the regulation of skeletal muscle protein synthesis as revealed by a new nonradioactive in vivo technique. *FASEB J* 25: 1028-1039, 2011.
8. **Schmidt EK, Clavarino G, Ceppi M, and Pierre P**. SUnSET, a nonradioactive method to monitor protein synthesis. *Nat Methods* 6: 275-277, 2009.
9. **Romero-Calvo I, Ocón B, Martínez-Moya P, Suárez MD, Zarzuelo A, Martínez-Augustin O, and Sánchez de Medina F**. Reversible Ponceau staining as a loading control alternative to actin in Western blots. *Anal Biochem* 401: 318-320, 2010.
10. **Tarum J, Folkesson M, Atherton PJ, and Kadi F**. Electrical pulse stimulation: an in vitro exercise model for the induction of human skeletal muscle cell hypertrophy. A proof-of-concept study. *Exp Physiol* 102: 1405-1413, 2017.
11. **Agley CC, Velloso CP, Lazarus NR, and Harridge SDR**. An Image Analysis Method for the Precise Selection and Quantification of Fluorescently Labeled Cellular Constituents: Application to the Measurement of Human Muscle Cells in Culture. *J Histochem Cytochem* 60: 428-438, 2012.
12. **Affourtit C, and Brand MD**. Measuring mitochondrial bioengertics in INS-1E insulinoma cells. *Methods Enzymol* 457: 2009.
13. **Divakaruni AS, Paradyse A, Ferrick DA, Murphy AN, and Jastroch M**. Analysis and interpretation of microplate-based oxygen consumption and pH data. *Methods Enzymol* 547: 309-354, 2014.
14. **Mookerjee SA, Gerencser AA, Nicholls DG, and Brand MD**. Quantifying intracellular rates of glycolytic and oxidative ATP production and consumption using extracellular flux measurements. *J Biol Chem* 292: 7189-7207, 2017.
15. **Mookerjee SA, Goncalves RLS, Gerencser AA, Nicholls DG, and Brand MD**. The contributions of respiration and glycolysis to extracellular acid production. *Biochim Biophys Acta* 1847: 171-181, 2015.
16. **Romero N, Swain P, Neilson P, and Dranka BP**. White paper: Improving quantification of cellular glycolytic rate using aglient seahorse XF technology. https://www.agilent.com/cs/library/whitepaper/public/whitepaper-improve-quantification-of-cellular-glycolytic-rate-cell-analysis-5991-7894en-agilent.pdf

17. **Seabright AP, Fine NHF, Barlow JP, Lord SO, Musa I, Gray A, Bryant JA, Banzhaf M, Lavery GG, Hardie DG, Hodson DJ, Philp A, and Lai YC**. AMPK activation induces mitophagy and promotes mitochondrial fission while activating TBK1 in a PINK1-Parkin independent manner. *FASEB J* 34: 6284-6301, 2020.
18. **Allen GFG, Toth R, James J, and Ganley IG**. Loss of iron triggers PINK1/Parkin-independent mitophagy. *EMBO Rep* 14: 1127-1135, 2013.
19. **McWilliams TG, Prescott AR, Allen GRG, Tamjar J, Munson MJ, Thomson C, Muqit MMK, and Ganley IG**. mito-QC illuminates mitophagy and mitochondrial architecture in vivo. *J Cell Biol* 214: 333-345, 2016.
20. **Sullivan GM, and Feinn R**. Using Effect Size-or Why the P Value Is Not Enough. *J Grad Med Educ* 4: 279-282, 2012.

CHAPTER 3 – DEVELOPMENT OF AN IN VITRO MODEL OF AGEING

The Effect of Young and Old *Ex Vivo* Human Serum on Cellular Protein Synthesis and Growth in an *In Vitro* Model of Ageing

Sophie L. Allen [1,2], Ryan N. Marshall [1,3], Sophie J. Edwards [1], Janet M. Lord [2,3,4], Gareth G. Lavery [2,3,5,6], Leigh Breen [1,2,3*]

Affiliations

[1] School of Sport, Exercise and Rehabilitation Sciences, University of Birmingham, UK.

[2] National Institute for Health Research, Birmingham Biomedical Research Centre at University Hospitals Birmingham NHS Foundation Trust and University of Birmingham, Birmingham, UK.

[3] MRC-Versus Arthritis Centre for Musculoskeletal Ageing Research, University of Birmingham, UK.

[4] Institute of Inflammation and Ageing, University of Birmingham, UK.

[5] Institute of Metabolism and Systems Research, University of Birmingham, UK.

[6] Centre for Endocrinology, Diabetes and Metabolism, Birmingham Health Partner, Birmingham, UK.

*Corresponding Author: Leigh Breen

School of Sport, Exercise and Rehabilitation Sciences

University of Birmingham

Edgbaston, Birmingham B15 2TT

Email: [redacted]

3.1 Abstract

In vitro models of muscle ageing are useful for understanding mechanisms of age-related muscle loss and aiding the development of targeted therapies. To investigate mechanisms of age-related muscle loss *in vitro* utilising *ex vivo* human serum, fasted blood samples were obtained from 4 old (72 ± 1 years) and 4 young (26 ± 3 years) men. Older individuals had elevated levels of plasma CRP, IL-6, HOMA-IR, and lower concentric peak torque and work-per-repetition compared with young participants ($P < 0.05$). C2C12 myotubes were serum and amino acid starved for 1-hour and conditioned with human serum (10%) for 4- or 24-hours. After 4-hours C2C12 cells were treated with 5mM leucine for 30-minutes. Muscle protein synthesis (MPS) was determined through the surface sensing of translation (SUnSET) technique and regulatory signalling pathways measured via western blot. Myotube diameter was significantly reduced in myotubes treated with serum from old, in comparison to young donors (45%, $P < 0.001$). MPS was reduced in myotubes treated with old donor serum, compared to young serum prior to leucine treatment (32%, $P < 0.01$). MPS and the phosphorylation of Akt, p70S6K and eEF2 were increased in myotubes treated with young serum in response to leucine treatment, with a blunted response identified in cells treated with old serum ($P < 0.05$). Muscle protein breakdown signalling pathways did not differ between groups. In summary, we show that myotubes conditioned with serum from older individuals had decreased myotube diameter and MPS compared with younger individuals, potentially driven by low-grade systemic inflammation.

3.2 Introduction

Sarcopenia (1), defined as the age-related loss of skeletal muscle mass, strength and function is associated with an increased risk of mortality, physical disability and metabolic disease which can reduce quality of life and independence (2-6). This phenomenon is predicted to affect ~32 million older individuals (>65 years) across Europe by 2045 (7), placing a significant strain on healthcare resources (8, 9). A number of factors contribute to the aetiology of sarcopenia, including alterations in lifestyle, hormone concentrations and peripheral nervous system changes (10). In particular, ageing is often associated with a state of chronic low-grade inflammation, termed inflammaging, consisting of raised levels of c-reactive protein (CRP) and pro-inflammatory cytokines such as interleukin-6 (IL-6) and tumor necrosis factor-α (TNF-α), which have been associated with reductions in muscle mass, strength (11-16), and diminished muscle protein synthesis (MPS) (17, 18). Previous acute metabolic investigations show that the postprandial MPS response to protein/amino acid ingestion is blunted in older individuals, particularly at moderate-to-low protein doses (<20g) (19), which may contribute to the progression of sarcopenia (20, 21). Due to the significant costs, complexities and often invasive nature of *in vivo* human studies of muscle protein turnover, there is a need for *in vitro* models to identify mechanisms of sarcopenia and expedite the development of targeted therapeutic interventions.

To date, *in vitro* models to probe mechanisms of sarcopenia have been conducted using pharmacological treatments to induce myotube atrophy, such as TNF-α (22, 23) and dexamethasone (DEX) (24-27). While these models provide an insight to the potential mechanisms of muscle wasting, the supraphysiological dosages used hinders the translation of this work to humans. Alternatively, C2C12 skeletal muscle cells subjected to replicative ageing, a process in which a population of cells undergo multiple passages, provides a potential *in vitro* model of musculoskeletal ageing. Using this approach Sharples *et al*, demonstrated

reductions in insulin growth factor-1 (IGF-1), myogenic regulatory factors and a diminished capacity for myoblast differentiation that was associated with impaired protein kinase B (Akt) signalling (28). However, undergoing multiple passages within cell lines such as C2C12 skeletal muscle cells does not induce senescence (28). In fact, immortalised cell lines have been shown to maintain their telomerase activity (29, 30). Thus, as senescence is considered to be a key hallmark of ageing (31), replicative ageing may not closely represent inherent ageing processes.

To overcome the potential drawbacks of *in vitro* experimental models outlined above, studies have used *ex vivo* human plasma (32, 33) and serum (34-37) to condition cell culture media. These studies have investigated a range of factors including changes in myotube diameter (32), MPS (34, 35), anabolic and catabolic regulatory signalling (33, 36) in response to divergent nutrient status, states of disease and injury (i.e. septic shock and burns) and ageing. Recently, Kalampouka *et al* (32) identified an increase in myotube diameter in C2C12 cells in response to 24- and 48-hour treatments with 5% plasma from young vs. older participants. Additionally, Carson *et al* (34) identified an increase in MPS in response to an acute 4-hour treatment with *ex vivo* human serum in comparison to serum-free control cells. Furthermore, the authors detected differences in anabolic signalling with the addition of serum obtained after the ingestion of a bolus of whey protein compared with the ingestion of non-essential amino acids (35) or fasted serum (34). Collectively, this evidence suggests that *ex vivo* human serum or plasma can be used to condition cell culture media in order to investigate changes in MPS and muscle cell morphology.

Although there is growing evidence demonstrating the use of *ex vivo* human serum to condition cell culture media *in vitro*, no studies have used serum to create an *in vitro* model of ageing in response to an acute stimulus. Additionally, no studies have conditioned media with human serum prior to *in vitro* nutritional treatment, which would enhance our understanding

of mechanisms of age-related muscle anabolic resistance. Therefore, the primary purpose of this study was to assess acute changes in MPS and regulatory signalling in response to leucine treatment, after conditioning media with *ex vivo* human serum from young and old participants to investigate mechanisms of age-related muscle wasting. Secondly, we aimed to investigate age-related alterations in myotube growth in response to a chronic 24-hour conditioning period with *ex vivo* human serum, to identify whether acute signalling responses correlated with chronic morphological changes. We hypothesized that myotubes conditioned with serum from older men would display impairments in MPS and lower myotube diameter in comparison to those treated with serum from young men.

3.3 Materials and Methods

3.3.1 Subject Characteristics and Ethical Approval

Four young (26 $\pm$ 3 years) and four old (72 $\pm$ 1 years) healthy male participants provided their written, informed consent to participate in this study. All participants were screened with a general health questionnaire and deemed healthy for the completion of this study. Participants were expected to be normotensive (<140/90), free from inflammatory and metabolic disease conditions (i.e. rheumatoid arthritis, type II diabetes, hyperlipidemia), not prescribed any medications such as anticoagulants or non-steroidal anti-inflammatory drugs (NSAIDs) and be habitually and / or recreationally active i.e. participate in regular physical activity such as walking. Ethical approval for this study was obtained through the local ethics committee at the University of Birmingham (ERN_19-0831) and conformed to the standards set by the Declaration of Helsinki.

3.3.2 Study Design

Participants reported to the laboratory after an overnight fast and were asked to refrain from the consumption of caffeine on the morning of the trial. Participants were additionally asked

to refrain from involvement in strenuous forms of exercise 24-hours prior to their visit. A fasted blood sample was obtained from the antecubital vein and collected into ethylenediaminetetraacetic (EDTA) and serum separator vacutainers (BD, Oxford, UK). After collection the serum separator tubes were allowed to sit for 30-minutes at room temperature to enable the blood to clot. Both types of tube were then centrifuged at 3,000 rpm for 10-minutes at 4°C to obtain serum and plasma. Aliquots were frozen at -80°C for further analysis. Finally, participants underwent body composition analysis and completed basic functional assessment in the form of isokinetic functional assessment and handgrip strength (HGS).

3.3.3 Body Composition

Body mass was measured using digital scales by weighing each participant in loose, light clothing without shoes to the closest 0.1kg. Height was measured using a stadiometer and made to the nearest 0.1cm. After assessment of body mass and height, body composition was measured using 8-electrode bioelectrical impedance analysis (BIA), allowing for the non-invasive measurement of fat-mass (FM), fat-free mass (FFM) and skeletal muscle mass (SMM) (mBCA 525, SECA, Hamburg, Germany). BIA has previously been observed to be a valid and clinically reliable measure of body composition in younger and older adults (38).

3.3.4 Handgrip Strength

HGS assessment was utilised as a clinically relevant measure of muscle strength (39). Participants were asked to hold a handheld dynamometer (Jamar hydraulic handheld dynamometer, Patterson Medical, Warrenville, IL, USA) with their arm straight and palm facing medially in a semi-pronated position. Participants completed 3 trials on each hand with a 30-second rest period between each test. Participants were asked to exert their maximal grip strength throughout the test with standardised verbal encouragement. The highest recording across all 6 measurements was used for analysis (39).

3.3.5 Leg Strength

Eccentric and concentric muscle strength of the knee flexors and extensors was assessed using an isokinetic dynamometer (Cybex, division of Lumex Inc., Ronkonkoma, New York, USA) for the evaluation of isokinetic muscle strength of both limbs. Participants were seated with their hips and knees flexed at a 90° angle, with the tested limb, hips and chest secured. The rotational axis of the lever arm was aligned with the lateral epicondyle of the femur. The knee range of motion as set between 5° and 90° of knee flexion. Participants were asked to start the test at full flexion, extend their leg and return to flexion with as much force as possible, completing a total of 5 repetitions at an angular velocity of 60deg/s. After the procedure was explained in full, participants were asked to complete a short warm-up set of 5 repetitions to ensure familiarity with the test, without reaching the point of fatigue. Standardised verbal encouragement was given by the operator throughout the test.

3.3.6 Blood Analyses

Fasting plasma glucose concentrations were measured utilising a Glucose-Glo^{TM} Assay (J6021, Promega Corporation, Madison Wisconsin, USA) following the manufacturer's instructions. Plasma insulin (DINS00), IL-6 (D6050) and CRP (DCRP00) concentrations were determined through the use of commercially available enzyme-linked immunosorbent assay (ELISA) kits following the manufacturer's instructions (R&D systems Inc., Minneapolis, MN, USA).

3.3.7 Cell Culture

A detailed account of the methodology utilised for the *in vitro* work described in this chapter is provided in Chapter 2. Briefly, C2C12 skeletal muscle cells were cultured in growth media and maintained in standard conditions as previously described (section 2.1.4). Cells were then seeded onto 6-well plates, or 24-well plates at a density of $2.0x10^5$ and $5.0x10^4$ cells. mL^{-1} respectively. At a confluency of ~90% myoblasts were differentiated in differentiation media

over the course of 5 days (section 2.1.6). During the differentiation period media was changed every 24-hours. All *in vitro* experiments were performed with n=4 in each group and were repeated in triplicate.

3.3.8 Myotube Diameter

C2C12 cells were prepared for experiments as previously described within Chapter 2 (section 2.5) of this thesis. On day 6 of differentiation, myotubes were incubated in differentiation media supplemented with 10% *ex vivo* human serum from either fasted young or old male donors for 24-hours. A subset of myotubes were maintained in differentiation media throughout the treatment period, providing a comparison to normal growth conditions. After a 24-hour incubation period, media was removed and myotubes were prepared for immunofluorescent imaging as previously described (section 2.5.1). The analysis of myotube diameter and nuclear fusion index (NFI) was conducted as described in section 2.5.2.

3.3.9 Muscle Protein Synthesis

C2C12 myoblasts were seeded in 6-well plates as described in section 2.2.1. Once a confluency of ~90% was reached, growth media was replaced with differentiation media and changed every 24-hours. On day 7 of differentiation myotubes were changed to an amino acid and serum free media and underwent a 1-hour serum and amino acid starvation period prior to treatment. Myotubes were subsequently treated with media containing 10% *ex vivo* human serum from fasted young or old participants for 4-hours. In a subset of C2C12 myotubes, 5mM leucine was added to wells for 30-minutes after the 4-hour serum conditioning treatment with *ex vivo* human serum with either young or old donor serum in order to investigate the anabolic response to the addition of an essential amino acid (section 2.2.3). This *in vitro* leucine stimulation provides an alternative model to investigate the effect of a nutritional supplement, providing

us with an alternative ‘fed’ state. A detailed justification of leucine dosage can be identified within section 2.2.2.

Acute measures of MPS were assessed using the surface sensing of translation (SUnSET) technique, as previously described (section 2.3). Briefly, myotubes were incubated with puromycin (1µmol/L) for the final 30-minutes of treatment. Subsequently, cellular protein lysates were obtained as previously described in section 2.4.1. Samples were then stored at -80°C for further analysis.

3.3.10 Immunoblotting

Cellular protein lysate concentrations were determined through the use of a detergent compatible (DC) assay using an FLUOstar Omega plate reader and prepared for western blot analysis as previously described (section 2.4.2). Protein (15-30μg) were separated on 4-20% linear graded pre-cast gels by sodium dodecyl sulphate polyacrylamide gel electrophoresis (SDS-PAGE) for 1-hour as previously described (section 2.4.3). After electrophoresis proteins were transferred to a nitrocellulose membrane at 100V for 1-hour and subsequently stained with Ponceau S as previously described (section 2.4.4). Membranes were then blocked with 5% (BSA) or 5% milk diluted in Tris-buffered saline and 0.1% Tween-20 (TBST) for 1-hour. Membranes were incubated overnight at 4°C with the following antibodies: mouse IgG2a monoclonal anti-puromycin, phospho- mammalian target of rapamycin (mTOR) Ser2448, total mTOR, phospho-protein kinase B (Akt) Ser473, total Akt, phospho-ribosomal protein S6 kinase (p70S6K) Thr389, total p70S6K1, phospho-eukaryotic translation initiation factor 4E-binding protein 1 (4EBP-1) Thr37/46, total 4EBP1, phospho-S6 protein (RPS6) Ser240/244, total RPS6, phospho-eukaryotic elongation factor 2 (eEF2) Thr56, total eEF2, microtubule-associated protein 1A/B- light chain (LC3A/B), caspase-3 (D3R6Y), muscle RING finger 1 (MuRF-1), and muscle atrophy F-box (MAFbx) (section 2.4.5). After 15-minutes of washing

with TBST membranes were incubated for 1-hour in an anti-rabbit IgG horseradish peroxidase (HRP)-conjugated secondary antibody with the exception of MAFbx (anti-rat IgG, HRP-linked antibody), puromycin and MuRF-1 (anti-mouse IgG, HRP-linked antibody). Details of the antibodies used within this chapter are outlined in Table 2.1. Following 15-minutes of washing in TBST protein content was quantified using immobilon western chemiluminescent HRP substrate and imaged on a G:BOX Chemi XT4 imager using GeneSys capture software as previously described (section 2.4.6). Once the image was captured, band quantification was conducted through the use of ImageJ software as described in section 2.4.6.

3.3.11 Statistical Analysis

Statistical analysis was performed using IBM SPSS Statistics version 26 (IBM SPSS inc. Chicago, Illinois, USA). Data were tested for normality using Shapiro-Wilk test, and for homogeneity of variances using Levene's test. Independent samples t-tests were used to assess differences in anthropometric measures and body composition components (FFM, SMM, FM and body fat %). Additionally, measures of muscle strength; both HGS, and isokinetic dynamometry measures were also assessed using an independent samples t-test. Independent sample t-tests were also used to analyse differences in plasma insulin, glucose and IL-6. A one-way ANOVA was utilised for the analysis of myotube diameter, NFI, puromycin incorporation, and markers anabolic and catabolic signalling. Where the results of the one-way ANOVA revealed a positive interaction effect, post-hoc analysis t-tests were completed using Tukey's HSD. Effect size was calculated using Cohen's d for t-test and post-hoc comparisons, while partial eta squared (η^2) was used for omnibus tests. Statistical significance was set at $p < 0.05$. The data presented include the mean of each participant, over the 3 passage numbers to provide one data point per participant $\pm$ standard deviation, unless stated otherwise. Figures were generated in GraphPad Prism V8.4.3.

3.4 Results

Table 3.1 Participant characteristics for anthropometric, body composition and strength data in young and old males

	Young (n=4)	Old (n=4)	P value
Anthropometrics			
Age (years)	26.5 ± 3.1	72.7± 0.8	<0.001
Body mass (kg)	80.6±19.2	77.1 ±12.0	0.77
Height (cm)	174.9 ±11.8	179.3 ± 4.4	0.50
BMI (kg m^{-2})	26.1 ± 3.1	24.0±3.8	0.43
Body Composition			
FFM (kg)	62.4 ± 11.8	59.4 ± 6.3	0.67
WBFM (kg)	18.2 ± 8.8	17.7 ± 9.7	0.95
BF (%)	21.6 ± 8.0	22.2 ± 8.9	0.92
SMM (kg)	31.7 ± 6.3	27.0 ± 3.7	0.25
Strength			
HGS (kg)	54.75 ± 12.1	45.8 ± 10.4	0.30
Con PT (nm)	209.0 ± 69.1	91.0 ± 18.3	0.016*
Ecc PT (nm)	93.8 ± 46.1	63.0 ± 19.2	0.27
Con WPR (nm)	217.5 ± 74.8	90.3 ± 51.1	0.03*
Ecc WPR (nm)	97.3 ±23.7	69.5 ± 28.1	0.18
Blood Analyses			
Fasting plasma insulin (μIU/mL)	6.4±0.8	8.22±1.6	0.08
Fasting plasma glucose (mmol/L)	4.5±0.4	4.9±0.04	0.11
HOMA-IR	1.3±0.13	1.8±0.4	0.03*
Plasma IL-6 (pg/mL)	0.41±0.07	0.78±0.08	<0.001‡
Plasma CRP (ng/mL)	0.40±0.05	0.53±0.01	<0.001‡

BMI, Body Mass Index, FFM (Fat Free Mass), WBFM (Whole Body Fat Mass), BF (Body Fat %), SMM (Skeletal Muscle Mass) HGS, handgrip strength, Con PT, concentric peak torque, Ecc PT, eccentric peak torque, Con WPR, concentric work per repetition, Ecc WPR, eccentric work per repetition, HOMA-IR, homeostatic model assessment of insulin resistance, IL-6, interleukin-6, CRP, c-reactive protein.
***** Significantly different from young ($P < 0.05$)
‡ Significantly different from young ($P < 0.001$)

3.4.1 Body Composition and Strength

Body composition and strength measures are shown in Table 3.1. No significant difference was observed between young and old participants for whole-body FM, body fat percentage, FFM or SMM. Concentric peak torque ($P = 0.02$, $d = 2.70$) and concentric WPR ($P = 0.03$, $d = 2.03$)

were significantly greater in the young compared to old participants. No significant difference was identified in eccentric peak torque, eccentric WPR or HGS between groups.

3.4.2 Inflammatory Markers and Blood Analysis

Plasma IL-6 and CRP were significantly greater in old, compared with young participants ($P < 0.001$, $d = 4.92$, $P = 0.002$, $d = 4.3$) respectively (Table 3.1). No significant difference was identified in fasting plasma insulin ($P = 0.08$, $d = 1.52$) and plasma glucose ($P = 0.11$, $d = 1.71$) between young and old participants. Homeostatic model assessment of insulin resistance (HOMA-IR) was significantly greater in old, compared with young participants ($P = 0.03$, $d = 2.2$).

3.4.3 Myotube Diameter and Nuclear Fusion Index

Differentiated myotubes were cultured in media conditioned with *ex vivo* human serum from young and old participants over a 24-hour time period. A one-way ANOVA revealed a significant main effect between groups ($P < 0.001$, $\eta^2 = 0.98$, $F = 196.1$) (Figure 3.1). Myotube diameter was significantly greater (45%) in response to conditioning with *ex vivo* human serum from young participants, in comparison to serum from old participants ($p < 0.001$, $d = 14.11$). Additionally, myotube diameter of those treated with serum from young participants was significantly greater (48%) than untreated control myotubes, receiving normal differentiation media over the 24-hour treatment period ($P < 0.0001$, $d = 9.82$). In contrast, cells treated with serum from older participants showed a significant decrease (20%) in myotube diameter in comparison to the untreated control myotubes ($P = 0.0009$, $d = 4.05$).

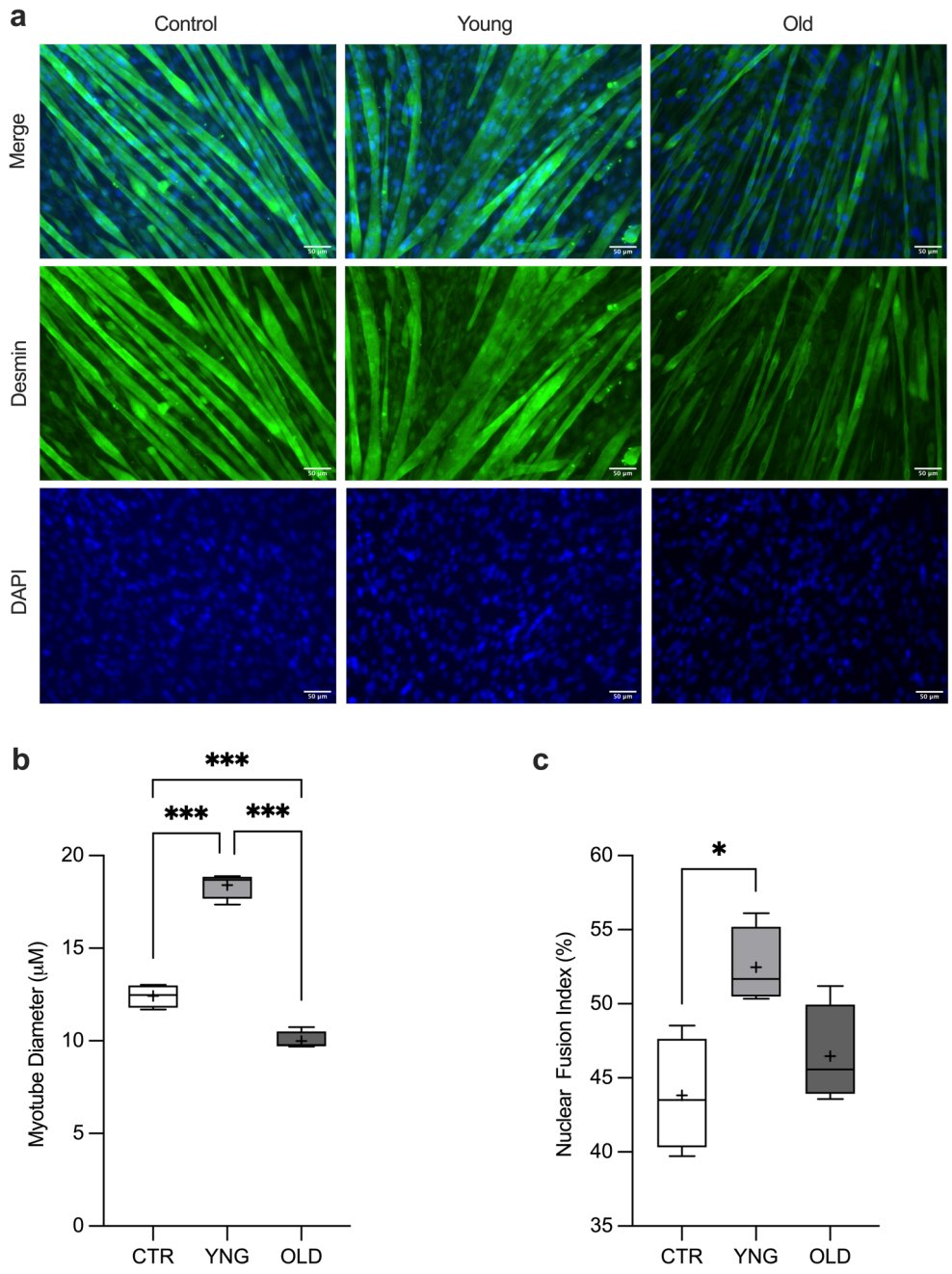

Figure 3.1. Myotube diameter and nuclear fusion index. The effect of *ex vivo* human serum conditioned media on myotube diameter and nuclear fusion index (NFI) *in vitro*. (A) representative images illustrating atrophy in myotubes conditioned with serum from older males in comparison to untreated control C2C12 myotubes and myotubes treated with serum from young males, (B) mean myotube diameter, (C) mean NFI. Data are expressed as the mean (cross), median (central horizontal line), 25th and 75th percentiles (box) and the

minimum and maximum values (vertical lines), with n=4 per group, corresponding to treatment of each participant's serum, repeated in triplicate. * $P < 0.05$, *** $P < 0.001$.

A one-way ANOVA revealed a significant main effect between groups for the analysis of NFI ($P < 0.5$, $\eta^2 = 0.62$, $F = 7.3$) (Figure 3.1). NFI was significantly greater (20%) in myotubes conditioned with young serum, in comparison to the untreated control myotubes ($P = 0.2$, $d = 2.71$). The NFI tended to be greater in myotubes conditioned with young serum, in comparison to old serum, though significance was not reached ($P = 0.06$, $d = 2.02$). No difference was identified in NFI between myotubes conditioned with old serum and untreated control myotubes ($P = 0.5$, $d = 0.7$).

3.4.4 Muscle Protein Synthesis

There was a significant main effect of MPS, measured by the incorporation of puromycin through the SUnSET technique ($P < 0.001$, $\eta^2 = 0.83$, $F = 20.11$) (Figure 3.2). After conditioning with serum from young participants, MPS was significantly increased (32%) in comparison to serum from old participants ($P = 0.008$, $d = 3.7$). Additionally, leucine treatment significantly elevated MPS in myotubes conditioned with young serum compared with myotubes treated with young serum only (25%, $P = 0.04$, $d = 1.7$) and myotubes treated with old serum and leucine (14%, $P < 0.0001$, $d = 3.8$). The addition of leucine did not significantly increase MPS in myotubes conditioned with old serum ($P = 0.6$, $d = 1.5$).

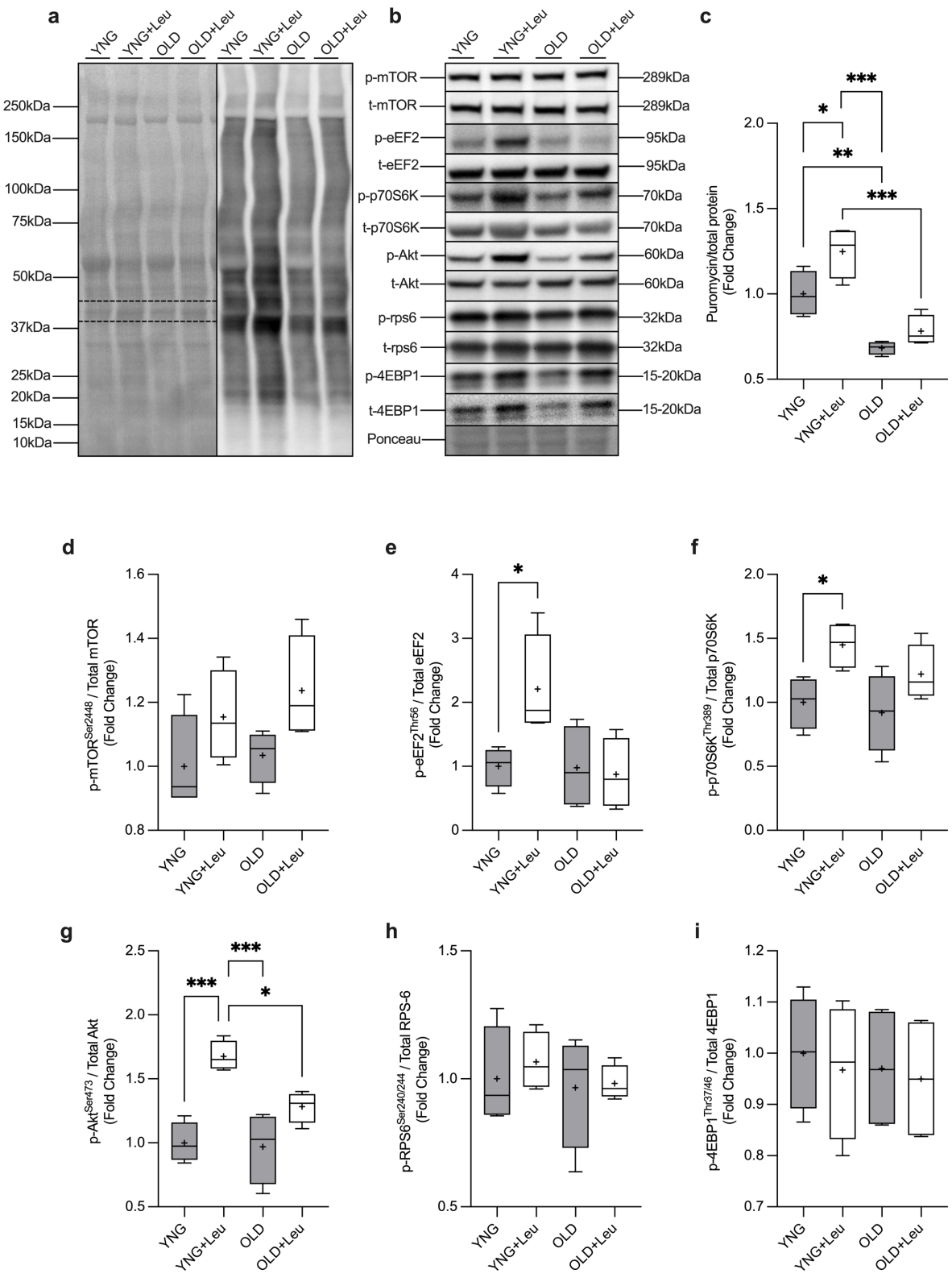

Figure 3.2. Measures of MPS and anabolic signalling in response to the addition of *ex vivo* human serum with and without leucine treatment. Data are represented as fold change in relation to the myotubes treated with *ex vivo* serum from young males. (A)

representative western blot images for puromycin incorporation and total protein, (B) representative western blot images for anabolic signaling markers, (C) puromycin incorporation, (D) phospho-mTORSer^{2448} / total-mTOR, (E) phospho-eEF2^{Thr56} / total-eEF2, (F) phospho-p70S6K^{Thr389} / total-p70S6K, (G) phospho-Akt^{Ser473} / total-Akt, (H) phospho-RPS6$^{Ser240/244}$ / total-RPS6, (I) phospho-4EBP-1$^{Thr37/46}$ / total-4EBP-1. Data are expressed as the mean (cross), median (central horizontal line), 25th and 75th percentiles (box) and the minimum and maximum values (vertical lines), with n=4 per group, corresponding to treatment of each participant's serum, repeated in triplicate. * $P < 0.05$, ** $P < 0.01$, *** $P < 0.001$.

3.4.5 Anabolic Signalling

In response to conditioning media with human serum, with and without the addition of leucine treatment, significant main effects were identified in the phosphorylation of Akt ($P < 0.001$, $\eta^2 = 0.77$, $F = 13.1$), p70S6K ($P = 0.03$, $\eta^2 = 0.51$, $F = 4.2$) and eEF2 ($P = 0.03$, $\eta^2 = 0.51$, $F = 4.3$) (Figure 3.2). No significant difference was identified in the phosphorylation of Akt, eEF2, and p70S6K in response to conditioning with fasted *ex vivo* serum, from young and old participants. However, the activation of Akt (68%, $P = 0.001$, $d = 4.97$), eEF2 (120%, $P = 0.032$, $d = 2.2$) and p70S6K (45%, $P = 0.02$, $d = 2.35$) significantly increased in response to leucine treatment in myotubes conditioned with *ex vivo* serum from young participants. In contrast, there was no significant increase in the activation of Akt and p70S6K in response to the addition of leucine in myotubes conditioned with serum from older individuals. Additionally, no significant difference in eEF2 phosphorylation was identified between myotubes treated with *ex vivo* human serum from older participants, and with the addition of leucine. Akt phosphorylation was significantly elevated in myotubes conditioned with young serum and leucine treatment in comparison to those conditioned with old serum prior to leucine treatment (73%, $P < 0.05$, $d = 3.29$).

There were no significant differences identified in the phosphorylation of mTOR (P = 0.77, $\eta^2 = 0.38$, F = 2.46), RPS6 (P = 0.82, $\eta^2 = 0.07$, F = 0.30) and 4EBP-1 (P = 0.95, $\eta^2 = 0.03$, F = 0.12) between myotubes treated with *ex vivo* human serum from young and old males alone, and with additional leucine treatment.

3.4.6 Catabolic Signalling

No significant differences were identified between myotubes conditioned with young and old serum, with or without leucine treatment, in MuRF-1 (P = 0.74, $\eta^2 = 0.1$, F = 0.42), MAFbx (P = 0.81, $\eta^2 = 0.1$, F = 0.31), caspase 3 (P = 0.9, $\eta^2 = 0.1$, F = 0.25) and LC3A/B I / LC3A/B II (P = 0.056, $\eta^2 = 0.5$, F = 3.33) protein content (Figure 3.3).

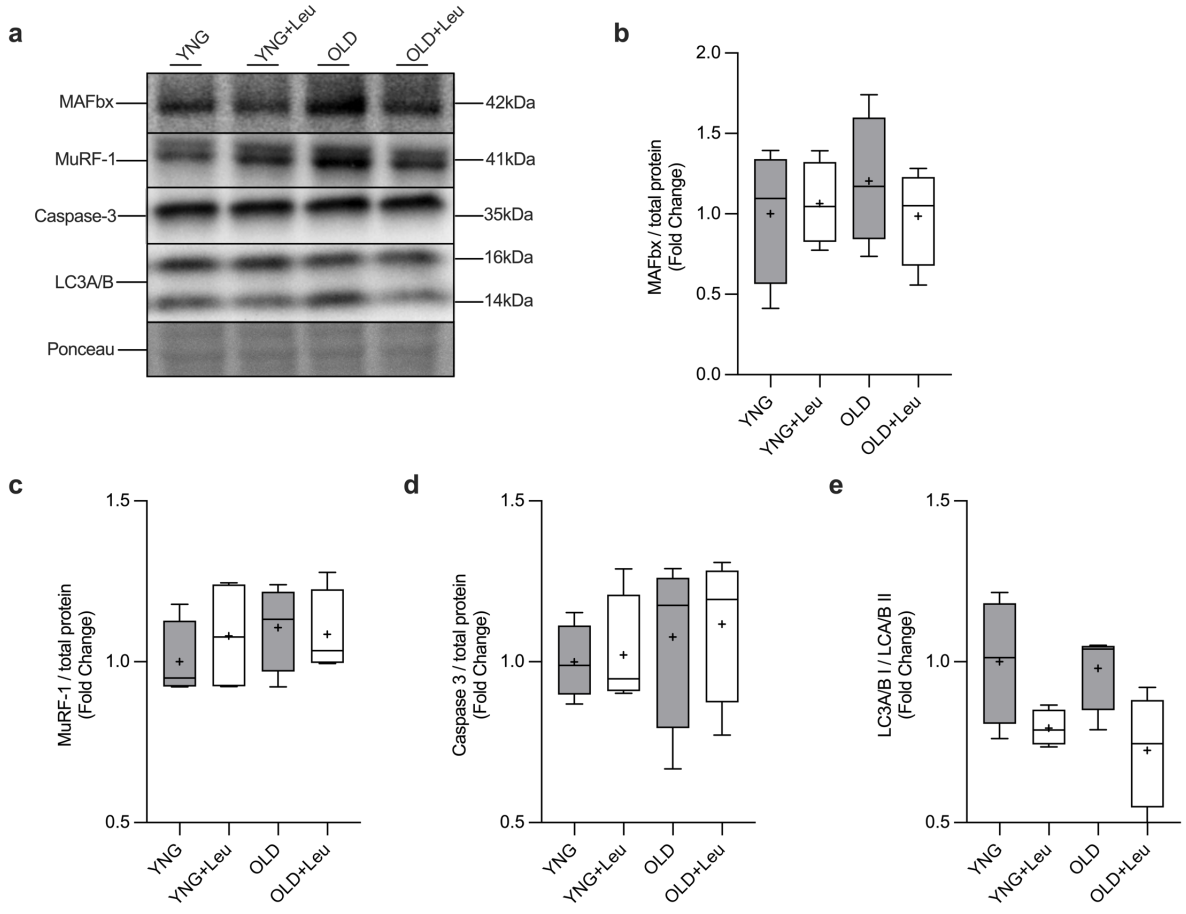

Figure 3.3. Changes in markers of catabolic signalling in response to the addition of *ex vivo* human serum with and without leucine treatment. Data are represented as fold

change in relation to the myotubes treated with *ex vivo* serum from young males. (A) representative western blot images, (B) MAFbx, (C) MuRF-1, (D) caspase-3, (E) LC3A/B. Data are expressed as the mean (cross), median (central horizontal line), 25th and 75th percentiles (box) and the minimum and maximum values (vertical lines), with n=4 per group, corresponding to treatment of each participant's serum, repeated in triplicate.

3.5 Discussion

The development of an *in vitro* model of age-related muscle wasting is useful for the investigation of potential mechanisms and interventions, with potential application to myriad disease conditions. Recent developments have involved the use of replicative ageing (28), TNF-α (22, 23) and DEX (24-27) treatment, but these approaches may not closely represent inherent physiological ageing processes. Therefore, we used *ex vivo* human serum from young and old men to condition C2C12 skeletal muscle myotubes, with and without subsequent *in vitro* anabolic treatment with leucine, in order to develop a more physiologically relevant model to study regulatory mechanisms of muscle ageing. In line with our hypotheses, we demonstrated that cells conditioned with serum from older men led to a decrease in myotube diameter compared with serum from young men. Mechanistically, the smaller myotube diameter appeared to be underpinned by a reduced MPS in older vs. younger serum treated cells. In addition, myotubes treated with old vs. young serum showed a blunted MPS and anabolic signalling response to *in vitro* leucine treatment (i.e., anabolic resistance). The impairment in diameter, MPS and anabolic signalling dysregulation of MPS in myotubes treated with old serum showed associations with markers of inflammation. Collectively, these data highlight that conditioning cell culture media with human serum can be effectively used to study mechanisms of age-related muscle loss, and that systemic inflammatory factors may contribute to age-related muscle loss through impaired anabolism, though blockade of cytokine signalling would be required to confirm this.

Following a 24-hour treatment with *ex vivo* human serum, we found that serum from young men led to a significant increase in myotube diameter in comparison to old serum and untreated control myotubes, whereas old serum decreased myotube diameter compared with untreated control myotubes. This observation is consistent with work by Kalampouka *et al* (32), who identified a reduction in myotube diameter after 24 and 48 hours of treatment with *ex vivo* human plasma from old vs. young humans. In contrast, previous work investigating myotube diameter within human primary skeletal muscle cells failed to identify a difference between young and old donor cells, when cultured under standard conditions (44). It is possible that the absence of any age-related atrophic effect in this study, may result from primary skeletal muscle cells not retaining their phenotype. Similar to the effects of young and old serum on myotube growth, conditioning media with *ex vivo* human serum from young participants resulted in a significant increase in NFI compared with untreated control myotubes, whereas NFI was numerically lower in myotubes treated with old compared with young serum (large effect size). Previous work investigating myogenic fusion index in primary myoblasts identified a decrease in myoblast fusion in cultures from older compared with younger donors (45). In contrast, no difference in myogenic fusion index was observed in myoblasts treated with serum from young and old participants, suggesting that myoblasts sustain the capacity to fuse, independent of the donor age (46). However, the absence of an age-related difference in NFI herein, may be due to the lower percentage (2%) serum enriched media used throughout the experiment. Notwithstanding, the present data reinforce the concept that serum from human participants can modulate myotube growth and NFI and be applied to probe mechanisms and countermeasures to age and disease-related muscle atrophy.

Analogous to myotube growth data, we report that acute MPS stimulation and anabolic signalling were dysregulated in myotubes conditioned with serum from old donors.

This observation is in line with *in vivo* human trials highlighting a reduction in basal MPS in older men (47-49). However, it is important to note that others have suggested that basal MPS rates are not influenced by the ageing process (50). Despite the age-related difference in MPS, no difference in the phosphorylation of mTOR, p70S6K, Akt, 4EBP-1 and RPS6 was found between young and old serum treated myotubes. Whilst this observation is generally consistent with data from *in vivo* human trials showing no age-related impairment in basal anabolic signalling (20, 51, 52), it should be noted that the phosphorylation of mTOR, p70S6K and Akt increased only in myotubes conditioned with young serum. Similarly, in response to the addition of leucine, a blunted MPS response and mTOR, p70S6K and Akt phosphorylation was observed in myotubes conditioned with older vs. younger donor serum. This suggests that old serum treated myotubes experience a diminished anabolic response to leucine treatment, which aligns with the concept of age-related muscle anabolic resistance to protein provision demonstrated in *in vivo* human and animal experimental studies (20, 21, 53, 54). Additionally, we identified no difference in markers of MPB, including MuRF-1 and MAFbx, in response to the addition of young vs. old serum alone, which is consistent with previous *in vivo* work in rats which identified no difference in MuRF-1 protein content between middle-aged and older mice (55). However, despite the fact that MuRF-1 and MAFbx have been shown to be upregulated in models of atrophy such as immobilization and limb unloading, the role of the ubiquitin proteasome pathway in sarcopenia progression is unclear (56, 57). Overall, this suggests that the addition of serum from older individuals contributes to a dysregulation in MPS, that may underpin changes in myotube atrophy identified.

The differences in myotube growth and MPS between cells treated with *ex vivo* serum from young and old individuals, may partially be underpinned by the low-grade inflammatory status that is a hallmark of ageing (31). Ageing is often associated with chronic elevations in

concentrations of pro-inflammatory cytokines including CRP, IL-6 and TNF-α (58) and may increase sarcopenia risk (11) through association with MPS (17). Indeed, the present data show elevated concentrations of pro-inflammatory cytokines in old vs. young individuals. In rodents, it has been suggested that low-grade inflammation (LGI) influences the age-related anabolic resistance to food intake, whereas rodents without LGI appear to restore robust postprandial MPS responses (59, 60). Further *in vivo* human studies are required to resolve the role of LGI on postprandial MPS in older humans, which is currently unclear (61, 62). Other systemic factors, such as glucose (63) and insulin (64), have been suggested to influence the growth of C2C12s through myogenesis, although these factors did not differ between young and old donors in the present study. We acknowledge that alterations in factors not measured in this study including: myostatin (65), irisin (66), testosterone (67), insulin growth factor-1 and growth hormone (68) may also influence age-related muscle atrophy. Finally, the relative role of inherent ageing processes (e.g. senescence (69), endocrine changes and mitochondrial dysfunction (70)) and artefacts of biological ageing, (e.g. inactivity (71-73) and raised BMI (74)), that induce LGI, in age-related muscle loss and MPS dysregulation requires further attention. It is likely that all of these factors play some role in sarcopenia progression, with the degree varying between individuals.

Although this *in vitro* model provides a novel, valuable means of investigating mechanisms of age-related muscle loss, it is worth noting that there are limitations to this approach. In the present study, myotubes were conditioned with only 10% human serum in order to maintain cell viability. Although this induced some changes in anabolic signalling markers, this low concentration may not maximally stimulate changes in MPS, anabolic or catabolic markers. Additionally, we did not condition primary human skeletal muscle cells with young and old human serum, instead using C2C12 murine cells, which may cause issues related to cross-species differences. While this approach is beneficial for use when human

primary skeletal muscle cells are unavailable, we are unable to discount the potential role of intrinsic muscle properties and cellular environmental factors on the regulation of growth with serum treatment. Future research should therefore aim to replicate this work using human primary skeletal muscle cells from young and old donors, matched with serum from these participants. Finally, the dose of leucine applied herein could be deemed 'supraphysiological' and repeat experiments using fed vs. fasted serum would be a useful means of confirming and expanding on the current findings.

In conclusion, conditioning cell culture media with *ex vivo* human serum enabled us to establish a novel model to study the effects of the young and old systemic milieu on regulatory mechanisms of myotube growth. We report that *ex vivo* serum from young participants increased MPS and induced myotube hypertrophy, while serum from old participants induced myotube atrophy in comparison to untreated control myotubes and young treated myotubes, allied to lower rates of MPS. Furthermore, we showed that myotubes conditioned with old serum display a diminished anabolic response to the addition of leucine treatment, in comparison to those treated with young serum. Collectively, this study indicates that *ex vivo* human serum can be successfully utilised to create an *in vitro* model to study potential mechanisms of and countermeasures to age-related muscle loss, providing a more physiologically relevant model than current pharmacological treatments.

Acknowledgements: The authors would like to thank Alex Seabright for his assistance in data analysis. The authors would like to extend our thanks to the research participants.

Author Contributions: S.L.A., G.G.L and L.B conceived and designed the research. S.L.A conducted all *in vitro* experiments. S.L.A and R.N.M completed human participant data collection. S.L.A and S. J.E analyzed the data. S.L.A, L.B., and G.G.L wrote the manuscript.

S.L.A, R.N.M, S.J.E, J.M.L, G.G.L and L.B contributed to the interpretation of the results, edited and approved of the final manuscript.

Funding: The study was funded by the National Institute for Health Research (NIHR) Birmingham Biomedical Research Centre (BRC-1215-20009). The views expressed are those of the authors and not necessarily those of the NIHR, or the Department of Health and Social Care.

Disclosures: The authors declare no conflicts of interest.

3.6 References

1. **Cruz-Jentoft AJ, Bahat G, Bauer J, Boirie Y, Bruyere O, Cederholm T, Cooper C, Landi F, Rolland Y, Sayer AA, and Schneider SM**. Sarcopenia: revised European consensus on definition and diagnosis. *Age Ageing* 48: 16-31, 2019.
2. **Arango-Lopera VE, Arroyo P, Gutierrez-Robledo LM, Perez-Zepeda MU, and Cesari M**. Mortality as an adverse outcome of sarcopenia. *J Nutr Health Aging* 17: 259-262, 2013.
3. **Schaap LA, van Schoor NM, Lips P, and Visser M**. Associations of Sarcopenia Definitions, and Their Components, With the Incidence of Recurrent Falling and Fractures: The Longitudinal Aging Study Amsterdam. *J Gerontol A Biol Sci Med Sci* 73: 1199-1204, 2018.
4. **Janssen I, Heymsfield SB, and Ross R**. Low relative skeletal muscle mass (sarcopenia) in older persons is associated with functional impairment and physical disability. *J Am Geriatr Soc* 50: 889-896, 2002.
5. **Srikanthan P, Hevener AL, and Karlamangla AS**. Sarcopenia exacerbates obesity-associated insulin resistance and dysglycemia: findings from the National Health and Nutrition Examination Survey III. *PLoS One* 5: e10805, 2010.
6. **Rizzoli R, Register JY, Arnal JF, Bautmans I, Beaudart C, Bischoff-Ferrari H, Biver E, Boonen S, Brandi ML, Chines A, Cooper C, Epstein S, Fielding RA, Goodpaster B, Kanis JA, Kaufman JM, Laslop A, Malafarina V, Manas LR, Mitlack BH, Oreffo RO, Petermans J, Reid K, Rolland Y, Sayer AA, Tsouderos Y, Visser M, and Bruyere O**. Quality of life in sarcopenia and frailty. *Calcif Tissue Int* 93: 101-120, 2013.
7. **Ethgen O, Beaudart C, Buckinx F, Bruyere O, and Reginster JY**. The Future Prevalence of Sarcopenia in Europe: A Claim for Public Health Action. *Calcif Tissue Int* 100: 229-234, 2017.
8. **Pinedo-Villanueva R, Westbury LD, Syddall HE, Sanchez-Santos MT, Dennison EM, Robinson SM, and Cooper C**. Health Care Costs Associated With Muscle Weakness: A UK Population-Based Estimate. *Calcif Tissue Int* 104: 137-144, 2018.
9. **Goates S, Du K, Arensberg MB, Gaillard T, Guralnik J, and Pereira SL**. Economic Impact of Hospitalizations in US Adults with Sarcopenia. *J Frailty Aging* 8: 93-99, 2019.
10. **Narici MV, and Maffulli N**. Sarcopenia: characteristics, mechanisms and functional significance. *British Medical Bulletin* 95: 139-159, 2010.
11. **Schaap LA, Pluijm SM, Deeg DJ, and Visser M**. Inflammatory markers and loss of muscle mass (sarcopenia) and strength. *Am J Med* 119: 526 e529-517, 2006.
12. **Schaap LA, Pluijm SM, Deeg DJ, Harris TB, Kritchevsky SB, Newman AB, Colbert LH, Pahor M, Rubin SM, Tylavsky FA, Visser M, and Health ABCS**. Higher inflammatory marker levels in older persons: associations with 5-year change in muscle mass and muscle strength. *J Gerontol A Biol Sci Med Sci* 64: 1183-1189, 2009.
13. **Visser M, Pahor M, Taaffe DR, Goodpaster BH, Simonsick EM, Newman AB, Nevitt M, and Harris TB**. Relationship of interleukin-6 and tumor necrosis factor-alpha with muscle mass and muscle strength in elderly men and women: the health ABC study. *J Gerontol A Biol Sci Med Sci* 57: M326-332, 2002.
14. **Cesari M, Penninx BW, Pahor M, Lauretani F, Corsi AM, Rhys Williams G, Guralnik JM, and Ferrucci L**. Inflammatory markers and physical performance in older persons: the InCHIANTI study. *J Gerontol A Biol Sci Med Sci* 59: 242-248, 2004.
15. **Brinkley TE, Leng X, Miller ME, Kitzman DW, Pahor M, Berry MJ, Marsh AP, Kritchevsky SB, and Nicklas BJ**. Chronic inflammation is associated with low physical

function in older adults across multiple comorbidities. *J Gerontol A Biol Sci Med Sci* 64: 455-461, 2009.
16. **Cesari M, Kritchevsky SB, Baumgartner RN, Atkinson HH, Penninx BW, Lenchick L, Palla SL, Ambrosius WT, Tracy RP, and Pahor M**. Sarcopenia, obesity, and inflammation--results from the Trial of Angiotensin Converting Enzyme Inhibition and Novel Cardiovascular Risk Factors study. *Am J Clin Nutr* 82: 428-434, 2005.
17. **Toth MJ, Matthews DE, Tracy RP, and Previs MJ**. Age-related differences in skeletal muscle protein synthesis: relation to markers of immune activation. *Am J Physiol Endocrinol Metab* 288: E883-E891, 2005.
18. **Wahlin-Larsson B, Wilkinson DJ, Strandberg E, Hosford-Donovan A, Atherton PJ, and Kadi F**. Mechanistic Links Underlying the Impact of C-Reactive Protein on Muscle Mass in Elderly. *Cell Physiol Biochem* 44: 267-278, 2017.
19. **Moore DR, Churchward-Venne TA, Witard O, Breen L, Burd NA, Tipton KD, and Phillips SM**. Protein ingestion to stimulate myofibrillar protein synthesis requires greater relative protein intakes in healthy older versus younger men. *J Gerontol A Biol Sci Med Sci* 70: 57-62, 2015.
20. **Cuthbertson D, Smith K, Babraj J, Leese G, Waddell T, Atherton P, Wackerhage H, Taylor PM, and Rennie MJ**. Anabolic signaling deficits underlie amino acid resistance of wasting, aging muscle. *FASEB J* 19: 422-424, 2005.
21. **Katsanos CS, Kobayashi H, Sheffield-Moore M, Aarsland A, and Wolfe RR**. Aging is associated with diminished accretion of muscle proteins after the ingestion of a small bolus of essential amino acids. *Am J Clin Nutr* 82: 1065-1073, 2005.
22. **Stewart CE, Newcomb PV, and Holly JM**. Multifaceted roles of TNF-alpha in myoblast destruction: a multitude of signal transduction pathways. *J Cell Physiol* 198: 237-247, 2004.
23. **Sharples AP, Al-Shanti N, and Stewart CE**. C2 and C2C12 murine skeletal myoblast models of atrophic and hypertrophic potential: relevance to disease and ageing? *J Cell Physiol* 225: 240-250, 2010.
24. **Crossland H, Smith K, Atherton PJ, and Wilkinson DJ**. A novel stable isotope tracer method to simultaneously quantify skeletal muscle protein synthesis and breakdown. *Metabol Open* 5: 100022, 2020.
25. **Desler MM, Jones SJ, Smith CW, and Woods TL**. Effects of Dexamethasone and Anabolic Agents on Proliferation and Protein Synthesis and Degradation in C2C12 Myogenic Cells. *J Anim Sci* 74: 1265-1273, 1996.
26. **Stitt TN, Drujan D, Clarke BA, Panaro F, Timofeyva Y, Kline WO, Gonzalez M, Yancopoulos GD, and Glass DJ**. The IGF-1/PI3K/Akt pathway prevents expression of muscle atrophy-induces ubiquitin ligases by inhibiting FOXO transcription factors. *Mol Cell* 14: 395-403, 2004.
27. **Sandri M, Sandri C, Gilbert A, Skurk C, Calabria E, Picard A, Walsh K, Schiaffino S, Lecker SH, and Goldberg AL**. Foxo Transcription Factors Induce the Atrophy-Related Ubiquitin Ligase Atrogin-1 and Cause Skeletal Muscle Atrophy. *Cell* 117: 399-412, 2004.
28. **Sharples AP, Al-Shanti N, Lewis MP, and Stewart CE**. Reduction of myoblast differentiation following multiple population doublings in mouse C2 C12 cells: a model to investigate ageing? *J Cell Biochem* 112: 3773-3785, 2011.
29. **Holt SE, Wright WE, and Shay JW**. Regulation of telomerase activity in immortal cell lines. *Mol Cell Biol* 16: 2932-2939, 1996.
30. **O'Connor MS, Carlson ME, and Conboy IM**. Differentation rather than aging of muscle stem cells abolishes their telomerase activity. *Biotechnol Prog* 25: 1130-1137, 2019.

31. **Lopez-Otin C, Blasco MA, Partridge L, Serrano M, and Kroemer G**. The hallmarks of aging. *Cell* 153: 1194-1217, 2013.
32. **Kalampouka I, van Bekhoven A, and Elliott BT**. Differing effects of younger and older human plasma on C2C12 myocytes in vitro. *Front Physiol* 9: 152, 2018.
33. **van Hees HW, Schellekens WJ, Linkels M, Leenders F, Zoll J, Donders R, Dekhuijzen PN, van der Hoeven JG, and Heunks LM**. Plasma from septic shock patients induces loss of muscle protein. *Crit Care* 15: R233, 2011.
34. **Carson BP, Patel B, Amigo-Benavent M, Pauk M, Kumar Gujulla S, Murphy SM, Kiely PA, and Jakeman PM**. Regulation of muscle protein synthesis in an in vitro cell model using ex vivo human serum. *Exp Physiol* 103: 783-789, 2018.
35. **Patel B, Pauk M, Amigo-Benavent M, Nongonierma AB, Fitzgerald RJ, Jakeman PM, and Carson BP**. A cell-based evaluation of a non-essential amino acid formulation as a non-bioactive control for activation and stimulation of muscle protein synthesis using ex vivo human serum. *PLoS One* 14: e0220757, 2019.
36. **Corrick KL, Stec MJ, Merritt EK, Windham ST, Thomas SJ, Cross JM, and Bamman MM**. Serum from human burn victims impairs myogenesis and protein synthesis in primary myoblasts. *Front Physiol* 6: 184, 2015.
37. **Catteau M, Gouzi F, Blervaque L, Passerieux E, Blaquière M, Ayoub B, Bughin F, Mercier J, Hayot M, and Pomiès P**. Effects of a human microenvironment on the differentiation of human myoblasts. *Biochem Biophsy Res Commun* 525: 968-973, 2020.
38. **Bosy-Westphal A, Jensen B, Braun W, Pourhassan M, Gallagher D, and Muller MJ**. Quantification of whole-body and segmental skeletal muscle mass using phase-sensitive 8-electrode medical bioelectrical impedance devices. *Eur J Clin Nutr* 71: 1061-1067, 2017.
39. **Roberts HC, Denison HJ, Martin HJ, Patel HP, Syddall H, Cooper C, and Sayer AA**. A review of the measurement of grip strength in clinical and epidemiological studies: towards a standardised approach. *Age Ageing* 40: 423-429, 2011.
40. **Tarum J, Folkesson M, Atherton PJ, and Kadi F**. Electrical pulse stimulation: an in vitro exercise model for the induction of human skeletal muscle cell hypertrophy. A proof-of-concept study. *Exp Physiol* 102: 1405-1413, 2017.
41. **Agley CC, Velloso CP, Lazarus NR, and Harridge SDR**. An Image Analysis Method for the Precise Selection and Quantification of Fluorescently Labeled Cellular Constituents: Application to the Measurement of Human Muscle Cells in Culture. *J Histochem Cytochem* 60: 428-438, 2012.
42. **Goodman CA, Mabrey DM, Frey JW, Miu MH, Schmidt EK, Pierre P, and Hornberger TA**. Novel insights into the regulation of skeletal muscle protein synthesis as revealed by a new nonradioactive in vivo technique. *FASEB J* 25: 1028-1039, 2011.
43. **Romero-Calvo I, Ocón B, Martínez-Moya P, Suárez MD, Zarzuelo A, Martínez-Augustin O, and Sánchez de Medina F**. Reversible Ponceau staining as a loading control alternative to actin in Western blots. *Anal Biochem* 401: 318-320, 2010.
44. **Alsharidah M, Lazarus NR, George TE, Agley CC, Velloso CP, and Harridge SD**. Primary human muscle precursor cells obtained from young and old donors produce similar proliferative, differentiation and senescent profiles in culture. *Aging Cell* 12: 333-344, 2013.
45. **Brzeszczynska J, Meyer A, McGregor R, Schilb A, Degen S, Tadini V, Johns N, Langen R, Schols A, Glass DJ, Roubenoff R, Ross JA, Fearon KCH, Greig CA, and Jacobi C**. Alterations in the in vitro and in vivo regulation of muscle regeneration in healthy ageing and the influence of sarcopenia. *J Cachexia Sarcopenia Muscle* 9: 93-105, 2018.
46. **George T, Velloso CP, Alsharidah M, Lazarus NR, and Harridge SD**. Sera from young and older humans equally sustain proliferation and differentiation of human myoblasts. *Exp Gerontol* 45: 875-881, 2010.

47. **Welle S, Thornton C, Jozefowicz R, and Statt M**. Myofibrillar protein synthesis in young and old men. *Am J Physiol* 264: E693-698, 1993.
48. **Rooyackers OE, Adey DB, Ades PA, and Sreekumaran Nair K**. Effect of age on in vivo rates of mitochondrial protein synthesis in human skeletal muscle. *Proc Natl Acad Sci U S A* 93: 15364-15369, 1996.
49. **Yarasheski K, Zacharewicz E, and Bier D**. Acute effects of resistance exercise on muscle protein synthesis rate in young and elderly men and women. *Am J Physiol* 265: E210-214, 1993.
50. **Volpi E, Sheffield-Moore M, Rasmussen BB, and Wolfe RR**. Basal muscle amino acid kinetics and protein synthesis in healthy young and older men. *JAMA* 286: 1206-1212, 2001.
51. **Kumar V, Selby A, Rankin D, Patel R, Atherton P, Hildebrandt W, Williams J, Smith K, Seynnes O, Hiscock N, and Rennie MJ**. Age-related differences in the dose-response relationship of muscle protein synthesis to resistance exercise in young and old men. *J Physiol* 587: 211-217, 2009.
52. **Drummond MJ, Dreyer HC, Pennings B, Fry CS, Dhanani S, Dillon EL, Sheffield-Moore M, Volpi E, and Rasmussen BB**. Skeletal muscle protein anabolic response to resistance exercise and essential amino acids is delayed with ageing. *J Appl Physiol* 104: 1452-1461, 2008.
53. **Wall BT, Gorissen SH, Pennings B, Koopman R, Groen BB, Verdijk LB, and van Loon LJ**. Aging Is Accompanied by a Blunted Muscle Protein Synthetic Response to Protein Ingestion. *PLoS One* 10: e0140903, 2015.
54. **Dardevet D, Sornet C, Balage M, and Grizard J**. Stimulation of in Vitro Rat Muscle Protein Synthesis by Leucine Decreases With Age. *J Nutr* 130: 2630-2635, 2000.
55. **Gaugler M, Brown A, Merrell E, DiSanto-Rose M, Rathmacher JA, and Reynolds THt**. PKB signaling and atrogene expression in skeletal muscle of aged mice. *J Appl Physiol (1985)* 111: 192-199, 2011.
56. **Dalle S, Rossmeislova L, and Koppo K**. The Role of Inflammation in Age-Related Sarcopenia. *Front Physiol* 8: 1045, 2017.
57. **Bodine SC, and Baehr LM**. Skeletal muscle atrophy and the E3 ubiquitin ligases MuRF1 and MAFbx/atrogin-1. *Am J Physiol Endocrinol Metab* 307: E469-484, 2014.
58. **Ferrucci L, and Fabbri E**. Inflammageing: chronic inflammation in ageing, cardiovascular disease and frailty. *Nat Rev Cardiol* 15: 505-522, 2018.
59. **Balage M, Averous J, Remond D, Bos C, Pujos-Guillot E, Papet I, Mosoni L, Combaret L, and Dardevet D**. Presence of low-grade inflammation impaired postprandial stimulation of muscle protein synthesis in old rats. *J Nutr Biochem* 21: 325-331, 2010.
60. **Rieu I, Magne H, Savary-Auzeloux I, Averous J, Bos C, Peyron MA, Combaret L, and Dardevet D**. Reduction in low grade inflammation restores blunting of postprandial muscle anabolism and limits sarcopenia in old rats. *J Physiol* 587: 5483-5492, 2009.
61. **Buffière C, Mariotti F, Savary-Auzeloux I, Mignè C, Hercberg S, Rèmond D, Duclos M, and Dardevet D**. Slight chronic elevation of C-reactive protein is associated with lower aerobic fitness but does not impair meal-induced stimulation of muscle protein metabolism in healthy old men. *J Physiol* 593: 1259-1272, 2015.
62. **Dideriksen K, Reitelseder S, Malmgaard-Clausen NM, Bechshoeft R, Petersen RK, Mikkelsen UR, and Holm L**. No effect of anti-inflammatory medication on postprandial and postexercise muscle protein synthesis in elderly men with slightly elevated systemic inflammation. *Exp Gerontol* 83: 120-129, 2016.
63. **Luo W, Ai L, Wang BF, and Zhou Y**. High glucose inhibits myogenesis and induces insulin resistance by down-regulating AKT signalling. *Biomed Parmacother* 120: 109498, 2019.

64. **Conejo R, Valverde AM, Benito M, and Loernzo M**. Insulin produces myogenesis in C2C12 myoblasts by induction of NF-kappaB and downregulation of AP-1 activities. *J Cell Physiol* 186: 82-94, 2001.
65. **Baczek J, Silkiewicz M, and Wojszel ZB**. Myostatin as a Biomarker of Muscle Wasting and other Pathologies-State of the Art and Knowledge Gaps. *Nutrients* 12: 2401, 2020.
66. **Planella-Farrugia C, Comas F, Sabater-Masdeu M, Moreno M, Moreno-Navarrete JM, Rovira O, Ricart W, and Fernandez-Real JM**. Circulating Irisin and Myostatin as Markers of Muscle Strength and Physical Condition in Elderly Subjects. *Front Physiol* 10: 871, 2019.
67. **Saad F, Rohrig G, von Haehling S, and Traish A**. Testosterone Deficiency and Testosterone Treatment in Older Men. *Gerontology* 63: 144-156, 2017.
68. **Bian A, Ma Y, Zhou X, Guo Y, Wang W, Zhang Y, and Wang X**. Association between sarcopenia and levels of growth hormone and insulin-like growth factor-1 in the elderly. *BMC Musculoskelet Disord* 21: 214, 2020.
69. **Lutz CT, and Quinn LS**. Sarcopenia, obesity, and natural killer cell immune senescence in aging: Altered cytokine levels as a common mechanism. *Aging (Albany NY)* 4: 535-546, 2012.
70. **Marzetti E, Calvani R, Cesari M, Buford TW, Lorenzi M, Behnke BJ, and Leeuwenburgh C**. Mitochondrial dysfunction and sarcopenia of aging: from signaling pathways to clinical trials. *Int J Biochem Cell Biol* 45: 2288-2301, 2013.
71. **Dirks ML, Wall BT, van den Valk B, Holloway TM, Chabowski A, Goossens GH, and van Loon LJ**. One week of bed rest leads to substantial muscle atrophy and induces whole-body insulin resistance in the abscence of skeletal muscle lipid accumulation. *Diabetes* 65: 2862-2875, 2016.
72. **Breen L, Stokes KA, Churchward-Venne TA, Moore DR, Baker SK, Smith K, Atherton PJ, and Phillips SM**. Two weeks of reduced activity decreases leg lean mass and induces "anabolic resistance" of myofibrillar protein synthesis in healthy elderly. *J Clin Endocrinol Metab* 98: 2604-2612, 2013.
73. **Tanner RE, Brunker LB, Agergaard J, Barrows KM, Briggs RA, Kwon OS, Young LM, Hopkins PN, Volpi E, Marcus RL, LaStayo PC, and Drummond MJ**. Age-related differences in lean mass, protein synthesis and skeletal muscle markers of proteolysis after bed rest and exercise rehabilitation. *J Physiol* 593: 4259-4273, 2015.
74. **Smeuninx B, Greig CA, and Breen L**. Amount, Source and Pattern of Dietary Protein Intake Across the Adult Lifespan: A Cross-Sectional Study. *Front Nutr* 7: 25, 2020.

CHAPTER 4 – THE DEVELOPMENT OF A NOVEL IN VITRO MODEL OF LIVER DISEASE

The Effect of *Ex Vivo* Human Serum From Liver Disease Patients on Cellular Protein Synthesis and Growth

Sophie L. Allen [1,2], Alex P. Seabright [1], Jonathan I. Quinlan [1,2], Amritpal Dhaliwal [2,4,5], Felicity R. Williams [2,4,5], Nicholas H. F. Fine [6], David J. Hodson [6,7], Matthew J. Armstrong [2,5], Ahmed M. Elsharkawy [2,5], Carolyn A. Greig [1,2,3], Yu-Chiang Lai [1,3,6], Janet M. Lord [2,3,4], Gareth G. Lavery [2,6], Leigh Breen [1,2,3*]

Affiliations: [1] School of Sport, Exercise and Rehabilitation Sciences, University of Birmingham, UK. [2] National Institute for Health Research, Birmingham Biomedical Research Centre at University Hospitals Birmingham NHS Foundation Trust, Birmingham, UK. [3] MRC-Versus Arthritis Centre for Musculoskeletal Ageing Research, University of Birmingham, UK. [4] Institute of Inflammation and Ageing, University of Birmingham, UK. [5] Liver Unit, Queen Elizabeth Hospital Birmingham, Nuffield House, Mindelsohn Way, Birmingham, UK. [6] Institute of Metabolism and Systems Research, University of Birmingham, UK. [7] Centre for Endocrinology, Diabetes and Metabolism, Birmingham Health Partners, Birmingham, UK.

*Corresponding Author: Leigh Breen

School of Sport, Exercise and Rehabilitation Sciences

University of Birmingham

Edgbaston

B15 2TT

Email [redacted]

Running title: *In vitro* model of Chronic Liver Disease

Word Count (excluding abstract and references):5780

Key Words: Chronic Liver Disease, Sarcopenia, Leucine, Mitochondria

4.1 Abstract

Background: Sarcopenia is a common complication affecting liver disease patients, yet the underlying mechanisms remain unclear. We aimed to elucidate the cellular mechanisms that underpin sarcopenia development in liver disease through the use of an *in vitro* model utilising C2C12 muscle cells and serum from End-Stage Liver Disease (ESLD) and non-alcoholic fatty liver disease (NAFLD) patients.

Methods: Fasted blood samples were obtained from 4 non-cirrhotic NAFLD patients (aged 61.8±7.6 years), 4 decompensated ESLD patients (aged 60.5±1.7 years) and 4 age-matched healthy controls (CON; aged 64.7±10.0 years). C2C12 myotubes were serum and amino acid starved for 1-hour and subsequently conditioned with serum from CON, NAFLD and ESLD patients for 4- or 24-hours. After 4-hours C2C12 myotubes were treated with 5mM leucine for 30-minutes to provide an anabolic stimulus. Myotube diameter was assessed using fluorescence microscopy. Mitochondrial function was measured through respiration utilising a mitochondrial stress test on an XFe24 Seahorse Analyser and mitophagy was assessed using a C2C12 mitoQC cell line. Muscle protein synthesis (MPS) was determined using the surface sensing of translation (SUnSET) technique and markers of anabolic and catabolic signalling were measured via western blotting.

Results: ESLD patients exhibited increased serum ammonia, CRP, IL-6 and HOMA-IR vs. CON and NAFLD ($p < 0.05$). Myotube diameter was reduced following treatment with serum from ESLD compared with CON (-45%) and NAFLD (-35%; $p < 0.001$ for both) serum. A reduction in maximal mitochondrial respiration (24% and 29%, respectively), coupling efficiency (~12%) and mitophagy (~13%) was identified in myotubes conditioned with NAFLD and ESLD serum compared with CON ($p < 0.05$ for both). Mitochondrial protein content was unchanged. Myostatin (43%, $p = 0.04$) and MuRF-1 (41%, $p = 0.03$) protein content was elevated in myotubes treated with ESLD serum compared with CON. No

change in basal or leucine-stimulated MPS or anabolic signalling was identified within or between groups.

Conclusions: We show myotube atrophy in cells conditioned with *ex vivo* serum from ESLD patients in comparison to CON and NAFLD patients, which was accompanied by mitochondrial dysfunction and increased markers of proteolysis. This work provides an experimental platform to further probe changes in circulating markers associated with chronic liver disease which may drive sarcopenia and develop targeted therapeutic interventions to mitigate sarcopenia.

4.2 Introduction

A loss of muscle mass, quality and strength, termed sarcopenia, is a common complication affecting ~25-70% of cirrhotic patients (1) and is considered a major component of malnutrition (2, 3). Sarcopenic cirrhotic patients have been shown to have an increase in pre- and post- liver transplant complications including infections, length of hospital stay (4), mortality (5) and a decrease in quality of life (QoL) (6). Despite the recognised clinical complications and socio-economic burden of sarcopenia in chronic liver disease, the underlying mechanisms remain poorly understood (7).

Muscle atrophy is underscored by a negative net muscle protein balance arising from differences in muscle protein synthesis (MPS) and muscle protein breakdown (MPB). Impaired muscle protein turnover in chronic liver disease patients may be driven by hyperammonemia (8), inflammation (9), alcohol (10), physical inactivity (11) and insulin resistance (12). Limited evidence in humans suggests that end stage liver disease (ESLD) patients experience a diminished MPS and anabolic signalling response to amino acid provision (13) compared with healthy individuals. Whole-body protein breakdown (WbPB) and MPB are also reportedly elevated in cirrhotic patients compared with healthy individuals, alongside increased markers of autophagy (14, 15). Finally, the myogenesis inhibitor myostatin has been found to be elevated in cirrhosis (8) and may be linked to alterations in protein turnover (9). Given the paucity of evidence from human studies, the mechanisms of sarcopenia in liver disease patients across different aetiologies and disease stages remain unclear. This is compounded by safety concerns around serial muscle biopsy sampling in liver disease patients due to their altered coagulation status and thrombocytopenia (14).

Beyond *in vivo* human studies, alternative *in vitro* (8) and *in vivo* (16) models of ESLD-like muscle atrophy have been developed through the use of ammonia treatment. These models highlight reductions in myotube atrophy *in vitro* (8) and muscle mass in

portacaval anastomosis (PCA) rats (16). However, the physiological relevance of *in vivo* animal and *in vitro* cell models of liver disease has been questioned (17). Recently, an *in vitro* model in which C2C12 cells were conditioned with *ex vivo* human serum was used to demonstrate differences in cell morphology and MPS in the context of age-related sarcopenia (18), with findings aligned to evidence from *in vivo* human studies (19). This novel experimental approach offers a potential avenue to probe mechanisms of sarcopenia in liver disease patients across different aetiologies (e.g., alcohol-related and non-alcoholic fatty liver disease; NAFLD) and stages of disease severity (cirrhotic and non-cirrhotic).

Alterations in muscle protein turnover in chronic liver disease may arise due to a number of contributing factors, including impairments in mitochondrial function (20). Specifically, mitochondrial dysfunction may contribute to a reduction in MPS through the diminution of tricarboxylic acid cycle (TCA) intermediates and adenosine triphosphate (ATP) synthesis, as shown with *in vitro* and *in vivo* hyperammonemia treatment (20). This reduction in ATP may impair MPS, as translation initiation is known to be an energy intensive process (21). Additionally, hyperammonemia has been shown to increase reactive oxygen species (ROS) and oxidative damage in rats and cirrhotic patients (20). This increase in ROS may in turn lead to tissue injury and subsequent muscle loss (20). Additionally, the removal of damaged mitochondria, termed mitophagy has been implicated in age-related sarcopenia (22) and cancer cachexia (23), but has not been investigated in the context of chronic liver disease.

The aim of the present study was to use a physiologically relevant *in vitro* model to elucidate the mechanisms of sarcopenia progression in chronic liver disease, through conditioning C2C12 skeletal muscle cells with *ex vivo* human serum from decompensated ESLD and non-cirrhotic NAFLD patients. To achieve this, we investigated myotube diameter and the regulatory mechanisms of myotube morphology, including mitochondrial respiration

and mitophagy in response to 24-hours of treatment with patient serum, as well as markers of MPS and proteolysis in response to a 4-hour treatment with patient serum, with and without a 30-minute leucine treatment. We hypothesized that serum from ESLD patients would lead to the development of myotube atrophy, alongside impairments in mitochondrial function, MPS and elevated proteolysis in comparison to myotubes treated with serum from non-cirrhotic NAFLD and age-matched controls (CON).

4.3 Methods

4.3.1 Participant Characteristics and Ethical Approval

Four decompensated ESLD, four non-cirrhotic NAFLD and four age-matched healthy CON participants provided their written, informed contest to participate in this study. CON participants were screened with a general health questionnaire and deemed eligible to participate. CON participants were expected to be normotensive (<140/90), free from metabolic disease conditions (i.e., type II diabetes and hyperlipidaemia) and chronic inflammatory disease (i.e., chronic liver disease, inflammatory bowel disease and rheumatoid arthritis). ESLD patients with cirrhosis, who were assessed for liver transplant (LT) and non-cirrhotic NAFLD patients, were recruited after screening in a clinical setting. Presence of cirrhosis in ESLD was confirmed through elastography, with or without a liver biopsy, or through consistent imaging and clinical findings. All ESLD patients had alcohol-related liver disease (ArLD) as the underlying etiology. The non-cirrhotic NAFLD patients were recruited through a dedicated liver clinic and a diagnosis of cirrhosis was excluded in these through transient elastography or liver biopsy. Patients were not assessed for sarcopenia prior to recruitment to this study in order to allow for the assessment of prevalence to be determined in the ESLD and NAFLD cohorts. Ethical approval for this study was obtained through the local ethics committee at the University of Birmingham (ERN_19-0831) for the recruitment

of CON participants and the Health Research Authority – West Midlands Solihull Research Ethics Committee Authority (REC reference: 18/WM/0167) for the recruitment of NAFLD and ESLD patients and conformed to the standards set by the Declaration of Helsinki. This was a registered clinical trial (clinicaltrials.gov, ID: NCT04734496).

4.3.2 Study Design

All participants reported to the laboratory after a minimum of a 4-hour fast and were asked to refrain from the consumption of caffeine on the morning of the trial. Participants were also asked to refrain from strenuous exercise for 24-hours prior to their visit to the laboratory. Upon arrival, a fasted blood sample was obtained from the antecubital vein and collected in a serum separator vacutainer (BD, Oxford, UK). The serum vacutainer was allowed to stand for 30-minutes at room temperature to allow the blood to clot and was then centrifuged at 3,000 g for 10-minutes at 4°C to obtain serum. Serum was stored at -80°C until required. Finally, participants underwent basic body composition (body mass index (BMI), fat free mass (FFM), whole body fat mass (WBFM), body fat (BF) percentage) and functional strength assessment through handgrip strength (HGS), as previously described (18).

4.3.3 Blood Analyses

Serum C-reactive protein (CRP) (DCRP00), interleukin-6 (IL-6) (D6050) and insulin (DINS00) concentrations were determined using commercially available enzyme-linked immunosorbent assay (ELISA) kits following manufacturer's instructions (R&D systems Inc., Minneapolis, MN, USA). Serum glucose concentrations were measured using a Glucose-Glo™ Assay (J6021, Promega Corporation, Madison Wisconsin, USA). Serum ammonia concentrations were measured utilising an ammonia assay kit (ab83360; abcam, Cambridge, UK).

4.3.4 Cell Culture

C2C12 skeletal muscle cells were maintained in growth media under standard conditions as previously described in section 2.1.4 and were seeded for experiments as described in section 2.1.5. Once a confluency of ~90% was reached, growth media was replaced with differentiation media (section 2.1.6). For myotube diameter and respirometry analysis, myotubes were incubated with differentiation media supplemented with 10% *ex vivo* human serum from CON, NAFLD and ESLD patients for 24-hours, on day 6 of differentiation. In order to investigate MPS, anabolic and catabolic signalling, myotubes were nutrient and serum starved in amino acid and serum free media for 1-hour, following which they were treated with media containing 10% *ex vivo* human serum from CON, NAFLD and ESLD patients for 4-hours. This preconditioning time period and serum dilution was selected based upon previous work described in section 2.2.1 and was performed with n=4 per group, replicated in triplicate.

4.3.5 Myotube Diameter

C2C12s were seeded in 24-well plates for experiments as described in section 2.1.5. Once a confluency of ~90% was reached, growth media was replaced with differentiation media (section 2.1.6) and media was changed every 48-hours. On day 6 of differentiation, myotubes were treated with 10% *ex vivo* human serum from CON, NAFLD and ESLD patients. After treatment, media was removed and myotubes were fixed in 2% paraformaldehyde and prepared for immunofluorescent imaging as outlined in section 2.5.1. Myotube diameter and nuclear fusion index (NFI) analysis was conducted as described in section 2.5.2.

4.3.6 Muscle Protein Synthesis

C2C12 myoblasts were seeded in 6-well plates and differentiated as outlined in section 2.2.1. On day 7 of differentiation, myotubes underwent a 1-hour amino acid and serum starvation, prior to treatment. Subsequently, myotubes were treated with media containing 10% *ex vivo* human serum from CON, NAFLD and ESLD patients. In a subset of samples, 5mM leucine was added for 30-minutes at the end of the 4-hour conditioning period to assess the anabolic response to leucine as previously described (section 2.2.3). MPS was assessed using the surface sensing of translation (SUnSET) technique, previously described in section 2.3. Briefly, the SUnSET technique utilises the antibiotic puromycin, a tyrosyl-tRNA analogue and immunoblotting to assess the incorporation level of puromycin (1μM) into new synthesised peptide chains during the final 30-minutes of treatment (24). Subsequently, cellular lysates were obtained as described in section 2.4.1. Lysates were stored at -80°C until further analysis.

4.3.7 Immunoblotting

The concentration of protein within cellular lysates was determined using a detergent compatible (DC) protein assay, with absorbance measured using a FLUOstar Omega plate reader and prepared as described previously (section 2.4.2). Protein was then separated on 4-20% linear graded pre-cast gels by sodium dodecyl sulphate (SDS) – polyacrylamide gel electrophoresis (PAGE) as previously described (section 2.4.3). Following electrophoresis protein were transferred to a nitrocellulose membrane as outlined previously (section 2.4.4). As a loading control, membranes were stained with Ponceau S solution and blocked with 5% milk or bovine serum albumin (BSA) diluted in Tris-buffered saline and 0.1% Tween-20 (TBST) for 1-hour (section 2.4.4). Overnight, the membranes were incubated at 4°C with the following primary antibodies: phospho- mammalian target of rapamycin (mTOR) Ser2448,

total mTOR, phospho-eukaryotic elongation factor 2 (eEF2) Thr56, total eEF2, phospho-ribosomal protein S6 kinase (p70S6K) Thr389, total p70S6K1, phospho-protein kinase B (Akt) Ser473, total Akt, phospho- S6 protein (RPS6) Ser240/244, total RPS6, phospho- eukaryotic translation initiation factor 4E-binding protein 1 (4EBP-1) Thr37/46, total 4EBP1, mouse IgG2a monoclonal anti-puromycin, total oxidative phosphorylation (OXPHOS) rodent cocktail, myostatin, muscle RING finger 1 (MuRF-1) and muscle atrophy F-box (MAFbx), microtubule-associated protein 1A/1B light chain 3 (LC3A/B) and caspase-3 (D3R6Y). The following day, membranes were washed for 15-minutes with TBST and incubated for 1-hour with the following secondary antibodies: anti-rabbit IgG horseradish peroxidase (HRP)-conjugated secondary antibody with the exception of MAFbx (anti-rat IgG, HRP-linked antibody), puromycin, OXPHOS and MuRF-1 (anti-mouse IgG, HRP-linked antibody). Details of all antibodies utilised herein are outlined in Table 2.1. Membranes were washed for 15-minutes in TBST prior to the quantification of protein content using Immobilon Western chemiluminescent HRP substrate. Images were captured on a G:BOX Chemi XT4 imager using GeneSys capture software (Syngene, Cambridge, UK), and band quantification was conducted using ImageJ software as previously described (section 2.4.6). Normalisation of relative arbitrary units was conducted using the protein band stained with Ponceau S solution.

4.3.8 Mitochondrial Respirometry

Mitochondrial respiration was measured in C2C12 skeletal muscle cells, which were seeded as described in section 2.6.1 on XFe24 cell culture plates. On day 5 of differentiation, myotubes were treated with differentiation media containing 10% *ex vivo* human serum from CON, NAFLD and ESLD patients for 24-hours. Additionally, a number of wells were maintained under normal growth conditions to provide an untreated control condition. After treatment, myotubes underwent a mitochondrial stress test as described in detail in section 2.6.2. Measurements for respiratory analysis were obtained as described in Table 2.2.

Additionally, estimations of ATP production were made, as described in section 2.6.3 and Table 2.3. All data was normalised to the total protein content quantified by a DC protein assay (26) as described in section 2.6.4.

4.3.9 Mitophagy Assay

Mitophagy was assessed using a mito-QC cell line outlined in section 2.7.1. Briefly, mito-QC cells were seeded onto imaging dishes as previously described (section 2.7.2). Once a confluency of ~40% was reached, mito-QC myoblasts were treated with serum from CON, NAFLD or ESLD patients for 24-hours. Following treatment, cells were prepared for immunofluorescent imaging as previously described (section 2.7.2). After an overnight incubation, images were taken using a Crest X-Light spinning disk system coupled to a Nikon Ti-E base, 60x/1.4 NA (CFI Plan Apo Lambda) air objective and Photometrics Delta Evolve EM-CCD, outlined previously in section 2.7.3.

Mitophagy was quantified using the mean fluorescence intensity of mCherry/ green florescent protein (GFP) measured in 25 cells across at least 15 fields of view for each condition using ImageJ software (26). The mCherry/GFP ratio was normalised to CON treated samples (see section 2.7.3).

4.3.10 Statistical Analysis

Statistical analysis was performed using GraphPad Prism V8 4.3. Data were tested for homogeneity of variances (Levene's test) and normality (Shapiro-Wilk test). A one-way ANOVA was used to investigate differences in anthropometrics, body composition (FFM, FM, BF %), HGS and plasma analytes/hormones (glucose, insulin, IL-6, CRP and serum ammonia) and the analysis of myotube diameter, NFI, respirometry, mitophagy and the protein content of OXPHOS between groups (i.e., CON, NAFLD, ESLD). A 3 (group) x 2 (leucine vs serum only) ANOVA was used to investigate differences in the protein content of

anabolic and catabolic signaling and puromycin incorporation. Where the results of the one-way or two-way ANOVAs revealed a significant interaction or main effect, post-hoc analysis t-tests were completed using Tukey's HSD. Effect size was calculated using Cohen's d for t-test and post-hoc comparisons, while partial eta squared (η^2) was used for omnibus tests. Statistical significance was set at $p < 0.05$. Data are reported as mean $\pm$ standard deviation in tables and as the mean (cross), median (central horizontal line), 25th and 75th percentiles (box) and the minimum and maximum values (vertical lines) in figures.

4.4 Results

4.4.1 Body Composition and Strength

Measures of anthropometrics, body composition and strength are shown in Table 4.1. No significant between-group difference was observed in age (P = 0.7, η^2= 0.07), body mass (P = 0.08, η^2= 0.4) and BMI (P = 0.06, η^2= 0.5). Additionally, no significant between-group difference was identified between FFM (P = 0.2, η^2= 0.3) and WBFM (P = 0.06, η^2= 0.5). However, BF percentage was significantly elevated in both NAFLD (100%, P < 0.01, d = 3.9) and ESLD patients (75%, P < 0.05, d = 2.6) compared with CON. No significant difference in HGS was identified between groups (P = 0.08, η^2 = 0.42).

Table 4.1. Participant characteristics for anthropometric, body composition and strength data in healthy control, NAFLD and ESLD patients

	CON (n=4)	NAFLD (n=4)	ESLD (n=4)
Anthropometrics			
Age (years)	64.7±10.0	61.8 ±7.6	60.5±1.7
Body mass (kg)	74.8±7.6	108.4±31.3	108.1±18.5
Height (cm)	179.0±7.4	171.6±3.6	174.3±4.3
BMI (kg m^{-2})	23.3±1.6	37.1±11.33	35.7±7.3
FFM (kg)	61.4±6.1	67.9±11.4	73.2±6.7
WBFM (kg)	13.4±2.2	40.6±20.1	34.9±15.5
BF (%)	17.8±1.9	35.7±7.3*	31.3±8.7*
Strength			
HGS (kg)	54.0±9.8	41.1±7.1	40.2±8.2
Blood Analyses			
Fasting Serum Insulin (μIU/mL)	9.6±4.1	16.88±3.5	24.6±10.1*
Fasting Serum Glucose (mmol/L)	4.4±0.1	4.3±0.1	4.3±0.1
HOMA-IR	1.8±0.7	3.2±0.6	4.8±2.0*
Serum IL-6 (pg/mL)	0.68±0.1	2.1±0.3	3.7±2.2*
Serum CRP (ng/mL)	1.2±0.7	1.6±0.5	6.1±0.8**†
Serum Ammonia	11.5±0.09	11.62±0.1	11.73±0.04*

BF, body fat, BMI, body mass index, CRP, c-reactive protein, FFM, fat free mass, HGS, hand grip strength, HOMA-IR, homeostatic model assessment of insulin resistance, IL-6, interleukin-6, WBFM, whole body fat mass.
*= P < 0.05 significantly different from CON
**= P < 0.01 significantly different from CON
***= P < 0.001 significantly different from CON
† = P < 0.001 significantly different from NAFLD

4.4.2 Blood Analysis

Serum ammonia concentration was significantly greater in ESLD patients compared with CON participants (p = 0.01, d = 3.5). No significant difference was found between CON and NAFLD patients (P = 0.2, d = 1.2), and NAFLD and ESLD patients (P = 0.2, d = 1.4) (Table 4.1). Serum IL-6 was significantly greater in ESLD patients compared with CON (P = 0.02, d = 2.7). Serum CRP was significantly increased in ESLD patients compared with CON (P < 0.001, d = 7.0) and NAFLD (P < 0.001, d = 6.6) patients. No significant difference in CRP concentration was found between CON and NAFLD patients (P = 0.7, d = 0.7). Serum insulin was significantly greater in ESLD patients in comparison to CON participants (158%,

P = 0.02, d = 2.2). No significant difference in serum insulin concentration was identified in NAFLD patients when compared to both CON and ESLD patients, however a large effect size was observed for both (P = 0.3, d = 2.2; P = 0.2, d = 1.2 respectively). Serum glucose was not significantly different between groups (P = 0.5, $\eta^2 = 0.16$). Homeostatic model assessment of insulin resistance (HOMA-IR) was significantly increased in ESLD patients in comparison to CON participants (159%, P = 0.02, d = 2.6). No significant difference in serum IL-6 (P = 0.3, d = 1.2; P = 0.3, d = 8.4 respectively), and HOMA-IR (P = 0.2, d = 1.2; P = 0.3, d = 2.0 respectively) was identified in NAFLD compared with both ESLD and CON participants.

Myotube Diameter and Nuclear Fusion Index

A one-way ANOVA revealed a significant main effect between groups (P < 0.001, $\eta^2 = 0.86$) (Figure 4.1b). Myotube diameter was significantly reduced in response to conditioning with serum from ESLD patients compared with CON (45%, P < 0.0001, d = 5.9) and NAFLD (35%, P = 0.001, d = 17.4) patients. Myotube diameter was numerically lower in myotubes conditioned with serum from NAFLD compared with CON patients, but this did not reach significance (15%, P = 0.081, d = 1.7). No significant difference in NFI was identified between experimental groups (P = 0.3, $\eta^2 = 0.24$) (Figure 4.1c).

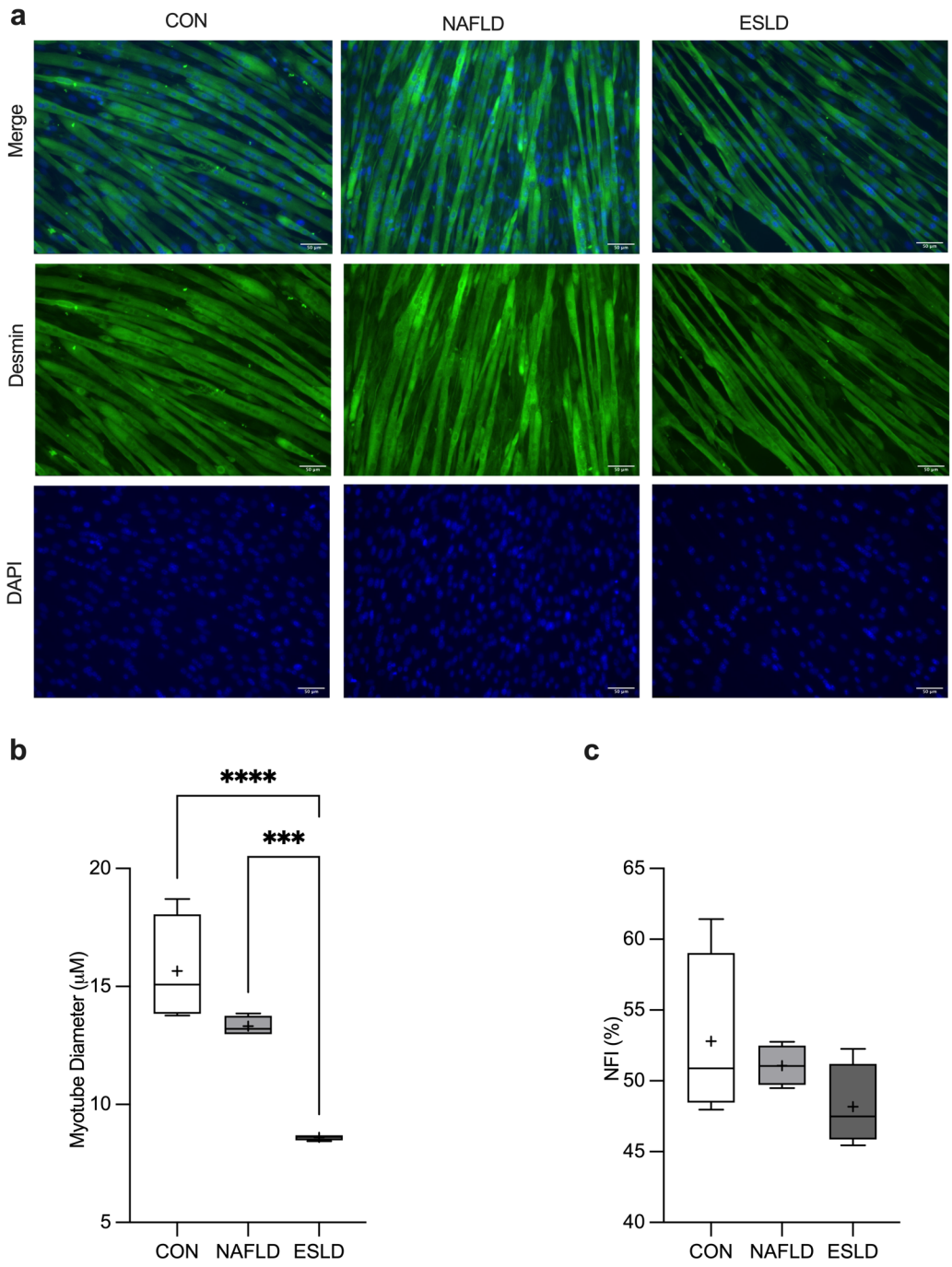

Figure 4.1. Serum from NAFLD and ESLD patients induces myotube atrophy. (A) representative Images illustrating atrophy in myotubes treated with *ex vivo* serum from non-alcoholic fatty liver disease (NAFLD) and end stage liver disease (ESLD) patients, in comparison to myotubes treated with serum from age-matched control participants (CON). (B) Mean myotube diameter (C) mean nuclear fusion index (NFI). Data are expressed as the mean (cross), median (central horizontal line), 25th and 75th percentiles (box) and the

minimum and maximum values (vertical lines), with n=4 per group, corresponding to the mean of treatment of each participant's serum, replicated in triplicate. *** P = 0.001, **** P < 0.0001.

4.4.3 Muscle Protein Synthesis and Anabolic Signalling

After conditioning myotubes with serum from CON, NAFLD and ESLD patients, we found no significant difference in MPS between groups ($F(2, 18) = 0.7$, $P = 0.5$), in basal conditions or following the addition of leucine ($F(1, 18) = 0.7$, $P = 0.4$) (Figure 4.2). Additionally, we found no significant difference in the phosphorylation of mTOR, 4EBP-1 and eEF2 between groups, with and without leucine treatment (Figure 2). A two-way ANOVA revealed a significant interaction effect between the effects of group and treatment in the phosphorylation of RPS6 ($F(2, 18) = 5.6$, $P = 0.01$). Additionally, a significant main effect for treatment (i.e., serum only vs. leucine) was identified for the phosphorylation of p70S6K ($F(1, 18) = 5.4$, $P = 0.03$). Furthermore, a significant main effect for treatment ($F(1, 18) = 6.1$, $P = 0.02$) and group (i.e., CON, NAFLD, ESLD) ($F(2, 18) = 4.1$, $P = 0.04$) was identified for the phosphorylation of Akt. Despite the interaction and main effects identified here, post-hoc analysis revealed no significant difference in the phosphorylation of RPS6, p70S6K and Akt between groups with and without leucine (Figure 4.2).

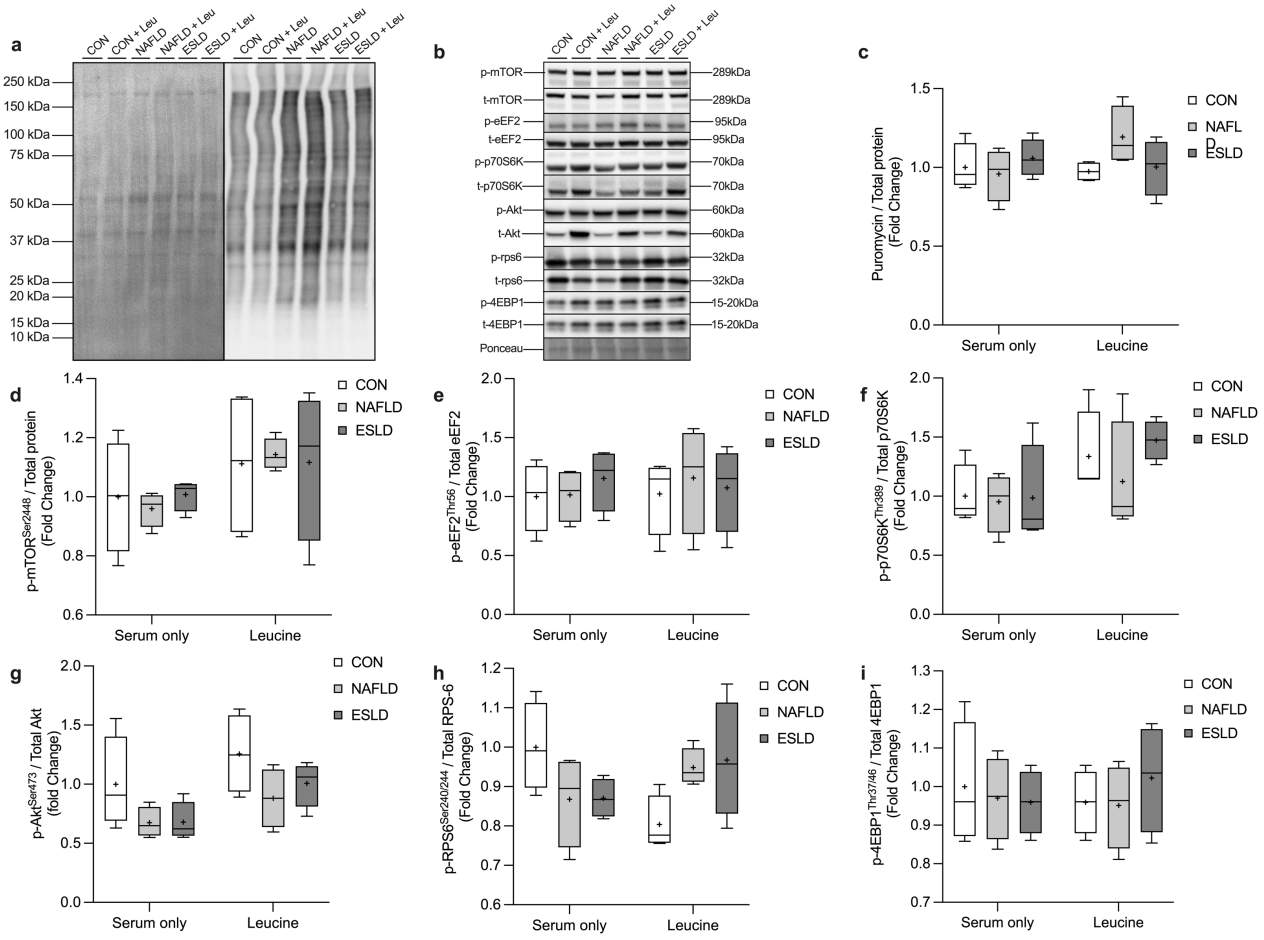

Figure 4.2. Measures of MPS and anabolic signalling in response to treatment with CON, NAFLD and ESLD serum. Myotubes were treated for 4 hours with *ex vivo* serum from age-matched control (CON), non-alcoholic fatty liver disease (NAFLD) and end stage liver disease (ESLD) patients**.** (A) representative western blot for puromycin and total protein, (B) representative western blots for anabolic signalling targets and loading control, (C) puromycin incorporation, (D) phospho-mTOR^{Ser2448} / total-mTOR, (E) phospho-eEF2^{Thr56} / total-eEF2, (F) phospho-p70S6K^{Thr389} / total-p70S6K, (G) phospho-Akt^{Ser473} / total-Akt, (H) phospho-RPS6$^{Ser240/244}$ / total-RPS6, (I) phospho-4EBP-1$^{Thr37/46}$ / total-4EBP-1. Data are expressed as fold change in comparison to the CON. All data are expressed as the mean (cross), median (central horizontal line), 25th and 75th percentiles (box) and the minimum and

maximum values (vertical lines), with an n=4 per group, with each data point corresponding to the average of 3 technical repeats.

4.4.4 Proteolytic Signalling

A two-way ANOVA revealed a significant main effect for group for the protein content of myostatin ($F(2, 18) = 6.3$, $P = 0.008$), MuRF-1 ($F(2, 18) = 6.9$, $P = 0.006$), MAFbx ($F(2, 18) = 12.1$, $P = 0.0005$), caspase-3 ($F(2, 18) = 6.7$, $P = 0.007$) and LC3A/B ($F(2, 18) = 11.8$, $P = 0.0005$) (Figure 3). Additionally, a significant main effect for treatment was identified for the protein content of myostatin ($F(1, 18) = 7.1$, $P = 0.02$).

Post-hoc analysis revealed that myostatin protein content was significantly increased in myotubes treated with serum from NAFLD (42%, $P = 0.05$, $d = 2.5$) and ESLD (44%, $P = 0.04$, $d = 3.6$) compared with those treated with serum from CON. Similarly, MuRF-1 protein content was significantly increased in myotubes treated with serum from ESLD patients compared with CON ($P = 0.03$, $d = 3.5$). No difference in the protein content of MAFbx, caspase 3 and LC3A/B was identified in myotubes in basal conditions between groups. In response to the addition of leucine we found a further increase in MAFbx (51%) and caspase 3 (99%) above basal conditions in ESLD treated myotubes, which was significantly greater than myotubes treated with CON serum, in a basal non-leucine state ($P = 0.02$, $d = 2.0$; $P = 0.02$, $d = 2.6$ respectively). Similarly, in the presence of leucine stimulation myotubes treated with serum from ESLD patients showed elevated levels of MAFbx (59%), caspase 3 (102%) and LC3A/B (237%) compared with CON treated myotubes with leucine ($P = 0.007$, $d = 2.4$; $P = 0.01$, $d = 2.2$; $P = 0.02$, $d = 2.8$ respectively). The protein content of MAFbx was also found to be elevated in myotubes treated with serum from ESLD patients compared with those treated with serum from CON with leucine (46%, $P = 0.05$, $d = 2.8$). Additionally, in comparison to CON leucine-stimulated myotubes, NAFLD and ESLD basal conditions showed an increase in myostatin protein content (12%, $P = 0.04$, $d = 0.6$, 23%, $P = 0.03$, $d =$

1.4 respectively). The protein content of caspase 3 was also shown to be elevated in myotubes treated with ESLD serum and leucine compared with NAFLD serum alone (173%, P = 0.03, d = 2.2). No difference in the protein content of myostatin, MuRF-1, MAFbx and LC3A/B was detected between myotubes treated with serum from NAFLD and ESLD patients without the presence of leucine.

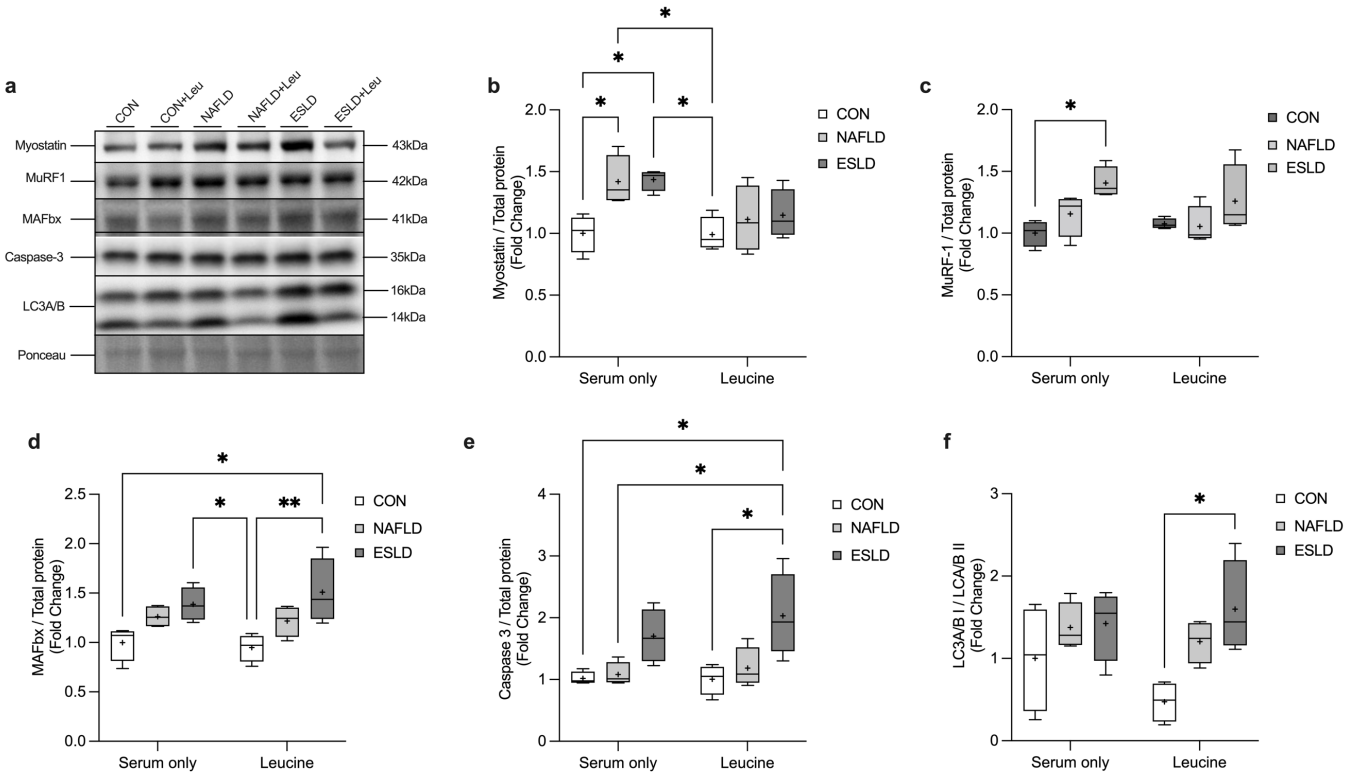

Figure 4.3. Markers of catabolic signalling are elevated within myotubes treated with serum from ESLD patients for 4 hours and a 30 minute treatment with leucine.

Myotubes were treated with *ex vivo* human serum from age-matched control (CON), non-alcoholic fatty liver disease (NAFLD) and end stage liver disease (ESLD) patients for 4-hours, with and without a 30-minute treatment with 5mM leucine. (A) representative western blot images of catabolic signalling markers, (B) myostatin, (C) MAFbx, (D) MuRF-1, (E) caspase-3, (F) LC3A/B. Data are expressed as fold change in comparison to the CON. Data

are expressed as the mean (cross), median (central horizontal line), 25th and 75th percentiles (box) and the minimum and maximum values (vertical lines), with an n=4 accounting for each participant group, with each data point corresponding to the average of 3 technical repeats. * P > 0.05.

4.4.5 Mitochondrial Respiration

We assessed oxygen consumption through the completion of a mitochondrial stress test after a 24-hour treatment with serum from CON, NAFLD and ESLD cohorts (Figure 4.4a). No significant difference was identified in basal mitochondrial respiration (P = 0.6, η^2 = 0.1) (Figure 4.4b). However, a significant main effect was identified in maximal mitochondrial respiration (P < 0.001, η^2 = 0.9) (Figure 4.4c). Indeed, maximal mitochondrial respiration significantly decreased in myotubes treated with serum from NAFLD (24%, P < 0.001, d = 4.20) and ESLD patients (30%, P < 0.001, d = 6.3) compared with CON, with no significant difference between NAFLD and ESLD treated myotubes (P = 0.4, d = 0.9). Furthermore, a significant main effect of spare respiratory capacity was identified between groups (P < 0.001, η^2 = 0.87) (Figure 4d). Spare respiratory capacity was significantly greater in myotubes treated with serum from CON, in comparison to NAFLD (31%, P < 0.001, d = 4.02) and ESLD (35%, P < 0.001, d = 5.61). No significant difference was identified between myotubes treated with NAFLD and ESLD serum (P = 0.7, d = 0.6). A significant main effect was identified for proton leak respiration between groups (P = 0.02, η^2 = 0.57) (Figure 4.4e). Proton leak respiration was significantly increased in myotubes treated with serum from NAFLD patients compared with CON (39%, P = 0.02, d = 2.3). While a large effect size was observed, no significant difference in proton leak respiration was identified between CON and ESLD treated myotubes (28%, P = 0.09, d = 1.7). No significant difference was identified between NAFLD and ESLD serum treated myotubes (P = 0.6, d = 1.0). Similarly, a significant main effect was identified between groups in coupling efficiency (P = 0.02, η^2 =

0.6) (Figure 4.4g). Coupling efficiency was significantly decreased in myotubes treated with serum from NAFLD (12%, P = 0.03, d = 2.2) and ESLD patients (12%, P = 0.04, d = 2.6) compared with CON, with no significant difference between myotubes treated with serum from NAFLD and ESLD patients (P = 0.9, d = 0.1). No significant difference in ATP coupled respiration was identified between groups (P = 0.2, $\eta^2 = 0.3$) (Figure 4.4f).

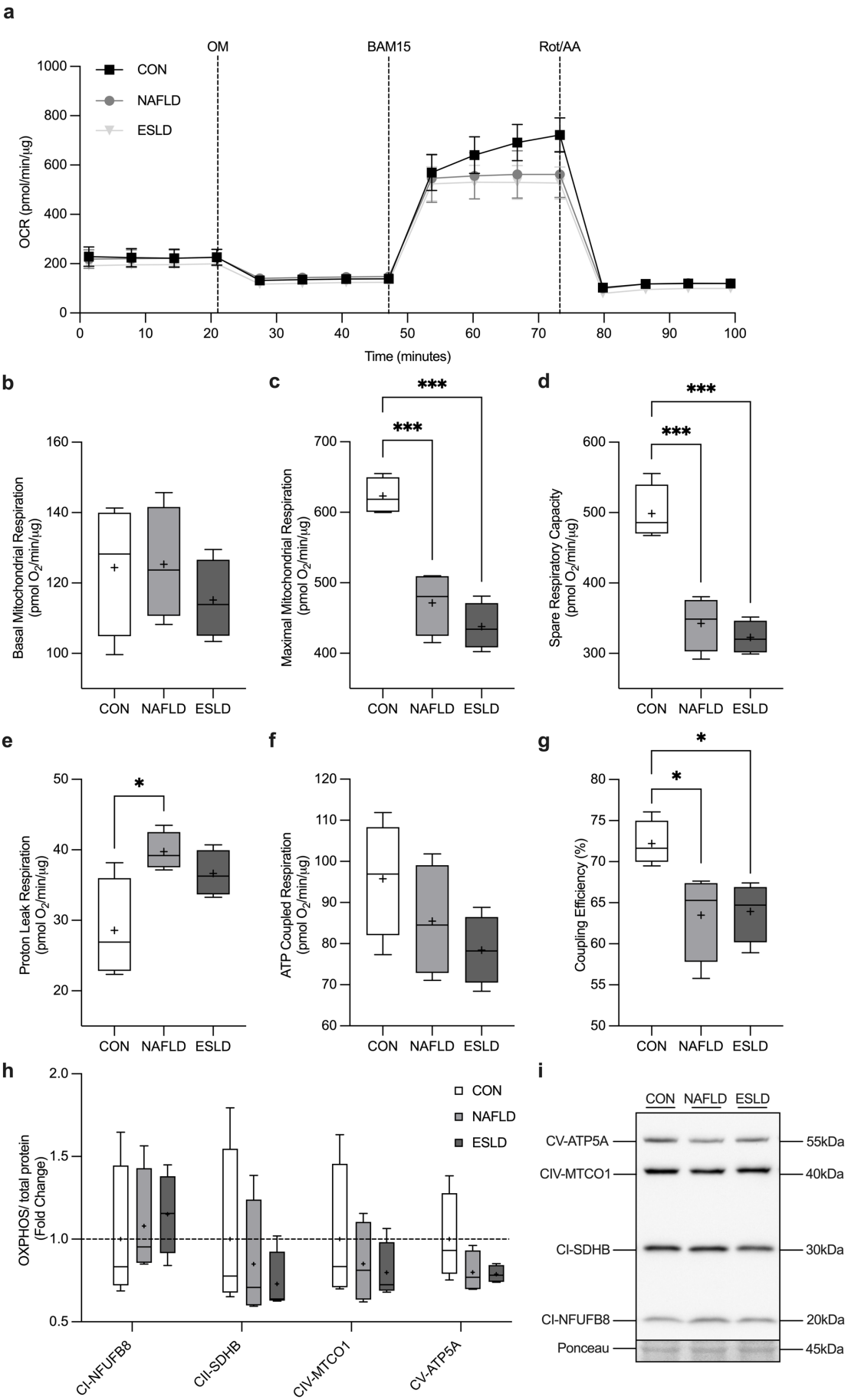
a
OM
BAM15
Rot/AA
CON
NAFLD
ESLD
OCR (pmol/min/µg)
Time (minutes)
b
Basal Mitochondrial Respiration (pmol O2/min/µg)
c
Maximal Mitochondrial Respiration (pmol O2/min/µg)
d
Spare Respiratory Capacity (pmol O2/min/µg)
e
Proton Leak Respiration (pmol O2/min/µg)
f
ATP Coupled Respiration (pmol O2/min/µg)
g
Coupling Efficiency (%)
h
OXPHOS/ total protein (Fold Change)
CI-NFUFB8
CII-SDHB
CIV-MTCO1
CV-ATP5A
i
CV-ATP5A
CIV-MTCO1
CI-SDHB
CI-NFUFB8
Ponceau
55kDa
40kDa
30kDa
20kDa
45kDa

Figure 4.4. Serum from NAFLD and ESLD patients induces impairments in mitochondrial respiration, despite no changes in markers of mitochondrial protein content. (A) raw trace of oxygen consumption rate (OCR) for myotubes treated with *ex vivo* serum from non-alcoholic fatty liver disease (NAFLD), end stage liver disease (ESLD) and age-matched controls (CON), (B) basal mitochondrial respiration was assessed prior to the addition of oligomycin (OM), an ATP synthase inhibitor and represents the energetic demand of the cell in baseline conditions, (C) maximal mitochondrial respiration was calculated after the addition of the uncoupler, N^5,N^6-bis(2-Fluorophenyl)-[1,2,5]oxadiazolo[3,4-B]pyrazine-5,6-diamine (BAM-15), (D) spare respiratory capacity indicates the ability of a cell to respond to an increase in energetic demand (E) proton leak respiration represents the portion of basal respiration not associated with ATP production, (F) ATP coupled respiration was calculated upon the addition of OM, (G) coupling efficiency was calculated as the percentage of respiration accounted for by ATP production, (H) quantification of OXPHOS/total protein, (I) representative western blot of OXPHOS. Respirometry data was normalized to protein content. Western blot data are expressed as fold change in comparison to CON. All data are expressed as the mean (cross), median (central horizontal line), 25^{th} and 75^{th} percentiles (box) and the minimum and maximum values (vertical lines), with an n=4 per group, with each data point corresponding to the average of 3 technical repeats. *** $P > 0.001$, * $P > 0.05$.

4.4.6 Mitophagy

Mitophagy was assessed using a mitophagy reporter cell line (mitoQC) in C2C12 skeletal muscle cells, in which C2C12s express a stable functional insert tandem mCherry-GFP tag, which is fused to the mitochondrial targeting sequence of FIS1 (residues 101-152) (27). Under basal conditions, the mitochondria fluoresce both red (mCherry) and green (GFP), which when merged appear gold in colour. However, mitophagy induces an acidic environment in the lysosomes which quench the signal of GFP, but not mCherry (26). As a

consequence, an increase in mCherry signal is visible in the mitochondrial network. A one-way ANOVA revealed a significant main effect between groups for the analysis of mCherry/GFP ($P < 0.001$, $\eta^2 = 0.9$) (Figure 4.6a). Specifically, in comparison to myoblasts treated with serum from CON there was a significant reduction in the level of mitophagy, as shown by a decrease in the ratio of mCherry/ GFP reported in myoblasts treated with serum from NAFLD (14%, $P < 0.001$, $d = 3.9$) and ESLD (13%, $P < 0.001$, $d = 5.1$) patients. No significant difference in mitophagy was evident between myotubes treated with serum from NAFLD and ESLD patients ($P = 1.0$, $d = 0.2$).

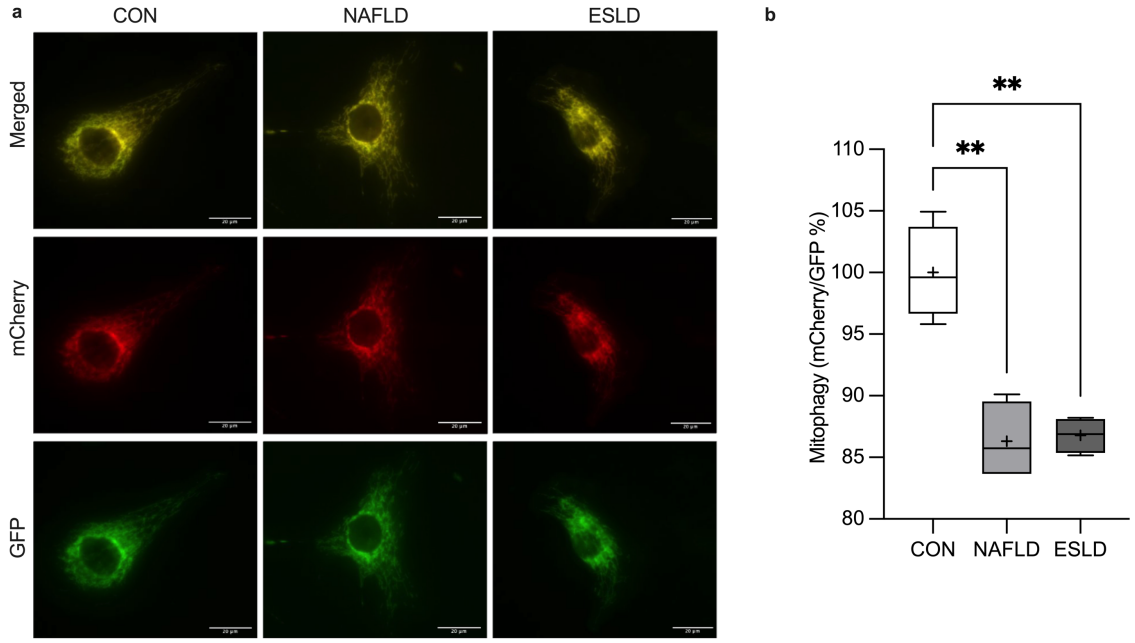

Figure 4.5. Serum from NAFLD and ESLD patients induces a reduction in mitophagy. (A) representative images illustrating that treatment of mitoQC cells with *ex vivo* serum from patients with non-alcoholic fatty liver disease (NAFLD) and end stage liver disease (ESLD) in comparison to age-matched control (CON) patients in C2C12 myoblasts stably expressing mCherry-GFP-FIS1101-152, (B) quantification of mitophagy, expressed as mCherry/GFP. Data are represented a fold change from CON. Data are expressed as the mean (cross), median (central horizontal line), 25th and 75th percentiles (box) and the minimum and

maximum values (vertical lines), with each data point corresponding to the mean of 25 measurements per condition. An n=4 was utilized within each group. ** P > 0.01.

4.4.7 Mitochondrial Content

Treatment with serum from CON, NAFLD and ESLD patients showed no significant difference in markers of mitochondrial protein content measured through the expression of OXPHOS subunits; complex I (NFUFB8) (P = 0.8, η^2 = 0.04), complex II (SDHB) (P = 0.6, η^2 = 0.1), complex IV (P = 0.6, η^2 = 0.1) and complex V (MTCO1) (P = 0.2, η^2 = 0.3) (Figure 4.4h).

4.5 Discussion

The use of an *in vitro* model utilising *ex vivo* human serum from CON, NAFLD and ESLD patients to condition C2C12 skeletal muscle cells, provides a model to investigate the potential mechanisms which underpin the progression of sarcopenia in chronic liver disease patients of different underlying aetiologies and clinical stages of disease. This model is advantageous as it circumvents concerns associated with muscle biopsies in ESLD patients (14) and provides a more physiologically relevant basis to study mechanisms of muscle atrophy compared with typical *in vitro* approaches (18). In line with our hypotheses, we demonstrated that conditioning myotubes with serum from ESLD patients induced myotube atrophy compared with those treated with CON serum. Mechanistically, we identified mitochondrial dysfunction in myotubes treated with serum from NAFLD and ESLD patients compared with CON. Additionally, we identified an increase in myostatin and proteolytic markers in myotubes treated with ESLD serum compared with CON. Fasted and fed state MPS and anabolic signalling did not differ between groups. Collectively, these data demonstrate potential mechanisms of sarcopenia progression in ESLD and NAFLD patients (Figure 4.6).

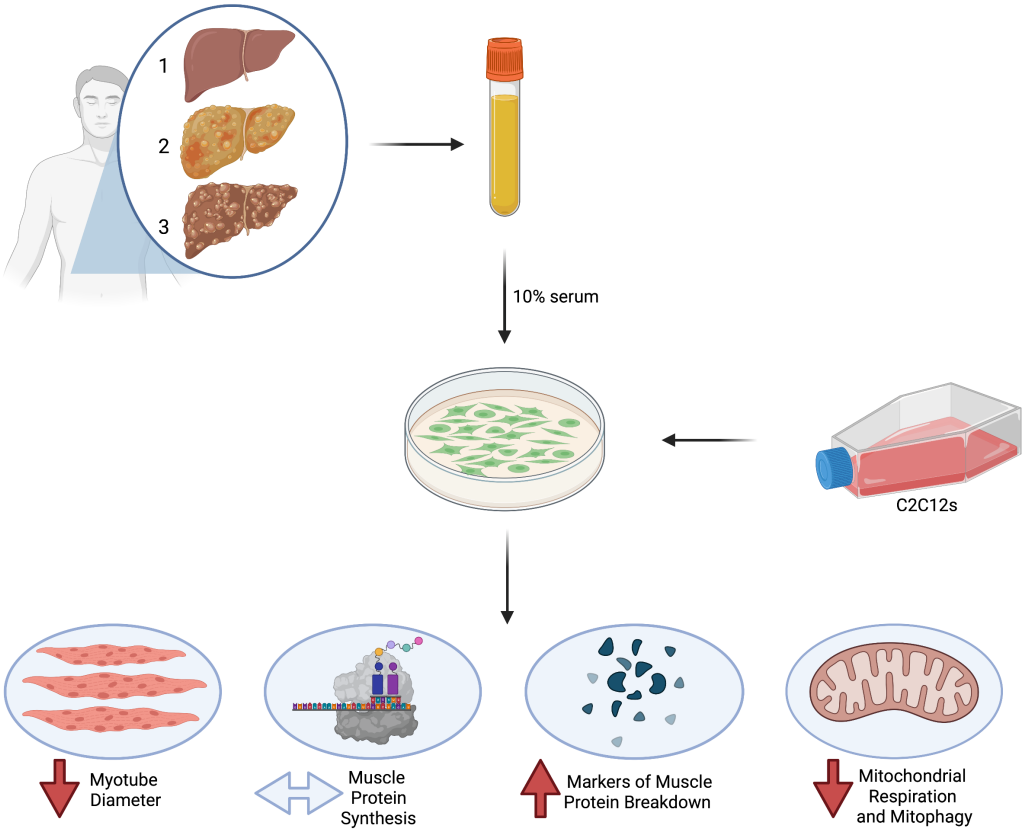

Figure 4.6. ESLD serum induces a reduction in myotube diameter, mitochondrial function and an increase in markers of MPB, with no change in MPS. Blood samples were obtained from age-matched controls (1), non-cirrhotic NAFLD (2) and decompensated ESLD (3) patients. C2C12 cells were treated with 10% *ex vivo* serum for 4- or 24-hours. Treatment with ESLD serum led to a decline in myotube diameter, which may be characterised by a reduction in mitochondrial function, shown through a reduction in respiration and mitophagy and an increase in markers of muscle protein breakdown. No change in muscle protein synthesis was identified.

After 24-hours of conditioning with *ex vivo* human serum, we found that serum from ESLD patients led to a significant decrease in myotube diameter in comparison to CON and NAFLD treated myotubes (~45% and 35%, respectively). This observation is consistent with

in vivo animal work, highlighting muscle atrophy in a PCA rat model of cirrhosis (28). Potential underlying factors that may contribute to the observed myotube atrophy and sarcopenia in ESLD include increased inflammation (29, 30) and ammonia (15), which are exacerbated with liver disease progression and were markedly greater in ESLD compared with CON and NAFLD in the present study (9). Further *in vitro* and *in vivo* research is required to understand the systemic factors which may contribute to myotube atrophy and sarcopenia progression in chronic liver disease, including other aetiologies (e.g., alcohol-related liver disease; ArLD).

The observed myotube atrophy in response to ESLD patient serum would undoubtedly be underscored by dysregulation of muscle protein turnover. In contrast to our hypothesis, we did not observe an impairment in fasted-state MPS or markers of anabolic signalling in response to ESLD serum treatment compared with CON and NAFLD patients. These findings are in contrast to previous work showing a reduction in fasted-state anabolic signalling in cirrhotic ArLD patients compared with healthy controls (14). The lack of fasted-state anabolic signalling impairment identified in this study could be partially explained by the differences between experimental models, patient status (i.e., compensated vs decompensated), anthropometrics and age. Although previous *in vitro* and *in vivo* animal ArLD models have demonstrated an impairment in mTOR signalling with ethanol treatment (10), patient donors with an ArLD etiology in the present study had abstained from alcohol prior to recruitment, which may explain the absence of any impairment in fasted-state anabolic signalling herein.

Alongside no differences in fasted-state MPS, we found no increase in leucine-stimulated MPS in any of the groups. As CON participants in this study had a mean age of ~65 years, it is plausible that the absence of a leucine-stimulated MPS or anabolic signalling response could be due to older age, as demonstrated in our recent work using this *in vitro*

model (18). Interestingly, previous *in vivo* work reported a similar increase in anabolic signalling in ArLD cirrhotic and healthy controls in response to leucine-enriched branched-chain amino acid (BCAA) ingestion (14), although the large dose of leucine provided in this study (7.5g) may have masked any potential muscle anabolic resistance (31). Nonetheless, it is surprising that we did not detect an impairment in postprandial MPS stimulation in ESLD or NAFLD compared with CON, particularly as BMI and body fat mass was greater in the liver disease cohorts and obesity exacerbates age-related muscle anabolic resistance to protein provision (29). Notwithstanding, the present findings suggest that myotube atrophy in response *ex vivo* ESLD serum treatment is not due to an impairment in fasted-sate or leucine-stimulated MPS or anabolic signalling. However, *in vivo* human studies of fasted and postprandial MPS in liver disease patients across different aetiologies are required fully elucidate whether MPS dysregulation contributes to sarcopenia in chronic liver disease.

Despite the absence of any difference in MPS, we report an increase in the myogenesis inhibitor, myostatin in myotubes treated with serum from NAFLD and ESLD patients. This finding is consistent with the observation that myostatin expression is increased in cirrhotic patients alongside reduced skeletal muscle mass (8). Similarly, ammonia and ethanol treatment have been shown to increase myostatin expression and reduce myotube diameter in C2C12 (32). Mechanistically, increased myostatin has been linked to the suppression of MPS and anabolic signalling (33); however we did not detect alterations in MPS herein. Myostatin has also been linked to an increase in MPB, through an increase in ubiquitin proteasome markers (34). In cirrhotic patients, elevated myostatin has also been reported alongside increased autophagy and WbPB compared with healthy controls (14, 15). Similarly, we identified an increase in autophagy and the ubiquitin proteasome markers in ESLD treated myotubes compared with CON. We also observed an increase in MuRF-1 protein content in response to ESLD serum treatment, which has not been detected in earlier

human studies (14, 15). Beyond fasted-state proteolytic signalling, BCAA treatment in ArLD cirrhotics has been reported to attenuate autophagy (14). In contrast, markers of proteolysis were not altered by leucine treatment in the present study across groups. This discrepancy may be due to differences in signalling responsiveness in leucine-treated C2C12 cells and human skeletal muscle with orally ingested high-dose BCAA/leucine. Interestingly, despite elevated myostatin expression in ESLD and NAFLD compared with CON serum treated cells, markers of proteolysis differed between ESLD and CON only. This finding may partly explain why differences in myotube atrophy in NAFLD vs. CON did not reach significance, whereas ESLD serum treated cells experienced significant atrophy compared with NAFLD and CON. We acknowledge that the stage of disease severity differed between NAFLD and ESLD donors in this study, and that serum treated cells from decompensated cirrhotic NAFLD patients may have undergone greater proteolysis and myotube atrophy compared with the noncirrhotic NAFLD patients included herein. Taken together, the present findings suggest that myotube atrophy with *ex vivo* ESLD serum treatment, may be partially underpinned by elevated myostatin and markers of proteolysis. Although these purported mechanisms of myotube atrophy in ESLD require further exploration, interventions targeting myostatin and proteolytic pathway regulators may provide a promising approach to offset sarcopenia progression in chronic liver disease.

In the present study, we report for the first time that mitochondrial respiration and coupling efficiency was impaired in C2C12s treated with serum from NAFLD and ESLD patients compared with CON. Previously, reduced mitochondrial oxidative capacity has been observed in conditions of muscle atrophy including age-related sarcopenia (35) and cancer cachexia (36), but has not been studied in chronic liver disease. *In vitro* work has shown impairments in cellular respiration in response to ammonia (20) and ethanol (10) treatment, and reversal in the reduction of ATP content with ammonia removal from culture media.

Expanding on these observations by using a physiologically relevant *in vitro* model, our novel findings support the notion that mitochondrial dysfunction could play an important role in sarcopenia progression in chronic liver disease. Additionally, we observed a reduction in mitophagy in both NAFLD and ESLD treated C2C12 mitoQC cells compared with CON. This is in line with previous *in vivo* work highlighting a reduction in mitophagy in the context of age-related sarcopenia (37) and NAFLD models (38). Although the mechanisms of mitophagy across the chronic liver disease spectrum remain unclear, this process is considered to be beneficial for the clearance of damaged mitochondria (39). Indeed, the inhibition of mitophagy leads to the accumulation of dysfunctional mitochondria (22). As a consequence, this may explain the reduction in mitochondrial respiration observed in the present study.

Changes in mitochondrial respiration and mitophagy occurred independently of changes in mitochondrial protein content, similar to observations from an *in vitro* ArLD model (10). Despite a similar degree of mitochondrial dysfunction in NAFLD and ESLD treated myotubes compared with CON, significant myotube atrophy was only present in ESLD treated myotubes. Previous *in vivo* mouse models of cancer cachexia have shown that mitochondrial dysfunction develops prior to the loss of muscle mass (23). Therefore, it is plausible that mitochondrial dysfunction may arise at an early stage of liver disease (e.g., non-cirrhotic NAFLD patients) prior to accelerated sarcopenia and myotube atrophy that is observed in ESLD (40). Additionally, ESLD patients were found to be insulin resistant in comparison to CON participants, a factor which has also been linked to the development of mitochondrial dysfunction (41). It is worth noting that the mitochondrial dysfunction identified here may be related to increased myostatin, which can influence glucose metabolism and the development of insulin resistance (42). Further exploratory research is

required to understand the causes of mitochondrial dysfunction and potential links to impairments in muscle protein turnover that underlie sarcopenia in chronic liver disease.

Although this *in vitro* work provides a valuable platform to investigate the mechanisms which underpin muscle atrophy in ESLD, there are limitations to this approach. Firstly, we did not treat human primary skeletal muscle cells with serum from NAFLD and ESLD patients or CON individuals, but instead used C2C12 murine cells, which may cause potential cross-species issues. As a result, future research should aim to replicate this work using human primary muscle cells, from the patient cohorts where possible, to investigate the potential links between the systemic factors driving this atrophy shown in this study. Secondly, as an extensive blood analysis was not completed, the systemic factors which drive the myotube atrophy and/or mechanistic dysregulation identified in ESLD and NAFLD serum treated cells remain unclear. Whilst hyperammonemia (15), inflammation (9) and alcohol (10) may drive sarcopenia progression in chronic liver disease, other systemic factors including insulin resistance (9), decreased testosterone (43) and IGF-1 (44) may influence sarcopenia progression. Finally, beyond the mechanisms explored in the present study, others have suggested that increased oxidative stress (20, 45), impaired ribosomal biogenesis (46) and satellite cell function (28) may contribute to the dysregulated muscle protein turnover in cirrhotic animals. It is likely that all of these factors may underpin the development of sarcopenia in ESLD, with the degree varying between individuals due to disease aetiology and possibly gender (1) and lifestyle factors (diet, physical activity; (47, 48)).

In conclusion, our data suggest that sarcopenia progression in ESLD may be linked to mitochondrial dysfunction, increased myostatin and potentially proteolysis. *In vivo* human studies are now required in order to confirm these observations and to resolve the systemic factors that drive sarcopenia across complex multi-faceted chronic liver disease pathologies and disease stage.

Acknowledgements: The authors would like to thank Dr. Jonathan Barlow from the Mitochondrial Profiling Centre for his assistance in seahorse respirometry training. The authors would like to extend our thanks to research participants and research staff within the Clinical Research Facility and Inflammation Research Facility who helped with collection of samples.

Author Contributions: S.L.A., G.G.L. and L.B conceived and designed the research. S.L.A. A.D., J.I.Q. and F.R.W. completed human data collection. S.L.A. conducted all *in vitro* work. A.P.S., Y.C.L., N.H.F.F. and D.J.H. provided mitoQC cells as well as access to microscopy and imaging expertise. S.L.A, G.G.L., L.B wrote the manuscript. All authors contributed to the interpretation of results, edited and approved of the final manuscript.

Funding: This study was funded by the National Institute for Health Research (NIHR) Birmingham Biomedical Research Centre (BRC-1215-20009). The views expressed are those of the authors and not necessarily of those of the NIHR, or the Department of Health and Social Care. D.J.H. was supported by MRC (MR/N00275X/1 and MR/S025618/1) Project and Diabetes UK (17/0005681) Project Grants. This project has received funding from the European Research Council (ERC) under the European Union's Horizon 2020 research and innovation programme (Starting Grant 715884 to D.J.H.).

Clinical trial number: NCT04734496

Disclosures: The authors declare no conflicts of interest.

Ethical Approval: The authors of this manuscript certify that they comply with the ethical guidelines for authorship and publishing in the Journal of Cachexia, Sarcopenia Muscle (49).

4.6 References

1. **Kim G, Kang SH, Kim MY, and Back SK**. Prognostic value of sarcopenia in patients with liver cirrhosis: A systematic review and meta-analysis. *PLoS One* 12: e0186990, 2017.
2. **Cruz-Jentoft AJ, Bahat G, Bauer J, Boirie Y, Bruyere O, Cederholm T, Cooper C, Landi F, Rolland Y, Sayer AA, and Schneider SM**. Sarcopenia: revised European consensus on definition and diagnosis. *Age Ageing* 48: 16-31, 2019.
3. **Dasarathy S**. Consilience in sarcopenia of cirrhosis. *J Cachexia Sarcopenia Muscle* 3: 225-237, 2012.
4. **van Vugt JL, Levolger S, de Bruin RW, van Rosmalen J, Metselaar HJ, and Ijzermans JN**. Systematic review and meta-analysis of the impact of computed tomography-assessed skeletal muscle mass on outcome in patients awaiting or undergoing liver transplantation. *Am J Transplant* 16: 2277-2292, 2016.
5. **Montano-Loza AJ, Meza-Junco J, Prado CM, Lieffers JR, Baracos VE, Bain VG, and Sawyer MB**. Muscle wasting is associated with mortality in patients with cirrhosis. *Clin Gastroenterol Hepatol* 10: 166-173, 2012.
6. **Yadav A, Chang YH, Carpenter S, Silva AC, Rakela J, Aqel BA, Byrne TJ, Douglas DD, Vargas HE, and Carey EJ**. Relationship between sarcopenia, six-minute walk distance and health-related quality of life in liver transplant candidates. *Clin Transplant* 29: 134-141, 2015.
7. **Dasarathy S**. Etiology and Management of Muscle Wasting in Chronic Liver Disease. *Curr Opin Gastroenterol* 32: 159-165, 2016.
8. **Qiu J, Thapaliya S, Runkana A, Yang Y, Tsien C, Mohan ML, Narayanan A, Eghtesad B, Mozdziak PE, McDonald C, Stark GR, Welle S, Naga Prasad SV, and Dasarathy S**. Hyperammonemia in cirrhosis induces transcriptional regulation of myostatin by an NF-kappaB-mediated mechanism. *Proc Natl Acad Sci U S A* 110: 18162-18167, 2013.
9. **Allen SL, Quinlan JI, Dhaliwal A, Armstrong MJ, Elsharkawy AM, Greig CA, Lord JM, Lavery GG, and Breen L**. Sarcopenia in Chronic Liver Disease: Mechanisms and Countermeasures. *Am J Physiol Gastrointest Liver Physiol* 320: G241-G257, 2021.
10. **Singh SS, Kumar A, Welch N, Sekar J, Mishra S, Bellar A, Gangadhariah M, Attaway A, Al Khafaji H, Wu X, Pathak V, Agrawal V, McMullen MR, Hornberger TA, Nagy LE, Davuluri G, and Dasarathy S**. Multiomics-Identified Intervention to Restore Ethanol-Induced Dysregulated Proteostasis and Secondary Sarcopenia in Alcoholic Liver Disease. *Cell Physiol Biochem* 55: 91-116, 2021.
11. **Ohashi K, Ishikawa T, Hoshi A, Suzuki M, Mitobe Y, Yamada E, Abeywickrama HM, Seki N, Koyama C, Aoki H, and Koyama Y**. Relationship Between Sarcopenia and Both Physical Activity and Lifestyle in Patients With Chronic Liver Disease. *J Clin Med Res* 10: 920-927, 2018.
12. **El Sherif O, Dhaliwal A, Newsome PN, and Armstrong MJ**. Sarcopenia in nonalcoholic fatty liver disease: new challenges for clinical practice. *Expert Rev Gastroeterol Hepatol* 23: 1-9, 2020.
13. **Tsien C, McCullough AJ, and Dasarathy S**. Late evening snack: exploiting a period of anabolic opportunity in cirrhosis. *J Gastroenterol Hepatol* 27: 430-441, 2012.
14. **Tsien C, Davuluri G, Singh D, Allawy A, Ten Have GA, Thapaliya S, Schulze JM, Barnes D, McCullough AJ, Engelen MP, Deutz NE, and Dasarathy S**. Metabolic and molecular responses to leucine-enriched branched chain amino acid supplementation in the skeletal muscle of alcoholic cirrhosis. *Hepatology* 61: 2018-2029, 2015.
15. **Qiu J, Tsien C, Thapalaya S, Narayanan A, Weihl CC, Ching JK, Eghtesad B, Singh K, Fu X, Dubyak G, McDonald C, Almasan A, Hazen SL, Naga Prasad SV, and**

Dasarathy S. Hyperammonemia-mediated autophagy in skeletal muscle contributes to sarcopenia of cirrhosis. *Am J Physiol Endocrinol Metab* 303: E983-E993, 2012.
16. **Kumar A, Davuluri G, Silva RNE, Engelen M, Ten Have GAM, Prayson R, Deutz NEP, and Dasarathy S**. Ammonia lowering reverses sarcopenia of cirrhosis by restoring skeletal muscle proteostasis. *Hepatology* 65: 2045-2058, 2017.
17. **Gao B, Xu MJ, Bertola A, Wang H, Zhou Z, and Liangpunsakul S**. Animal Models of Alcoholic Liver Disease: Pathogenesis and Clinical Relevance. *Gene Expr* 17: 173-186, 2017.
18. **Allen SL, Marshall RN, Edwards SJ, Lord JM, Lavery GG, and Breen L**. The effect of young and old ex vivo human serum on cellular protein synthesis and growth in an in vitro model of ageing. *Am J Physiol Cell Physiol* 321: C26-C37, 2021.
19. **Cuthbertson D, Smith K, Babraj J, Leese G, Waddell T, Atherton P, Wackerhage H, Taylor PM, and Rennie MJ**. Anabolic signaling deficits underlie amino acid resistance of wasting, aging muscle. *FASEB J* 19: 422-424, 2005.
20. **Davuluri G, Allawy A, Thapaliya S, Rennison JH, Singh D, Kumar A, Sandlers Y, Van Wagoner DR, Flask CA, Hoppel C, Kasumov T, and Dasarathy S**. Hyperammonaemia-induced skeletal muscle mitochondrial dysfunction results in cataplerosis and oxidative stress. *J Physiol* 594: 7341-7360, 2016.
21. **Dasarathy S, and Merli M**. Sarcopenia from mechanism to diagnosis and treatment in liver disease. *J Hepatol* 65: 1232-1244, 2016.
22. **Hood DA, Memme JM, Oliveira AN, and Triolo M**. Maintenance of Skeletal Muscle Mitochondria in Health, Exercise, and Aging. *Annu REv Physiol* 81: 19-41, 2019.
23. **Brown JL, Rosa-Caldwell ME, Lee DE, Blackwell TA, Brown LA, Perry RA, Haynie WS, Hardee JP, Carson JA, Wiggs MP, Washington TA, and Greene NP**. Mitochondrial degeneration precedes the development of muscle atrophy in progression of cancer cachexia in tumour-bearing mice. *J Cachexia Sarcopenia Muscle* 8: 926-938, 2017.
24. **Goodman CA, Mabrey DM, Frey JW, Miu MH, Schmidt EK, Pierre P, and Hornberger TA**. Novel insights into the regulation of skeletal muscle protein synthesis as revealed by a new nonradioactive in vivo technique. *FASEB J* 25: 1028-1039, 2011.
25. **Affourtit C, and Brand MD**. Measuring mitochondrial bioengertics in INS-1E insulinoma cells. *Methods Enzymol* 457: 405-424, 2009.
26. **Seabright AP, Fine NHF, Barlow JP, Lord SO, Musa I, Gray A, Bryant JA, Banzhaf M, Lavery GG, Hardie DG, Hodson DJ, Philp A, and Lai YC**. AMPK activation induces mitophagy and promotes mitochondrial fission while activating TBK1 in a PINK1-Parkin independent manner. *FASEB J* 34: 6284-6301, 2020.
27. **Allen GFG, Toth R, James J, and Ganley IG**. Loss of iron triggers PINK1/Parkin-independent mitophagy. *EMBO Rep* 14: 1127-1135, 2013.
28. **Dasarathy S, Dodig M, Muc SM, Kalhan SC, and McCullough AJ**. Skeletal muscle atrophy is associated with an increased expression of myostatin and impaired satellite cell function in the portacaval anastamosis rat. *Am J Physiol Gastrointest Liver Physiol* 287: G1124-1130, 2004.
29. **Smeuninx B, McKendry J, Wilson D, Martin U, and Breen L**. Age-Related Anabolic Resistance of Myofibrillar Protein Synthesis Is Exacerbated in Obese Inactive Individuals. *J Clin Endocrinol Metab* 102: 3535-3545, 2017.
30. **Wahlin-Larsson B, Wilkinson DJ, Strandberg E, Hosford-Donovan A, Atherton PJ, and Kadi F**. Mechanistic Links Underlying the Impact of C-Reactive Protein on Muscle Mass in Elderly. *Cell Physiol Biochem* 44: 267-278, 2017.
31. **Katsanos CS, Kobayashi H, Sheffield-Moore M, Aarsland A, and Wolfe RR**. A high proportion of leucine is required for optimal stimulation of the rate of muscle protein

synthesis by essential amino acids in the elderly. *Am J Physiol Endocrinol Metab* 291: E381-E387, 2006.
32. **Kant S, Davuluri G, Alchirazi KA, Welch N, Heit C, Kumar A, Gangadhariah M, Kim A, McMullen MR, Willard B, Luse DS, Nagy LE, Vasiliou V, Marini AM, Weiner ID, and Dasarathy S**. Ethanol sensitizes skeletal muscle to ammonia-induced molecular perturbations. *J Biol Chem* 294: 7231-7244, 2019.
33. **Trendelenburg AU, Meyer A, Rohner D, Boyle J, Hatakeyama S, and Glass DJ**. Myostatin reduces Akt/TORC1/p70S6K signaling, inhibiting myoblast differentiation and myotube size. *Am J Physiol Cell Physiol* 296: C1258-C1270, 2009.
34. **Lokireddy S, Mouly V, Butler-Browne G, Gluckman PD, Sharma M, Kambadur R, and McFarlane C**. Myostatin promotes the wasting of human myoblast cultures through promoting ubiquitin-proteasome pathway-mediated loss of sarcomeric proteins. *Am J Physiol Cell Physiol* 301: C1316-C1324, 2011.
35. **Porter C, Hurren NM, Cotter MV, Bhattarai N, Reidy PT, Dillon EL, Durham WJ, Tuvdendorj D, Sheffield-Moore M, Volpi E, Sidossis LS, Rasmussen BB, and Borsheim E**. Mitochondrial respiratory capacity and coupling control decline with age in human skeletal muscle. *Am J Physiol Endocrinol Metab* 309: E224-232, 2015.
36. **Julienne CM, Dumas JF, Goupille C, Pinault M, Berri C, Collin A, Tesseraud S, Couet C, and Servais S**. Cancer cachexia is associated with a decrease in skeletal muscle mitochondrial oxidative capacities without alteration of ATP production efficiency. *J Cachexia Sarcopenia Muscle* 3: 265-275, 2012.
37. **Sebastian D, Sorianello E, Segales J, Irazoki A, Ruiz-Bonilla V, Sala D, Planet E, Berenguer-Llergo A, Munoz JP, Sanchez-Feutrie M, Plana N, Hernandez-Alvarez MI, Serrano AL, Palacin M, and Zorzano A**. Mfn2 deficiency links age-related sarcopenia and impaired autophagy to activation of an adaptive mitophagy pathway. *EMBO J* 35: 1677-1693, 2016.
38. **Zhou H, Du W, Li Y, Shi C, Hu N, Ma S, Wang W, and Ren J**. Effects of melatonin on fatty liver disease: The role of NR4A1/DNA-PKcs/p53 pathway, mitochondrial fission, and mitophagy. *J Pineal Res* 64: 2018.
39. **Lemasters JJ**. Selective mitochondrial autophagy, or mitophagy, as a targeted defense against oxidative stress, mitochondrial dysfunction, and aging. *Rejuvenation Res* 8: 3-5, 2005.
40. **Dornas W, and Schuppan D**. Mitochondrial oxidative injury: a key player in nonalcoholic fatty liver disease. *Am J Physiol Gastrointest Liver Physiol* 319: G400-G411, 2020.
41. **Sergi D, Naumovski N, Heilbronn LK, Abeywardena M, O'Callaghan N, Lionetti L, and Luscombe-Marsh N**. Mitochondrial (Dys)function and Insulin Resistance: From Pathophysiological Molecular Mechanisms to the Impact of Diet. *Front Physiol* 10: 532, 2019.
42. **Consitt LA, and Clark BC**. The Vicious Cycle of Myostatin Signaling in Sarcopenic Obesity: Myostatin Role in Skeletal Muscle Growth, Insulin Signaling and Implications for Clinical Trials. *J Frailty Aging* 7: 21-27, 2018.
43. **Sinclair M, Grossmann M, Gow PJ, and Angus PW**. Testosterone in men with advanced liver disease: abnormalities and implications. *J Gastroenterol Hepatol* 30: 244-251, 2015.
44. **Niu L, Geyer PE, Wewer Albrechtsen NJ, Gluud LL, Santos A, Doll S, Treit PV, Holst JJ, Knop FK, Vilsboll T, Junker A, Sachs S, Stemmer K, Muller TD, Tschop MH, Hofmann SM, and Mann M**. Plasma proteome profiling discovers novel proteins associated with non-alcoholic fatty liver disease. *Mol Syst Biol* 15: e8793, 2019.

45. **Kumar A, Davuluri G, Welch N, Kim A, Gangadhariah M, Allawy A, Priyadarshini A, McMullen MR, Sandlers Y, Willard B, Hoppel CL, Nagy LE, and Dasarathy S**. Oxidative stress mediates ethanol-induced skeletal muscle mitochondrial dysfunction and dysregulated protein synthesis and autophagy. *Free Radic Biol Med* 145: 284-299, 2019.
46. **Davuluri G, Giusto M, Chandel R, Welch N, Alsabbagh K, Kant S, Kumar A, Kim A, Gangadhariah M, Ghosh PK, Tran U, Krajcik DM, Vasu K, DiDonato AJ, DiDonato JA, Willard B, Monga SP, Wang Y, Fox PL, Stark GR, Wessely O, Esser KA, and Dasarathy S**. Impaired Ribosomal Biogenesis by Noncanonical Degradation of beta-Catenin during Hyperammonemia. *Mol Cell Biol* 39: 2019.
47. **Periyalwar P, and Dasarathy S**. Malnutrition in cirrhosis: contribution and consequences of sarcopenia on metabolic and clinical responses. *Clin Liver Dis* 16: 95-131, 2012.
48. **Hallsworth K, Thoma C, Moore S, Ploetz T, Anstee QM, Taylor R, Day CP, and Trenell MI**. Non-alcoholic fatty liver disease is associated with higher levels of *objectively* measured sedentary behaviour and lower levels of physical activity than matched healthy controls. *Frontline Gastroenterol* 6: 44-51, 2015.
49. **von Haehling S, Morley JE, Coats AJS, and Anker SD**. Ethical guidelines for publishing in the journal of cachexia, sarcopenia and muscle: update 2017. *J Cachexia Sarcopenia Muscle* 8: 1081-1083, 2017.

CHAPTER 5 – THE REGULATORY PROTEIN AND GENE EXPRESSION PROFILE OF SKELETAL MUSCLE IN CHRONIC LIVER DISEASE PATIENTS

The Regulatory Protein and Gene Expression Profile of Skeletal Muscle in Chronic Liver Disease Patients

Sophie L. Allen [1,2], Jonathan I. Quinlan [1,2], Amritpal Dhaliwal [2,3,4], Thomas Nicholson [2,3], Felicity R. Williams [2,3,4], Matthew J. Armstrong [2,4], Ahmed, M. Elsharkawy[2,4], Simon W. Jones [3,5], Carolyn A. Greig [1,2,5], Janet M. Lord [2,3,5], Gareth G. Lavery [2,6,7], Leigh Breen [1,2,5]

Affiliations: [1] School of Sport, Exercise and Rehabilitation Sciences, University of Birmingham, UK. [2] National Institute for Health Research, Birmingham Biomedical Research Centre at University Hospitals Birmingham NHS Foundation Trust, Birmingham, UK. [3] Institute of Inflammation and Ageing, University of Birmingham, UK. [4] Liver Unit, Queen Elizabeth Hospital Birmingham, 3rd Floor, Nuffield House, Mindelsohn Way, Birmingham, UK. [5] MRC-Versus Arthritis Centre for Musculoskeletal Ageing Research, University of Birmingham, UK. [6] Institute of Metabolism and Systems Research, University of Birmingham, UK. [7] Centre for Endocrinology, Diabetes and Metabolism, Birmingham Health Partner, Birmingham, UK.

*Corresponding Author: Leigh Breen

School of Sport, Exercise and Rehabilitation Sciences

University of Birmingham

Edgbaston

B15 2TT

Email: [redacted]

Running title: Mechanisms of sarcopenia in Chronic Liver Disease

Word Count (excluding abstract and references):6168

Key Words: Chronic Liver Disease, Sarcopenia, Protein Turnover, Mitochondria

5.1 Abstract

Background: Low muscle mass, quality and strength (sarcopenia) commonly affects patients with chronic liver disease (CLD). However, the intracellular regulatory pathways which may underpin sarcopenia in CLD patients are unclear. The aim of this study was to characterise the intracellular regulatory signalling pathways that may underscore sarcopenia in CLD patients of different aetiologies and disease stages.

Methods: Muscle biopsy and blood samples were obtained from 9 non-cirrhotic non-alcoholic fatty liver disease patients (NAFLD; aged 61.1±9.0), 12 decompensated end-stage liver disease patients (ESLD; aged 55.7±5.7) and 12 healthy, age-matched healthy controls (CON; aged 55.7±8.7), alongside physical function and body composition tests. The protein content of skeletal muscle anabolic, catabolic, mitochondrial and other regulatory signalling intermediates was determined via western blot. The muscle transcriptome was analysed using RNA-sequencing and pathway analysis.

Results: Body mass and BMI was higher in NAFLD and ESLD patients compared with CON ($P < 0.05$). Serum ammonia was higher in ESLD vs. NAFLD patients ($P < 0.001$), whereas insulin was higher in NAFLD and ESLD compared with CON ($P < 0.001$). Citrate synthase (CS) activity (~43%) and the protein content of OXPHOS complex I was significantly lower (~26%) in ESLD vs. CON ($P < 0.01$) whereas OXPHOS complex IV was significantly lower in ESLD vs. CON (71%; $P < 0.01$) and NAFLD (61%; $P = 0.04$). Total-mTOR protein was significantly lower in NAFLD (62%, $P = 0.01$) and ESLD (52%, $P = 0.03$) vs. CON. Myostatin protein content was significantly greater in NAFLD vs. CON (77%; $P < 0.01$) and ESLD (70%; $P < 0.01$). Gene pathway analysis revealed a significant enrichment in pathways related to oxidative stress and protein ubiquitination in ESLD vs. CON. A significant enrichment in genes related to senescence was evident in NAFLD vs. CON.

Conclusion: Here we show a reduction in total-mTOR protein content in ESLD and NAFLD patients. Additionally, mitochondrial dysfunction and the activation of pathways related to oxidative stress were evident in ESLD patient muscle, while elevated myostatin protein content and genes related to senescence were evident in NAFLD patient muscle. Collectively these findings highlight some similar but largely distinct signalling pathways that may underscore sarcopenia in CLD patients across different aetiologies and disease stages.

5.2 Introduction

Sarcopenia, defined low muscle quality, mass and strength is a common disease complication, affecting an estimated ~25-70% of cirrhotic patients (1). The burden of sarcopenia in end-stage liver disease (ESLD) is considered to be extensive due to its association with pre- and post- liver transplant (LT) complications including; length of hospital stay, mortality and risk of infection (2, 3). Although there is increasing understanding of the clinical complications of sarcopenia in chronic liver disease, investigations into the intracellular signalling pathways which may contribute to the onset of sarcopenia in liver disease patients are scarce (4).

A range of factors may influence the development of sarcopenia in chronic liver disease, including severity or stage of disease (5) and underlying aetiology, with higher sarcopenia prevalence identified amongst alcoholic related liver disease (ArLD) compared with non-alcoholic fatty liver disease (NAFLD) (6). Mechanistically, alterations in muscle protein synthesis (MPS) and muscle protein breakdown (MPB) (7) underpin sarcopenia progression in chronic liver disease and may be driven by a number of systemic factors including; hyperammonemia (8), inflammation (9, 10) and alcohol (11, 12). How these factors influence the intracellular signalling pathways that regulate muscle protein turnover has largely been investigated in cellular and animal models (8, 12-14). The translation of findings from pre-clinical models of intracellular signalling regulation in patients across the spectrum of liver disease, is unclear and is compounded by difficulty in obtaining muscle biopsy samples from cirrhotic patients (15).

A number of intracellular molecular pathways have been implicated in the regulation of muscle protein turnover, including the mammalian target of rapamycin (mTOR) pathway (15), autophagy (13), mitochondrial-related signalling (8, 16) and satellite cell (SC)

signalling (17). Indeed, a decline in mTOR-anabolic signalling and increased proteolysis have been identified in skeletal muscle biopsies from cirrhotic patients, compared with healthy participants (13, 15). Furthermore, we (Chapter 4) and others have suggested that mitochondrial dysfunction may drive myotube atrophy in cellular models of liver disease, induced by *ex vivo* patient serum (Chapter 4), hyperammonemia (8) and ethanol (16) treatment. At the genome level, the downregulation of genes associated with mTOR signalling, mitochondrial oxidative phosphorylation and the tricarboxylic acid cycle (TCA), alongside an upregulation in genes related to reactive oxygen species (ROS) generation have been identified in ethanol treated myotubes (11, 16). Similarly, an upregulation of genes related to mitochondrial dysfunction has been reported in obese individuals (e.g., representative of early-onset NAFLD) (18). Furthermore, pathways related to oxidative stress, senescence and cell cycle regulation are differentially expressed in cirrhotic patients, as well as ammonia-treated mice and myotubes (19). Collectively, these studies highlight the potential role of mTOR-related signalling, and mitochondrial dysfunction in the development of liver disease-related sarcopenia. In order to implicate dysregulated intracellular signalling pathways in liver disease-related sarcopenia, and identify appropriate targets for therapeutic intervention, comprehensive intracellular protein-to-gene analysis across different aetiologies and disease stages is now required.

The aim of the present study was to characterise the intracellular protein content of key regulatory markers of skeletal muscle morphology and metabolism in muscle biopsy tissue from decompensated, alcohol related-ESLD, non-cirrhotic NAFLD patients and healthy control participants (CON). In addition, we conducted pathway enrichment analysis through ribonucleic acid (RNA)-sequencing to investigate gene enrichment patterns in CON, NAFLD and ESLD. We hypothesized that muscle from ESLD patients would exhibit impaired signalling related to mitochondrial function and anabolism alongside an increase in

proteolytic markers compared with CON. We hypothesized that NAFLD patients would show a similar pattern of intracellular signalling dysregulation to ESLD, albeit at a lesser magnitude.

5.3 Methods

5.3.1 Participant Characteristics and Ethical Approval

12 healthy CON, 12 decompensated alcohol related-ESLD, and 9 non-cirrhotic NAFLD patients were recruited and provided their written informed consent to participate in this study. ESLD patients and NAFLD patients were recruited after screening in a clinical setting. ESLD patients were assessed for LT and presence of cirrhosis in ESLD was confirmed through consistent imaging, clinical findings and elastography with or without a liver biopsy. All ESLD patients recruited to this study had an underlying etiology of ArLD. The NAFLD patients were non-cirrhotic and were recruited through a dedicated liver clinic, with cirrhosis excluded by a liver biopsy or transient elastography. Prior to recruitment of this study, participants were not assessed for sarcopenia to allow the opportunity to assess the prevalence in both ESLD and NAFLD cohorts. A number of comorbidities were present in NAFLD and ESLD patients which are detailed in Table 5.1. CON participants were expected to be free from chronic inflammatory disease (i.e., chronic liver disease, inflammatory bowel disease and rheumatoid arthritis), metabolic disease conditions (i.e., type II diabetes and hyperlipidaemia) and normotensive (<140/90). Ethical approval for this study was obtained through the local ethics committee at the Health Research Authority – West Midlands Solihull Research Ethics Committee Authority (REC reference: 18/WM/0167) and conformed to the standards set by the Declaration of Helsinki. This was a registered clinical trial (clinicaltrials.gov, ID: NCT04734496).

Table 5.1. Co-morbidities in NAFLD and ESLD patients

	NAFLD (n=9)	ESLD (n=12)
Hepatic encephalopathy	0	9
Portal hypertension	0	12
Cardiovascular disease	0	2
Stroke	2	0
Hypertension	6	2
Chronic obstructive pulmonary disease	2	0
Diabetes mellitus	6	4
Insulin dependence	3	4
Oral hypoglycaemic treatment	5	0
Hypercholesterolemia	4	1
Chronic kidney disease	1	4
Asthma	0	1

5.3.2 Study Design

Participants reported to the laboratory after a minimum of a 4-hour fast and were asked to refrain from the consumption of caffeine on the morning of the trial. Participants were also asked to refrain from strenuous exercise for 24-hours prior to their visit to the laboratory. Upon arrival, a fasted blood sample was obtained from the antecubital vein and collected in ethylenediaminetetraacetic acid (EDTA) and serum separator vacutainers (BD, Oxford, UK). After the collection of blood samples, a subset was allowed to sit for 30-minutes at room temperature to allow the blood to clot. Blood was centrifuged at 3,000 g for 10-minutes at 4°C to obtain plasma and serum. Participants underwent basic body composition analysis and functional assessment through handgrip strength (HGS) and short physical performance battery (SPPB) testing. Both HGS and SPPB have previously been utilised to assess muscle strength and physical performance respectively in older, and cirrhotic populations (20-23). Additionally, a muscle biopsy of the vastus lateralis was performed after confirmation participants had a platelet count of >30 and an international normalised ratio (INR) of ≤ 1.6.

5.3.3 Blood Analyses

Concentrations of serum myostatin and insulin growth factor-1 (IGF-1) were analysed using commercially available DuoSet enzyme-linked immunosorbent assays (ELISA) (DY788-05, R&D Systems; DY291, R&D Systems respectively) and were completed in line with manufacturer's instructions. Serum interleukin (IL)-1β, IL-4, IL-9, IL-16, tumor necrosis factor-beta (TNF-β), hepatocyte growth factor (HGF), insulin and c-peptide were analysed using commercially available Bio-Plex Pro immunoassays (171A7001M Bio-Rad; 12007283 Bio-Rad) and were completed following manufacturer's instructions. Immunoassays were imaged using a Luminex multiplex platform (Luminex, R&D Systems).

5.3.4 Muscle Sample Preparation

After blood samples were obtained, a muscle biopsy (~100mg) was obtained from the vastus lateralis muscle of the dominant leg under local anaesthesia (1% lidocaine) using the Bergström needle. After extraction from the needle, muscle tissue was washed in sodium chloride (saline) and any visible adipose, or connective tissue was removed. Samples were snap frozen in liquid nitrogen and stored for future protein and RNA analysis at -80°C.

5.3.5 Immunoblotting

For protein analysis, approximately 20-30mg of muscle tissue was homogenised in ice-cold radio-immunoprecipitation assay (RIPA) lysis buffer (10μl /mg) (Merck Millipore, Watford, UK) with protease (1x complete protease inhibitor tablet (Roche, Switzerland) and phosphatase inhibitors (1x PhosSTOP tablet (Roche) using a TissueLyser II. Once homogenised, samples were centrifuged for 10-minutes at 8,000g at 4°C. The concentration of protein lysates was determined using a detergent compatible (DC) protein assay and concentrations were read at an absorbance of 750nm using a FLUOstar Omega plate reader, as previously described (section 2.4.2). Equal amounts of protein from each sample were

added to 1x Laemmli sample buffer and left on the bench-top for 24-hours to denature, before immunoblotting.

Protein (15-30 μg) was loaded onto 4-20% pre-cast gels and subjected to electrophoresis at 100V for 10-minutes, followed by 140V for ~1-hour to separate samples as outlined previously in section 2.4.3. Protein was then transferred from the gel to a nitrocellulose membrane at 100V for 1-hour as previously described (section 2.4.4). Membranes were stained with Ponceau S solution as a loading control and subsequently blocked with 5% bovine serum albumin (BSA) or 5% milk diluted in Tris-buffered saline and 0.1% Tween-20 (TBST) for 1-hour (section 2.4.5). Afterwards, membranes were incubated overnight at 4°C with the following primary antibodies: phospho-mTOR Ser2448, total-mTOR, phospho-eukaryotic elongation factor 2 (eEF2) Thr56, total-eEF2, phospho- protein kinase B (Akt) (Ser473), total-Akt, phospho- S6 kinase (RPS6) Ser240/244, total-RPS6, phospho- eukaryotic translation initiation factor 4E- binding protein 1 (4EBP-1) Thr37/46, total-4EBP-1, muscle ring finger-1 (MuRF-1), muscle atrophy box (MAFbx), caspase-3, microtubule-associated protein 1A/B light chain 3 (LC3A/B), myostatin, oxidative phosphorylation (OXPHOS) human cocktail, optic atrophy protein 1 (OPA-1), dynamic related protein 1 (DRP1) (D8H5), fission-1 (FIS-1), mitofusin-2 (MFN-2) (D2D10), mitochondrial fission factor (MFF), anti-myosin (skeletal muscle, fast), anti-myosin (skeletal muscle, slow), paired box 7 (Pax7), myoblast determination protein 1 (MyoD), myogenin and anti-ubiquitinylated proteins, clone FK2. Finally, membranes were washed in TBST for 15-minutes and incubated for 1-hour with an anti-rabbit IgG horseradish peroxidase (HRP)-conjugated secondary antibody with the exception of MAFbx (anti-rat IgG, HRP-linked antibody), MuRF-1, OXPHOS, OPA-1, anti-myosin (skeletal muscle, slow), anti-myosin (skeletal muscle, fast), myogenin and anti-ubiquitinylated proteins, clone FK2 (anti-mouse IgG, HRP-linked antibody). Detailed information of both primary and secondary antibodies can be found in Table 2.1. Following a

further 15-minutes of TBST washes, protein was quantified using Immobilon Western chemiluminescent HRP substrate and imaged on a G:BOX Chemi XTR imager using GeneSys capture software as described previously in Section 2.4.6. Upon image capture, band quantification was conducted using ImageJ software and normalized as described previously (section 2.4.6).

5.3.6 RNA Sequencing Analysis

Snap frozen muscle tissue was homogenised in RLT lysis buffer (74704, Qiagen, Manchester, UK), supplemented with 2-mercaptoethanol using a TissueRupter II (Qiagen). Next, total RNA was extracted using a RNeasy Fibrous Tissue Kit (74704, Qiagen) and treated with DNase (79254, Qiagen). Values of RNA integrity number were >7 (Aglient Bioanalyser). Library preparation and RNA-sequencing was performed using a QuantSeq 3' kit (Lexogen, Austria) and sequenced on an Illumina's NextSeq 500 by the Genomics Facility at the University of Birmingham. Once sequenced, RNA data was imported into Galaxy, a web platform (usegalaxy.org) and aligned to the human reference genome (hg38) with HISAT2 (24). Subsequently, aligned binary alignment (BAM) files were imported into Qlucore Omics Explorer v3.6 (Qlucore, AB, Lund, Sweden). Differential analysis was then performed following Trimmed Mean of M values normalization. Data was filtered to allow for the identification of differentially expressed genes using a multi-group statistical comparison set at $p < 0.05$. To establish differences between CON and either NAFLD and ESLD data was filtered using a two-group analysis with parameters set at $P < 0.05$ and a fold change > 1.5.

Differentially expressed genes from each patient cohort ($P < 0.05$, fold Change > 1.5) were analysed using Ingenuity Pathway Analysis (IPA, Qiagen, UK) in order to determine the significance of the association with certain functions and pathways. To calculate the p-values

of the association between pathways and genes a Fisher's exact test was used. To predict upstream regulators, p-values and z-scores were generated based upon the significant overlap present between the genes within the differentially expressed data set and known targets that are regulated by the transcriptional regulator.

5.3.7 Citrate Synthase Activity Assay

For the assessment of citrate synthase (CS) activity, protein (20μg) was loaded into each well. CS activity was measured in 50mmol/L Tris (pH 8.0), 100μmol/L 5,5-dithio-bis-(2-nitrobenzoic acid) (DTNB) and 120μmol/L acetyl CoA. The reaction was started with the addition of 100 μmol/L oxaloacetic acid to each well. CS activity was assessed spectrophotometrically through the measurement of 5-thio-2-nitrobenzoic acid (TNB) at an absorbance of 412 nm at 37°C with measurements taken every 15-seconds over a 3-minute period.

5.3.8 Statistical Analysis

Statistical analysis was performed using GraphPad Prism Version 9.2. Data was tested for normality using a Shapiro-Wilk test, and for homogeneity of variances through a Levene's test. A one-way ANOVA was used to investigate differences in anthropometric measures, body composition components and muscle strength between groups (i.e., CON, NAFLD, ESLD). A one-way ANOVA was also used to investigate changes in myostatin, IGF-1, INR, alanine aminotransferase (ALT), bilirubin, albumin, insulin, c-peptide, IL-1β, IL-4, IL-9, IL-16, TNF-β and HGF. An independent samples t-test was used to investigate changes in ammonia. A one-way ANOVA was used to analyse the protein content of markers of anabolic, catabolic, regulatory and mitochondrial signalling and CS activity. Where the results of a one-way ANOVA revealed a positive interaction effect, post-doc analysis t-tests were completed using Tukey's HSD. Effect size was calculated using partial eta squared (η^2)

for omnibus tests and Cohen's d for post-hoc comparisons. RNA-sequencing analysis was performed using two-group comparisons in Qlucore Omics Explorer v3.7 and IPA software (i.e., CON vs. NAFLD, CON vs. ESLD). Statistical significance was set at $p < 0.05$. The data presented in this chapter include the mean of each participant ± standard deviation unless stated otherwise. Figures were generated in GraphPad Prism version 9.2.

5.4 Results

5.4.1 Body Composition, Muscle Mass and Strength

Participant characteristics can be found in Table 5.2. No significant difference was identified in age, height, body fat (BF) (%) (P = 0.3, $\eta^2 = 0.09$) and lean body mass (% of total body mass) (P = 0.2, $\eta^2 = 0.1$) between CON, NAFLD and ESLD. A one-way ANOVA revealed a significant main effect for BMI (P = 0.004, $\eta^2 = 0.3$, F= 6.6), weight, (P = 0.005, $\eta^2 = 0.3$, F = 6.4) fat mass (P = 0.03, $\eta^2 = 0.2$, F = 4.0) and fat free mass (FFM) (P = 0.02, $\eta^2 = 0.2$, F = 4.6) between groups. BMI was found to be significantly higher in NAFLD (~36%, P = 0.007, d = 10.1) and ESLD (~30%, P = 0.02, d= 11.2) compared with CON. Similarly, body mass was significantly greater in NAFLD (~48%, P = 0.07, d = 7.7) and ESLD (~38%, P = 0.02, d = 9.8) patients, compared with CON. However, body fat mass was significantly elevated in NAFLD patients only compared with CON (~ 99%, P = 0.3, d = 4.1). No significant difference in body fat mass was identified between ESLD and both NAFLD and CON participants. Additionally, FFM was significantly greater in ESLD patients compared with CON (~32%, P = 0.02, d = 9.1). No difference in FFM was identified between NAFLD in comparison to ESLD and CON participants.

A one-way ANOVA revealed a significant main effect for SPPB between groups (P = 0.001, $\eta^2 = 0.4$, F = 8.8). SPPB scores were significantly lower in ESLD patients compared with NAFLD (~ 2.8%, P = 0.02, d = 24.6) and CON (~ 12.5%, P = 0.001, d = 31.1). No significant

difference in SPPB was identified between NAFLD and CON participants. No significant difference in HGS was identified between groups.

Table 5.2 Participant characteristics for anthropometric, body composition and strength data in CON, NAFLD and ESLD patients.

	CON (n=12)	NAFLD (n=9)	ESLD (n=12)
Gender (Male: Female)	6:6	6:3	7:5
Age (years)	55.7 ± 8.7	61.1± 9.0	55.7±5.7
Body mass (kg)	72.7±13.5	107.3±33.2**	100.4±22.0*
Height (m)	1.7±0.08	1.7±0.08	1.7±0.07
BMI (kg m^{-2})	25.3±3.8	34.5±8.0**	32.9±6.6*
FM (kg)	22.2±6.4	42.1±24.9*	33.6±13.3
BF (%)	30.6±7.1	38.1±13.3	33.1±9.1
FFM (kg)	50.5±11.3	63.1±13.8	66.7±14.4*
Lean Mass (% of body mass)	69.4±7.1	61.2±12.9	66.9±8.9
HGS (kg)	35.0±8.1	33.7±9.8	32.6±7.7
SPPB	12.0±0.0	11.67±0.5	10.5±1.5***†
Serum ALT (IU/L)	20.6±6.5	43.2±40.6	24.3±12.6
Serum Bilirubin (μmol/L)	12.1±5.2	8.8±2.9	49.3±41.2**†
Serum Albumin (g/L)	41.8±2.7	41.1±3.0	33.7±6.6***††
International Normalised Ratio	0.9±0.07	1.0±0.1	1.4±0.2***‡
Serum Ammonia (μmol/L)	N/A	32.9±8.9	73.9±25.5‡
Serum Insulin (pg/mL)	179.7±144.8	812.3±691.8*	675.7±453.5*
Serum C-peptide (pg/mL)	574.4±311.0	1153.0±561.6	1311.0±620.1**
Serum IGF-1 (pg/mL)	1199±1907	1719±2617	990±857
Serum Myostatin (pg/mL)	1579±1010	1059±372.4	3163±387
Serum HGF (pg/mL)	185.3±77.7	282.6±166.5	528.2±151.4***††
Serum TNF-$\boldsymbol{\beta}$ (pg/mL)	38.5±12.5	33.77±9.5	53.1±27.7
Serum IL-1$\boldsymbol{\beta}$ (pg/mL)	1.1±1.0	0.6±0.2	1.1±1.0
Serum IL-4 (pg/mL)	2.1±1.4	0.9±0.3*	1.5±0.4
Serum IL-9 (pg/mL)	40.7±8.9	34.07±10.1	54.0±24.3
Serum IL-16 (pg/mL)	6.6±3.6	4.5±3.6	14.9±12.6†

ALT, alanine aminotransferase, BMI, Body Mass Index, FM, Fat Mass, BF, Body Fat, FFM, Fat Free Mass, HGS, Handgrip Strength, SPPB, Short Physical Performance Battery, IGF-1, insulin growth factor-1, HGF, hepatocyte growth factor, TNF-$\boldsymbol{\beta}$, tumor necrosis factor-beta, IL-1$\boldsymbol{\beta}$, interleukin-1 beta, IL-4, interleukin-4, IL-9, interleukin-9, IL-16, interleukin-16

* Significantly different from CON ($P < 0.05$)
** Significantly different from CON ($P < 0.01$)
***Significantly different from CON ($P < 0.001$)
† Significantly different from NAFLD ($P < 0.05$)
††Significantly different from NAFLD ($P < 0.01$)
‡ Significantly different from NAFLD ($P < 0.001$)

5.4.2 Blood Analysis

Clinical blood markers are shown in Table 5.2. ESLD patients had significantly greater bilirubin (P = 0.003, d = 1.6; P = 0.01, d = 1.4), INR (P < 0.001, d = 3.2; P < 0.001, d =2.4), and a significant reduction in serum albumin concentration (P < 0.001, d = 2.9; P = 0.002, d = 1.5) compared with CON and NAFLD patients, respectively. Additionally, serum ammonia was significantly elevated in ESLD compared with NAFLD patients (P < 0.001, d = 2.4). No significant difference in alanine aminotransferase (P = 0.07, η^2 = 0.2), serum IGF-1 (P = 0.7, η^2 = 0.02), myostatin (P = 0.2, η^2 = 0.1), TNF-β (P = 0.09, η^2 = 0.2) or IL-1β (P = 0.5, η^2 = 0.06) concentration was found between groups. Although a significant main effect was identified for the concentration of IL-9 (P = 0.05, η^2 = 0.2), no significant difference was identified in CON vs. NAFLD and ESLD (P = 0.7, d = 0.7; P = 0.2, d = 0.8 respectively), nor NAFLD vs. ESLD (P = 0.053, d = 1.2). Serum insulin was significantly greater in both NAFLD (P = 0.02, d = 1.5) and ESLD (P = 0.04, d = 1.6) compared with CON. Serum c-peptide concentration was also significantly greater in ESLD compared with CON (P = 0.006, d = 1.6). C-peptide concentration in NAFLD did not differ from CON (P = 0.06, d = 1.3) or ESLD (P = 0.8, d = 0.3). Serum HGF was significantly elevated in ESLD compared with CON (P < 0.0001, d = 3.0) and NAFLD patients (P = 0.002, d = 1.5). IL-4 concentration was significantly greater in CON compared with NAFLD patients (P = 0.03, d = 1.4). No difference in IL-4 concentration was identified between ESLD and CON (P = 0.2, d = 0.8) or NAFLD (P = 0.4, d = 1.5) patients. In addition, IL-16 was significantly greater in ESLD compared with NAFLD patients (P = 0.04, d = 1.3). No significant difference in IL-16 was found between CON and both ESLD (P = 0.07, d = 1.0) and NAFLD (P = 0.8, d = 0.6) patients.

5.4.3 Anabolic Signalling

No significant difference in the phosphorylation of mTOR (P = 0.3, η^2 = 0.1), eEF2 (P = 0.9, η^2 = 0.004), Akt (P = 0.1, η^2 = 0.1), RPS6 (P = 0.5, η^2 = 0.04) and 4EBP-1 (P = 0.2, η^2 = 0.1)

in basal-fasted muscle biopsy tissue between groups (Figure 5.1). Additionally, we found no significant difference in total eEF2 (P = 0.9, η^2 = 0.007), Akt (P = 0.5, η^2 = 0.04), RPS6 (P = 0.9, η^2 = 0.005) and 4EBP-1 (P = 0.5, η^2 = 0.04) between groups. However, a significant main effect was identified for the protein content of total-mTOR between groups (P = 0.006, η^2 = 0.3), with lower total-mTOR protein in NAFLD (62%, P = 0.01, d = 2.8) and ESLD (52%, P = 0.03, d = 3.6) compared with CON. No significant difference in total-mTOR protein was evident between NAFLD and ESLD patients (P = 0.9, d = 0.3).

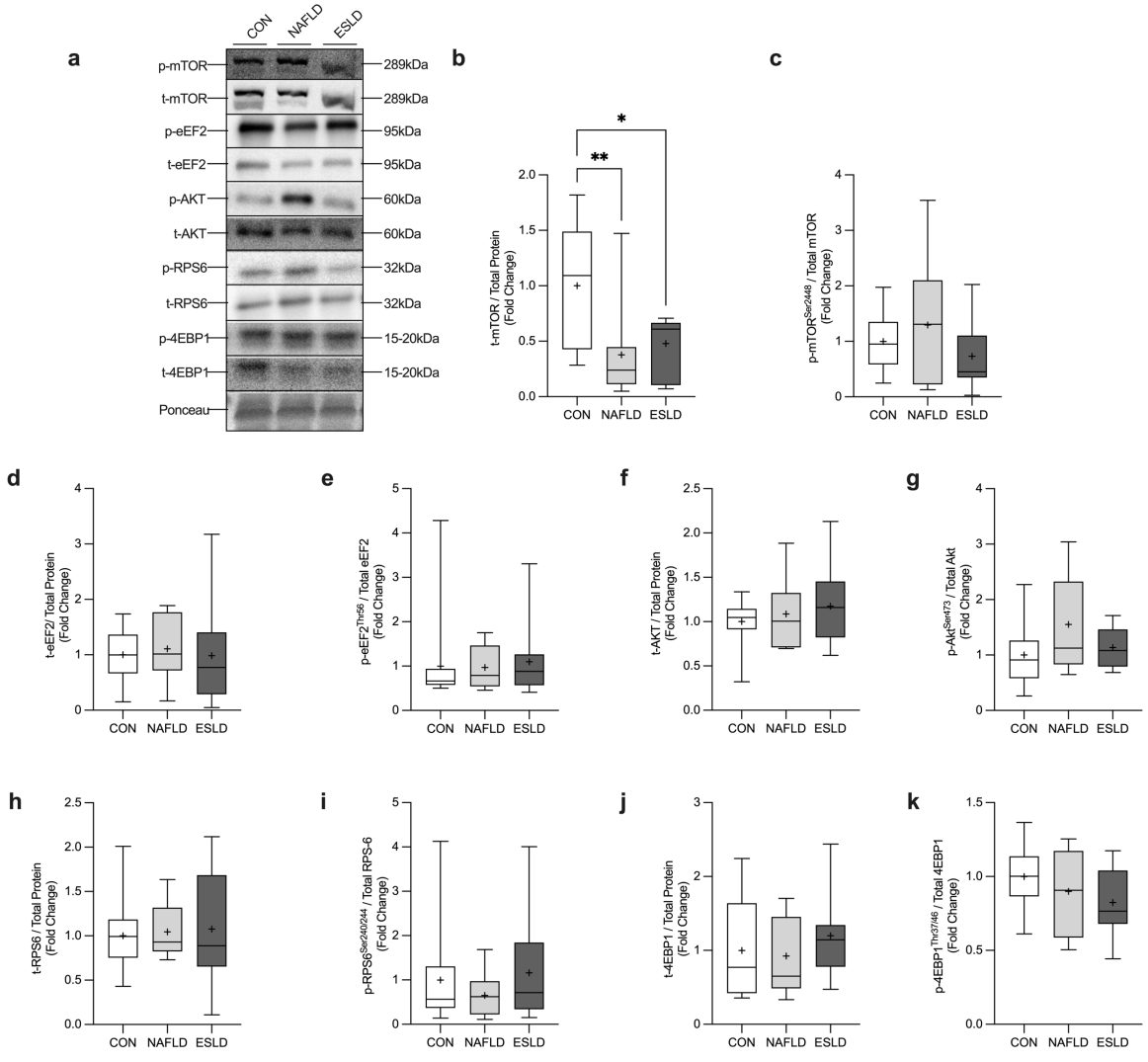

Figure 5.1. Western blot analysis of anabolic signalling targets in CON, NAFLD and ESLD patients. (A) representative western blot images of anabolic markers and loading

control, (B) total-mTOR, (C) phospho-mTOR^{Ser2448} / total-mTOR, (D) total-eEF2, (E) phospho-eEF2^{Thr56} / total-eEF2, (F) total-Akt, (G) phospho-Akt^{Ser473} / total-Akt, (H) total-RPS6, (I) phospho-RPS6$^{Ser240/244}$ / total RPS6, (J) total-4EBP-1, (K) phospho-4EBP-1$^{Thr37/46}$ / total-4EBP-1. Data are expressed as fold change in comparison to the CON participants. Data are expressed as the mean (cross), median (central horizontal line), 25th and 75th percentiles (box) and the minimum and maximum values (vertical lines). * $P < 0.05$, ** $P < 0.01$.

5.4.4 Catabolic Signalling

No significant difference in the protein content of FK2 ($P = 0.1$, $\eta^2 = 0.1$), MuRF-1 ($P = 0.4$, $\eta^2 = 0.1$), MAFbx ($P = 0.6$, $\eta^2 = 0.1$), caspase-3 ($P = 0.9$, $\eta^2 = 0.01$) or LC3A/B ($P = 0.4$, $\eta^2 = 0.03$) was identified between CON, NAFLD and ESLD (Figure 5.2). However, a significant main effect was identified in myostatin protein content between groups ($P = 0.003$, $\eta^2 = 0.3$). Myostatin protein content was increased in NAFLD patients compared with CON (77%, $P = 0.006$, $d = 5.5$) and ESLD (70%, $P = 0.007$, $d = 5.2$). No significant difference was identified between CON and ESLD ($P = 1.0$, $d = 0.04$).

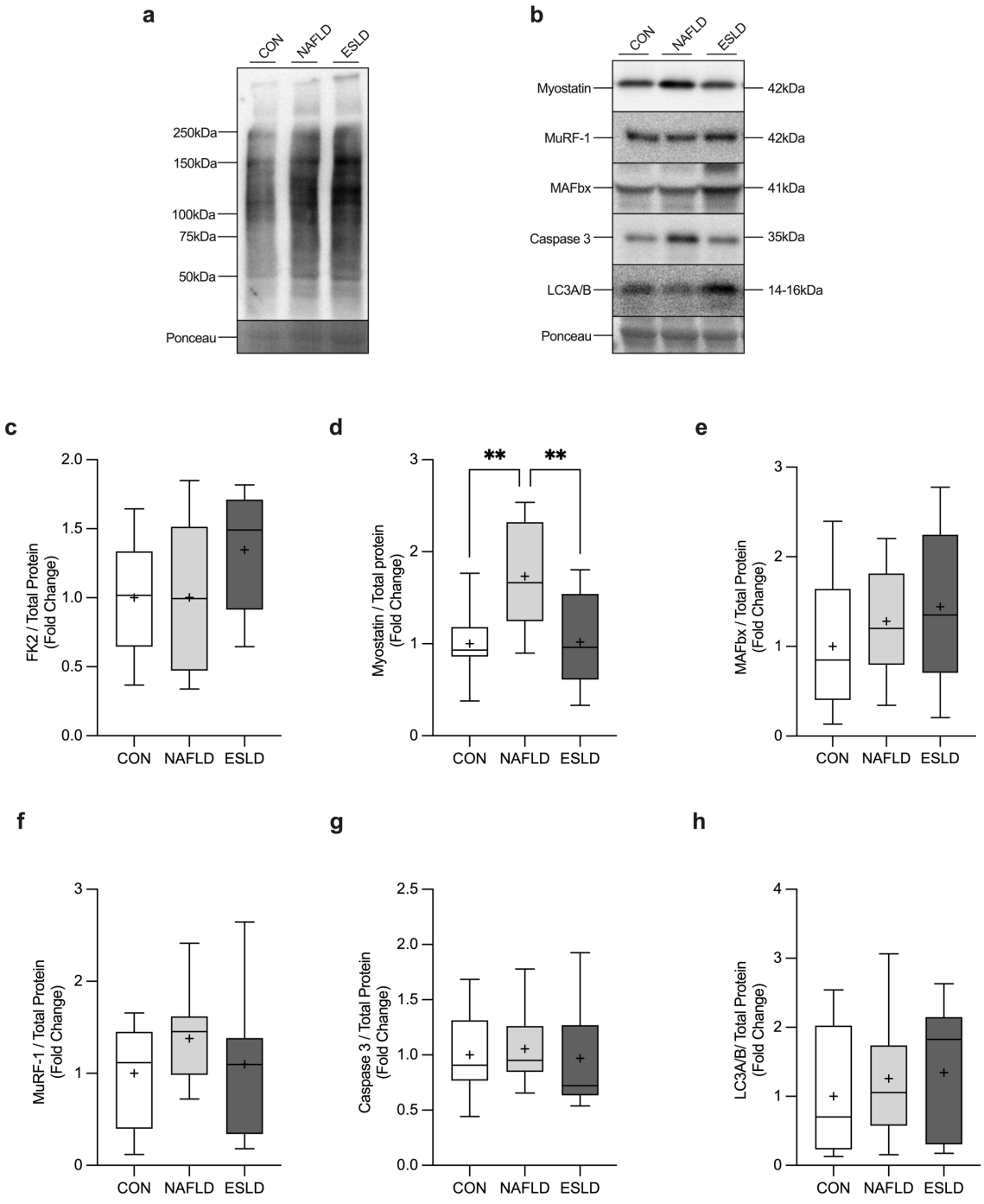

Figure 5.2. Markers of proteolytic signalling in CON, NAFLD and ESLD patients. (A) representative western blot image of FK2 and loading control, (B) Representative western blot images of proteolytic markers and loading control, (C) FK2, (D) myostatin, (E) MAFbx, (F) MuRF-1, (G) caspase-3, (H) LC3A/B. Data are expressed as fold change in comparison to

the CON participants. Data are expressed as the mean (cross), median (central horizontal line), 25th and 75th percentiles (box) and the minimum and maximum values (vertical lines). ** $P < 0.01$.

5.4.5 Mitochondrial Markers and Activity

No significant difference in the protein content of fission markers; FIS1 ($P = 0.7$, $\eta^2 = 0.02$), DRP1 ($P = 0.6$, $\eta^2 = 0.04$) and MFF ($P = 1.0$, $\eta^2 = 0.002$) was found between CON, NAFLD and ESLD. Similarly, no significant difference in the protein content of fusion markers; OPA1 ($P = 0.2$, $\eta^2 = 0.1$) and MFN2 ($P = 0.3$, $\eta^2 = 0.02$) was found between CON, NAFLD and ESLD. A one-way ANOVA revealed a significant main effect of CS activity between groups ($P = 0.007$, $\eta^2 = 0.3$). CS activity was significantly lower in ESLD patients compared with CON (43.4%, $P = 0.005$, $d = 4.6$). No difference was found between NAFLD and both CON and ESLD patients ($P = 0.4$, $d = 0.6$; $P = 0.2$, $d = 1.0$, respectively). Additionally, a significant main effect was identified in the protein content of OXPHOS complex I ($P = 0.006$, $\eta^2 = 0.3$) and complex IV ($P = 0.007$, $\eta^2 = 0.3$, $F = 5.9$) between groups. The protein content of complex I (26%, $P = 0.005$, $d = 6.0$) and complex IV (71%, $P = 0.008$, $d = 2.8$) was significantly lower in ESLD patients compared with CON. The protein content of complex IV was significantly lower in ESLD compared with NAFLD patients (67%, $P = 0.04$, $d = 2.7$).

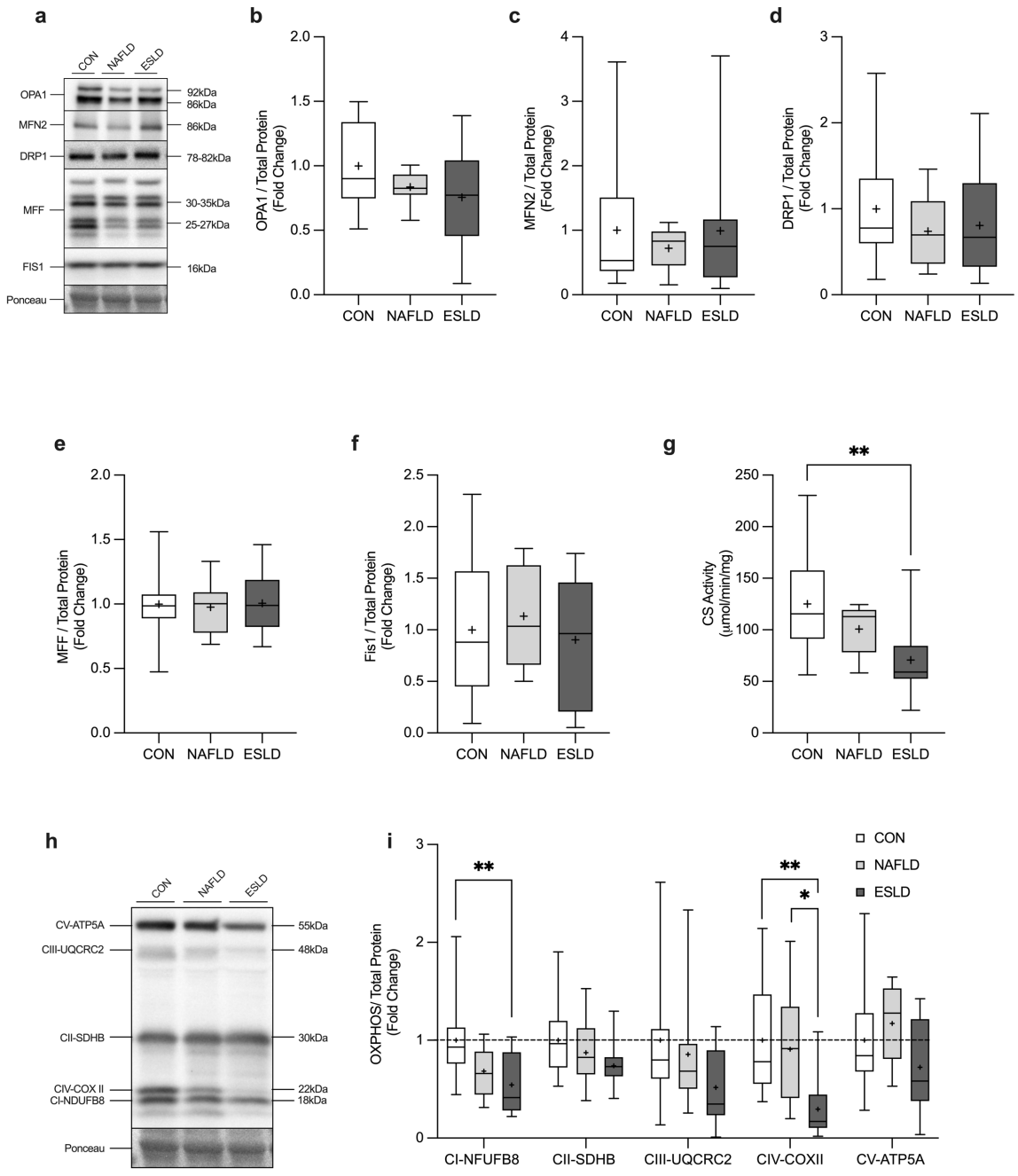

Figure 5.3 Markers of mitochondrial fission, fusion and content in CON, NAFLD and ESLD patients. (A) representative western blot images of markers of mitochondrial fusion, fission and loading control, (B) OPA1, (C) MFN2, (D) DRP1, (E) MFF, (F) FIS1, (G) citrate synthase activity, (H) representative western blot image of the human OXPHOS complex and loading control, (I) OXPHOS. Data are expressed as fold change in comparison to the CON participants. Data are expressed as the mean (cross), median (central horizontal line), 25th and

75th percentiles (box) and the minimum and maximum values (vertical lines). * P < 0.05, ** P < 0.01.

5.4.6 Regulatory Markers

No significant difference was identified in the protein content of myosin fast (P = 0.8, η^2 = 0.02) and slow (P = 0.5, η^2 = 0.1), Pax7 (P = 0.2, η^2 = 0.1), MyoD (P = 0.6, η^2 = 0.04) and myogenin (P = 0.3, η^2 = 0.1) between CON, NAFLD and ESLD (Figure 5.4).

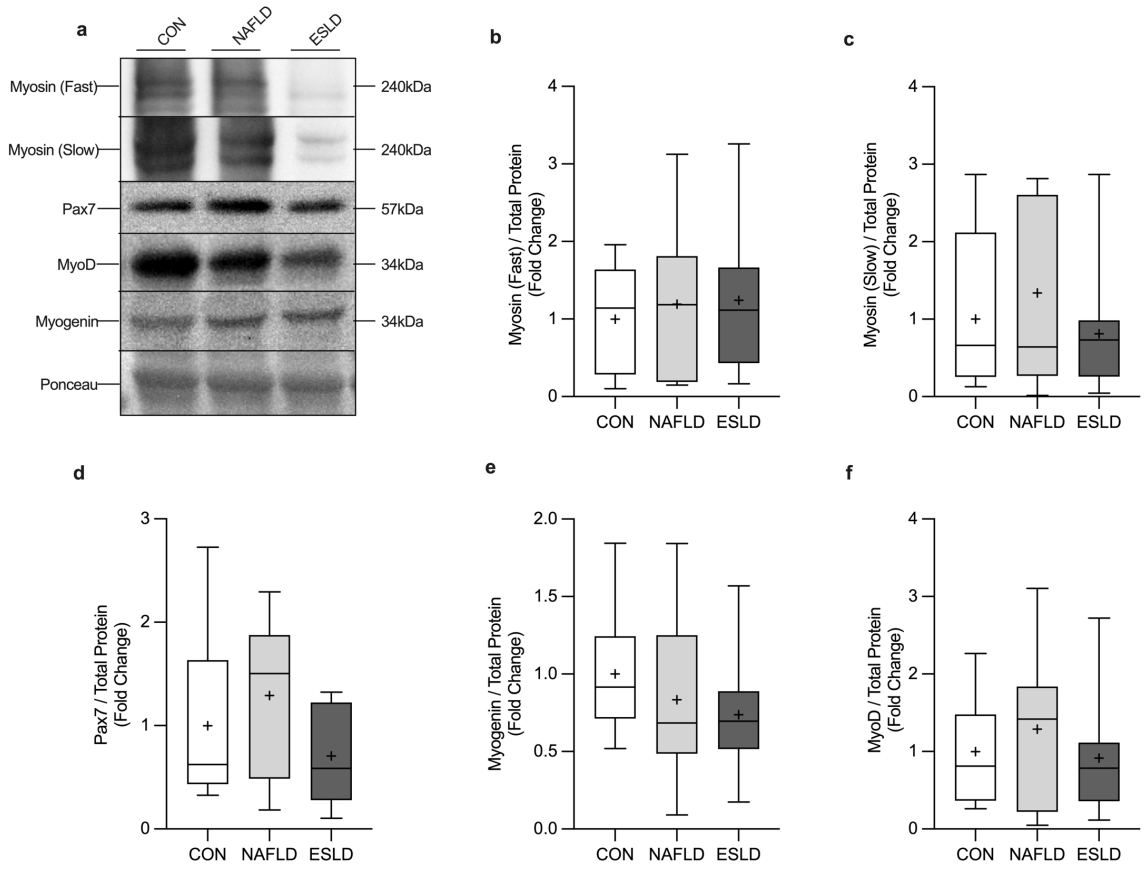

Figure 5.4 Regulatory protein content in CON, NAFLD and ESLD patients. (A) Representative western blot images of regulatory markers and loading control, (B) myosin (Fast), (C) myosin (Slow), (D) Pax7, (E) myogenin, (F) MyoD. Data are expressed as fold change in comparison to the CON participants. Data are expressed as the mean (cross),

median (central horizontal line), 25th and 75th percentiles (box) and the minimum and maximum values (vertical lines).

5.4.7 RNA Sequencing Analysis

To provide a more in-depth characterisation of intracellular signalling, RNA-sequencing analysis was performed. When comparing CON to NAFLD patients, a total of 2,161 genes were differentially expressed ($P < 0.0001$, fold change < 2), of which 1 was downregulated and 2,160 were upregulated. Functional pathway analysis (IPA) of these differentially expressed genes revealed that the most significant canonical pathways were 'endoplasmic reticulum stress pathway', 'ceramide signalling', 'lipopolysaccharide (LPS)-stimulated mitogen-activated protein kinase (MAPK) signalling' and 'senescence pathway'. Furthermore, amongst the top 20 most significant pathways were 'phosphoinositide 3-kinase (PI3K) /AKT signalling', 'PI3K signalling by lymphocytes' and 'tumor growth factor-β (TGF-β) signalling'. In line with pathway analysis the most differentially expressed genes were related to mitochondrial respiration, ribosomal and structural proteins.

When comparing CON to ESLD patients a total of 635 genes were differentially expressed ($P < 0.05$, Fold Change > 1.5) of which 54 were downregulated and 581 were upregulated. Functional pathway analysis revealed that of these differentially expressed genes, the most significant canonical pathways were 'integrin linked kinase (ILK) signalling', 'actin cytoskeleton signalling', 'RAC signalling' and 'unfolded protein response'. Furthermore, amongst the top 20 most significant pathways were 'nuclear factor erythroid factor 2 related factor 2 (NRF2)-mediated oxidative stress response', 'endoplasmic reticulum stress pathway' and 'protein ubiquitination'. The most differentially expressed genes were related to oxidative stress and regulation of the cytoskeleton.

Of interest, a large number of genes were differentially expressed in NAFLD, compared with ESLD patients (Figure 5.5G). To further investigate these changes, we performed an upstream analysis to identify any inhibited, or activated upstream regulators of the CLD transcriptomes. In NAFLD patients, glutathione reductase (GSR), IKARSO family zinc finger 3 (IKZF3), nitric oxide synthase trafficking (NOSTRIN), Cpb/P300 interacting transactivator 2 (CITED2), N-myc downstream regulated 1 (NDRG1) were identified as inhibited upstream regulators, while transforming growth factor beta 1 (TGFB1), forkhead box O (FOXO) 1, insulin like growth factor binding protein 2 (IGFBP2), eukaryotic translation initiation factor 4 gamma 1 (EIF4G1), v-Raf-1 murine leukaemia viral oncogene homolog 1 (RAF1) were identified as activated upstream regulators compared with CON. In ESLD patients, protein kinase AMP-activated catalytic subunit alpha 2 (PRKAA2), apolipoprotein E (APOE), tuberous sclerosis complex 2 (TSC2) and PPAR coactivator alpha (PPARGC1A) were identified as inhibited upstream regulators, while IGF-1, PI3K, AKT1 and TGFB1 were identified as activated upstream regulators compared with CON.

Furthermore, we examined selected genes related to mTOR, mitochondrial and proteolytic pathways identified using gene sets obtained from the Molecular Signatures Database (MSigDB) (25). We found that NAFLD patients exhibited an upregulation of genes related to mTOR, including mTORC1, RPS6KB1, proline-rich Akt1 substrate 1 (Akt1S1) and eukaryotic translation initiation factor 4E (eIF-4E) in comparison to both CON and ESLD patients ($P < 0.05$, $q < 0.08$). Additionally, genes related to autophagy ($P < 0.01$, $q < 0.02$) and protein ubiquitination ($P < 0.05$, $q < 0.06$) were also upregulated in NAFLD patients compared with CON and ESLD. Finally, a number of genes related to autophagy were shown to be upregulated in ESLD patients compared with CON ($P < 0.05$, $q = 0.42$, fold change < 2).

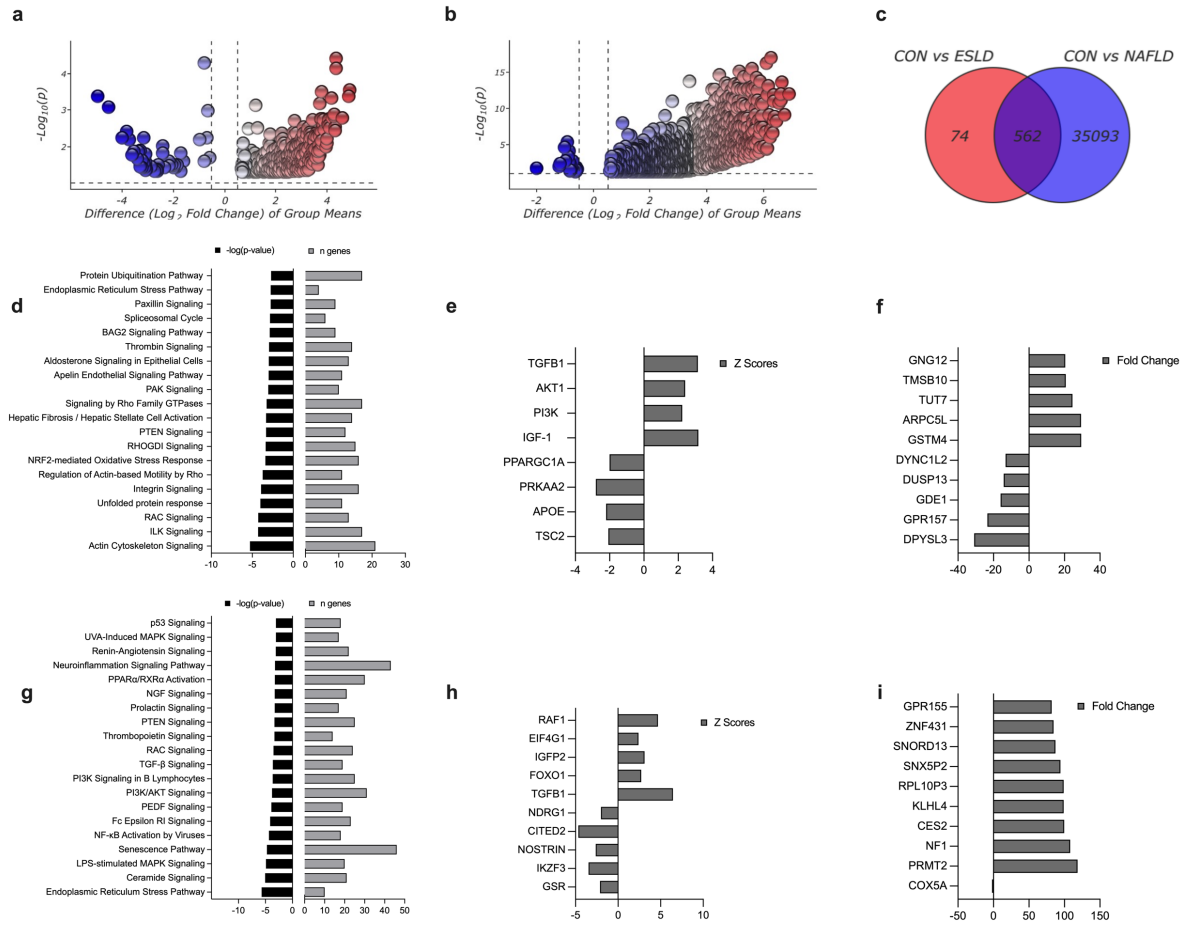

Figure 5.5. RNA-sequencing analysis of CON, NAFLD and ESLD muscle biopsy samples. (A) volcano plot of differential gene expression between CON and ESLD patients. Fold change (Log2) of gene expression is plotted against p value (-Log10) ($P < 0.05$, Fold Change > 1.5, (B) volcano plot of differential gene expression between CON and NAFLD patients. Fold change (Log2) of gene expression is plotted against p value (-Log10) ($P < 0.05$, Fold Change > 1.5), (C) venn diagram showing the overlap and total numbers of differentially expressed genes in NAFLD and ESLD patients compared to CON, (D) most significant canonical signalling pathways associated with the differential transcriptome of ESLD muscle tissue, (E) z-scores of the identified upstream regulators of the transcriptome of ESLD patients, (F) LogP and fold-change values of upregulated and downregulated genes in ESLD patients grouped into functional categories, (G) most significant canonical

signalling pathways associated with the differential transcriptome of NAFLD patients, (H) z-scores of the identified upstream regulators of the transcriptome of NAFLD patients, (I) logP and fold-change values of upregulated and downregulated genes in NAFLD patients grouped into functional categories. Positive Z-scores are presented as grey bars represent a predicted activated upstream regulator; negative Z-scores are presented as black bars represent a predicted inhibited upstream regulator.

5.5 Discussion

The use of a combined protein and gene enrichment analysis provides an in-depth characterisation of the intracellular regulatory pathways which may underpin sarcopenia progression across the spectrum of liver disease. We show that mitochondrial protein content and activity are decreased in decompensated alcohol related-ESLD patients compared with CON. Although there was no difference in the phosphorylation of intracellular anabolic markers, total-mTOR content was decreased in NAFLD and ESLD patients compared with CON. Additionally, myostatin protein content was elevated in NAFLD compared with ESLD and CON. We also observed an upregulation of genes related to the oxidative stress response, in ELSD, and senescence in NAFLD, compared with CON. Collectively, these findings highlight some similar, but largely distinct, intracellular regulatory signalling pathways between non-cirrhotic NAFLD and decompensated ESLD patients.

In fasted-state muscle biopsies obtained from ESLD, NAFLD and CON participants we found no significant difference in the phosphorylation of markers of muscle anabolic signalling. This contrasts with previous *in vivo* human work, highlighting a decrease in the protein content of p70S6K, RPS6 and 4EBP-1 in ArLD cirrhotic patients, compared with healthy controls (15), potentially due to the difference in cirrhosis severity (i.e., compensated vs. decompensated). However, we did identify lower total-mTOR content in both NAFLD

and ESLD patients compared with CON. The cause of the attenuated mTOR content identified herein is unclear, but may be driven mechanisms including elevated ammonia in ESLD patients (14), and lipotoxicity (26), or insulin resistance (27) in NAFLD. Additionally, SC proliferation and differentiation is believed to be an important process involved in muscle repair and regeneration (28). Although others have demonstrated a reduction in markers of SC differentiation in portacaval anastomosis (PCA) rats (17), our human study shows that protein markers of cell proliferation and differentiation did not differ between CON, NAFLD and ESLD. This may be explained by the fact that serum myostatin and IGF-1, two key regulators of satellite cell proliferation and differentiation (28), did not differ between groups. Similarly, we identified no change in the protein content of key structural slow and fast myosin proteins, whereas type II fibre myosin heavy chain protein has been reported to be lower in PCA rats (17). The absence of a difference in myogenic, or differentiation markers, between groups here, suggests that evidence from *in vivo* mouse models of cirrhosis may not readily translate to humans. Nonetheless, the clear reduction in the abundance of mTOR protein in ESLD and NAFLD could indicate a possible muscle anabolic impairment, although the present analysis does not allow us to comment on whether anabolic responsiveness/activity of mTOR signalling is adversely affected.

Alongside evidence of lower total-mTOR content in NAFLD and ESLD patients, we found a significant increase in myostatin protein content in NAFLD, compared with CON and ESLD, despite no difference in serum myostatin concentration between groups. This observation differs somewhat to previous work showing increased myostatin in both serum (29) and muscle (30) of cirrhotic patients. Previous work has shown an increase in myostatin protein content in adipose and muscle tissue from obese women (31) and type II diabetics (32). Thus, factors associated with metabolic disease, combined with the difference in disease aetiology (NAFLD vs. ArLD) and stage/severity may explain the divergence in myostatin

content identified here. Despite a moderate effect size (d = 0.65), the greater serum myostatin in ESLD over CON reported herein did not reach significance, likely due to the large within group variability in myostatin protein. Recent evidence suggests that serum myostatin may be a poor biomarker for muscle atrophy when taken alone, due to the vast range of factors which can influence circulating concentrations (33). Regarding intracellular markers of protein breakdown, we observed no difference in the protein content of MAFbx, FK2 and MuRF-1 between groups, in line with previous findings (13, 15). Surprisingly, we did not detect a difference in LC3A/B and caspase-3 protein content, inferring no change in autophagy or apoptosis. This observation is in contrast to previous work highlighting an increase in LC3 lipidation, beclin1 expression and sequestome 1 (P62) degradation in ArLD patients (15). Therefore, future research is required to investigate the role of autophagy and the ubiquitin proteasome pathway across liver disease to confirm its role in sarcopenia progression.

Mitochondrial dysfunction has consistently been identified in cellular models of ESLD and age-related sarcopenia (34, 35). Herein, we report that the protein content of mitochondrial OXPHOS complexes I and IV and CS activity was reduced in ESLD compared with CON. While the findings identified in ESLD patients show similarities with our previous *in vitro* work highlighting a reduction in oxidative respiration and coupling efficiency in ESLD and NAFLD serum-treated myotubes (Chapter 4), we did not find a similar decline in these parameters in muscle samples from NAFLD patients. The mitochondrial dysfunction observed in alcohol related-ESLD patients in the present study, aligns with evidence that *in vitro* and *in vivo* treatment with ethanol (16) leads to a decrease in function of complexes I, II and IV. Although ESLD patients in the present study were not diagnosed as sarcopenic, reductions in mitochondrial complex proteins and activity supports the notion that mitochondrial dysfunction may precede the development of sarcopenia in advanced liver disease (36).

Despite the observed decline in mitochondrial content, we identified no difference in the protein content of markers associated with mitochondrial dynamics. Of particular interest, we found no difference in the protein content of markers implicated in mitochondrial fission, which plays a key role in mitophagy through preparing cells to clear damaged mitochondria (37). This contrasts with our previous findings (Chapter 4), showing a reduction in mitophagy in an *in vitro* model of non-cirrhotic NAFLD and alcohol related-ESLD, thus highlighting a need for further investigation of mitochondrial kinetics across the spectrum of liver disease. Additionally, *in vitro* and *in vivo* animal models have shown a reduction in mitophagy is associated with age-related sarcopenia (38) and cancer cachexia (39). The absence of changes in mitochondrial dynamics herein compared with previous studies may be due to the models utilised to study mitophagy, and lack of capability to assess mitophagy directly within humans. Despite these findings, conflicting evidence shows that perturbations in the markers of mitochondrial fission may contribute to muscle atrophy in aged mice (40) and thus warrants further scrutiny in the context of chronic liver disease. Collectively, this evidence suggests that mitochondrial dysfunction in ESLD patients may be driven by a decline in mitochondrial content, and ultimately function, as opposed to any impairment in the removal of damaged mitochondria. Whether mitochondrial function is implicated in sarcopenia progression at more advanced stages of NAFLD (e.g., non-alcoholic steatohepatitis (NASH)) has yet to be probed.

Alongside protein analysis, we conducted RNA-sequencing analysis to provide an in-depth examination of the intracellular pathways which may underpin the development of sarcopenia at the transcriptome level. We observed alterations in multiple pathways which may relate to the development of sarcopenia in ESLD patients, including ‘NRF2 mediated oxidative stress response’, ‘unfolded protein response’ and ‘protein ubiquitination’. Indeed, previous work has highlighted an increase in ROS in response to *in vitro* ethanol (16) and

ammonia treatment (8). Consequently, this may be linked to the decline in mitochondrial content identified in ESLD compared with CON. Also similar to the present findings is evidence that the protein ubiquitination pathway has been identified amongst the top canonical pathways amongst ammonia treated myotubes (19). Furthermore, in NAFLD patients we found pathways related to senescence and PI3K/AKT signalling to be amongst the top canonical pathways differentially regulated compared with CON. Although, others have suggested that cirrhotic patients experience an accelerated state of senescence (41), similar to our findings in NAFLD patients, we did not identify senescence as one of the top differentially regulated canonical pathways in ESLD vs. CON. Indeed, a significant enrichment of genes related to senescence has been identified in cirrhotic patients, and ammonia treated myotubes (19), and thus warrants further investigation in ESLD patients. Additionally, targeted gene analysis revealed an upregulation in genes related to mTOR signalling in NAFLD compared with CON and ESLD patients, which contrasts somewhat with the lower total-mTOR protein content that was observed in both NAFLD and ESLD. One possible explanation for this discrepancy is that post-transcriptional signalling events may be impaired in NAFLD patients, potentially leading to a dysregulation in gene expression (42, 43). In support of this notion, we identified a number of genes related to RNA metabolic processes amongst the top upregulated genes identified in NAFLD compared with CON. Furthermore, despite a lack of change at the protein level we identified an upregulation in genes related to ubiquitination and autophagy in NAFLD and ESLD compared with CON. Disparities between protein and gene expression data in the present study are not overly surprising given previous evidence of weak correlation between the two (44, 45). These findings highlight a number of distinct intracellular gene pathways that are dysregulated in NAFLD and ESLD that may be influenced by disease aetiology and/or severity and linked to sarcopenia progression.

A number of factors may drive the differential gene expression between NAFLD and ESLD identified herein. Firstly, it is important to note that the ESLD patients in this study had an ArLD aetiology, therefore the drivers and regulatory mechanisms of sarcopenia progression may differ through liver disease progression in comparison to those with NAFLD cirrhosis (e.g., one or a combination of alcohol (46), inflammation (9), insulin resistance (47) or lipotoxicity (26)). However, it is worth noting that BIA, which was utilised for the measurement of body composition herein, may mask changes in FM and FFM due to the presence of ascites in ESLD patients (48). Hence, while both NAFLD and ESLD patients in this study may appear obese based on the reported anthropometric characteristics, the burden of metabolic disease may be more apparent in NAFLD. Furthermore, a number of risk factors are associated with the development of both NAFLD and sarcopenia, including insulin resistance and physical inactivity (47). Thus, it remains possible that the factors driving metabolic disease and obesity in NAFLD patients, may also underscore divergence at the skeletal muscle genome level compared with ESLD patients of an ArLD aetiology. As such, it would be prudent to investigate the mechanisms of sarcopenia across disease progression in a specific aetiology, such as NAFLD progression to NASH.

Changes associated with liver disease progression (i.e., an increase in ammonia concentration), may also contribute to differences in intracellular regulatory protein and gene signalling in ESLD and NAFLD patients. We observed a significantly greater concentration of ammonia in ESLD, compared with NAFLD patients, which may explain the evidence of mitochondrial dysfunction in ESLD only, aligned with evidence from *in vitro* hyperammonemia treatment (8). Inflammatory cytokines may also influence the divergent intracellular regulatory signalling profiles identified herein (9). However, of the cytokines measured, only HGF was shown to be significantly elevated in ESLD patients compared with CON and NAFLD, therefore the inflammatory markers measured here may not be key

inflammatory drivers of sarcopenia in ESLD. It is however important to note that HGF is activated in response to inflammation, as a protective mechanism and, thus, may reflect the high level of inflammation present in ESLD cohorts (49). Furthermore, an increase in TNF-α has been associated with sarcopenia in cirrhosis (9) and age-related related sarcopenia (50), therefore the potential role of inflammatory targets, beyond those available in the present study, in liver-disease related sarcopenia requires further investigation. Furthermore, other systemic (51, 52) and lifestyle factors not available in the present study may influence sarcopenia in liver disease (4, 53, 54). Taken together, it is likely that a combination of factors may influence the dysregulation of intracellular signalling identified herein, with insulin and ammonia related signalling identified as potential drivers in NAFLD and alcohol related-ESLD respectively.

Although this study provides important insights into the intracellular signalling pathways which may underpin sarcopenia progression in non-cirrhotic NAFLD and decompensated ESLD patients, we did not perform dynamic measures of *in vivo* muscle protein turnover or mitochondrial respiration. These dynamic measures can offer unique insights into habitual levels of protein turnover and mitochondrial respiration which could provide more revealing insights. Furthermore, we did not investigate differences in intracellular signalling between cohorts after a known stimulus (e.g., protein provision, or exercise). Previous research has speculated that cirrhotic patients experience a blunted anabolic response to protein ingestion, termed muscle anabolic resistance (55). The presence of muscle anabolic resistance may contribute to the development of sarcopenia, as previously highlighted in age-related sarcopenia (56). Additionally, we did not identify any difference in markers of SC proliferation. In order to truly establish whether markers of SC function are implicated in the development of sarcopenia in CLD, a remodelling stimulus (i.e., damaging exercise) may be required (57). Thus, future research should aim to combine the dynamic

measurement of muscle protein turnover and transcriptome analysis, as successfully used in the context of human disuse muscle atrophy (58), to reveal differences which are otherwise missed amongst static measurements in the absence of an appropriate stimulus.

In conclusion, we are the first to demonstrate a number of similar, but largely distinct intracellular regulatory pathways which may underpin sarcopenia progression in chronic liver disease patients of differing aetiology and disease stage. Specifically, we observed impairments in mitochondrial protein content and an increase in genes related to oxidative stress in ESLD skeletal muscle compared with CON. In NAFLD patient muscle, we show an increase in myostatin protein content and genes related to senescence compared with CON. Similarities between NAFLD and ESLD included a reduction in total-mTOR protein content and an upregulation in genes related to autophagy and ubiquitination compared with CON. These novel findings provide a valuable insight into intracellular regulatory targets that could be further exploited as potential therapeutic targets.

Acknowledgements: The authors would like to thank the nurses and laboratory support staff within the Inflammatory Research Facility and Clinical Research Facility for their assistance with data collection of this study. The authors would also like to express our thanks to the individuals who participated in this study.

Author Contributions: All authors contributed to the design of the research. S.L.A, A.D, J.I.Q, F.R.W and T.N completed data collection. S.L.A, J.I.Q and T.N completed data analysis. S.L.A., G.G.L. and L.B. wrote the manuscript. All authors contributed to the interpretation of results, edited and approved of the final manuscript.

Funding: This study was funded by the National Institute for Health Research (NIHR) Birmingham Biomedical Research Centre (BRC-1215-20009). The views expressed as those

of the authors and not necessarily those of the NIHR, or the Department of Health and Social Care.

Clinical trial number: NCT04734496

Disclosures: The authors declare no conflicts of interest

5.6 References

1. **Kim G, Kang SH, Kim MY, and Back SK**. Prognostic value of sarcopenia in patients with liver cirrhosis: A systematic review and meta-analysis. *PLoS One* 12: e0186990, 2017.
2. **van Vugt JL, Levolger S, de Bruin RW, van Rosmalen J, Metselaar HJ, and Ijzermans JN**. Systematic review and meta-analysis of the impact of computed tomography-assessed skeletal muscle mass on outcome in patients awaiting or undergoing liver transplantation. *Am J Transplant* 16: 2277-2292, 2016.
3. **Montano-Loza AJ, Meza-Junco J, Prado CM, Lieffers JR, Baracos VE, Bain VG, and Sawyer MB**. Muscle wasting is associated with mortality in patients with cirrhosis. *Clin Gastroenterol Hepatol* 10: 166-173, 2012.
4. **Allen SL, Quinlan JI, Dhaliwal A, Armstrong MJ, Elsharkawy AM, Greig CA, Lord JM, Lavery GG, and Breen L**. Sarcopenia in Chronic Liver Disease: Mechanisms and Countermeasures. *Am J Physiol Gastrointest Liver Physiol* 320: G241-G257, 2021.
5. **Tandon P, Low G, Mourtzakis M, Zenith L, Myers RP, Abraldes JG, Shaheen AA, Qamar H, Mansoor N, Carbonneau M, Ismond K, Mann S, Alaboudy A, and Ma M**. A Model to Identify Sarcopenia in Patients With Cirrhosis. *Clin Gastroenterol Hepatol* 14: 1473-1480 e1473, 2016.
6. **Welch N, Dasarathy J, Runkana A, Penumatsa R, Bellar A, Reen J, Rotroff D, McCullough AJ, and Dasarathy S**. Continued muscle loss increases mortality in cirrhosis: Impact of aetiology of liver disease. *Liver Int* 40: 1178-1188, 2020.
7. **Breen L, and Phillips SM**. Skeletal muscle protein metabolism in the elderly: Interventions to counteract the 'anabolic resistance' of ageing. *Nutr Metab* 8: 68, 2011.
8. **Davuluri G, Allawy A, Thapaliya S, Rennison JH, Singh D, Kumar A, Sandlers Y, Van Wagoner DR, Flask CA, Hoppel C, Kasumov T, and Dasarathy S**. Hyperammonaemia-induced skeletal muscle mitochondrial dysfunction results in cataplerosis and oxidative stress. *J Physiol* 594: 7341-7360, 2016.
9. **Han JW, Kim DI, Nam HC, Chang UI, Yang JM, and Song DS**. Association between serum TNF-a and sarcopenia in liver cirrhosis. *Clin Mol Hepatol* 2021.
10. **Kurosawa T, Goto M, Kaji N, Aikiyo S, Mihara T, Ikemoto-Uezumi M, Toyoda M, Kanazawa N, Nakazawa T, Hori M, and Uezumi A**. Liver fibrosis-induced muscle atrophy is mediated by elevated levels of circulating TNFalpha. *Cell Death Dis* 12: 11, 2021.
11. **Singh SS, Kumar A, Welch N, Sekar J, Mishra S, Bellar A, Gangadhariah M, Attaway A, Al Khafaji H, Wu X, Pathak V, Agrawal V, McMullen MR, Hornberger TA, Nagy LE, Davuluri G, and Dasarathy S**. Multiomics-Identified Intervention to Restore Ethanol-Induced Dysregulated Proteostasis and Secondary Sarcopenia in Alcoholic Liver Disease. *Cell Physiol Biochem* 55: 91-116, 2021.
12. **Kant S, Davuluri G, Alchirazi KA, Welch N, Heit C, Kumar A, Gangadhariah M, Kim A, McMullen MR, Willard B, Luse DS, Nagy LE, Vasiliou V, Marini AM, Weiner ID, and Dasarathy S**. Ethanol sensitizes skeletal muscle to ammonia-induced molecular perturbations. *J Biol Chem* 294: 7231-7244, 2019.
13. **Qiu J, Tsien C, Thapalaya S, Narayanan A, Weihl CC, Ching JK, Eghtesad B, Singh K, Fu X, Dubyak G, McDonald C, Almasan A, Hazen SL, Naga Prasad SV, and Dasarathy S**. Hyperammonemia-mediated autophagy in skeletal muscle contributes to sarcopenia of cirrhosis. *Am J Physiol Endocrinol Metab* 303: E983-E993, 2012.
14. **Davuluri G, Krokowski D, Guan BJ, Kumar A, Thapaliya S, Singh D, Hatzoglou M, and Dasarathy S**. Metabolic adaptation of skeletal muscle to hyperammonemia drives the beneficial effects of l-leucine in cirrhosis. *J Hepatol* 65: 929-937, 2016.

15. **Tsien C, Davuluri G, Singh D, Allawy A, Ten Have GA, Thapaliya S, Schulze JM, Barnes D, McCullough AJ, Engelen MP, Deutz NE, and Dasarathy S**. Metabolic and molecular responses to leucine-enriched branched chain amino acid supplementation in the skeletal muscle of alcoholic cirrhosis. *Hepatology* 61: 2018-2029, 2015.
16. **Kumar A, Davuluri G, Welch N, Kim A, Gangadhariah M, Allawy A, Priyadarshini A, McMullen MR, Sandlers Y, Willard B, Hoppel CL, Nagy LE, and Dasarathy S**. Oxidative stress mediates ethanol-induced skeletal muscle mitochondrial dysfunction and dysregulated protein synthesis and autophagy. *Free Radic Biol Med* 145: 284-299, 2019.
17. **Dasarathy S, Dodig M, Muc SM, Kalhan SC, and McCullough AJ**. Skeletal muscle atrophy is associated with an increased expression of myostatin and impaired satellite cell function in the portacaval anastamosis rat. *Am J Physiol Gastrointest Liver Physiol* 287: G1124-1130, 2004.
18. **Paczkowska-Abdulsalam M, Niemira M, Bielska A, Szalkowska A, Raczkowska BA, Junttila S, Gyenesei A, Adamska-Patruno E, Maliszewska K, Citko A, Szczerbinski L, and Kretowski A**. Evaluation of Transcriptomic Regulations behind Metabolic Syndrome in Obese and Lean Subjects. *Int J Mol Sci* 21: 2020.
19. **Welch N, Singh SS, Kumar A, Dhruba SR, Mishra S, Sekar J, Bellar A, Attaway AH, Chelluboyina A, Willard BB, Li L, Huo Z, Karnik SS, Esser K, Longworth MS, Shah YM, Davuluri G, Pal R, and Dasarathy S**. Integrated multiomics analysis identifies molecular landscape perturbations during hyperammonemia in skeletal muscle and myotubes. *J Biol Chem* 297: 101023, 2021.
20. **Volpato S, Cavalieri M, Sioulis F, Guerra G, Maraldi C, Zuliani G, Fellin R, and Guralnik JM**. Predictive value of the Short Physical Performance Battery following hospitalization in older patients. *J Gerontol A Biol Sci Med Sci* 66: 89-96, 2011.
21. **Lai JC, Dodge JL, Sen S, Covinsky K, and Feng S**. Functional decline in patients with cirrhosis awaiting liver transplantation: results from the functional assessment in liver transplantation (FrAILT) study. *Hepatology* 63: 574-580, 2016.
22. **Alvares-da-Silva MR, and Reverbel da Silveira T**. Comparison between handgrip strength, subjective global assessment, and prognostic nutritional index in assessing malnutrition and predicting clinical outcome in cirrhotic outpatients. *Nutrition* 21: 113-117, 2005.
23. **Roberts HC, Denison HJ, Martin HJ, Patel HP, Syddall H, Cooper C, and Sayer AA**. A review of the measurement of grip strength in clinical and epidemiological studies: towards a standardised approach. *Age Ageing* 40: 423-429, 2011.
24. **Afgan E, Baker D, van den Beek M, Blankenberg D, Bouvier D, Cech M, Chilton J, Clements D, Coraor N, Eberhard C, Gruning B, Guerler A, Hillman-Jackson J, Von Kuster G, Rasche E, Soranzo N, Turaga N, Taylor J, Nekrutenko A, and Goecks J**. The Galaxy platform for accessible, reproducible and collaborative biomedical analyses: 2016 update. *Nucleic Acids Res* 44: W3-W10, 2016.
25. **Liberzon A, Birger C, Thorvaldsdottir H, Ghandi M, Mesirov JP, and Tamayo P**. The Molecular Signatures Database (MSigDB) hallmark gene set collection. *Cell Syst* 1: 417-425, 2015.
26. **Montgomery MK, De Nardo W, and Watt MJ**. Impact of Lipotoxicity on Tissue "Cross Talk" and Metabolic Regulation. *Physiology (Bethesda)* 34: 134-149, 2019.
27. **Cleasby ME, Jamieson PM, and Atherton PJ**. Insulin resistance and sarcopenia: mechanistic links between common co-morbidities. *J Endocrinol* 229: R67-R81, 2016.
28. **Snijders T, Nederveen JP, McKay BR, Joanisse S, Verdijk LB, van Loon LJ, and Parise G**. Satellite cells in human skeletal muscle plasticity. *Front Physiol* 6: 283, 2015.

29. **Nishikawa H, Enomoto H, Ishii A, Iwata Y, Miyamoto Y, Ishii N, Yuri Y, Hasegawa K, Nakano C, Nishimura T, Yoh K, Aizawa N, Sakai Y, Ikeda N, Takashima T, Takata R, Iijima H, and Nishiguchi S**. Elevated serum myostatin level is associated with worse survival in patients with liver cirrhosis. *J Cachexia Sarcopenia Muscle* 8: 915-925, 2017.
30. **Qiu J, Thapaliya S, Runkana A, Yang Y, Tsien C, Mohan ML, Narayanan A, Eghtesad B, Mozdziak PE, McDonald C, Stark GR, Welle S, Naga Prasad SV, and Dasarathy S**. Hyperammonemia in cirrhosis induces transcriptional regulation of myostatin by an NF-kappaB-mediated mechanism. *Proc Natl Acad Sci U S A* 110: 18162-18167, 2013.
31. **Hittel DS, Berggren JR, Shearer J, Boyle K, and Houmard JA**. Increased secretion and expression of myostatin in skeletal muscle from extremely obese women. *Diabetes* 58: 30-38, 2009.
32. **Brandt C, Nielsen AR, Fischer CP, Hansen J, Pedersen BK, and Plomgaard P**. Plasma and muscle myostatin in relation to type 2 diabetes. *PLoS One* 7: e37236, 2012.
33. **Baczek J, Silkiewicz M, and Wojszel ZB**. Myostatin as a Biomarker of Muscle Wasting and other Pathologies-State of the Art and Knowledge Gaps. *Nutrients* 12: 2401, 2020.
34. **Sebastian D, Sorianello E, Segales J, Irazoki A, Ruiz-Bonilla V, Sala D, Planet E, Berenguer-Llergo A, Munoz JP, Sanchez-Feutrie M, Plana N, Hernandez-Alvarez MI, Serrano AL, Palacin M, and Zorzano A**. Mfn2 deficiency links age-related sarcopenia and impaired autophagy to activation of an adaptive mitophagy pathway. *EMBO J* 35: 1677-1693, 2016.
35. **Zhou H, Du W, Li Y, Shi C, Hu N, Ma S, Wang W, and Ren J**. Effects of melatonin on fatty liver disease: The role of NR4A1/DNA-PKcs/p53 pathway, mitochondrial fission, and mitophagy. *J Pineal Res* 64: 2018.
36. **del Campo A, Contreras-Hernández I, Castro-Sepúlveda MC, C. A., Figueroa R, Tevy MF, Eisner V, Casas M, and Jaimovich E**. Muscle function decline and mitochondrial changes in middle age precede sarcopenia in mice. *Aging (Albany NY)* 10: 34-55, 2018.
37. **Toyama EQ, Herzig S, Courchet J, Lewis TL, Jr., Loson OC, Hellberg K, Young NP, Chen H, Polleux F, Chan DC, and Shaw RJ**. Metabolism. AMP-activated protein kinase mediates mitochondrial fission in response to energy stress. *Science* 351: 275-281, 2016.
38. **Hood DA, Memme JM, Oliveira AN, and Triolo M**. Maintenance of Skeletal Muscle Mitochondria in Health, Exercise, and Aging. *Annu Rev Physiol* 81: 19-41, 2019.
39. **Brown JL, Rosa-Caldwell ME, Lee DE, Blackwell TA, Brown LA, Perry RA, Haynie WS, Hardee JP, Carson JA, Wiggs MP, Washington TA, and Greene NP**. Mitochondrial degeneration precedes the development of muscle atrophy in progression of cancer cachexia in tumour-bearing mice. *J Cachexia Sarcopenia Muscle* 8: 926-938, 2017.
40. **Dulac M, Leduc-Gaudet JP, Cefis M, Ayoub MB, Reynaud O, Shams A, Moamer A, Nery Ferreira MF, Hussain SN, and Gouspillou G**. Regulation of muscle and mitochondrial health by the mitochondrial fission protein Drp1 in aged mice. *J Physiol* 599: 4045-4063, 2021.
41. **Aravinthan AD, and Alexander GJM**. Senescence in chronic liver disease: Is the future in aging? *J Hepatol* 65: 825-834, 2016.
42. **Yeh HS, and Yong J**. mTOR-coordinated Post-Transcriptional Gene Regulations: from Fundamental to Pathogenic Insights. *J Lipid Atheroscler* 9: 8-22, 2020.
43. **Corbett AH**. Post-transcriptional regulation of gene expression and human disease. *Curr Opin Cell Biol* 52: 96-104, 2018.

44. **Schwanhausser B, Busse D, Li N, Dittmar G, Schuchhardt J, Wolf J, Chen W, and Selbach M**. Global quantification of mammalian gene expression control. *Nature* 473: 337-342, 2011.
45. **Ingolia NT, Ghaemmaghami S, Newman JR, and Weissman JS**. Genome-wide analysis in vivo of translation with nucleotide resolution using ribosome profiling. *Science* 324: 218-223, 2009.
46. **Davuluri G, Welch N, Sekar J, Gangadhariah M, Alsabbagh Alchirazi K, Mohan ML, Kumar A, Kant S, Thapaliya S, Stine M, McMullen MR, McCullough RL, Stark GR, Nagy LE, Naga Prasad SV, and Dasarathy S**. Activated protein phosphatase 2A disrupts nutrient sensing balance between mTORC1 and AMPK causing sarcopenia in alcoholic liver disease. *Hepatology* 73: 1892-1908, 2020.
47. **Lee YH, Jung KS, Kim SU, Yoon HJ, Yun YJ, Lee BW, Kang ES, Han KH, Lee HC, and Cha BS**. Sarcopenia is associated with NAFLD independently of obesity and insulin resistance: nationwide surveys (KNHANES 2008-2011). *J Hepatol* 63: 486-493, 2015.
48. **Carey EJ, Lai JC, Sonnenday C, Tapper EB, Tandon P, Duarte-Rojo A, Dunn MA, Tsien C, Kallwitz ER, Ng V, Dasarathy S, Kappus M, Bashir MR, and Montano-Loza AJ**. A North American Expert Opinion Statement on Sarcopenia in Liver Transplantation. *Hepatology* 70: 1816-1829, 2019.
49. **Molnarfi N, Benkhoucha M, Funakoshi H, Nakamura T, and Lalive PH**. Hepatocyte growth factor: A regulator of inflammation and autoimmunity. *Autoimmun Rev* 14: 293-303, 2015.
50. **Schaap LA, Pluijm SM, Deeg DJ, and Visser M**. Inflammatory markers and loss of muscle mass (sarcopenia) and strength. *Am J Med* 119: 526 e9-17, 2006.
51. **Sinclair M, Grossmann M, Gow PJ, and Angus PW**. Testosterone in men with advanced liver disease: abnormalities and implications. *J Gastroenterol Hepatol* 30: 244-251, 2015.
52. **Stokes CS, Volmer DA, Grunhage F, and Lammert F**. Vitamin D in chronic liver disease. *Liver Int* 33: 338-352, 2013.
53. **Hallsworth K, Thoma C, Moore S, Ploetz T, Anstee QM, Taylor R, Day CP, and Trenell MI**. Non-alcoholic fatty liver disease is associated with higher levels of *objectively* measured sedentary behaviour and lower levels of physical activity than matched healthy controls. *Frontline Gastroenterol* 6: 44-51, 2015.
54. **Zelber-Sagi S, Nitzan-Kaluski D, Goldsmith R, Webb M, Zvibel I, Goldiner I, Blendis L, Halpern Z, and Oren R**. Role of leisure-time physical activity in nonalcoholic fatty liver disease: a population-based study. *Hepatology* 48: 1791-1798, 2008.
55. **Tsien C, McCullough AJ, and Dasarathy S**. Late evening snack: exploiting a period of anabolic opportunity in cirrhosis. *J Gastroenterol Hepatol* 27: 430-441, 2012.
56. **Cuthbertson D, Smith K, Babraj J, Leese G, Waddell T, Atherton P, Wackerhage H, Taylor PM, and Rennie MJ**. Anabolic signaling deficits underlie amino acid resistance of wasting, aging muscle. *FASEB J* 19: 422-424, 2005.
57. **Nederveen JP, Joanisse S, Thomas ACQ, Snijders T, Manta K, Bell KE, Phillips SM, Kumbhare D, and Parise G**. Age-related changes to the satellite cell niche are associated with reduced activation following exercise. *FASEB J* 34: 8975-8989, 2020.
58. **Willis CRG, Gallagher IJ, Wilkinson DJ, Brook MS, Bass JJ, Phillips BE, Smith K, Etheridge T, Stokes T, McGlory C, Gorissen SHM, Szewczyk NJ, Phillips SM, and Atherton PJ**. Transcriptomic links to muscle mass loss and declines in cumulative muscle protein synthesis during short-term disuse in healthy younger humans. *FASEB J* 35: e21830, 2021.

CHAPTER 6 – GENERAL DISCUSSION

6.1 Introduction

A loss of muscle mass and function is known to occur with advancing age, but can also occur due to other causes e.g. chronic disease states; thus sarcopenia is described as primary if age is the main factor, and secondary sarcopenia when other causes exist (1). Due to the ever-growing ageing population (2), and an increase in the number of individuals suffering with liver disease (3), it is imperative to improve our understanding of the mechanisms which underpin the development of sarcopenia. Sarcopenia in end-stage liver disease (ESLD) is known to be problematic (4, 5) and thus warrants further investigation as the preservation of skeletal muscle mass and function are critical for improvements in clinical outcomes.

The underlying mechanisms of sarcopenia in ESLD are likely to be multifactorial but may arise due to an imbalance of muscle protein turnover in which patients exhibit a negative net protein balance (6). It is possible that this imbalance may be driven by an impairment in muscle protein synthesis (MPS) (7), an increase in muscle protein breakdown (MPB) (8) and an impairment in mitochondrial function (9). Previous research speculates that cirrhotic patients may experience anabolic resistance, in which patients experience a reduced muscle protein synthetic response to protein ingestion (10). In addition, proteolytic markers such as myostatin and autophagic related markers have been shown to increase in cirrhosis (11). Furthermore, mitochondrial dysfunction has been identified in response to *in vitro* and *in vivo* ammonia (9) and ethanol (12) treatment. At present, we are yet to fully understand the factors which contribute to the development of both age- and in particular, liver disease-related sarcopenia. This may be partially due to the lack physiologically relevant, *in vitro* models of sarcopenia to inform research prior to the progression to *in vivo* studies. As a result, there are currently limited interventions to treat and counteract the decline in muscle mass identified in ageing and cirrhotic patients. Therefore, this thesis had three main aims:

1. To develop a physiologically relevant *in vitro* model of age-related sarcopenia to enable the investigation of the molecular mechanisms of sarcopenia and anabolic resistance in response to leucine treatment, prior to completion of *in vivo* human trials.
2. To investigate the potential molecular mechanisms of sarcopenia in a novel *vitro* model of chronic liver disease (CLD) utilising *ex vivo* human serum.
3. To investigate the possible molecular pathways which may underpin the development sarcopenia in CLD patients, in fasted state muscle biopsies.

This discussion chapter provides a brief summary of the key findings from each of the studies described in chapters 3, 4 and 5 of this thesis. First, based on **Chapter 3** this section discusses the requirement of a more physiologically relevant *in vitro* model to study age-related sarcopenia, alongside the potential drivers of sarcopenia identified in this work. Second, based on findings in **Chapter 4** this section discusses the potential systemic, and intracellular mechanistic drivers which may contribute to the progression of sarcopenia across different stages of chronic liver disease. Finally, based upon the findings outlined in **Chapter 5** this section discusses the logistical challenges related to the completion of muscle biopsies in chronic liver disease patients, and how our *in vitro* findings translate to the findings outlined in *in vivo* work.

6.2 *In Vitro* Models of Age-Related Sarcopenia

The completion of *in vivo* human studies are often logistically challenging, thus combined with the multifactorial nature of sarcopenia (13), there is a need for the development of a more physiological model of age-related muscle atrophy. The development of such a model would allow researchers to probe further into the potential mechanisms of sarcopenia and potential countermeasures. Indeed, over recent years the use of *ex vivo* human plasma (14, 15) and serum (16-18) has been utilised to investigate a range of morphological and molecular responses to

various conditions. Furthermore, recent work by Kalampouka et al (14) investigated the effect of conditioning C2C12 myotubes with *ex vivo* human plasma (5%) from young and old individuals. The authors found an increased myotube diameter in cells treated with young in comparison to old plasma after 24- and 48-hours of treatment (14). Additionally, cells incubated with plasma from young males were able to regenerate at a quicker rate in response to a scratch assay (14). While this study highlighted the capability of *ex vivo* plasma to induce an *in vitro* model of ageing, the authors did not investigate the potential mechanisms which may contribute to the atrophy identified in this model. Therefore, in Chapter 3 we aimed to further this model through the investigation of acute anabolic and catabolic signalling in response to treatment with *ex vivo* human serum from young and old males. First, we completed a chronic 24-hour treatment period with *ex vivo* human serum from young and old males in order to investigate changes in myotube growth. In Chapter 3, we demonstrated that serum from young males induced myotube hypertrophy, while serum from old males induced myotube atrophy in comparison to untreated control cells maintained under normal differentiation conditions. These findings were similar to those found in response to plasma treatment, highlighting that we were able to successfully induce a model of hypertrophy and atrophy to mimic the effects of ageing (14).

Previous research has utilised *ex vivo* human serum to investigate MPS and anabolic signalling in response to an acute, 4-hour treatment with serum from fasted vs. fed individuals after the ingestion of different protein sources (16, 18, 19). The authors confirmed the suitability of *ex vivo* serum to condition C2C12 myotubes, alongside an increase in MPS in response to treatment with serum obtained 60-minutes after the ingestion of whey protein in contrast to fasted samples (16), and samples obtained 60-minutes post ingestion of non-essential amino acids (NEAA) (19). More recently, the authors furthered this work by investigating the ability of alternative protein sources to induce MPS, highlighting an increase in myotube diameter in

myotubes treated with serum obtained 60-minutes post whey protein and fish hydrolysate protein ingestion, in comparison to NEAA (18). Therefore, we aimed to apply this model to investigate potential differences in MPS, anabolic and catabolic signalling in C2C12s treated with serum from old and young males. However, unlike this previous work we did not have access to fed-state blood samples. Therefore, to investigate muscle anabolic resistance we utilised an *in vitro* leucine treatment. In Chapter 3, we show an increase in MPS in response to leucine treatment in myotubes conditioned with young serum, in contrast to a blunted response found in myotubes treated with old serum. These findings align with the concept of age-related muscle anabolic resistance to protein provision, previously identified *in vivo* (20-23). This therefore highlights the utility of the model to investigate the anabolic response to protein provision, after conditioning cells with *ex vivo* human serum. As a result, this model may be applicable for the investigation of the anabolic response of alternative protein sources, or nutraceutical compounds in pre-conditioned myotubes.

6.2.1 Inflammation, Insulin Resistance and Sarcopenia

Inflammation has clear implications in the development of sarcopenia, and is often associated with a blunted MPS, loss of muscle mass, strength and physical performance (24-30). Unsurprisingly, inflammatory-related atrophy has been studied through the use of tumor necrosis factor-α (TNF-α) (31) and c-reactive protein (CRP) (32) treatment, inducing myotube atrophy in C2C12 models. Treatment with inflammatory cytokines has also been shown to reduce the phosphorylation of anabolic targets, inhibit myogenesis and increase proteolysis (31-33). However, due to the supraphysiological treatments used in this work, we aimed to establish if *ex vivo* human serum could be used to unravel mechanisms of age-related sarcopenia, as levels of CRP and interleukin-6 (IL-6) are associated with sarcopenia in older adults (32, 34). In Chapter 3, we show a significant increase in concentrations of IL-6 and CRP in plasma from old, in comparison to younger individuals (Figure 6.1). This is consistent with

previous work suggesting that higher levels of IL-6 and CRP may be linked to sarcopenia progression in older individuals (24), and *in vivo* human evidence of an association between basal mixed-muscle and myosin heavy chain protein synthesis and plasma concentrations of CRP, IL-6 and TNF-α (29). In addition, pre-clinical investigations in rat models also suggest that low-grade inflammation (LGI) influences age-related anabolic resistance to food intake, whereas rodents without LGI appear to restore robust postprandial MPS responses (35, 36). At present, the role of LGI on postprandial MPS in older humans is unclear (37, 38) and further studies are required to resolve any potential associations. Nonetheless, our data support the notion that LGI may, at least in part, underpin the age-related dysregulation in MPS that drives muscle atrophy, further highlighting LGI as a potential target for therapeutic intervention.

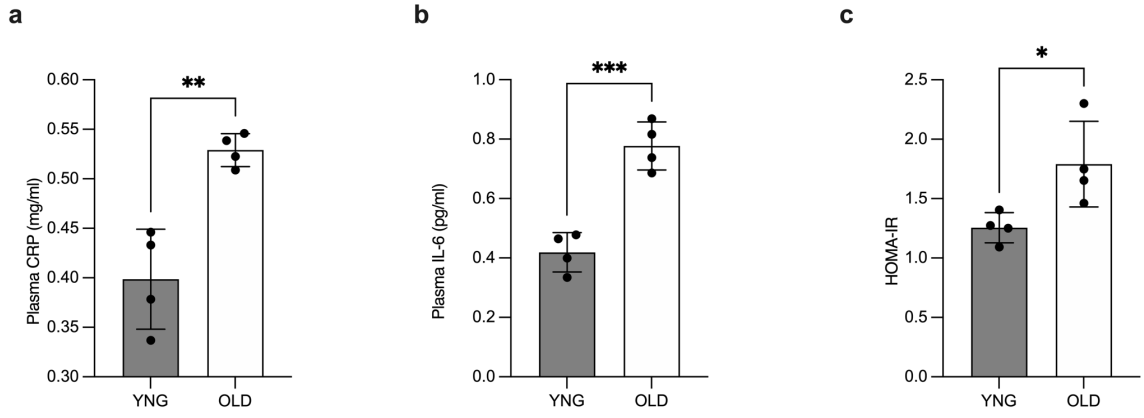

Figure 6.1. Plasma IL-6 and CRP concentrations and HOMA-IR in young and old males. (A) Plasma CRP concentrations, (B) Plasma IL-6 concentrations, (C) HOMA-IR Data are presented as mean ± SD. *** $P < 0.001$, **$P < 0.01$.

A state of chronic inflammation can lead to the development of insulin resistance and other metabolic diseases. Indeed, ageing is often associated with an increased risk of insulin resistance (39), which is associated with the development of sarcopenia, independent of obesity (40). Similarly, in Chapter 3 we identified an increase in homeostatic model assessment of insulin resistance (HOMA-IR) in older males, in comparison to young males (Figure 6.1). This

could partially be explained by the fact that individuals included in this study were of 'normal' BMI. In human trials, insulin resistance has been identified in older individuals with normal muscle mass, suggesting that insulin resistance may precede the progression of sarcopenia (41). Insulin may contribute to muscle atrophy through a blunted muscle protein synthetic response to protein provision (42). However, the contribution of insulin resistance to the development of sarcopenia is unclear. Previous work from our laboratory has identified a blunted myofibrillar protein synthesis after the ingestion of 15g milk protein in old obese males, in contrast to young lean and old lean males, which both experienced a significant increase in protein synthesis (43). Therefore, it is plausible to suggest that while a decline in insulin sensitivity may impair the anabolic response to protein ingestion, the presence of obesity may further contribute to the development of sarcopenia, termed sarcopenic obesity due to changes in metabolism and body composition i.e. an increase in intramuscular adipose tissue (44). Taken together, this suggests that inflammation, and to a degree insulin resistance may contribute to the development of myotube atrophy identified in Chapter 3 of this thesis. However, further research is required to investigate other systemic factors such as growth factors and cellular senescence which may contribute to the development of age-related sarcopenia, and the additional impact of obesity in *in vitro* experiments.

6.2.2 Future Directions and Implications

To date, limited research has been conducted to investigate the potential mechanisms of age-related sarcopenia in a more physiologically relevant *in vitro* model. Therefore, future research should aim to repeat the work outlined in this thesis with primary human skeletal muscle cells, to avoid potential cross-species effects. The combination of *ex vivo* serum, with human muscle cells is likely to be considered as the 'gold standard' approach to the improvement of physiological relevance in *in vitro* methodologies. While this model highlights the potential role of inflammation in the progression of sarcopenia, its development is considered

multifactorial (13). Therefore, the removal or inhibition of cytokines, alongside the investigation of alternative systemic factors may allow for an in-depth investigation into their contribution in the development of sarcopenia. Furthermore, the use of *in vitro* leucine treatment in this model was a supraphysiological dosage, which could limit translation to human work. Therefore, future research should aim to replicate these findings with fasted vs. fed serum. However, using *in vitro* treatment after conditioning with fasted *ex vivo* serum highlights that this model can be applied to investigate the potential effectiveness of *in vitro* treatments with nutraceutical or pharmacological compounds, prior to the completion of logistically challenging, invasive and expensive *in vivo* trials.

6.3 *In Vitro* Models of Chronic Liver Disease

Recently, a growing interest into the potential of mechanisms of sarcopenia in CLD has arisen, largely attributed to its association with negative clinical outcomes (4, 5). However, the completion of invasive human trials in cirrhotic patients are logistically challenging (7). Therefore*, in vitro* and *in vivo* models of are vital, in order to provide an insight into the mechanisms of sarcopenia prior to *in vivo* human trials. Current models focus on the treatment of ammonia (9, 45, 46) and ethanol (47, 48), which are considered to be key drivers of sarcopenia in CLD (49). The results presented in Chapter 4 are in line with previous *in vitro* work, highlighting a decline in myotube diameter in C2C12s in response to treatment with *ex vivo* human serum from ESLD patients. Furthermore, these findings are in line with *in vivo* animal work, highlighting a reduction in muscle mass in portacaval anastomosis (PCA) rats, confirming the induction of cirrhosis induced muscle atrophy (46).

A number of systemic factors may contribute to the myotube atrophy identified herein, including an increase in inflammation, ammonia and insulin resistance. This is in line with previous work which has shown a reduction in myotube diameter in C2C12 skeletal muscle

cells treated with ammonia, ethanol or a combination (45, 48, 50). Similarly, ethanol exposure in C2C12 myotubes, followed by ammonia exposure has been shown to cause a greater impairment in MPS, in comparison to the respective treatments alone (48). Although the potential link between sarcopenia and inflammation in ESLD has not been widely investigated, TNF-α has been shown to correlate with muscle loss in a model of liver disease and in patient cohorts (51, 52). Furthermore, *in vitro* treatment with CRP (32) and TNF-α (31), two proinflammatory cytokines has also been shown to decrease myotube diameter. In line with these *in vivo* and *in vitro* models, the myotube atrophy identified in Chapter 4, alongside analysis of basic blood parameters allowed for the validation of atrophy in an *in vitro* model of liver disease. Thus, this model enables the investigation of sarcopenia, with respect to both its mechanisms and potential countermeasures.

Surprisingly, we did not identify a difference in myotube diameter between control (CON) and non-alcoholic fatty liver disease (NAFLD) treated C2C12 skeletal muscle cells. However, ESLD treated myotubes were reduced ~45% and ~35% in comparison to CON and NAFLD treatments, respectively. The lack of change between CON and NAFLD treatments may be explained by the age of the CON group recruited. In Chapter 4, the CON group had a mean age of ~65 years, therefore these individuals may experience age-related muscle loss. Indeed, age-related loss of muscle mass and strength is thought to progress at an annual rate of ~0.7-1.2% and 3-4% respectively (53). The age of the CON group in Chapter 4 was similar to the older group utilised in Chapter 3 of this thesis. As previously discussed, the findings from Chapter 3 highlight that serum from older individuals induced myotube atrophy in comparison to untreated myotubes. Therefore, serum from the CON group in this study (Chapter 4) may have caused a degree of myotube atrophy. This can be outlined in Figure 6.2 which highlights a non-significant reduction in myotube diameter in CON vs. untreated control (UTC) and a

significant reduction in myotube diameter in NAFLD treated myotubes in comparison to the UTC.

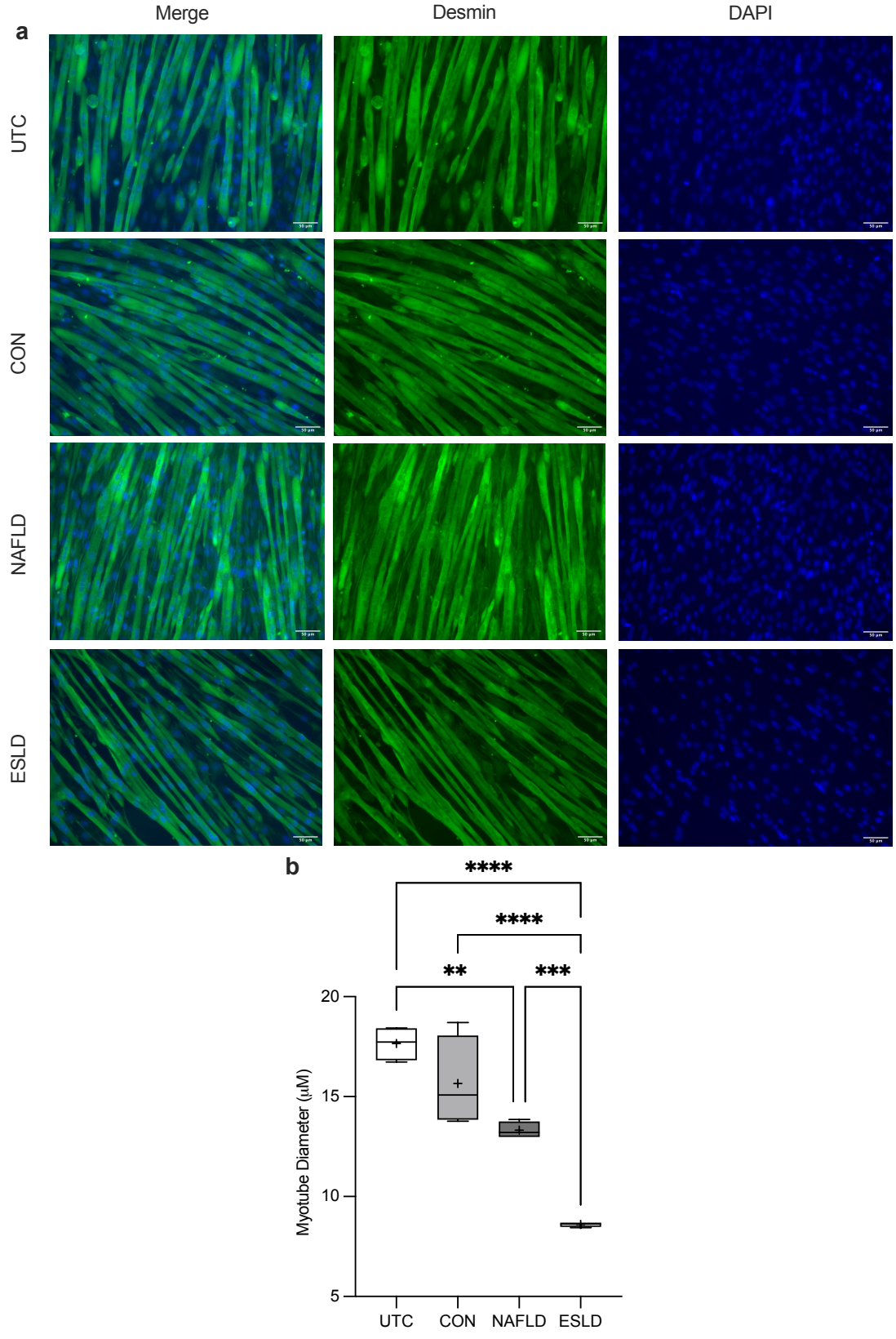

Figure 6.2. Myotube diameter is significantly decreased within NAFLD and ESLD treated myotubes compared to untreated control C2C12s. (A) representative images illustrating atrophy in myotubes maintained under normal differentiation conditions (UTC) in comparison to treatment with ex vivo serum from age-matched controls (CON), non-alcoholic fatty liver disease (NAFLD) and end-stage liver disease (ESLD), (B) mean myotube diameter. Data are expressed as the mean (cross), median (central horizontal line), 25^{th} and 75^{th} percentiles (box) and the minimum and maximum values (vertical lines), corresponding to the mean of treatment of each participant's serum, replicated in triplicate. ** $P < 0.01$, *** $P = 0.001$, **** $P < 0.0001$.

In addition, the substantial myotube atrophy identified in myotubes treated with decompensated ESLD serum in comparison to non-cirrhotic NAFLD serum could be a consequence of the differences in both the underlying disease aetiology and disease progression. Indeed, recent work by Welch et al (54) identified that cirrhotic patients with alcoholic related liver disease (ArLD) experience the lowest level of muscle mass, alongside the fastest rate of muscle loss in comparison to NAFLD and viral hepatitis aetiologies. This would suggest that disease aetiology may present an independent risk factor in the development of sarcopenia. However, we did not measure blood alcohol concentration in order to rule out an added influence of ethanol alongside ammonia and/or inflammatory factors on myotube atrophy, as has been demonstrated in C2C12 cells (45, 55). Nonetheless, all ESLD patients included in this study were awaiting liver transplant and were being carefully monitored for abstinence at the time of sample donation. If alcohol was detected in their regular blood work, patients were removed from the liver transplant list. Irrespective, ethanol appears to play a role in the progression of sarcopenia in liver disease (56) and has been reported to blunt postprandial MPS in healthy humans (57). Despite this current abstinence, previous ethanol exposure may have increased the sensitivity of muscle to the effects of hyperammonemia, and subsequently

impair MPS (48). Future research should therefore aim to utilise this *ex vivo* model to investigate potential differences in myotube atrophy across different aetiologies and disease stages.

6.3.1 Muscle Atrophy and Protein Turnover in Chronic Liver Disease

Muscle atrophy occurs due to an imbalance in muscle protein turnover caused by a decline in MPS, an increase in MPB, or a combination of the two (58). Previously, treatment with ethanol (59), ammonia (50), or a combination (48) in C2C12s has been shown to impair MPS, alongside a decline in the phosphorylation of mammalian target of rapamycin (mTOR), ribosomal S6 protein kinase (p70S6K) and S6 protein (RPS6). Similarly, ethanol-fed mice exhibit a reduction in MPS, alongside a reduction in the phosphorylation of mTOR, p70S6K and RPS6 (59). However, in Chapter 4, we did not identify a decline in MPS, or a decline in markers of anabolic signalling in myotubes treated with fasted serum from ESLD or NAFLD patients in comparison to CON. These results may seem surprising based on previous literature; however, it is possible that the supraphysiological nature of the ammonia and ethanol treatments resulted in greater declines in comparison to the more physiological approach utilised in Chapter 4. In our model, myotubes were exposed to a number of systemic factors including ammonia, inflammatory cytokines and insulin at lower concentrations. Additionally, as all ESLD patients abstained from alcohol consumption, it is plausible to suggest that there would have been little circulating ethanol in the serum used for treatment. Collectively, our findings suggest that myotubes treated with serum from ESLD and NAFLD serum do not show an impairment in m-TOR related anabolic signalling in comparison to age-matched CON.

In addition to the findings outlined herein, recent work beyond the scope of the study in Chapter 4 has begun to investigate the potential mechanisms which may contribute to the inhibition of mTOR and MPS identified in response to ethanol and ammonia treatments (59, 60), with a

focus on the integrated stress response (ISR) and AMP kinase (AMPK). Previous work by Davuluri et al (60), showed an increase in the phosphorylation of eukaryotic initiation factor 2α (eIF2α) and general control non-depressed 2 (GCN2) in skeletal muscle samples from cirrhotic patients, PCA rats and C2C12 myotubes treated with ammonia. In addition, treatment with ethanol has also been shown to increase the phosphorylation of eIF2α and GCN2 (48). Therefore, these treatments may induce cellular stress which leads to the activation of the ISR, thus the inhibition of mTOR signalling (60). Research suggests that in response to ammonia treatment, cells adopt an alternative ISR in which activating transcription factor 4 (ATF4) is inhibited, preventing a negative feedback loop, and the return of normal levels of MPS (60). Additionally, in response to ethanol treatment in C2C12s previous work has shown an inhibition of the phosphorylation of mTOR and AMPK, due to the activation of protein phosphatase 2A (PP2A) (59). This is in contrast to 'normal conditions' in which AMPK is phosphorylated during nutrient and energy deficiency, resulting in the inhibition of autophagy, and tuberous sclerosis complex 1/2 (TSC1/2) and subsequently mTOR (61). Similarly, no change in AMPK activation was identified in myotubes treated with ammonia (45). Together, this suggests that ESLD patients, particularly with an ArLD aetiology may experience a dysregulation in muscle protein turnover through the inhibition of mTOR via the ISR and activation of PP2A. However, future *in vivo* research is required to establish the translatability of these findings to cirrhotic patients.

Although no difference in MPS, or anabolic targets was identified, in Chapter 4 we showed an increase in myostatin content in myotubes treated with NAFLD and ESLD serum in contrast to CON participants. While this is consistent with previous findings in cirrhotic patients (8), highlighting an increase in skeletal muscle myostatin expression compared to healthy controls, myostatin has also been linked to the inhibition of MPS (62), in disagreement to our findings. However, our results are similar to those identified in an *in vivo* model of chronic kidney

disease, highlighting a reduction in muscle mass, alongside an increase in myostatin content with no change in MPS (63). In addition to the mTOR pathway, myostatin has been shown to negatively regulate satellite cell (SC) activation (64). In older individuals an increase in myostatin content has been associated with a decrease in SC content within type II fibres, in contrast to younger individuals (65). Furthermore, ageing is associated with an increased distance between the capillaries and type II fibre SCs in older skeletal muscle (66). It is therefore unsurprising that muscle atrophy is largely associated with a decline in type II muscle fibres. As a result, it is plausible to suggest that ESLD patients may experience an increase in myostatin, in line with a decline in SC content which may contribute to the development of sarcopenia. Thus, future research should investigate SC content and location in cirrhotic patients.

6.3.2 Mitochondrial Dysfunction and Chronic Liver Disease

Alterations in muscle protein turnover in CLD may also arise due to impairments in mitochondrial function (9). In Chapter 4 of this thesis, we identified a significant decline in mitophagy (i.e., the removal of damaged mitochondria) alongside a decline in maximal respiration and coupling efficiency. While these factors have not been investigated in intact, or permeabilised muscle fibres from CLD patients, these findings are similar to a reduction in mitochondrial oxidative capacity identified in permeabilised muscle fibres of older adults, when compared to younger individuals (67). In addition, *in vivo* models of cancer cachexia have also identified a decline in mitochondrial oxidative capacity, alongside a decline muscle atrophy (68). However, in contrast to our findings, an *in vivo* model of cachexia showed no change in the efficiency of adenosine triphosphate (ATP) production, suggesting that the decrease in oxidative capacity may be attributed to a decline in complex IV activity (68).

Previous *in vitro* and *in vivo* work has shown that ammonia treatment may contribute to a reduction in ATP synthesis and tricarboxylic acid cycle (TCA) intermediates, and thus may impair MPS (9). However, we showed no change in ATP coupled respiration between CON, NAFLD and ESLD treated myotubes (Figure 4.4). In an attempt to explain the lack of change identified in Chapter 4, we analysed proton efflux rate (PER) to investigate changes in both basal and compensatory glycolysis. We identified no significant difference in basal and compensatory glycolysis between conditions (Figure 6.3). Furthermore, we analysed the production of ATP through both oxidative and glycolytic capacities. Although NAFLD and ESLD cohorts appeared to show a decrease in the oxidative generation of ATP there was no significant difference in comparison to CON treated myotubes (Figure 6.3).

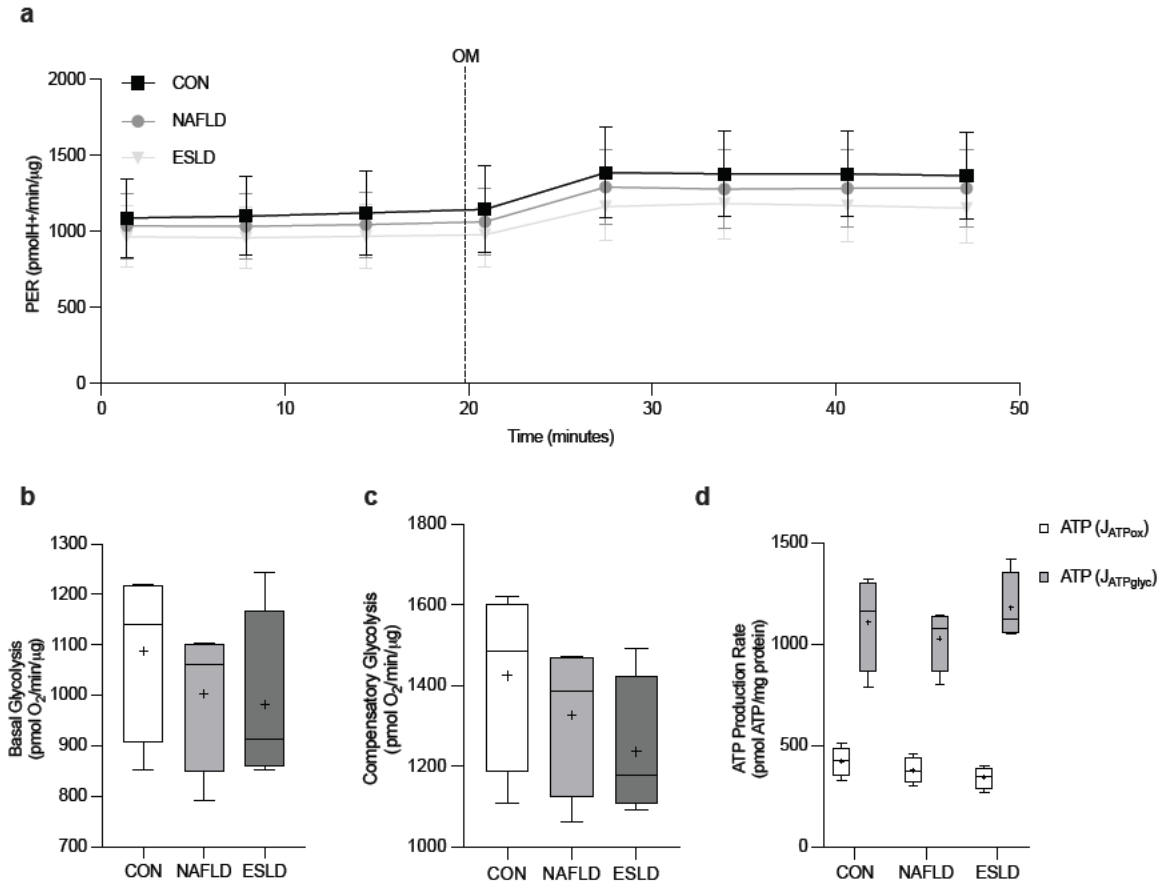

Fig. 6.3. Proton efflux rate and ATP production. (A) proton efflux rate raw trace for myotubes treated with *ex vivo* human serum from age matched controls (CON), non-alcoholic fatty liver disease (NAFLD) and end-stage liver disease (ESLD) patients, (B) basal glycolysis, (C) compensatory glycolysis, (D) ATP production. Data are expressed as the mean (cross), median (central horizontal line), 25^{th} and 75^{th} percentiles (box) and the minimum and maximum values (vertical lines), with each data point corresponding to the average of 3 technical repeats.

6.3.3 Model Limitations and Future Directions

While this *in vitro* model of liver disease provides a valuable platform for the investigation of a number of systemic factors which may underpin the development of muscle atrophy in ESLD, it is not without limitations. Firstly, and similar to Chapter 3, cross-species issues may be present as we did not use human primary skeletal muscle cells, as such C2C12s cannot fully replicate the conditions in human skeletal muscle tissue. As a result, future research should aim to replicate this treatment with *ex vivo* human serum on human primary skeletal muscle cells. Additionally, we are not able to distinguish between the primary drivers of myotube atrophy in this model. Therefore, further research should aim to remove, or knockout specific systemic drivers e.g., inflammatory cytokines and ammonia in order to establish their contribution to the development of sarcopenia. Furthermore, other systemic drivers such as testosterone and insulin growth factor-1 (IGF-1), which may influence sarcopenia progression should also be measured. Lastly, this model provides a beneficial platform for the investigation of potential countermeasures of sarcopenia in cirrhosis, prior to invasive human trials. Therefore, future research should use this model to investigate the effectiveness of nutraceutical and pharmacological treatments such as hydroxymethylbutyrate (HMB) (47), vitamin D (6).

6.4 Sarcopenia in Chronic Liver Disease: Translation of an *In Vitro* Model of ESLD, to *In Vivo* Work

In recent years, studies have been conducted to highlight the safety of muscle biopsies in cirrhotic patients (7), a pivotal step in improving our understanding of muscle loss across liver disease. Therefore, in Chapter 5 of the present thesis, we conducted an observational study in which fasted muscle biopsies were obtained from healthy age-matched controls, non-cirrhotic NAFLD and decompensated, alcohol related-ESLD patients. We aimed to investigate the translatability of our *in vitro* work, to *in vivo* human work. Additionally, we aimed to characterise the protein and gene expression of NAFLD and ESLD patients in this cohort, in comparison to CON participants.

Firstly, it is important to note that while we identified a significant decline in myotube diameter in Chapter 4 in response to treatment with ESLD serum, we did not show any difference in lean body mass (%) between groups in Chapter 5. While our *in vitro* model outlined in Chapter 4 represents the toxicity of human serum from ESLD, highlighted by a significant reduction in myotube diameter, this may not translate to our *in vivo* work, as patients were not sarcopenic. Ultimately, this suggests that our *in vitro* model of cell culture can be utilised to investigate the potential molecular mechanisms which may underpin the development of sarcopenia and reinforces the toxic systemic environment in ESLD patients, which if untreated may lead to the progression of sarcopenia.

In line with findings from our *in vitro* model of liver disease outlined in Chapter 4, we identified no change in the phosphorylation of anabolic markers in muscle biopsy samples obtained during a fasted state. We did however identify a decline in total-mTOR content in both NAFLD and ESLD patients in comparison to CON participants. This is in contrast to previous *in vivo* work conducted in human cirrhotic patients which found that patients

experience a decrease in the phosphorylation of anabolic signalling targets (7). While it may be surprising that we identified no difference in the phosphorylation of anabolic markers, we must consider that these findings only provide a single static measure. Indeed, previous work investigating age-related sarcopenia have identified no difference in basal levels of MPS, and anabolic signalling in comparison to young individuals (69). However, a blunted response to protein ingestion has been identified (20, 70). Therefore, it is plausible to suggest that as we did not measure MPS and anabolic signalling after the ingestion of a bolus protein solution, we may have missed potential differences in the anabolic response.

In addition to these findings, we also identified an upregulation of genes related to mTOR signalling in NAFLD, in comparison to both CON and ESLD in targeted gene analysis. This is in contrast to recent work by Singh et al (47), who identified a decline in mTOR signalling in a multi-omics analysis including gene expression in ethanol treated myotubes. However, we did identify a significant upregulation in genes related to ribonucleic acid (RNA) metabolism in NAFLD in comparison to CON participants (Chapter 5). Furthermore, messenger ribonucleic acid (mRNA) expression and protein levels have been shown to correlate to a limited extent (R^2 ~0.17-0.41) (71, 72). This dysregulation of protein and RNA is largely attributed to translation initiation, which is considered to be a rate limiting step (73). Translation initiation requires the binding of eukaryotic translation initiation factor (eIF4F) to the 5' cap of the mRNA (74). The rate of translation initiation can be influenced by the structural accessibility of the 5'cap (75) and the presence of small open reading frames (ORFs) in the 5' untranslated region (5' UTR) (72). Furthermore, a secondary structure in the 5' UTR of an mRNA may reduce the rate of protein synthesis through the impedance of the scanning ribosome (76). As a consequence, protein levels may vary to a greater extent than corresponding mRNAs (71). In addition, the rates of translation elongation may also contribute to the dysregulation of mRNA vs. protein levels. Translation elongation involves

the delivery of amino acids to the ribosomes by transfer ribonucleic acid (tRNA) (77). Previously, a number of factors have been linked to the variation in elongation rate including tRNA availability (78) and amino acid composition (79). Indeed, recent work has shown that amino acid composition of newly synthesized proteins is considered to be a key determinant of translation elongation rate (79). Taken together, it is therefore unsurprising that protein content does not fully correlate to changes in anabolic and catabolic signalling identified herein.

Furthermore, in Chapter 5, we identified an increase in myostatin protein content in NAFLD patients, in comparison to both CON and ESLD patients. Despite this, we found no significant change in serum myostatin between groups. This is in contrast to our *in vitro* work in chapter 4, highlighting an increase in myostatin protein content in myotubes treated with ESLD serum. In support of our *in vitro* model, previous *in vivo* work has shown a reduction in the concentration of myostatin within serum (80) and muscle (11) of cirrhotic patients. Furthermore, animal models of ESLD have also highlighted an increase in myostatin, alongside a reduction in myotube diameter and muscle mass within rats (11), suggesting an inverse correlation with muscle mass (81). Additionally, previous *in vitro* work has highlighted treatment with ammonia may upregulate myostatin through an nuclear factor- κB (NF-κB) mediated mechanism (11), while ammonia withdrawal has been shown to reduce myostatin expression in PCA rats and C2C12 myotubes (50). Although across the literature, there is strong support to suggest that cirrhotic patients show elevated levels of myostatin, it is worth noting that the use of serum myostatin as a biomarker for sarcopenia has been questioned, due to inconsistent results identified across studies (82). Thus, the role of myostatin in liver disease related muscle atrophy warrants further investigation.

In addition to alterations in myostatin protein content found in NAFLD, we observed no change in the protein content of FK2, muscle atrophy box (MAFbx), caspase-3 and

microtubule associated protein 1A/B light chain 3 (LC3 A/B) in fasted muscle biopsy samples. These results are in line with findings outlined in Chapter 4, highlighting no difference in these proteolytic markers. While previous work has identified no change in the expression of ubiquitinated proteins in models of cirrhosis and cirrhotic patients, an increase in autophagy, outlined by an increase in sequestome 1 (p62) degradation, LC3 lipidation and beclin3 content has been identified (7, 8, 46). This has led to the belief that an increase in MPB, identified in cirrhotic patients may be driven by an increase in myostatin and an increase in autophagy, with no change in ubiquitination (6, 7). However, we show conflicting results in relation to muscle ring finger-1 (MuRF-1) protein content in which MuRF-1 was elevated in our cellular model of ESLD, outlined in Chapter 4, but remained unchanged in ESLD patients in Chapter 5, despite an increase in genes related to protein ubiquitination shown amongst the top canonical pathways in ESLD vs. CON. In line with findings in Chapter 5, Dasarathy et al, identified an increase in mRNA of ubiquitinated proteins in PCA rats (83). However, the findings identified in our *in vivo* work, corresponds to previous human work highlighting no change in MuRF-1 protein content (7, 8), thus highlighting that PCA may translate poorly to work conducted in cirrhotic patients. It is however important to note that the data presented in this study may not reflect 'true disease conditions' as these samples were taken after an overnight fast. Cirrhotic patients are assumed to experience an accelerated state of starvation (10, 84); therefore, it is plausible to suggest that these patients may experience an increase in proteolytic markers at a more rapid rate, postprandial thus any difference may have been missed due to sample timing. Future research should aim to investigate proteolytic signalling related to muscle protein turnover over a time course postprandial. Taken together, I hypothesise that alternations in muscle protein turnover in both NAFLD and ESLD cohorts here may be driven by an increase in

MPB, as opposed an accompanied decline in MPS outlined within an update of Figure 1.2 of this thesis (Figure 6.4).

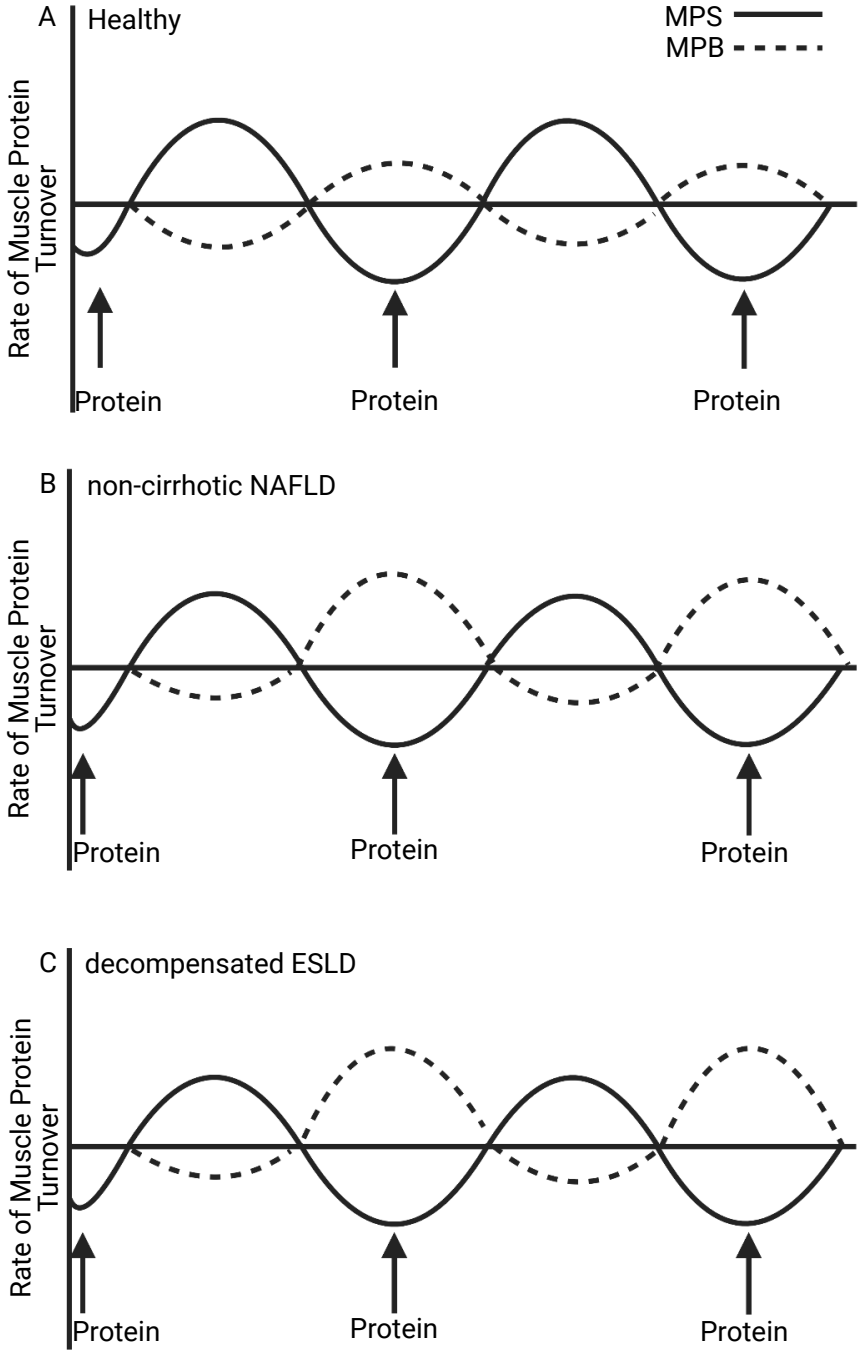

Figure 6.4. Updated schematic representation of muscle protein turnover in response to anabolic stimuli (protein feeding) in healthy, non-cirrhotic non-alcoholic fatty liver

disease. (NAFLD) and decompensated end-stage liver disease (ESLD). We hypothesise that the muscle protein breakdown (MPB) is the primary factor which contributes to alternations in muscle protein turnover. This alteration in muscle protein turnover may lead to muscle loss in liver disease patients.

In addition to anabolic and catabolic signalling pathways, we also investigated markers of mitochondrial function and regulation within ESLD patients. In Chapter 5, we identified a decline in citrate synthase (CS) activity, alongside a decline in the content of oxidative phosphorylation (OXPHOS) complexes I and IV. This contrasts with our *in vitro* work outlined in chapter 4 which identified no difference in OXPHOS content. Although, a decline in the content of complex I, IV and V has been identified in sedentary, compared to active elderly individuals has been shown (85, 86). However, while we observed a tendency for complex V protein content to decline with liver disease, this did not reach significance. Furthermore, electron transport chain (ETC) complex I content has been associated with a decline in physical performance in elderly males, highlighting that mitochondrial dysfunction may have a role in the development of sarcopenia (87).

In addition to markers of mitochondrial content, we found no change in protein content of markers of mitochondrial dynamics (i.e., fusion and fission). While we did not measure markers of mitochondrial regulation in Chapter 4, we did measure mitophagy through the use of a mito-QC reported cell line (88). These results highlight that cells treated with serum from both non-cirrhotic NAFLD and decompensated ESLD patients resulted in a decline in mitophagy when compared to CON treated cells. However, there are currently no appropriate methods to measure mitophagy in humans, which limit translatability. Therefore, human research investigating mitophagy currently relies on the use of static markers related to mitochondrial fusion and fission to highlight changes in mitochondrial structure. As a consequence, changes in mitochondrial dynamics may be missed in humans. Collectively,

Chapters 4 and 5 highlight that mitochondrial dysfunction may be a driver of sarcopenia in ESLD. Further research is required to investigate whether a reduction in number of mitochondria, or an accumulation of damaged mitochondria is the major contributor of mitochondrial dysfunction in ESLD.

6.4.3 Limitations and Future Directions

This study confirms that muscle biopsy samples can be safely obtained from ESLD patients, in line with previous work (7). Therefore, future research should aim to investigate the intracellular mechanisms which may contribute to the development of sarcopenia, in order to establish the translatability of supraphysiological models of cirrhosis, which we have begun to disentangle herein. However, this work is not without limitations. Firstly, we did not perform dynamic measures of muscle protein turnover. These dynamic measures provide a unique insight into basal and post-prandial levels of muscle protein turnover and mitochondrial respiration, thus targeting key gaps in the current literature. Additionally, while this research supports the notion that mitochondrial dysfunction may be a key driver of sarcopenia in ESLD, we did not measure oxidative stress or mitochondrial respiration directly. Therefore, future research should aim to probe further into the potential role of the mitochondria in the development of sarcopenia in cirrhosis. Furthermore, while we highlight the characterisation of protein and gene expression for non-cirrhotic NAFLD and ESLD patients with an underlying alcohol related aetiology, future research is required to investigate these findings over the course of different disease aetiologies such as the progression of NAFLD to non-alcoholic steatohepatitis (NASH).

6.4.4 Implications and Potential Therapeutic Targets

Although disease related complications such as hepatic encephalopathy (HE) and ascites can be treated by liver transplants, sarcopenia may develop or worsen post-transplant (89, 90).

Therefore, the management of sarcopenia in CLD is a high clinical priority. The findings of this thesis have allowed for the identification of several therapeutic targets, in particular the mitochondria and myostatin. Therefore, several innovative therapies, involving Bimagrumab, an antagonistic anti-activin receptor IIB (ActRIIB) antibody (91, 92), or urolithin A (UA) (93) which have previously been used for the treatment of age-related sarcopenia and chronic obstructive pulmonary disease (COPD) may prove beneficial treatments. While research into these pharmaceutical compounds have not been conducted in CLD patients, the underlying molecular mechanisms which contribute to the underpin the development of sarcopenia in CLD may be similar. Therefore, these treatments may provide a novel insight into potential pharmaceutical compounds which may be used for the treatment of sarcopenia in CLD.

Throughout this thesis we have identified an increase in myostatin in cellular models of ESLD, and muscle samples of non-cirrhotic NAFLD patients. Myostatin is known to regulate muscle growth by acting on the anti-ActRIIB receptor, which subsequently inhibits myoblast mTOR signalling and myoblast differentiation (62). Therefore, the inhibition of myostatin may provide a useful treatment for sarcopenia in CLD. Previous work has shown that Bimagrumab, can prevent the binding of myostatin to ActRIIB, and has been found to induce muscle hypertrophy (94). Indeed, a 16-week treatment of Bimagrumab in community-dwelling older adults resulted in improvements in gait speed, muscle mass and strength (95). Similarly, a 24-week treatment with Bimagrumab in COPD has been shown to induce improvements in lean body mass, thigh muscle volume, alongside a reduction in intermuscular and subcutaneous fat in comparison to a placebo (91). However, these changes occurred with no improvements in physical function. While Bimagrumab has not been investigated in patients with CLD patients, findings from other cohorts suggest that this may be a promising therapeutic treatment of muscle atrophy.

Additionally, in chapters 4 and 5 of this thesis, we identified elements of mitochondrial dysfunction in both an *in vitro* model of NAFLD and ESLD, and human muscle from ESLD patients. Therefore, improvements in mitochondrial function may be a suitable therapeutic target for ESLD patients. UA is a naturally occurring metabolite formed in response to the consumption of ellagitannin-rich food by the gut microbiota (96). Preclinical work in C2C12 skeletal muscle cells and Caenorhabditis elegans has shown that UA activates mitophagy and subsequently leads to improvements in mitochondrial biogenesis and respiratory capacity (97). Additionally, the induction of mitophagy through UA treatment in rodents lead to improvements in muscle function, measured through grip strength and voluntary wheel running (97). Furthermore, UA has been reported to have antioxidant and anti-inflammatory properties (98), two elements which we (Chapter 4) and others have shown may contribute to muscle atrophy in ESLD. Indeed, in sedentary older individuals, UA was shown to induce improvements in cellular and mitochondrial health (93). While no research surrounding the use of UA in ESLD has been conducted, previous work suggests that UA supplementation may have beneficial effects on mitochondrial health, which may lead to improvements in skeletal muscle function.

6.5 Conclusions

To conclude, this thesis has described the role of *ex vivo* human serum to create a more physiological *in vitro* model of age-related and liver disease-related atrophy. In this model, *ex vivo* human serum from older males induced myotube atrophy, alongside a blunted anabolic sensitivity to *in vitro* leucine treatment, providing rationale to conduct this experimental design with *ex vivo* human serum from liver disease patients. Myotube atrophy was observed alongside mitochondrial dysfunction in myotubes treated with serum from ESLD patients in comparison to both CON and NAFLD patients. As a result, we provide a suitable model for the investigation of the mechanisms and countermeasures of sarcopenia, prior to the

completion of *in vivo* human trials. These models allowed us to successfully investigate intracellular pathways of interest, prior to completion of human work. Finally, *in vivo* human work was conducted in non-cirrhotic NAFLD, decompensated-ESLD and age-matched CON participants. We found that ESLD patients showed mitochondrial dysfunction and the activation of pathways related to oxidative stress, while NAFLD patients showed elevated myostatin protein content, alongside an upregulation of genes related to senescence pathways. We also found a reduction in total-mTOR protein content, alongside an increase in gene expression related to ubiquitination and autophagy in both NAFLD and ESLD patients. These *in vivo* findings show several divergent and similar signalling pathways which may underpin the development of sarcopenia in non-cirrhotic NAFLD and decompensated ESLD. Collectively, this thesis highlights a number of potential therapeutic targets for the management of sarcopenia across the stages of CLD.

6.6 References

1. **Cruz-Jentoft AJ, Bahat G, Bauer J, Boirie Y, Bruyere O, Cederholm T, Cooper C, Landi F, Rolland Y, Sayer AA, and Schneider SM**. Sarcopenia: revised European consensus on definition and diagnosis. *Age Ageing* 48: 16-31, 2019.
2. **Ethgen O, Beaudart C, Buckinx F, Bruyere O, and Reginster JY**. The Future Prevalence of Sarcopenia in Europe: A Claim for Public Health Action. *Calcif Tissue Int* 100: 229-234, 2017.
3. **Pimpin L, Cortez-Pinto H, Negro F, Corbould E, Lazarus JV, Webber L, and Sheron N**. Burden of liver disease in Europe: Epidemiology and analysis of risk factors to identify prevention policies. *Journal of Hepatology* 69: 718-735, 2018.
4. **Kim G, Kang SH, Kim MY, and Back SK**. Prognostic value of sarcopenia in patients with liver cirrhosis: A systematic review and meta-analysis. *PLoS One* 12: e0186990, 2017.
5. **Montano-Loza AJ, Meza-Junco J, Prado CM, Lieffers JR, Baracos VE, Bain VG, and Sawyer MB**. Muscle wasting is associated with mortality in patients with cirrhosis. *Clin Gastroenterol Hepatol* 10: 166-173, 2012.
6. **Allen SL, Quinlan JI, Dhaliwal A, Armstrong MJ, Elsharkawy AM, Greig CA, Lord JM, Lavery GG, and Breen L**. Sarcopenia in Chronic Liver Disease: Mechanisms and Countermeasures. *Am J Physiol Gastrointest Liver Physiol* 320: G241-G257, 2021.
7. **Tsien C, Davuluri G, Singh D, Allawy A, Ten Have GA, Thapaliya S, Schulze JM, Barnes D, McCullough AJ, Engelen MP, Deutz NE, and Dasarathy S**. Metabolic and molecular responses to leucine-enriched branched chain amino acid supplementation in the skeletal muscle of alcoholic cirrhosis. *Hepatology* 61: 2018-2029, 2015.
8. **Qiu J, Tsien C, Thapalaya S, Narayanan A, Weihl CC, Ching JK, Eghtesad B, Singh K, Fu X, Dubyak G, McDonald C, Almasan A, Hazen SL, Naga Prasad SV, and Dasarathy S**. Hyperammonemia-mediated autophagy in skeletal muscle contributes to sarcopenia of cirrhosis. *Am J Physiol Endocrinol Metab* 303: E983-E993, 2012.
9. **Davuluri G, Allawy A, Thapaliya S, Rennison JH, Singh D, Kumar A, Sandlers Y, Van Wagoner DR, Flask CA, Hoppel C, Kasumov T, and Dasarathy S**. Hyperammonaemia-induced skeletal muscle mitochondrial dysfunction results in cataplerosis and oxidative stress. *J Physiol* 594: 7341-7360, 2016.
10. **Tsien C, McCullough AJ, and Dasarathy S**. Late evening snack: exploiting a period of anabolic opportunity in cirrhosis. *J Gastroenterol Hepatol* 27: 430-441, 2012.
11. **Qiu J, Thapaliya S, Runkana A, Yang Y, Tsien C, Mohan ML, Narayanan A, Eghtesad B, Mozdziak PE, McDonald C, Stark GR, Welle S, Naga Prasad SV, and Dasarathy S**. Hyperammonemia in cirrhosis induces transcriptional regulation of myostatin by an NF-kappaB-mediated mechanism. *Proc Natl Acad Sci U S A* 110: 18162-18167, 2013.
12. **Kumar A, Davuluri G, Welch N, Kim A, Gangadhariah M, Allawy A, Priyadarshini A, McMullen MR, Sandlers Y, Willard B, Hoppel CL, Nagy LE, and Dasarathy S**. Oxidative stress mediates ethanol-induced skeletal muscle mitochondrial dysfunction and dysregulated protein synthesis and autophagy. *Free Radic Biol Med* 145: 284-299, 2019.
13. **Narici MV, and Maffulli N**. Sarcopenia: characteristics, mechanisms and functional significance. *Br Med Bull* 95: 139-159, 2010.
14. **Kalampouka I, van Bekhoven A, and Elliott BT**. Differing effects of younger and older human plasma on C2C12 myocytes in vitro. *Front Physiol* 9: 152, 2018.
15. **van Hees HW, Schellekens WJ, Linkels M, Leenders F, Zoll J, Donders R, Dekhuijzen PN, van der Hoeven JG, and Heunks LM**. Plasma from septic shock patients induces loss of muscle protein. *Crit Care* 15: R233, 2011.

16. **Carson BP, Patel B, Amigo-Benavent M, Pauk M, Kumar Gujulla S, Murphy SM, Kiely PA, and Jakeman PM**. Regulation of muscle protein synthesis in an in vitro cell model using ex vivo human serum. *Exp Physiol* 103: 783-789, 2018.
17. **Patel B, Pauk M, Amigo-Benavent M, Nongonierma AB, Fitzgerald RJ, Jakeman PM, and Carson BP**. A cell-based evaluation of a non-essential amino acid formulation as a non-bioactive control for activation and stimulation of muscle protein synthesis using ex vivo human serum. *PLoS One* 14: e0220757, 2019.
18. **Lees MJ, Nolan D, Amigo-Benavent M, Raleigh CJ, Khatib N, Harnedy-Rothwell P, FitzGerald RJ, Egan B, and Carson BP**. A Fish-Derived Protein Hydrolysate Induces Postprandial Aminoacidaemia and Skeletal Muscle Anabolism in an In Vitro Cell Model Using Ex Vivo Human Serum. *Nutrients* 13: 2021.
19. **Patel B, Pauk M, Amigo-Benavent M, Nongonierma AB, Fitzgerald RJ, Jakeman PM, and Carson BP**. A cell-based evaluation of a non-essential amino acid formulation as a non-bioactive control for activation and stimulation of muscle protein synthesis using ex vivo human serum. *PLoS One* 14: e0220757, 2019.
20. **Cuthbertson D, Smith K, Babraj J, Leese G, Waddell T, Atherton P, Wackerhage H, Taylor PM, and Rennie MJ**. Anabolic signaling deficits underlie amino acid resistance of wasting, aging muscle. *FASEB J* 19: 422-424, 2005.
21. **Katsanos CS, Kobayashi H, Sheffield-Moore M, Aarsland A, and Wolfe RR**. Aging is associated with diminished accretion of muscle proteins after the ingestion of a small bolus of essential amino acids. *Am J Clin Nutr* 82: 1065-1073, 2005.
22. **Wall BT, Gorissen SH, Pennings B, Koopman R, Groen BB, Verdijk LB, and van Loon LJ**. Aging Is Accompanied by a Blunted Muscle Protein Synthetic Response to Protein Ingestion. *PLoS One* 10: e0140903, 2015.
23. **Dardevet D, Sornet C, Balage M, and Grizard J**. Stimulation of in Vitro Rat Muscle Protein Synthesis by Leucine Decreases With Age. *J Nutr* 130: 2630-2635, 2000.
24. **Schaap LA, Pluijm SM, Deeg DJ, and Visser M**. Inflammatory markers and loss of muscle mass (sarcopenia) and strength. *Am J Med* 119: 526 e529-517, 2006.
25. **Schaap LA, Pluijm SM, Deeg DJ, Harris TB, Kritchevsky SB, Newman AB, Colbert LH, Pahor M, Rubin SM, Tylavsky FA, Visser M, and Health ABCS**. Higher inflammatory marker levels in older persons: associations with 5-year change in muscle mass and muscle strength. *J Gerontol A Biol Sci Med Sci* 64: 1183-1189, 2009.
26. **Visser M, Pahor M, Taaffe DR, Goodpaster BH, Simonsick EM, Newman AB, Nevitt M, and Harris TB**. Relationship of interleukin-6 and tumor necrosis factor-alpha with muscle mass and muscle strength in elderly men and women: the health ABC study. *J Gerontol A Biol Sci Med Sci* 57: M326-332, 2002.
27. **Cesari M, Penninx BW, Pahor M, Lauretani F, Corsi AM, Rhys Williams G, Guralnik JM, and Ferrucci L**. Inflammatory markers and physical performance in older persons: the InCHIANTI study. *J Gerontol A Biol Sci Med Sci* 59: 242-248, 2004.
28. **Brinkley TE, Leng X, Miller ME, Kitzman DW, Pahor M, Berry MJ, Marsh AP, Kritchevsky SB, and Nicklas BJ**. Chronic inflammation is associated with low physical function in older adults across multiple comorbidities. *J Gerontol A Biol Sci Med Sci* 64: 455-461, 2009.
29. **Toth MJ, Matthews DE, Tracy RP, and Previs MJ**. Age-related differences in skeletal muscle protein synthesis: relation to markers of immune activation. *Am J Physiol Endocrinol Metab* 288: E883-E891, 2005.
30. **Cesari M, Kritchevsky SB, Baumgartner RN, Atkinson HH, Penninx BW, Lenchick L, Palla SL, Ambrosius WT, Tracy RP, and Pahor M**. Sarcopenia, obesity, and inflammation--results from the Trial of Angiotensin Converting Enzyme Inhibition and Novel Cardiovascular Risk Factors study. *Am J Clin Nutr* 82: 428-434, 2005.

31. **Sharples AP, Al-Shanti N, and Stewart CE**. C2 and C2C12 murine skeletal myoblast models of atrophic and hypertrophic potential: relevance to disease and ageing? *J Cell Physiol* 225: 240-250, 2010.
32. **Wahlin-Larsson B, Wilkinson DJ, Strandberg E, Hosford-Donovan A, Atherton PJ, and Kadi F**. Mechanistic Links Underlying the Impact of C-Reactive Protein on Muscle Mass in Elderly. *Cell Physiol Biochem* 44: 267-278, 2017.
33. **Li YP, Chen Y, John J, Moylan J, Jin B, Mann DL, and Reid MB**. TNF-alpha acts via p38 MAPK to stimulate expression of the ubiquitin ligase atrogin1/MAFbx in skeletal muscle. *FASEB J* 19: 362-370, 2005.
34. **Rong YD, Bian AL, Hu HY, Ma Y, and Zhou XZ**. Study on relationship between elderly sarcopenia and inflammatory cytokine IL-6, anti-inflammatory cytokine IL-10. *BMC Geriatr* 18: 308, 2018.
35. **Balage M, Averous J, Remond D, Bos C, Pujos-Guillot E, Papet I, Mosoni L, Combaret L, and Dardevet D**. Presence of low-grade inflammation impaired postprandial stimulation of muscle protein synthesis in old rats. *J Nutr Biochem* 21: 325-331, 2010.
36. **Rieu I, Magne H, Savary-Auzeloux I, Averous J, Bos C, Peyron MA, Combaret L, and Dardevet D**. Reduction in low grade inflammation restores blunting of postprandial muscle anabolism and limits sarcopenia in old rats. *J Physiol* 587: 5483-5492, 2009.
37. **Buffière C, Mariotti F, Savary-Auzeloux I, Mignè C, Hercberg S, Rèmond D, Duclos M, and Dardevet D**. Slight chronic elevation of C-reactive protein is associated with lower aerobic fitness but does not impair meal-induced stimulation of muscle protein metabolism in healthy old men. *J Physiol* 593: 1259-1272, 2015.
38. **Dideriksen K, Reitelseder S, Malmgaard-Clausen NM, Bechshoeft R, Petersen RK, Mikkelsen UR, and Holm L**. No effect of anti-inflammatory medication on postprandial and postexercise muscle protein synthesis in elderly men with slightly elevated systemic inflammation. *Exp Gerontol* 83: 2016.
39. **Shou J, Chen PJ, and Xiao WH**. Mechanism of increased risk of insulin resistance in aging skeletal muscle. *Diabetol Metab Syndr* 12: 14, 2020.
40. **Srikanthan P, Hevener AL, and Karlamangla AS**. Sarcopenia exacerbates obesity-associated insulin resistance and dysglycemia: findings from the National Health and Nutrition Examination Survey III. *PLoS One* 5: e10805, 2010.
41. **Rasmussen BB, Fujita S, Wolfe RR, Mittendorfer B, Roy M, Rowe VL, and Volpi E**. Insulin resistance of muscle protein metabolism in aging. *FASEB J* 20: 768-769, 2006.
42. **Volpi E, Mittendorfer B, Rasmussen BB, and Wolfe RR**. The response of muscle protein anabolism to combined hyperaminoacidemia and glucose-induces hyperinsulinemia is impaired in the elderly. *J Clin Endocrinol Metab* 85: 4481-4490, 2000.
43. **Smeuninx B, McKendry J, Wilson D, Martin U, and Breen L**. Age-Related Anabolic Resistance of Myofibrillar Protein Synthesis Is Exacerbated in Obese Inactive Individuals. *J Clin Endocrinol Metab* 102: 3535-3545, 2017.
44. **Batsis JA, and Villareal DT**. Sarcopenic obesity in older adults: aetiology, epidemiology and treatment strategies. *Nat Rev Endocrinol* 14: 513-537, 2018.
45. **Crossland H, Smith K, Atherton PJ, and Wilkinson DJ**. The metabolic and molecular mechanisms of hyperammonaemia- and hyperethanolaemia-induced protein catabolism in skeletal muscle cells. *J Cell Physiol* 233: 9663-9673, 2018.
46. **Dasarathy S, Dodig M, Muc SM, Kalhan SC, and McCullough AJ**. Skeletal muscle atrophy is associated with an increased expression of myostatin and impaired satellite cell function in the portacaval anastamosis rat. *Am J Physiol Gastrointest Liver Physiol* 287: G1124-1130, 2004.

47. **Singh SS, Kumar A, Welch N, Sekar J, Mishra S, Bellar A, Gangadhariah M, Attaway A, Al Khafaji H, Wu X, Pathak V, Agrawal V, McMullen MR, Hornberger TA, Nagy LE, Davuluri G, and Dasarathy S**. Multiomics-Identified Intervention to Restore Ethanol-Induced Dysregulated Proteostasis and Secondary Sarcopenia in Alcoholic Liver Disease. *Cell Physiol Biochem* 55: 91-116, 2021.
48. **Kant S, Davuluri G, Alchirazi KA, Welch N, Heit C, Kumar A, Gangadhariah M, Kim A, McMullen MR, Willard B, Luse DS, Nagy LE, Vasiliou V, Marini AM, Weiner ID, and Dasarathy S**. Ethanol sensitizes skeletal muscle to ammonia-induced molecular perturbations. *J Biol Chem* 294: 7231-7244, 2019.
49. **Dasarathy S, and Merli M**. Sarcopenia from mechanism to diagnosis and treatment in liver disease. *J Hepatol* 65: 1232-1244, 2016.
50. **Kumar A, Davuluri G, Silva RNE, Engelen M, Ten Have GAM, Prayson R, Deutz NEP, and Dasarathy S**. Ammonia lowering reverses sarcopenia of cirrhosis by restoring skeletal muscle proteostasis. *Hepatology* 65: 2045-2058, 2017.
51. **Han JW, Kim DI, Nam HC, Chang UI, Yang JM, and Song DS**. Association between serum TNF-a and sarcopenia in liver cirrhosis. *Clin Mol Hepatol*: 2021.
52. **Kurosawa T, Goto M, Kaji N, Aikiyo S, Mihara T, Ikemoto-Uezumi M, Toyoda M, Kanazawa N, Nakazawa T, Hori M, and Uezumi A**. Liver fibrosis-induced muscle atrophy is mediated by elevated levels of circulating TNFalpha. *Cell Death Dis* 12: 11, 2021.
53. **Mitchell WK, Williams J, Atherton P, Larvin M, Lund J, and Narici M**. Sarcopenia, dynapenia, and the impact of advancing age on skeletal muscle size and strength a quantitative review. *Front Physiol* 3: 260, 2012.
54. **Welch N, Dasarathy J, Runkana A, Penumatsa R, Bellar A, Reen J, Rotroff D, McCullough AJ, and Dasarathy S**. Continued muscle loss increases mortality in cirrhosis: Impact of aetiology of liver disease. *Liver Int* 40: 1178-1188, 2020.
55. **Wang DT, Yin Y, Yang YJ, Lv PJ, Shi Y, Lu L, and Wei LB**. Resveratrol prevents TNF-alpha-induced muscle atrophy via regulation of Akt/mTOR/FoxO1 signaling in C2C12 myotubes. *Int Immunopharmacol* 19: 206-213, 2014.
56. **Dasarathy J, McCullough AJ, and Dasarathy S**. Sarcopenia in Alcoholic Liver Disease: Clinical and Molecular Advances. *Alcohol Clin Exp Res* 41: 1419-1431, 2017.
57. **Parr EB, Camera DM, Areta JL, Burke LM, Phillips SM, Hawley JA, and Coffey VG**. Alcohol ingestion impairs maximal post-exercise rates of myofibrillar protein synthesis following a single bout of concurrent training. *PLoS One* 9: e88384, 2014.
58. **Breen L, and Phillips SM**. Skeletal muscle protein metabolism in the elderly: Interventions to counteract the 'anabolic resistance' of ageing. *Nutr Metab* 8: 68, 2011.
59. **Davuluri G, Welch N, Sekar J, Gangadhariah M, Alsabbagh Alchirazi K, Mohan ML, Kumar A, Kant S, Thapaliya S, Stine M, McMullen MR, McCullough RL, Stark GR, Nagy LE, Naga Prasad SV, and Dasarathy S**. Activated protein phosphatase 2A disrupts nutrient sensing balance between mTORC1 and AMPK causing sarcopenia in alcoholic liver disease. *Hepatology* 73: 1892-1908, 2020.
60. **Davuluri G, Krokowski D, Guan BJ, Kumar A, Thapaliya S, Singh D, Hatzoglou M, and Dasarathy S**. Metabolic adaptation of skeletal muscle to hyperammonemia drives the beneficial effects of l-leucine in cirrhosis. *J Hepatol* 65: 929-937, 2016.
61. **Laplante M, and Sabatini DM**. mTOR signalling in growth control and disease. *Cell* 149: 274-293, 2012.
62. **Trendelenburg AU, Meyer A, Rohner D, Boyle J, Hatakeyama S, and Glass DJ**. Myostatin reduces Akt/TORC1/p70S6K signaling, inhibiting myoblast differentiation and myotube size. *Am J Physiol Cell Physiol* 296: C1258-C1270, 2009.

63. **Wang DT, Yang YJ, Huang RH, Zhang ZH, and Lin X**. Myostatin Activates the Ubiquitin-Proteasome and Autophagy-Lysosome Systems Contributing to Muscle Wasting in Chronic Kidney Disease. *Oxid Med Cell Longev* 2015: 684965, 2015.
64. **McCroskery S, Thomas M, Maxwell L, Sharma M, and Kambadur R**. Myostatin negatively regulates satellite cell activation and self-renewal. *J Cell Biol* 162: 1135-1147, 2003.
65. **McKay BR, Ogborn DI, Bellamy LM, Tarnopolsky MA, and Parise G**. Myostatin is associated with age-related human muscle stem cell dysfunction. *FASEB J* 26: 2509-2521, 2012.
66. **Nederveen JP, Joanisse S, Snijders T, Ivankovic V, Baker SK, Phillips SM, and Parise G**. Skeletal muscle satellite cells are located at a closer proximity to capillaries in healthy young compared with older men. *J Cachexia Sarcopenia Muscle* 7: 547-554, 2016.
67. **Porter C, Hurren NM, Cotter MV, Bhattarai N, Reidy PT, Dillon EL, Durham WJ, Tuvdendorj D, Sheffield-Moore M, Volpi E, Sidossis LS, Rasmussen BB, and Borsheim E**. Mitochondrial respiratory capacity and coupling control decline with age in human skeletal muscle. *Am J Physiol Endocrinol Metab* 309: E224-232, 2015.
68. **Julienne CM, Dumas JF, Goupille C, Pinault M, Berri C, Collin A, Tesseraud S, Couet C, and Servais S**. Cancer cachexia is associated with a decrease in skeletal muscle mitochondrial oxidative capacities without alteration of ATP production efficiency. *J Cachexia Sarcopenia Muscle* 3: 265-275, 2012.
69. **Kumar V, Selby A, Rankin D, Patel R, Atherton P, Hildebrandt W, Williams J, Smith K, Seynnes O, Hiscock N, and Rennie MJ**. Age-related differences in the dose-response relationship of muscle protein synthesis to resistance exercise in young and old men. *J Physiol* 587: 211-217, 2009.
70. **Volpi E, Sheffield-Moore M, Rasmussen BB, and Wolfe RR**. Basal muscle amino acid kinetics and protein synthesis in healthy young and older men. *JAMA* 286: 1206-1212, 2001.
71. **Schwanhausser B, Busse D, Li N, Dittmar G, Schuchhardt J, Wolf J, Chen W, and Selbach M**. Global quantification of mammalian gene expression control. *Nature* 473: 337-342, 2011.
72. **Ingolia NT, Ghaemmaghami S, Newman JR, and Weissman JS**. Genome-wide analysis in vivo of translation with nucleotide resolution using ribosome profiling. *Science* 324: 218-223, 2009.
73. **Livingstone M, Atas E, Meller A, and Sonenberg N**. Mechanisms governing the control of mRNA translation. *Phys Biol* 7: 021001, 2010.
74. **Sonenberg N**. eIF4E, the mRNA cap-binding protein: from basic discovery to translational research. *Biochem Cell Biol* 86: 178-183, 2008.
75. **Richter JD, and Sonenberg N**. Regulation of cap-dependent translation by eIF4E inhibitory proteins. *Nature* 433: 477-480, 2005.
76. **Weinberg DE, Shah P, Eichhorn SW, Hussmann JA, Plotkin JB, and Bartel DP**. Improved Ribosome-Footprint and mRNA Measurements Provide Insights into Dynamics and Regulation of Yeast Translation. *Cell Rep* 14: 1787-1799, 2016.
77. **Kirchner S, and Ignatova Z**. Emerging roles of tRNA in adaptive translation, signalling dynamics and disease. *Nat Rev Genet* 16: 98-112, 2015.
78. **Varenne S, Buc J, Lloubes R, and Lazdunski C**. Translation is a non-uniform process. Effect of tRNA availability on the rate of elongation of nascent polypeptide chains. *J Mol Biol* 180: 549-576, 1984.
79. **Riba A, Di Nanni N, Mittal N, Arhne E, Schmidt A, and Zavolan M**. Protein synthesis rates and ribosome occupancies reveal determinants of translation elongation rates. *Proc Natl Acad Sci U S A* 116: 15023-15032, 2019.

80. **Nishikawa H, Enomoto H, Ishii A, Iwata Y, Miyamoto Y, Ishii N, Yuri Y, Hasegawa K, Nakano C, Nishimura T, Yoh K, Aizawa N, Sakai Y, Ikeda N, Takashima T, Takata R, Iijima H, and Nishiguchi S**. Elevated serum myostatin level is associated with worse survival in patients with liver cirrhosis. *J Cachexia Sarcopenia Muscle* 8: 915-925, 2017.
81. **Dasarathy S**. Myostatin and beyond in cirrhosis: all roads lead to sarcopenia. *J Cachexia Sarcopenia Muscle* 8: 864-869, 2017.
82. **Baczek J, Silkiewicz M, and Wojszel ZB**. Myostatin as a Biomarker of Muscle Wasting and other Pathologies-State of the Art and Knowledge Gaps. *Nutrients* 12: 2401, 2020.
83. **Dasarathy S, Muc S, Hisamuddin K, Edmison JM, Dodig M, McCullough AJ, and Kalhan SC**. Altered expression of genes regulating skeletal muscle mass in the portacaval anastomosis rat. *Am J Physiol Gastrointest Liver Physiol* 292: G1105-1113, 2007.
84. **Owen OE, Trapp VE, Reichard GAJ, Mozzoli MA, Moctezuma J, Paul P, Skutches CL, and Boden G**. Nature and quantity of fuels consumed in patients with alcoholic cirrhosis. *J Clin Invest* 72: 1821-1832, 1983.
85. **Broskey NT, Greggio C, Boss A, Boutant M, Dwyer A, Schlueter L, Hans D, Gremion G, Kreis R, Boesch C, Canto C, and Amati F**. Skeletal muscle mitochondria in the elderly: effects of physical fitness and exercise training. *J Clin Endocrinol Metab* 99: 1852-1861, 2014.
86. **Broskey NT, Boss A, Fares EJ, Greggio C, Gremion G, Schluter L, Hans D, Kreis R, Boesch C, and Amati F**. Exercise efficiency relates with mitochondrial content and function in older adults. *Physiol Rep* 3: e12418, 2015.
87. **Rygiel KA, Dodds RM, Patel HP, Syddall HE, Westbury LD, Granic A, Cooper C, Cliff J, Rocha MC, Turnball DM, and Sayer AA**. Mitochondrial respiratory chain deficiency in older men and its relationship with muscle mass and performance. *J Cachexia Sarcopenia Muscle* 2: 1-10(e00035), 2017.
88. **Seabright AP, Fine NHF, Barlow JP, Lord SO, Musa I, Gray A, Bryant JA, Banzhaf M, Lavery GG, Hardie DG, Hodson DJ, Philp A, and Lai YC**. AMPK activation induces mitophagy and promotes mitochondrial fission while activating TBK1 in a PINK1-Parkin independent manner. *FASEB J* 34: 6284-6301, 2020.
89. **Dasarathy S**. Posttransplant sarcopenia: an underrecognized early consequence of liver transplantation. *Dig Dis Sci* 58: 3103-3111, 2013.
90. **Tsien C, Garber A, Narayanan A, Shah SN, Barnes D, Eghtesad B, Fung J, McCullough AJ, and Dasarathy S**. Post-liver transplantation sarcopenia in cirrhosis: a prospective evaluation. *J Gastroenterol Hepatol* 29: 1250-1257, 2014.
91. **Polkey MI, Praestgaard J, Berwick A, Franssen FME, Singh D, Steiner MC, Casaburi R, Tillmann HC, Lach-Trifilieff E, Roubenoff R, and Rooks DS**. Activin Type II receptor blockade for treatment of muscle depletion in chronic obstructive pulmonary disease. A randomized trial. *Am J Respir Crit Care Med* 199: 313-320, 2019.
92. **Rooks DS, Laurent D, Praestgaard J, Rasmussen S, Bartlett M, and Tanko LB**. Effect of bimagrumab on thigh muscle volume and composition in men with casting-induced atrophy. *J Cachexia Sarcopenia Muscle* 8: 727-734, 2017.
93. **Andreux PA, Blanco-Bose W, Ryu D, Burdet F, Ibberson M, Aebischer P, Auwerx J, Singh A, and Rinsch C**. The mitophagy activator urolithin A is safe and induces a molecular signature of improved mitochondrial and cellular health in humans. *Nature Metabolism* 1: 595-603, 2019.
94. **Lach-Trifilieff E, Minetti GC, Sheppard K, Ibebunjo C, Feige JN, Hartmann S, Brachat S, Rivet H, Koelbing C, Morvan F, Hatakeyama S, and Glass DJ**. An antibody

blocking activin type II receptors induces strong skeletal muscle hypertrophy and protects from atrophy. *Mol Cell Biol* 34: 606-618, 2014.
95. **Rooks D, Praestgaard J, Hariry S, Laurent D, Petricoul O, Perry RG, Lach-Trifilieff E, and Roubenoff R**. Treatment of sarcopenia with bimagrumab: results from a phase II, randomized, controlled, proof-of-concept study. *J Am Geriatr Soc* 65: 1988-1995, 2017.
96. **Garcia-Munoz C, and Vaillant F**. Metabolic fate of ellagitannins: implications for health, and research perspectives for innovative functional foods. *Crit Rev Food Sci Nutr* 54: 1584-1598, 2014.
97. **Ryu D, Mouchiroud L, Andreux PA, Katsyuba E, Moullan N, Nicolet-Dit-Felix AA, Williams EG, Jha P, Lo Sasso G, Huzard D, Aebischer P, Sandi C, Rinsch C, and Auwerx J**. Urolithin A induces mitophagy and prolongs lifespan in C. elegans and increases muscle function in rodents. *Nat Med* 22: 879-888, 2016.
98. **Tomas-Barberan FA, Gonzalez-Sarrias A, Garcia-Villalba R, Nunez-Sanchez MA, Selma MV, Garcia-Conesa MT, and Espin JC**. Urolithins, the rescue of "old" metabolites to understand a "new" concept: Metabotypes as a nexus among phenolic metabolism, microbiota dysbiosis, and host health status. *Mol Nutr Food Res* 61: 2017.